

This electronic thesis or dissertation has been downloaded from the King's Research Portal at <https://kclpure.kcl.ac.uk/portal/>



The physicochemical properties of nonionic oil-in-water microemulsions.

Malcolmson, Carole A

The copyright of this thesis rests with the author and no quotation from it or information derived from it may be published without proper acknowledgement.

END USER LICENCE AGREEMENT



Unless another licence is stated on the immediately following page this work is licensed

under a Creative Commons Attribution-NonCommercial-NoDerivatives 4.0 International

licence. <https://creativecommons.org/licenses/by-nc-nd/4.0/>

You are free to copy, distribute and transmit the work

Under the following conditions:

- Attribution: You must attribute the work in the manner specified by the author (but not in any way that suggests that they endorse you or your use of the work).
- Non Commercial: You may not use this work for commercial purposes.
- No Derivative Works - You may not alter, transform, or build upon this work.

Any of these conditions can be waived if you receive permission from the author. Your fair dealings and other rights are in no way affected by the above.

Take down policy

If you believe that this document breaches copyright please contact librarypure@kcl.ac.uk providing details, and we will remove access to the work immediately and investigate your claim.

**The Physicochemical Properties of
Nonionic Oil-in-Water Microemulsions**

A thesis submitted for the degree of

DOCTOR OF PHILOSOPHY

in

The Faculty of Medicine

of

The University of London

Carole A Malcolmson

October 1992

Chelsea Department of Pharmacy

King's College London



Abstract

Oil-in-water microemulsions are attractive vehicles for the delivery of therapeutic agents which are not sufficiently soluble or stable in an aqueous environment to allow injection or other effective administration.

In this investigation eight commercially available polyoxyethylene ether surfactants (C_mE_n) have been investigated for their ability to produce 3-component o/w microemulsions, without the addition of cosurfactant. Modification of oil and surfactant altered microemulsion formation in a complex way, dependent on the relative size and structure of the surfactant hydrophobe, ethylene oxide chain, and the dispersed oil phase. The surfactant Brij 96 ($C_{18-1}E_{10}$) at concentrations of 8-28 %w/w was found to be particularly effective at forming o/w microemulsions at room temperature with a variety of oils.

Further studies involved o/w microemulsions produced from soybean oil, Brij 96 and water. Light scattering investigations indicated that the size of the microemulsion droplets increased with oil content and decreased with surfactant concentration. Results suggested greater interdroplet interaction and aggregation near the border of the region of microemulsion existence.

The addition of water soluble polyols in these microemulsions was tolerated up to concentrations which depressed the PIT below that of room temperature. In comparison medium straight chained alcohols (1-butanol and 1-pentanol) extended the area of existence of clear liquid systems, although reduced the existence of microemulsions with an o/w droplet structure.

The stability of the o/w microemulsions did not appear to be affected by the presence of up to 1 %w/w of six poorly water soluble drugs. Results suggested that the most important site of incorporation of these drugs was the area of dehydrated polyoxyethylene chains of the surfactant. In order for an improvement in the drug carrying capacity of microemulsions over micellar systems of the same surfactant concentration, high solubility of the drug in the dispersed oil phase was required.

Acknowledgements

I wish to thank my supervisor, Dr. M. Jayne Lawrence for her guidance, enthusiasm and encouragement throughout this research project, and the Royal Pharmaceutical Society of Great Britain for the award of a research grant.

I would also like to express my gratitude to Dr. David Barlow of Chelsea Department of Pharmacy for the time and effort he has spent helping me.

I wish to thank SmithKline Beecham in Worthing, and in particular Dr. Caroline Gooch, for permitting me access to their spinning drop tensiometer, Dr. Duncan Craig of the School of Pharmacy, Brunswick Square, London, for allowing me to use their dielectric spectrometer, and Dr. David Attwood of the Department of Pharmacy, Manchester University, for use of their refractometer.

Furthermore I would like to acknowledge the assistance I received in obtaining some of these results by Miss Amarlok Sidhu, Mr. Larry Lam and Mr. George Kilipiris.

Thanks are also due to Mr. Martin Jessop, of the Computer Advisory Centre, King's College London, for making it possible to store and reproduce many of my triangular phase diagrams by computer. I would also like to thank the academic and technical staff, and all my friends and colleagues at Chelsea Department of Pharmacy for their encouragement.

Finally, I would like to thank Mr. Andy Greensmith for his continued support throughout this project.

Contents

	Page
Abstract	2
Acknowledgements	3
Contents	4
List of figures	9
List of tables	12
Abbreviations and symbols	14
Chapter One: Introduction	
1.1 Definition of a microemulsion	19
1.2 Microemulsion properties	20
1.3 The structure of microemulsion systems	23
1.3.1 Experimental methods for determining microemulsion structure	24
1.3.2 Structure of ionic microemulsions	27
1.3.3 Structure of nonionic microemulsions	29
1.4 Models for microemulsion structure	31
1.4.1 Geometric considerations	32
1.4.1.1 The critical packing parameter	32
1.4.1.2 The hydrophilic/lipophilic ratio	34
1.4.1.3 Surfactant film curvature	35
1.4.2 The models	40
1.4.2.1 Droplet model	40
1.4.2.2 Talmon-Prager model	41
1.4.2.3 Cubic random cell model	43
1.4.2.4 Disordered open connected model	44
1.5 Potential applications of microemulsions	47
1.5.1 Microemulsions in tertiary oil recovery	47
1.5.2 Microemulsions for chemical reactions	47

1.5.3 Microemulsions as media for enzyme catalyzed reactions	49
1.5.4 Microemulsions as liquid membrane carrier agents	50
1.5.5 Microemulsion gels	51
1.5.6 Microemulsions as blood substitutes	55
1.5.7 Microemulsions for drug delivery	57
1.5.7.1 Water-in-oil microemulsions	61
1.5.7.2 Oil-in-water microemulsions	64
 Chapter Two: Experimental	
2.1 Materials	68
2.1.1 Surfactants	68
2.1.2 Oils	68
2.1.3 Cosurfactants	70
2.1.4 Drugs	70
2.1.5 Miscellaneous chemicals	70
2.2 Methods and apparatus	72
2.2.1 Microemulsion production	72
2.2.2 Determination of phase diagrams	72
2.2.3 Determination of maximum drug incorporation	74
2.2.4 Stability testing via temperature cycling	75
2.2.5 Determination of phase inversion temperature	75
2.2.6 Conductivity measurements	76
2.2.7 Density measurements	76
2.2.8 Interfacial tension measurements	76
2.2.9 Refractive index measurements	79
2.2.10 Light scattering studies	80
2.2.10.1 Photon correlation spectroscopy	82
2.2.10.2 Total intensity light scattering	84
2.2.10.3 Analysis of total intensity light scattering data	86

Chapter Three: Soybean oil/Brij 96/water microemulsions

3.1 Area of existence	94
3.2 Effect of temperature on the area of existence	99
3.3 Phase inversion temperatures	99
3.4 Light scattering investigations	103
3.4.1 Photon correlation spectroscopy	103
3.4.1.1 Variation with temperature	105
3.4.1.2 Reproducibility of data	105
3.4.1.3 Changes with increasing soybean oil content	107
3.4.1.4 Changes with increasing Brij 96 content	114
3.4.1.5 Changes with a fixed weight ratio of Brij 96:soybean oil	120
3.4.2 Total intensity light scattering	124
3.4.2.1 Brij 96 micellar systems	124
3.4.2.2 Microemulsion systems	129
3.4.3 Comparison of photon correlation spectroscopy and total intensity light scattering data	136
3.5 Stability of soybean oil/Brij 96/water microemulsions	138

Chapter Four: Other 3-component nonionic microemulsion systems

4.1 The influence of the surfactant	143
4.1.1 The surfactants used	143
4.1.1.1 Polydispersity of polyoxyethylene ether surfactants	143
4.1.1.2 The HLB and CPP of the surfactants used	146
4.1.2 The area of microemulsion existence found with soybean oil	148
4.2 The influence of the oil	151
4.2.1 The effect of different oils on C ₁₈₋₁ E ₁₀ systems	151
4.2.1.1 One component oils	151
4.2.1.1.1 Effect on the phase inversion temperature	152
4.2.1.1.2 Effect on areas of existence	154
4.2.1.2 Oil mixtures	159
4.2.1.2.1 Triglyceride oils	159

4.2.1.2.2 Binary hydrocarbon oils	160
4.2.1.3 Photon correlation spectroscopy studies	162
4.2.2 The effect of different oils on C ₁₂ E ₁₀ systems	165
4.2.3 The effect of oil on other surfactant systems	168
Chapter Five: Soybean oil/Brij 96 microemulsion systems with added cosurfactant	
5.1 The addition of straight chain alcohols	173
5.1.1 The effect of alcohols on the area of existence	173
5.1.1.1 Methanol as cosurfactant	173
5.1.1.2 Butanol as cosurfactant	177
5.1.1.3 Pentanol as cosurfactant	181
5.1.2 Changes in the area of existence with temperature	184
5.1.3 Conductivity and dilution of soybean oil/Brij 96/butanol/ water systems	186
5.1.4 Changes in interfacial tension with the addition of butanol or pentanol	191
5.1.5 The addition of butanol to soybean oil/Brij 76 systems	193
5.2 The addition of polyols	195
5.2.1 The effect of polyols on the area of existence	195
5.2.2 Changes in interfacial tension with the addition of glycerol	203
5.5.3 The effect of polyols on the phase inversion temperature	203
Chapter Six: Drug incorporation into Brij 96 microemulsion systems	
6.1 The incorporation of diazepam	209
6.1.1 Comparison between micellar and microemulsion incorporation	210
6.1.2 Possible sites of incorporation	210
6.2 The incorporation of testosterone, testosterone propionate and testosterone enanthate	215

6.2.1 Effect on the area of existence	215
6.2.2 Comparison between micellar and 2% soybean oil microemulsion incorporation	217
6.2.3 Testosterone propionate incorporation into o/w microemulsions produced with different oils	222
6.2.4 Light scattering investigations of microemulsions containing testosterone enanthate	227
6.2.4.1 Photon correlation spectroscopy studies	227
6.2.4.2 Total intensity light scattering studies	230
6.2.5 Stability testing of microemulsions containing testosterone enanthate	236
6.3 The incorporation of progesterone and medroxy- progesterone acetate	241
6.3.1 Comparison between micellar and 2% soybean oil microemulsion incorporation	241
 Chapter Seven: Conclusions and future work	 246
 References	 251

List of figures

	Page
1.1: Phase behaviour in microemulsions	22
1.2: Possible structures of microemulsion systems	25
1.3: Structure of nonionic microemulsions with HLB and temperature	30
1.4: Packing properties of surfactants	33
1.5: Variation of film curvature with surfactant shape	36
1.6: The Talmon-Prager model of microemulsion systems	42
1.7: DOC model for DDAB/water/cyclohexane microemulsions	46
1.8: Model of reversed lecithin w/o microemulsions	54
1.9: Proposed models for gelatin-containing microemulsion gels	56
1.10: <i>In vitro</i> permeation of azelaic acid from a microemulsion and a gel into mouse abdominal skin	59
1.11: <i>In vitro</i> transdermal water transport from water and DSS/octanol microemulsions	60
 2.1: Construction of triangular phase diagrams	 73
2.2: Apparatus used to determine interfacial tension	78
2.3: The Malvern 4700c light scatterer	81
 3.1: Existence of intially clear liquid regions found with soybean oil, Brij 96 and water	 95
3.2: Area of o/w soybean oil/Brij 96/water microemulsions	96
3.3: Postulated model for o/w soybean oil/Brij 96 microemulsion	98
3.4: Existence of soybean oil/Brij 96/water microemulsions after one month at 37°C	100
3.5: CP and PIT vs %w/w Brij 96 for systems containing 0, 2 & 5%w/w soybean oil	102
3.6: Apparent Z mean diameters within the o/w region	104
3.7: PCS results for increasing soybean oil content in systems containing 10 %w/w Brij 96	109
3.8: PCS results for increasing soybean oil content in systems containing 14 %w/w Brij 96	110
3.9: PCS results for increasing soybean oil content in systems containing 18 %w/w Brij 96	111
3.10: PCS results for increasing soybean oil content in systems containing	

22 %w/w Brij 96	112
3.11: PCS results for increasing soybean oil content in systems containing 26 %w/w Brij 96	113
3.12: PCS results for Brij 96 surfactant solutions	115
3.13: PCS results for increasing Brij 96 content in systems containing 2 %w/w soybean oil	117
3.14: PCS results for increasing Brij 96 content in systems containing 4 %w/w soybean oil	118
3.15: PCS results for increasing Brij 96 content in systems containing 6 %w/w soybean oil	119
3.16: PCS results for microemulsions with fixed ratios of Brij 96:soybean oil	122
3.17: Z mean diameter and polydispersity vs weight fraction for microemulsions with fixed Brij 96:oil ratio	123
3.18: TILS results for Brij 96 surfactant solutions	125
3.19: TILS results for microemulsion systems	130
3.20: Calculated radii with increasing soybean oil and Brij 96 from TILS data	135
3.21: Comparison of radii obtained by PCS and TILS	137
3.22: Apparent Z mean diameter vs time for microemulsions subjected to temperature cycling	140
4.1: Variation in CP for different batches or brands of C ₁₈₋₁ E ₁₀	145
4.2: Partial phase diagram for systems with soybean oil and C ₁₂ E ₁₀	149
4.3: Partial phase diagrams for alkane hydrocarbons with C ₁₈₋₁ E ₁₀	155
4.4: Partial phase diagrams for 1-alkene hydrocarbons with C ₁₈₋₁ E ₁₀	156
4.5: Partial phase diagram for IPM/C ₁₈₋₁ E ₁₀ /water	158
4.6: Partial phase diagram for Miglyol 812/C ₁₈₋₁ E ₁₀ /water	161
4.7: Partial phase diagrams for alkane hydrocarbons with C ₁₂ E ₁₀	166
4.8: Partial phase diagrams for IPM and 1-alkene hydrocarbons with C ₁₂ E ₁₀	167
4.9: Partial phase diagrams for heptane and 1-heptene with C ₁₈ E ₂₀	169
4.10: Partial phase diagrams for heptane, 1-heptene and IPM with C ₁₈₋₁ E ₂₀	170
5.1: Change in the phase diagram with the addition of methanol	175
5.2: Phase diagrams for methanol systems with 2 and 5% soybean oil	176

5.3: Change in the phase diagram with the addition of butanol	179
5.4: Phase diagrams for butanol systems with 2, 5 & 10% soybean oil	180
5.5: Change in the phase diagram with the addition of pentanol	182
5.6: Phase diagrams for pentanol systems with 2, 5, & 10% soybean oil	183
5.7: Change in the phase diagram of methanol or butanol-containing systems with increasing temperature	185
5.8: Conductivity and dilution of butanol systems (a)	187
5.9: Conductivity and dilution of butanol systems (b)	188
5.10: Conductivity and dilution of butanol systems (c)	189
5.11: Phase diagrams for butanol/Brij 76 systems with 2 and 5% soybean oil	194
5.12: Change in the phase diagram with the addition of glycerol	196
5.13: Phase diagrams glycerol systems with 2 and 5% soybean oil	197
5.14: Change in the phase diagram with the addition of xylitol	199
5.15: Phase diagrams for xylitol systems with 2 and 5% soybean oil	200
5.16: Change in the phase diagram with the addition of sorbitol	201
5.17: Phase diagrams for sorbitol systems with 2 and 5% soybean oil	202
5.18: PIT vs %w/w Brij 96 for 2% soybean oil microemulsions containing glycerol, xylitol or sorbitol	205
5.19: PIT vs Brij 96 concentration for 2% soybean oil using a combined surfactant of Brij 96(2):glycol(3)	208
6.1: Log diazepam incorporation vs %w/w DMTG	214
6.2: Phase diagrams for microemulsions containing testosterone, testosterone propionate or testosterone enanthate	216
6.3: Log drug incorporation vs %w/w DMTG for testosterone, testosterone propionate and testosterone enanthate	221
6.4: PCS results for microemulsions with added testosterone enanthate	228
6.5: TILS results for microemulsions with added testosterone enanthate	231
6.6: TILS radii for 2 %w/w soybean oil microemulsions with and without 1% testosterone enanthate	235
6.7: TILS radii for microemulsions with increasing concentration of testosterone enanthate	238
6.8: Log drug incorporation vs %w/w DMTG for progesterone and medroxyprogesterone acetate	245

List of tables

	Page
2.1: Composition of polyoxyethylene surfactants used	69
2.2: Drugs used in the study	71
3.1: PIT for Brij 96 systems containing 0, 2 & 5 %w/w soybean oil	102
3.2: Apparent Z mean diameter and polydispersity for repeated microemulsion samples	106
3.3: Calculated dimensions of Brij 96 micelles with an aggregation number of 112	127
3.4: TILS radii for microemulsions with increasing soybean oil content determined for four values of a_o	132
3.5: TILS radii for microemulsions with constant soybean oil content determined for four values of a_o	133
3.6: Z mean diameters of samples before and after stability testing	141
4.1: Mean ethylene oxide units found by NMR for surfactants used	145
4.2: CPP and HLB values of the surfactants used	147
4.3: PIT of microemulsions with 2% of various oil phases	153
4.4: Apparent Z mean diameter for C₁₈₋₁E₁₀ o/w microemulsions with various oils	163
4.4: Ability of surfactants and oils to form o/w microemulsions at room temperature	172
5.1: Interfacial tension between soybean oil and 20% Brij 96 with the addition of butanol or pentanol	192
5.2: Interfacial tension between soybean oil and 20% Brij 96 with the addition of glycerol	204
6.1: Incorporation of diazepam into Brij 96 micelles and 2% soybean oil microemulsions	211
6.2: Solubilities of diazepam at 25°C	213
6.3: Incorporation of testosterone drugs into Brij 96 micelles and 2% soybean oil microemulsions	218
6.4: Solubilities of testosterone drugs at 25°C	220

6.5: Solubilities of testosterone propionate in various oil phases at 25⁰C	224
6.6: Incorporation of testosterone propionate into microemulsions of different oil phases	225
6.7: TILS radii for microemulsions containing 1 %w/w testosterone enanthate	234
6.8: TILS radii for microemulsions with increasing testosterone enanthate concentration	237
6.9: Apparent Z mean diameters of microemulsions with testosterone enanthate before and after stability testing	240
6.10: Solubilities of progesterone and medroxyprogesterone acetate at 25⁰C	242
6.11: Incorporation of progesterone and medroxyprogesterone acetate into Brij 96 micelles and 2% soybean oil microemulsions	243

Abbreviations and symbols

a	molecular length
a_c	long axis of prolate ellipsoid
a_o	area occupied by surfactant polar headgroup at the interface
A	temperature-dependent constant used in TILS
b_c	short axis of prolate ellipsoid
AOT	aerosol-OT = sodium bis(2-ethylhexyl)sulphosuccinate
c	concentration
C	curvature of microemulsion droplet (R^{-1})
C_1	one of two principle curvatures of the surfactant film
C_2	one of two principle curvatures of the surfactant film
C_mE_n	polyoxyethylene glycol ether surfactant, with m C atoms in the hydrocarbon chain and n ethylene oxide units in the hydrophile
CMC	critical micellar concentration
C_o	spontaneous curvature of the interface
CP	cloud point
CPP	critical packing parameter = $v/a_o l_c$
CRC	critical random cell
C_s	number of surfactant molecules per unit volume
d	diameter
D	diffusion coefficient determined by PCS
DDAB	didodecyldimethyl ammonium bromide
DMTG	dimethoxytetraethylene glycol
DOC	disordered random connected
DSS	dioctyl sodium sulphosuccinate
e	constant for Kruss spinning drop tensiometer (3.427×10^{-7})
f	molar ratio of oil to surfactant in a microemulsion droplet
f_d	molar ratio of drug to surfactant in a microemulsion droplet
F	bending energy
g	fraction of drug within r_1 a microemulsion droplet
$g(r_s)$	particle pair radial distribution function
$G(p)$	shape factor used to fit PCS data to ellipsoidal micelles
$G(t)$	correlation function used in PCS
H/L	hydrophile/lipophile ratio
HLB	hydrophile lipophile balance

HLK	hydrophile lipophile index
IPM	isopropyl myristate
k	Boltzmann constant ($1.380662 \times 10^{-23} \text{ JK}^{-1}$)
K	elastic modulus (or rigidity)
\bar{K}	saddle splay (or gaussian) elastic modulus
K_1	optical constant used for analysis of TILS data of micelles
K_2	derived optical constant used for analysis of TILS data from microemulsions
K_o	optical constant used for analysis of TILS data from microemulsions
K_s	light scattering vector in PCS
l_c	critical alkyl chain length
l_{\max}	fully extended alkyl chain length
L	dispersion size ($2R$ for microemulsion droplets, E_k for bicontinuous microemulsions)
m	number of carbon atoms in the hydrophobe of a C_mE_n surfactant
M	molecular mass of scattering unit in TILS
M_r	molecular weight
n	number of ethylene oxide units in a C_mE_n surfactant
n_c	value close to, but smaller than the number of carbon atoms per alkyl chain
n_{cis}	number of cis double bonds in the surfactant hydrophobe
n_d	number of drug molecules in a microemulsion droplet
n_o	number of oil molecules in a microemulsion droplet
n_r	revolutions per minute (rpm) used in spinning drop tensiometer
n_s	number of surfactant molecules in a microemulsion droplet
n_w	number of water molecules surrounding a microemulsion droplet
N	density of spherical centres in space used in DOC model
N'	average intensity (photons / unit time) in PCS
N_A	Avogadro number ($6.022045 \times 10^{23} \text{ mol}^{-1}$)
N_s	number of scattering units per cm^3 in TILS
NMR	nuclear magnetic resonance
p	axial ratio of an ellipsoid ($= b/a$)
o/w	oil-in-water
P(Q)	TILS particle scattering form factor at scattering vector Q
P(90)	TILS form factor at 90°
PCS	photon correlation spectroscopy
PIT	phase inversion temperature

Q	scattering vector used in TILS
QELS	quasielastic light scattering
QLS	quasielastic light scattering
r	cylinder radius in DOC model
r₁	radius of inner sphere of an o/w microemulsion droplet containing oil and the hydrophobic portion of the surfactant
r_{1d}	radius of inner sphere of o/w microemulsion drop containing drug
r₂	radius of o/w microemulsion droplet including oil and all of the surfactant molecule
r_{2d}	outer radius of o/w microemulsion droplet containing drug
r_c	cylinder radius of droplet in spinning drop tensiometer
r_s	distance between centres of scattering particles in TILS
R	radius of microemulsion droplet
R₁	radius corresponding to the principle curvature, C ₁
R₂	radius corresponding to the principle curvature, C ₂
R₉₀	Rayleigh ratio of sample relative to a standard at 90°
R_θ	Rayleigh ratio of sample relative to a standard measured at angle θ
RGD	Rayleigh-Gans-Debye
R_{HS}	hard sphere radius used in TILS
RI	refractive index of sample
RI_{benzene}	refractive index of benzene
RI_o	refractive index of solvent
RI_s	refractive index of scattering unit in TILS
R_o	radius of droplet corresponding to the spontaneous curvature
R_{max}	maximum radius which can be achieved due to swelling of microemulsion droplets
S(Q)	TILS structure factor at scattering vector Q
S(90)	TILS structure factor at measurement angle 90°
S₉₀	ratio of scatter relative to standard at 90°, corrected for scatter by solvent
SANS	small angle neutron scattering
SAXS	small angle x-ray scattering
SDS	sodium dodecyl sulphate
t	delay time in PCS
t₁	difference between r ₂ , or r _{2d} , and R _{HS} in TILS hard sphere model
t_c	characteristic decay time in PCS
T	absolute temperature (Kelvin)
TEM	transmission electron microscopy

TILS	total intensity light scattering
TOW	transparent oil-water (gels)
v	volume of the surfactant alkyl chain
v_d	volume of drug molecule
v_h	volume of surfactant hydrophile
v_o	volume of oil molecule
V	magnification factor used in spinning drop tensiometer
V_c	volume of micellar hydrocarbon core
V_H	volume of the interfacial hydrophilic layer
V_H^O	volume of the surfactant headgroup
V_L	volume of the interfacial hydrophobic layer
V_L^O	volume of the surfactant hydrocarbon chains
V_O^L	volume of oil dissolved in surfactant chains
V_W^H	volume of water dissolved in surfactant headgroups
V_{r2}	volume of microemulsion droplet of radius r_2
V_w	volume of water associated with each microemulsion droplet
V_x	volume of surfactant head group shell in o/w microemulsion droplet
w/o	water-in-oil
$Y(t)$	log of correlation function in PCS
z	average coordination number in DOC model
γ	interfacial tension
γ_d	tension at the droplet surface
ΔG_f	free energy of formation
Δn	change in interfacial area
ΔS_{disp}	entropy change due to dispersion
$\Delta \rho$	density difference
η	viscosity of external medium
λ	wavelength of light
λ_o	wavelength of light <i>in vacuo</i>
ξ	characteristic length of cells in CRC models
ξ_k	persistence length of surfactant layer
ξ_o	maximum of E_k before emulsion failure occurs
ρ_s	density of scattering units in TILS
θ	scattering angle of observed light
Σ	total surfactant interfacial area
Φ_d	dispersed phase volume fraction
Φ_{HS}	hard sphere volume fraction in TILS

Φ_o	oil phase volume fraction
Φ_p	critical volume fraction of the dispersed phase
Φ_{r2}	volume fraction of microemulsion droplets of radius r_2
Φ_w	water phase volume fraction
ω	angular velocity of spinning drop tensiometer

CHAPTER ONE: Introduction

1.1 Definition of a microemulsion

The term *microemulsion* was first introduced by Schulman and coworkers in 1959 [1] to describe clear systems brought about spontaneously by adding a short chain alcohol to a coarse macroemulsion of benzene, hexanol and potassium oleate, which had been prepared originally in 1943 [2]. Since then there has been much debate on the definition that best encompasses these isotropic, optically clear, macroscopically homogeneous systems containing two immiscible phases stabilised by the presence of one, or more, amphiphiles [3, 4, 5].

One of the difficulties which appears to prevent the acceptance of a universal definition for microemulsion systems is the argument of whether or not microemulsions are separate entities to swollen micellar systems. Some workers believe that the name *microemulsion* should be reserved for systems that contain more than a few percent of the dispersed phase [6] and that there is a distinction between swollen micelles (which have no strictly hydrophobic core) and microemulsions, which exhibit the properties of nonassociating hard spheres [7]. Other workers believe there is no difference in nature between a micelle with an added solute (a swollen micelle) and a microemulsion [8].

The surfactants used to produce a microemulsion may be ionic (cationic or anionic) or nonionic. With a few notable exceptions, such as the double chained ionic surfactants sodium di-2-ethyl-hexyl sulphosuccinate (AOT) and didodecyldimethylammonium bromide (DDAB), ionic surfactants will not

form microemulsions without the presence of a cosurfactant. The cosurfactants used are usually medium to long chained alcohols, although other compounds such as amines have also been successfully employed [9]. On the other hand, a number of nonionic surfactants, can produce microemulsions without the presence of a cosurfactant [10].

1.2 Microemulsion properties.

Microemulsions can be water-continuous, oil-continuous or bicontinuous, low viscosity fluids (see section 1.3). The droplet size in the water or oil continuous microemulsions is generally less than 100nm. As a result of their very small size (less than the wavelength of light) microemulsion systems appear optically transparent. They are also isotropic and non-birefringent when viewed through crossed polaroids. Unlike macroemulsions, microemulsions form spontaneously, without the requirement of high shear conditions. Although energy barriers may need to be overcome to obtain spontaneous clearing [11], once formed the microemulsions are thermodynamically stable as their properties do not change with time.

When microemulsions were first studied by Schulman and coworkers an ultralow, or even negative, interfacial tension was presented as an explanation of the spontaneous formation of these systems. Although this is now considered to be an oversimplification, an extreme lowering of interfacial tension is a key factor in the formation and stability of microemulsion systems [6]. The interfacial tension between the oil and aqueous phases must be small enough to compensate for the increase in entropy resulting from the dispersion of one phase in another. This relationship is described mathematically by [12];

$$\Delta G_f = \gamma_d \Delta n - T \Delta S_{disp} \quad \text{eqn.1}$$

where;

ΔG_f = the free energy of formation

γ_d = tension at the droplet surface

Δn = change in interfacial area

T = temperature

ΔS_{disp} = entropy change due to the dispersion of droplets in the external phase.

For a spontaneous process to occur ΔG_f must be negative. In order to achieve a negative value of ΔG_f , γ_d should usually be less than 10^{-2}mNm^{-1} [13]. Usually the addition of cosurfactant is required to achieve such low interfacial tensions, although some nonionic surfactants and double hydrocarbon chained ionic surfactants alone can lead to values of $<10^{-2} \text{mNm}^{-1}$. This balance of entropy, interfacial tension and interfacial area has been included in most thermodynamic models of microemulsion formation, such as those of Ruckenstein and coworkers [13, 14, 15] and Overbeek and coworkers [16, 17].

From a standpoint of entropy a large number of small droplets are favoured over a small number of large ones. However, the surfactant layers surrounding the droplets have a certain rigidity and resistance so that the actual size of the droplets is a compromise [12]. Miller & Neogi [18] were the first to present a theory (for dilute microemulsions) which included both the entropy of dispersion of the droplets and the energy effects associated with the bending of the surfactant film at the drop interface (see section 1.4.1.3).

Microemulsions tend to form when a high concentration of surfactant is present (typically about 20%). When lower surfactant concentrations are used, multiphase systems can be obtained in which a microemulsion phase exists in equilibrium with excess oil and/or excess water. Such equilibrated systems were first described, and categorized into four types by Winsor [19]. In Winsor Type I systems, two phases exist in which the lower microemulsion phase is in equilibrium with excess oil. In Type II systems an upper microemulsion phase is in equilibrium with excess aqueous phase, and in Type III there are three phases; a middle microemulsion phase in equilibrium with both excess oil and water. A Winsor Type IV system is one in which the surfactant concentration is sufficiently high to result in only one clear microemulsion phase. A systematic shift between lower, middle and upper phase microemulsions ($\text{I} \rightleftharpoons \text{III} \rightleftharpoons \text{II}$) is thought to reflect changes in temperature, salinity, oil composition and the hydrophilic vs lipophilic (HLB) character of the surfactant [20] as illustrated in figure 1.1.

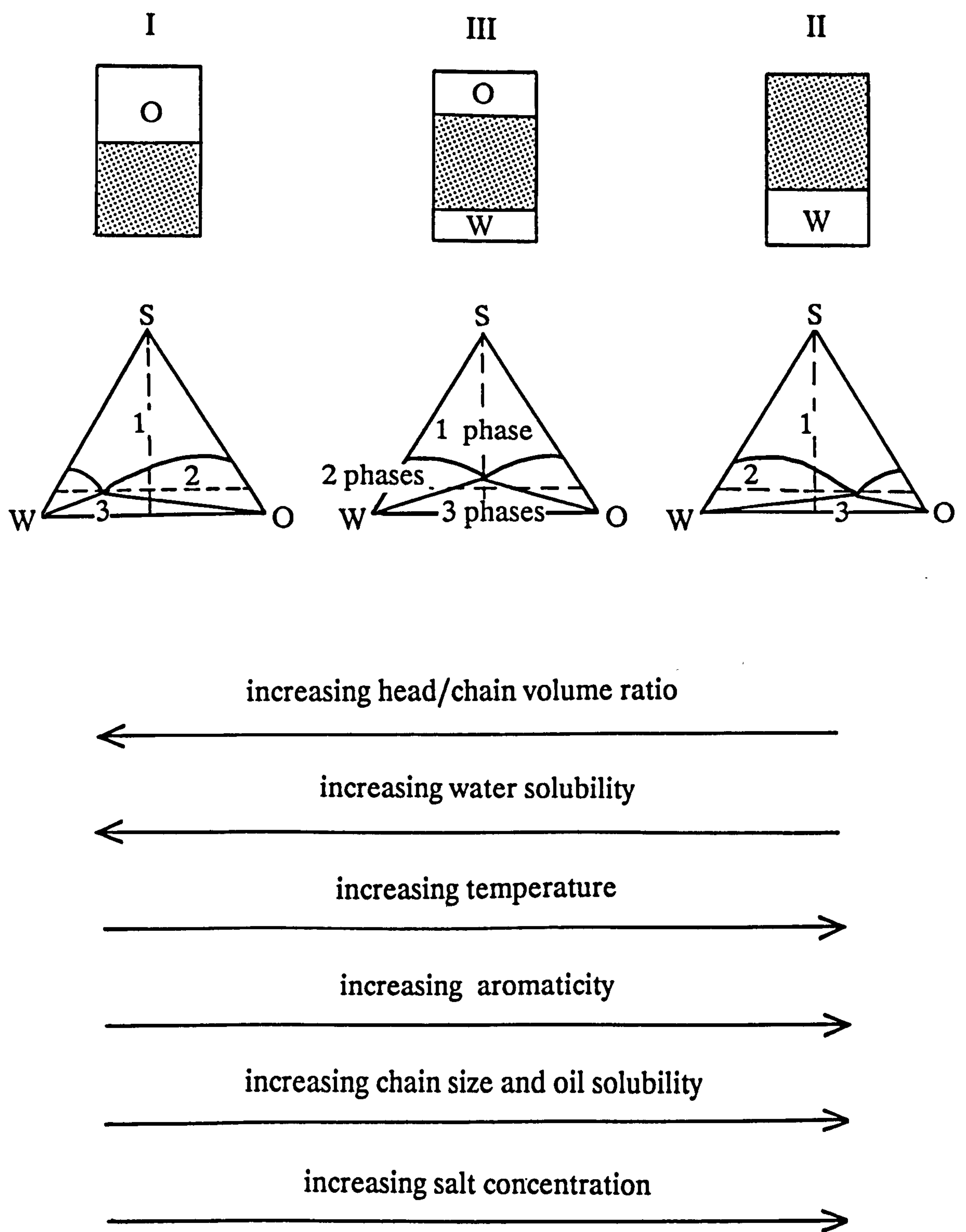


Figure 1.1: Phase behaviour in microemulsions. The transition between Winsor's $I \rightleftharpoons II \rightleftharpoons III$ microemulsions systems; appearance of the equilibrated systems (top), representation of phase phase boundaries on the idealised ternary diagram (centre) and factors effecting a shift in behaviour (bottom). Copied from reference 20.

1.3 The structure of microemulsion systems

Ternary oil, surfactant and water systems can show very complex phase equilibria, and it is not always easy to distinguish microemulsions from liquid crystalline phases, or from molecular mixtures of oil, surfactant and water [21]. There has been much experimental and theoretical work carried out in order to determine the structure(s) of systems found within the area of existence of a clear microemulsion region. Much of this work is included in a review of the structure of microemulsions (and micelles) written by Chevalier and Zemb [8].

Traditionally microemulsions are described in similar terms to those of macroemulsions, hence their classification into either oil-in-water (o/w), or water-in-oil (w/o) microemulsions. O/w systems consist of an oil droplet, stabilised by an interfacial layer of surfactant (or surfactants) surrounded by an external aqueous media. W/o microemulsions have a water core and an external oil phase (Fig.1.2a and 1.2b). Often o/w and w/o microemulsions have been found to invert from one to another by altering the composition or by external influences, such as changing the temperature. This inversion may occur via a separate viscoelastic or lamellar phase [22] or the w/o and o/w regions may appear to merge into one single phase [23]. It is unlikely that a fixed microstructure will exist throughout such extended areas of existence, especially for single phase systems which encompass a large range of composition [24]. For example, Rushforth *et al* [25] have distinguished five regions within one clear isotropic area in microemulsion systems containing sodium dodecyl sulphate, 1-butanol, toluene and brine solution. The microstructure is not however frozen as microemulsions are dynamic systems in which the interface is continuously and spontaneously fluctuating [26].

The structure of clear, stable non-birefringent microemulsion systems occurring at very high surfactant concentrations, or at comparable volumes of oil and water, is unlikely to consist of spherical droplets. There has been considerable work undertaken to try to identify the structure of microemulsion systems within these regions. In 1976 Scriven [27] introduced the concept of a bicontinuous structure for some microemulsion domains, in particular those with comparable volumes of oil and water. In a bicontinuous structure both the water and oil domains, which are separated by a connected

amphiphile-rich interfacial layer, can be joined continuously from one side of a specimen to the opposite side. A bicontinuous structure may be regular (as in figure 1.2ci), or can be topologically chaotic (fig.1.2cii) [28].

Evidence appears to suggest that when a small amount of oil is present, o/w microemulsion droplets are likely, and when only a small amount of water is present, w/o droplets occur. If however there are comparable amounts of both oil and water, bicontinuous systems are most probable [29]. The amount of the internal phase that can be considered *small* will depend on the composition and chemical structure of the components of the microemulsions.

1.3.1 Experimental methods for determining microemulsion structure.

The determination of microemulsion structure is difficult. Any single technique can only provide a limited amount of information, and hence it is usually necessary to consider results obtained for the same microemulsion system by different techniques [24].

Direct visual evidence is elusive because of the very small sizes involved. Transmission electron microscopy (TEM) can in principle go to the required resolution of size and some success has been achieved using freeze fracture TEM [30, 31, 32, 33]. The freeze fracture technique is not however without experimental difficulties. It involves freezing, fracturing and replication procedures before a carbon replica (rather than the sample itself) can be investigated, and in particular the rate of cooling must be fast enough to avoid any phase changes and prevent the introduction of artifacts [30, 34 & 35].

Macroscopic methods of studying microemulsions are useful for the observation of transitions, as an abrupt variation in macroscopic properties will be indicative of a change in microscopic structure [8]. Such techniques include the measurement of electrical conductivity in both ionic surfactant microemulsion systems [36, 37, 38], and in microemulsions produced with nonionic surfactants and containing added electrolyte [39]. The measurement of viscosity has been used to investigate the hydration and interaction of microemulsion droplets [7, 40] and changes in the rheological behaviour across a region of microemulsion existence is thought to be indicative of a change in microstructure [41].

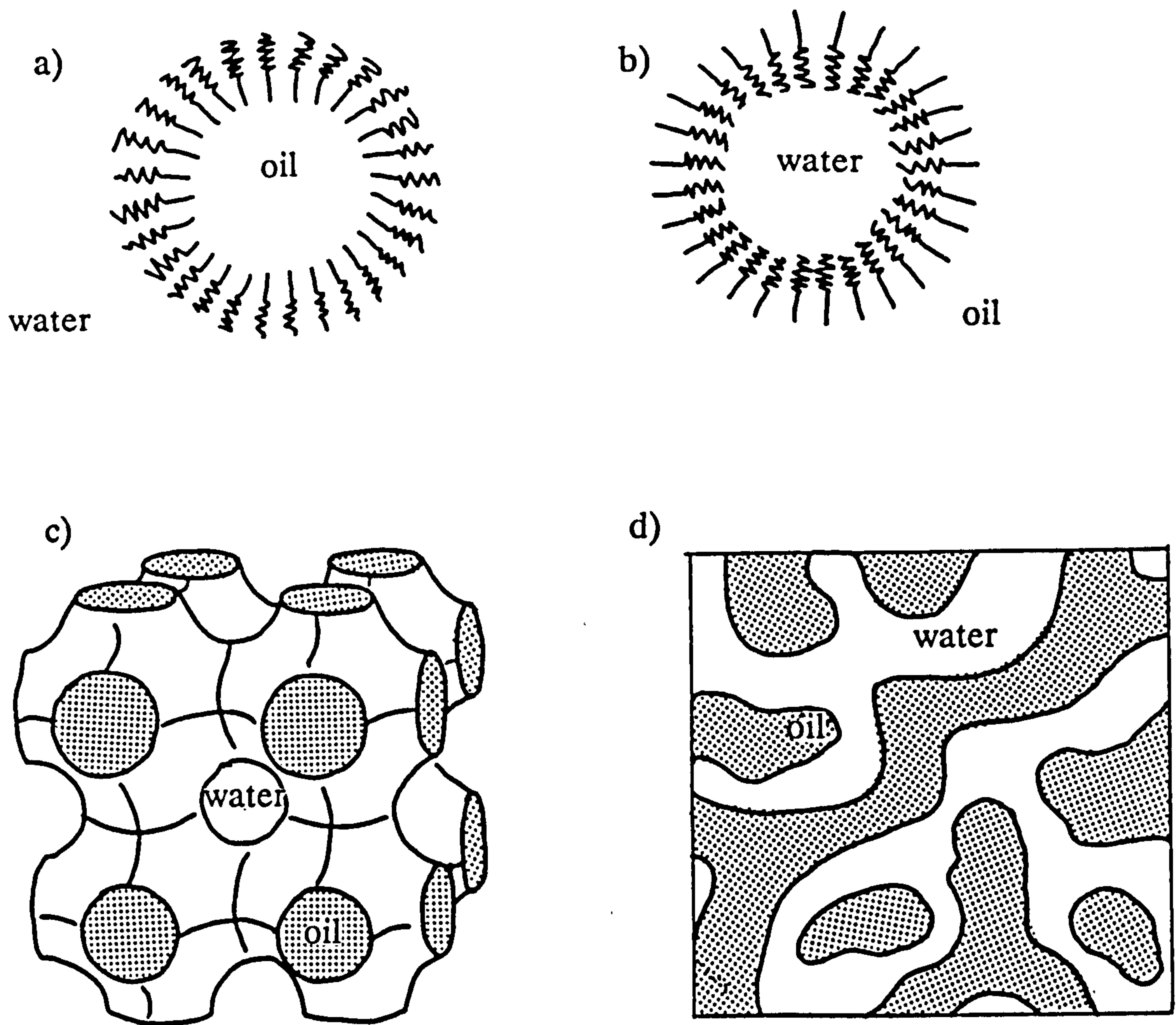


Figure 1.2: Possible structures in microemulsion systems. Droplet microemulsion structures; a) oil-in-water and b) water-in-oil. Two extremes of bicontinuous structures; c) cubically symmetrical and d) completely random. Copied from reference 21.

Methods involving the introduction of various probes are also employed to study microemulsion structure. The addition of the foreign molecule is assumed not to perturb the system, which may or may not be the case. Hence these methods are best employed to confirm conclusions reached by more reliable methods [8]. Probes reside in different regions of the microemulsion depending on their hydrophobicity, and are presumed to give information about the environment in which they are situated. Probe studies in microemulsions have included the use of fluorescent molecules such as oil-soluble pyrene [42, 43] and ferrocene derivatives as electroactive probes [44].

Nuclear magnetic resonance (NMR) is a basic tool for investigating geometric and dynamic properties at a molecular level. This method has the highest resolution of all methods and is best employed for microemulsion structure refinement once some lower resolution data is already known [8]. There have been many studies on microemulsion systems employing NMR techniques. In particular NMR self-diffusion studies have been used to test the suggested structural models of a microemulsion phase by comparing the rate of diffusion of molecules present in the microemulsion system to the rate found for a pure sample of the component [45].

Scattering measurements employed to study microemulsions include small angle neutron scattering (SANS), small angle x-ray scattering (SAXS) and light scattering. Any scattering technique measures the intensity of radiation (of wavelength λ) scattered at an angle of 2θ from an applied beam. The lower experimental limit is usually about 2nm and the largest distance measured is about 100nm for SANS or SAXS, and a few μm for light scattering [8]. Hence the application of such techniques in the study of microemulsions is promising. In cases of monodisperse spheres, fitting procedures can be used to estimate microemulsion droplet size, aggregation number and hydration. Polydisperse systems are however more difficult to investigate, and although scattering studies are very powerful techniques to eliminate some structural models, scattering experiments alone cannot be taken as proof of microstructure [8]. A major difficulty in scattering studies of microemulsions is that in many cases the systems need to be diluted before testing which is likely to modify the structure and composition of the different domains [24], and possibly result in the disappearance of microemulsion droplets [46]. Good reviews on the application and interpretation of SANS data in relation to microemulsion systems have been written by Chen [47] and

Magid [48]. Light scattering techniques will be further discussed in section 2.2.10.

1.3.2 Structure of ionic microemulsions.

The structure of ionic microemulsions will change with the quantity and quality of the components present. Some of the most well characterised ionic microemulsion systems are those employing the double chained surfactant AOT, in combination with water and various oils [49, 50, 51, 52, 53, 54, 55, 56]. Oil-continuous ternary microemulsion systems, which are stable over a relatively wide range of concentration and temperature, can form with this surfactant without the addition of a cosurfactant. The dominating structure within the area of existence for these microemulsion systems appears to be that of closed, essentially spherical aggregates containing an aqueous core of water and counterions surrounded by an interface of surfactant molecules. Huang and Kotlarchyk [53] suggest that in these AOT three-component microemulsions which do not contain any alcohol, the molecular packing of the cone shaped surfactant molecules plays a dominant role and that due to this geometry, droplet structures may persist into regions containing equal volumes of oil and water.

Applying NMR spin relaxation data of AOT w/o microemulsions formed with isooctane however revealed substantial shape polydispersity [49]. These authors suggest that for any particular instant there is thought to be a large fraction of nonspherical droplets, although an equilibrium shape which is spherical is still possible. Using SANS techniques, Robinson *et al* [50] have also found an increased tendency of the SANS data for AOT microemulsions not to fit a model of monodisperse spheres as the alkane chain of the external phase was increased from n-heptane to n-dodecane. This effect was attributed to an increase in polydispersity of the w/o droplet size distributions found in the longer alkane systems. Light-scattering techniques have shown an increase in droplet size and interdroplet attractive interaction with both an increase in the ratio of water to AOT, or an increase in the chain length of the oil [56]. The addition of a water soluble polymer (polyethylene oxide) to AOT/water/heptane microemulsions was also found to induce droplet aggregation and increase the polydispersity [57].

Other ionic surfactants capable of forming three component oil- continuous microemulsions include DDAB. Spherical water droplets have been found in DDAB/water/oil systems with a weight ratio of water to surfactant of 0.95 and less than 5 %w/w DDAB [58]. The interaction between the spheres was found to be attractive, and it was proposed that the spheres might be connected for volume fractions of water greater than 5% [58]. The presence of a bicontinuous microstructure over at least some of the area of existence has been illustrated [59]. The structure of DDAB/water/oil microemulsions has been found to be significantly influenced by the oil phase used [60, 61] and by the introduction of electrolyte [62].

The addition of butanol to an AOT/water/hydrocarbon system has been shown to reduce the size of the w/o droplets (hence increasing the interfacial area) suggesting that butanol is present in the interface of these systems [63, 64]. In comparison to systems without cosurfactant, the polydispersity increases, there is a reduced rigidity of the interface [63, 64] and less molecular organisation throughout the system [55].

In addition, AOT surfactant systems can form o/w microemulsions when cosurfactants are added. Light scattering studies of o/w AOT/isopropyl myristate/water microemulsions with ten cosurfactants have revealed a maximum of diffusion coefficient (minimum of droplet size) in the plots of diffusion coefficient vs alcohol concentration for each of the cosurfactants. The concentration of alcohol required to give a maximum of diffusion coefficient was found to be proportional to the aqueous solubility of the alcohol, suggesting that saturation of the aqueous phase is important in order to achieve a maximum reduction in diameter [65].

The introduction of a straight chain alcohol to an ionic surfactant microemulsion system can greatly extend the region of existence found. In many cases investigations applying a variety of techniques confirm a transition in the microstructure within the area of existence from oil-continuous to water-continuous via a bicontinuous arrangement [42, 66, 67, 68, 69, 70]; although the possibility of more than three structural regions are also suggested [25, 71].

The structures found within the region of four-component ionic microemulsion systems are strongly influenced by the chain length of the

alcohol, and hence by the amount of disorder introduced into the interfacial film by the alcohol [72]. Studies using NMR self diffusion techniques have found that if a long chain alcohol is introduced the degree of structure remains quite high and microemulsion droplets are favoured. If however a shorter chained alcohol, such as butanol or pentanol, is added a much lower degree of organisation is detected and the interfacial film is found to be in a highly dynamic state [73, 74, 75, 76].

1.3.3 Structure of nonionic microemulsions.

Unlike most ionic surfactants, many nonionic surfactants can produce microemulsion systems without the addition of a cosurfactant. Three-component nonionic surfactant microemulsion systems appear to possess the same characteristic structural features as more complex microemulsions, including multicomponent systems containing ionic surfactant and cosurfactant [10, 77]; frequently exhibiting a composition-dependent gradual transition between droplet and bicontinuous structures [78].

Systems which have been widely studied are those produced from hydrocarbon, water and a nonionic surfactant of the polyoxyethylene glycol alkyl ether type; C_mE_n (where m is the chain length of the hydrocarbon, and n is the number of ethylene oxide units that make up the hydrophilic headgroup). Using $C_{12}E_5$ as surfactant, a number of techniques have indicated, over a broad range of composition, the presence of bicontinuous structures [30, 79] in which there may be considerable penetration of the water and alkane into the surfactant film [80]. However, evidence for o/w and w/o droplet structure has also been found [81].

In addition to the composition of a nonionic microemulsion system, the microstructure is also highly dependent on temperature [82, 83]. Each combination of nonionic surfactant, hydrocarbon and water is characterised by a narrow temperature range called the HLB temperature, or phase inversion temperature (PIT). At the HLB temperature the hydrophilic-lipophilic properties of the surfactant balance for a given hydrocarbon-water system [84]. Below the HLB temperature the surfactant is preferentially soluble in the water, and above the PIT the surfactant prefers to reside in the hydrocarbon [85]. Furthermore, for a specific oil there appears to be a linear

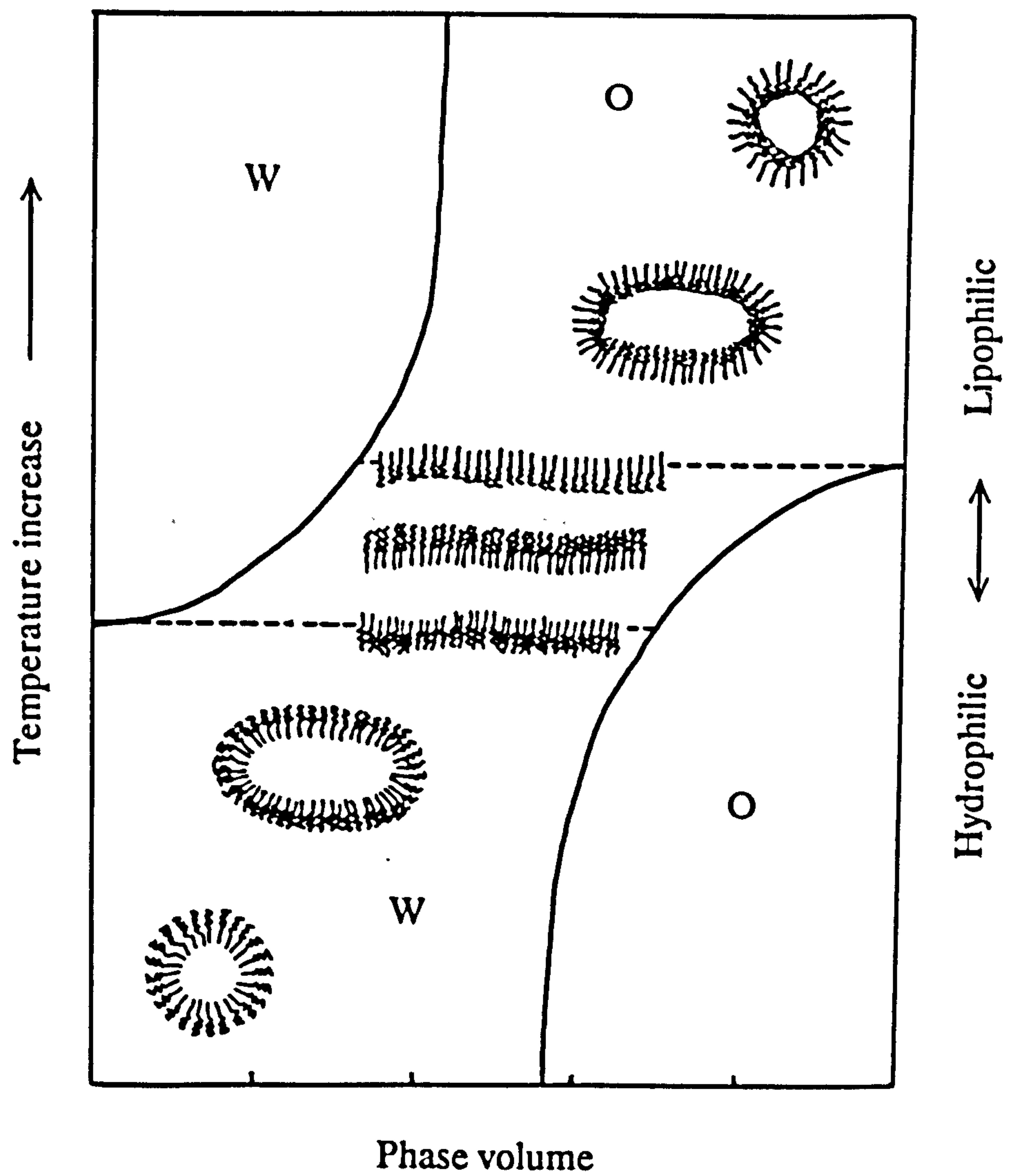


Figure 1.3: The change of microemulsion structure with temperature and surfactant HLB of a hydrocarbon/nonionic surfactant/water system. Copied from reference 83.

relationship between the HLB value and the HLB temperature for pure C_mE_n surfactants [86].

Isotropic, water-rich and hydrocarbon-rich phases may appear connected in a composition/temperature diagram via a bicontinuous phase (also referred to as the surfactant phase, S). Low temperatures and high water concentrations tend to favour distinct o/w droplets [87]. Increasing the temperature encourages more cylindrical o/w structures until at, or near, the HLB temperature, bicontinuous microemulsions are possible over a wide range of water to oil ratios [83]. Increasing the temperature beyond the PIT favours the formation of w/o droplets [88] which have been found, at constant water concentration, to decrease in size with increasing temperature [89]. This transition with temperature is illustrated diagrammatically in figure 1.3.

1.4 Models for microemulsion structure.

The definition of microemulsions as clear, stable, multicomponent liquids containing both oil and water encompasses a range of possible microemulsion structures. Any structural model needs to include the droplet structures proposed by Schulman, and the bicontinuous structures of Scriven, with (in some cases) a transition between the two which is macroscopically undetectable.

The structural models for microemulsion structure considered here are divided into four sections; the droplet, Talmon-Prager, cubic random cell (CRC) and disordered open connected (DOC) models. Before describing them however, the geometric considerations of the critical packing parameter (CPP), hydrophile-lipophile (H/L) ratio, and surfactant film curvature are discussed.

1.4.1 Geometric considerations.

1.4.1.1 The critical packing parameter.

Based on packing considerations of surfactants, a fundamental geometric quantity for structural descriptions has been proposed in the form of the critical packing parameter or CPP [90]. If v is the alkyl chain volume, a_0 the area occupied at the interface by the polar head group, and l_c the critical alkyl chain length, a value can be obtained for $v/a_0 l_c$, which can be used to indicate the preferred structure of the surfactant system (as illustrated in figure 1.4).

Values of v and l_c can be calculated from the equations of Tanford [92];

$$v = 27.4 + 26.9n_c (\text{\AA}^3) \quad \text{eqn.2}$$

$$l_{\max} = 1.5 + 1.265n_c (\text{\AA}) \quad \text{eqn.3}$$

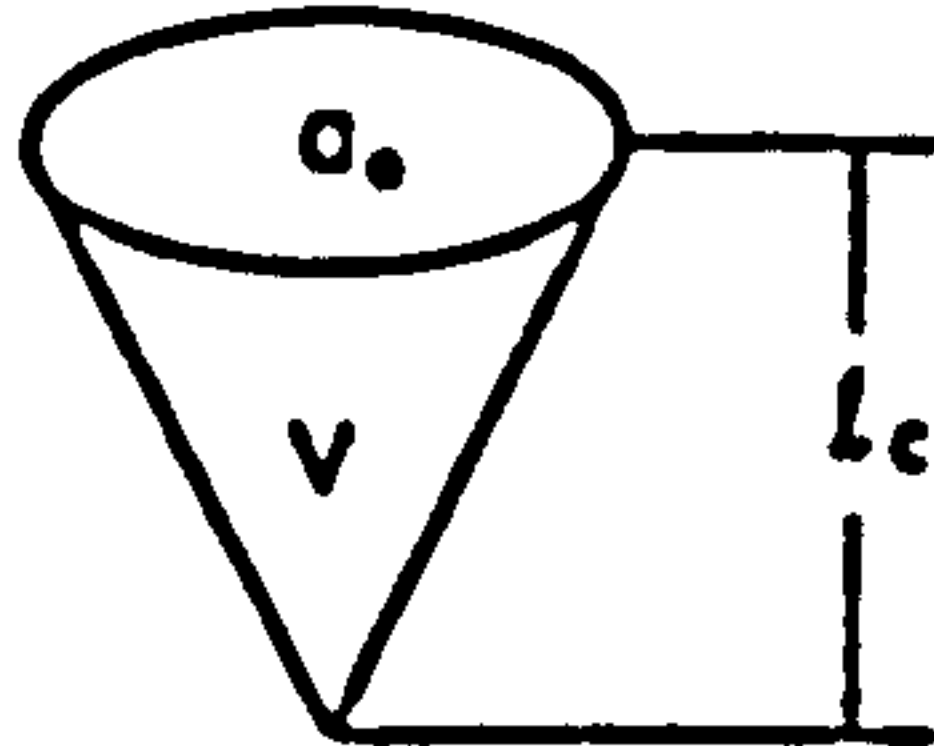
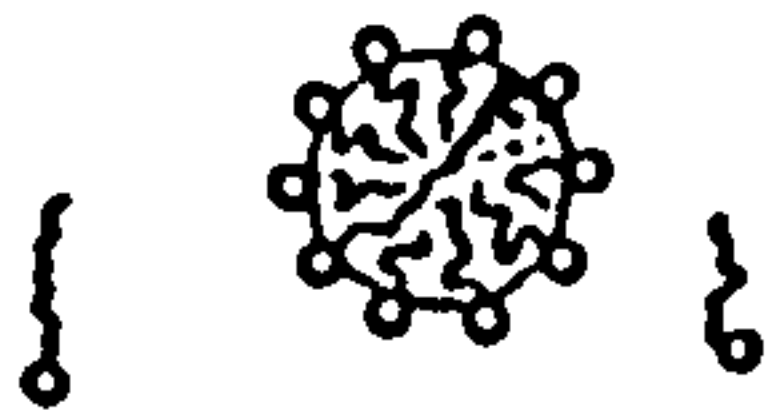
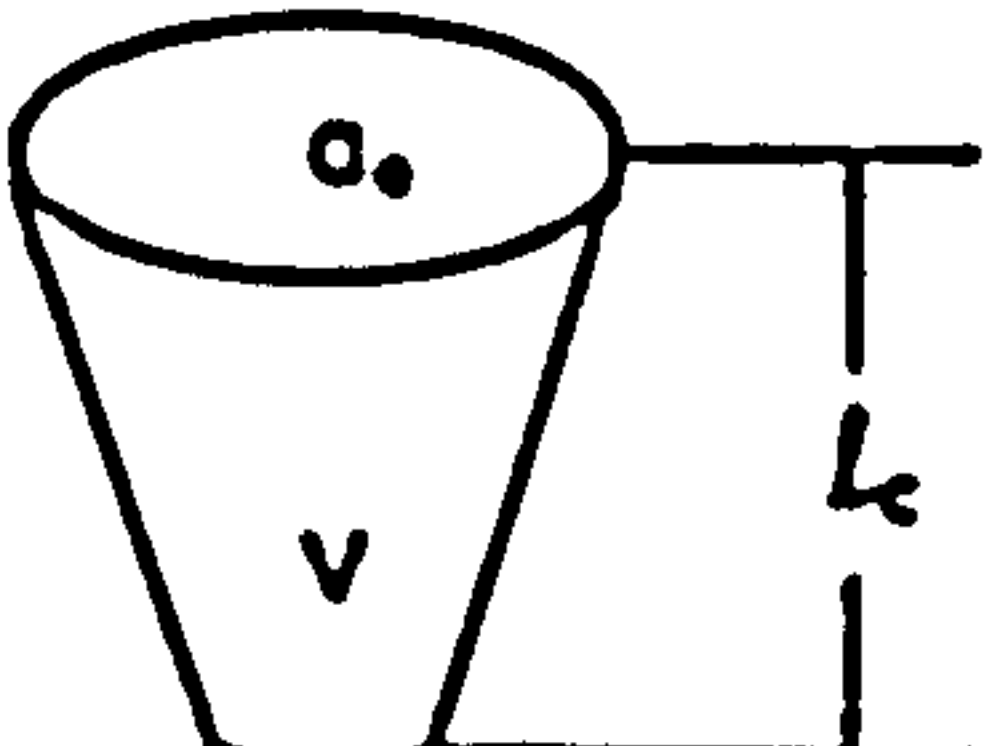

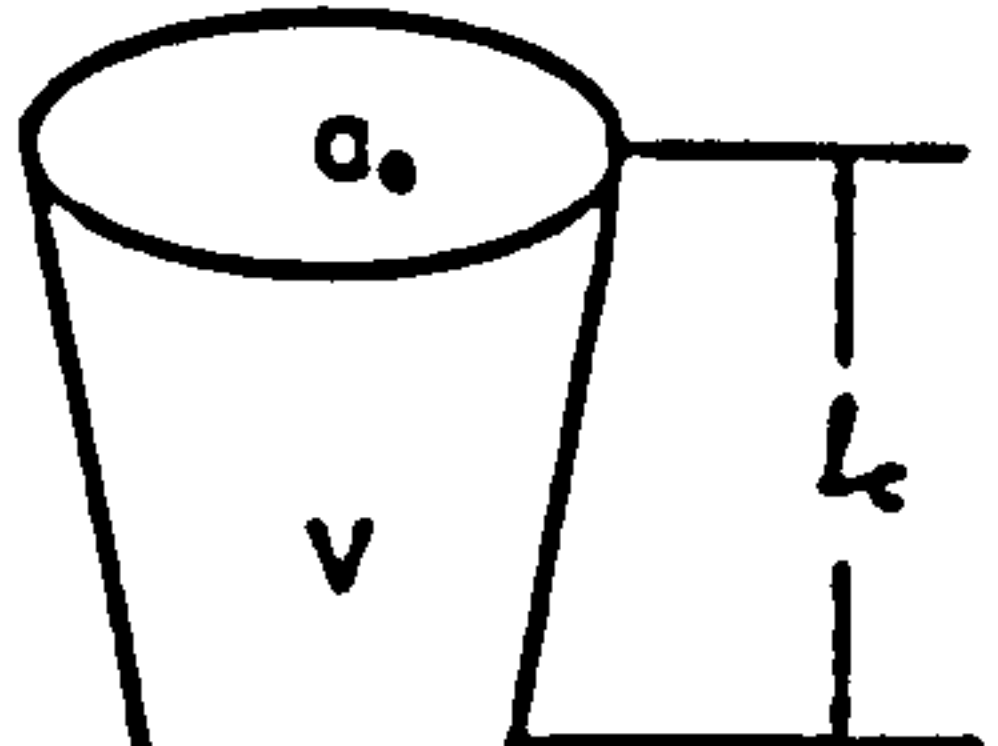
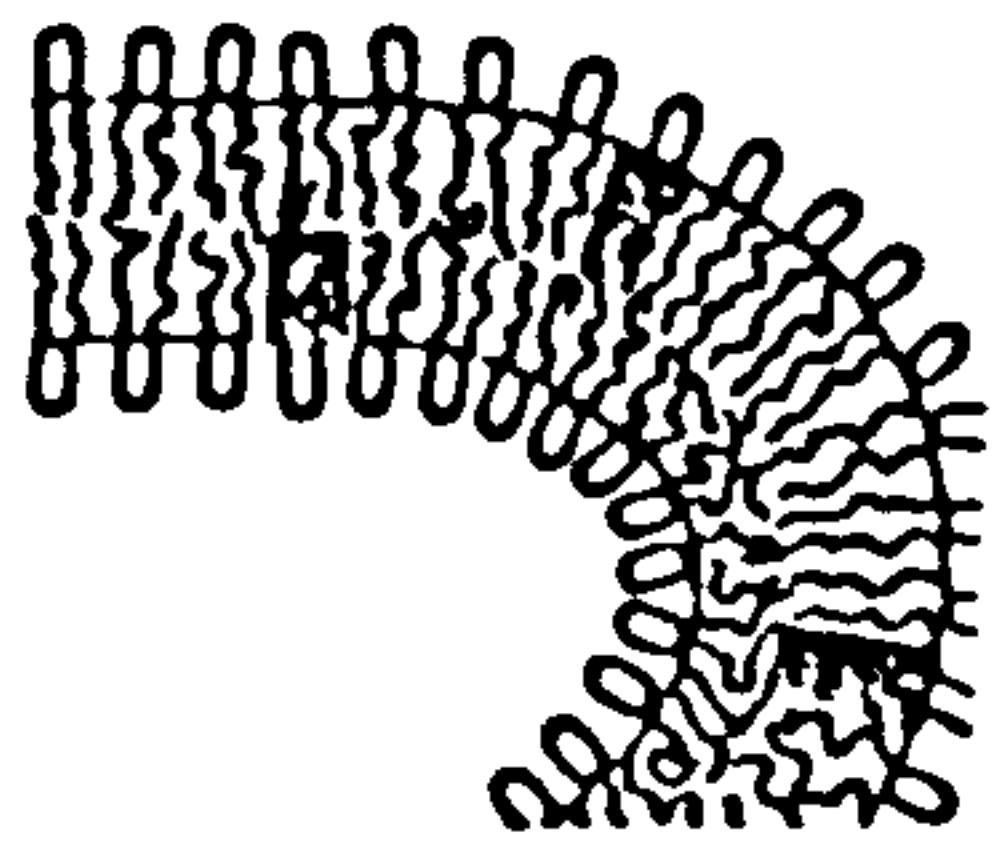
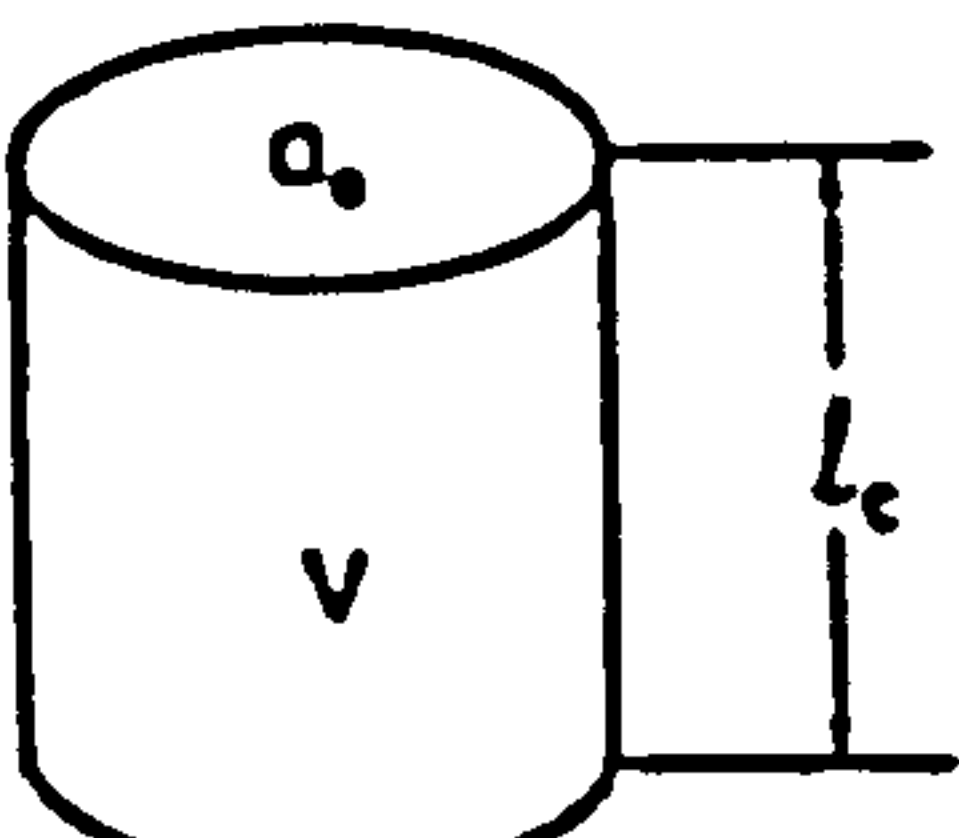
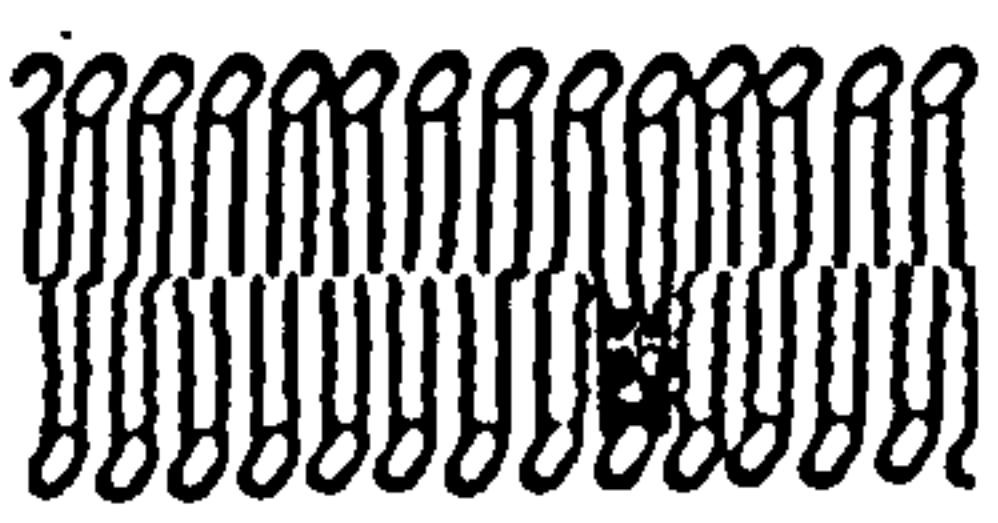
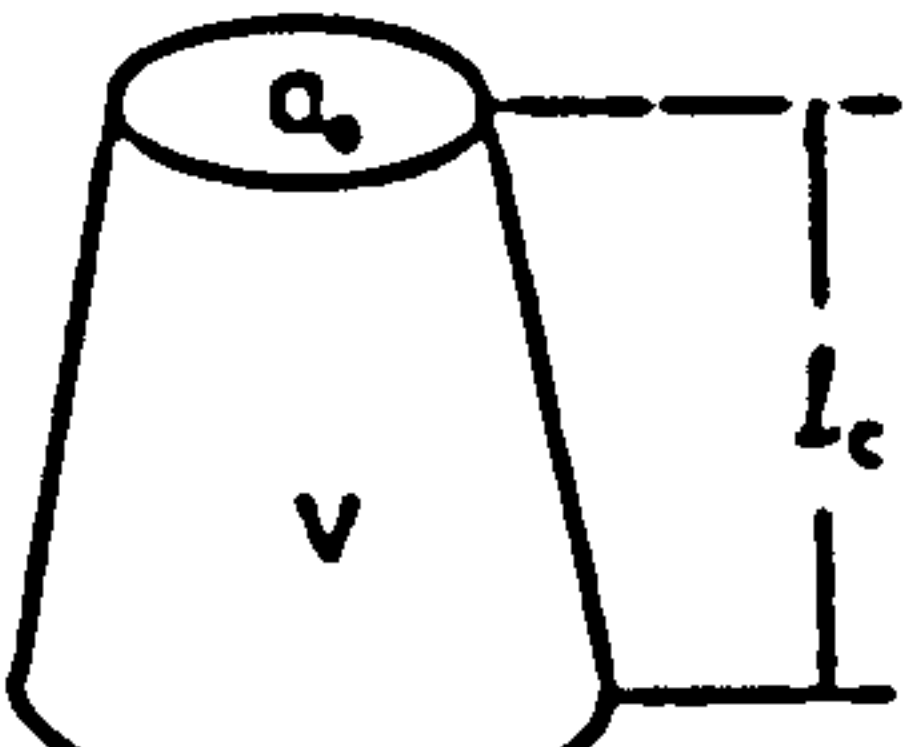
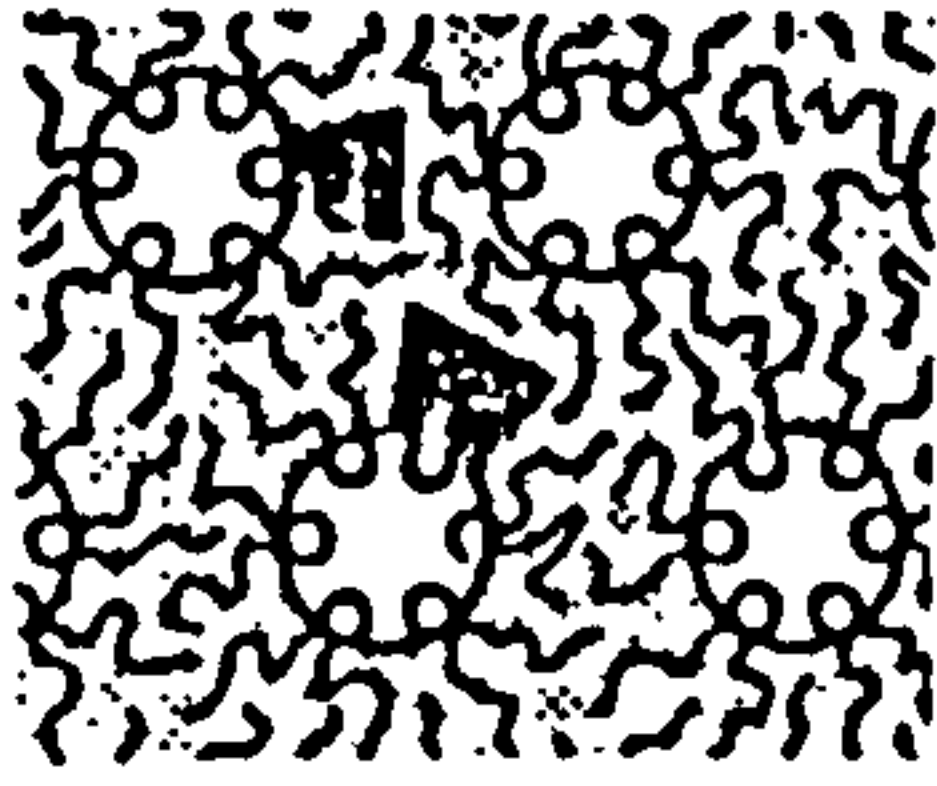
where n_c is some value close to, but smaller than the number of carbon atoms per alkyl chain. The surfactant hydrocarbon chain length (l_c) will be in a liquid state, rather than fully extended (l_{\max}). Therefore the value of l_c is expected to be somewhat less than l_{\max} . Values of l_c of 75-80% of the fully extended length of the alkyl chain have been proposed [93, 94].

Similarly, the choice of n_c can also be arbitrary to some degree. For example, it has been suggested that for the nonionic surfactant $C_{12}E_8$, the CH_2 group adjacent to the hydrophilic moiety would not enter the hydrophobic core, and in which case a value of n_c which is one less than the number of carbon atoms in the alkyl chain has been proposed [93].

If the CPP relationship is extended to microemulsions; a CPP less than one will encourage oil-swollen aggregates to form, and when greater than one reverse systems will occur. If the CPP is close to one the mean curvature is zero and bicontinuous microemulsions will be formed [21].

The application of the CPP to microemulsions cannot however be used without caution, as it only accounts for geometric considerations of the surfactant. The environment of the surfactant at the interface must also be considered, and the addition of cosurfactant and oil will alter the ratio.

Figure 1.4: Packing properties of surfactants, their CPP and the structures they form. Copied from reference 91.

Shape	CPP	Surfactant	Examples	Structures formed
cone 	$< 1/3$	single chain SAA with large headgroup areas	NaDS in low salt some lysophospholipids	spherical micelles 
truncated cone or wedge 	$1/3 - 1/2$	single chain SAA with very small headgroup areas	NaDS in high salt lysolecithin nonionic surfactants	globular or cylindrical micelles 
truncated cone 	$1/2 - 1$	double chain SAA with large headgroup areas	lecithin sphingomyelin DPPC, DPPS	vesicles flexible bilayers 
cylinder 	~ 1	double chain SAA with small headgroup areas	DPPE DPPS + Ca^{2+}	planar bilayers 
inverted truncated cone 	> 1	double chain SAA with small headgroup areas	monosugar-diglycerides unsaturated DPPE cholesterol	inverted micelles 

Alcohols which act as cosurfactants have an alkyl chain length shorter than that of the surfactant. With the same number of surfactant molecules, the area of the interface will increase by approximately 0.2nm^2 per alcohol molecule penetrating the interfacial film [8]. However, the predominating influence of the alcohol will be to increase v without a corresponding increase in l_c , and hence increase the CPP [95].

For a given surfactant, the CPP may also differ when different oils are used. If the alkane length of the oil is much less than l_c , it will penetrate strongly and swell the hydrocarbon side of the surfactant interface [61]. The value of the parameter may furthermore depend on the water content, because the headgroup area is sensitive to hydration effects, especially at low water fractions [96]. It is therefore necessary that the CPP used is in fact the $(v/a_0 l_c)_{\text{eff}}$ which will take into account any oil penetration or dehydration effects.

1.4.1.2 The H/L Ratio.

An extension of the hydrophile lipophile balance (HLB) system, the H/L ratio was used by Robbins and coworkers [20, 97, 98, 99] to postulate a model for spherical o/w or w/o droplets. The ratio is defined;

$$\text{H/L ratio} = \frac{V_H}{V_L} = \frac{(V_H^O + V_W^H)}{(V_L^O + V_O^L)} \quad \text{eqn.4}$$

where;

V_H = volume of the interfacial hydrophilic layer

V_H^O = volume of the surfactant head groups

V_W^H = volume of water dissolved in the head groups

V_L = volume of the interfacial hydrophobic layer

V_L^O = volume of the surfactant chains

V_O^L = volume of oil dissolved in the chains

The model developed by Robbins assumes a monodisperse w/o droplet structure which consists of a water core surrounded firstly by a shell of hydrophilic surfactant headgroups, and then by a shell of hydrophobic surfactant chains. In o/w microemulsions the inner oil core is surrounded by

concentric shells of surfactant chains and surfactant head groups.

As with the application of the CPP, the Robbins model focuses on the structure of the surfactant at the oil/water interface, and relates water and oil uptake to the relative thickness and volumes of the surfactant head groups and tails. The curvature of the interface is imposed by the differing tendencies of the water to swell the headgroups versus the oil to swell the surfactant chains [20], and hence the influence of salinity, temperature and oil composition can be included [97]. The theory has been further extended to generate theoretical phase diagrams for the transition between Winsor I, II and III microemulsion systems [98] (section 1.2), and to make predictions of microemulsion droplets size [99].

1.4.1.3 Surfactant film curvature

For any particular microemulsion composition (at constant temperature and pressure) structure will depend on the curvature, bending energy and elasticity of the surfactant layer [100]. The spontaneous, or preferred, curvature of the interface is defined as C_0 . By convention, o/w microemulsion droplets have a $C_0 > 0$, while a negative C_0 is applied to w/o systems.

Curvature of surfactant films can help to explain the formation and structure of microemulsions by the application of a steric model of surfactant molecules as either truncated cones or cylinders. Depending on the bulk of the hydrophobic and hydrophilic portions of a surfactant o/w or w/o droplet systems form. If the surfactant shape can be represented as a cylinder, or if a surfactant with $C_0 > 0$ is mixed with a cosurfactant of $C_0 < 0$, zero spontaneous curvature can be achieved, as illustrated in figure 1.5. With nonionic surfactants, C_0 can be inverted by changing the temperature [101]. If $C_0 \neq 0$, the radius of the resulting droplet microemulsion, R_0 , is the inverse of the spontaneous curvature ($|C_0|^{-1}$). If $C_0 \approx 0$ the surfactant layers tend to become planar, although subject to thermal fluctuations.

The actual curvature in a microemulsion system however may not necessarily equal the preferred curvature of the surfactant layer, and microemulsions may not necessarily consist solely of droplet structures. Hence two principle

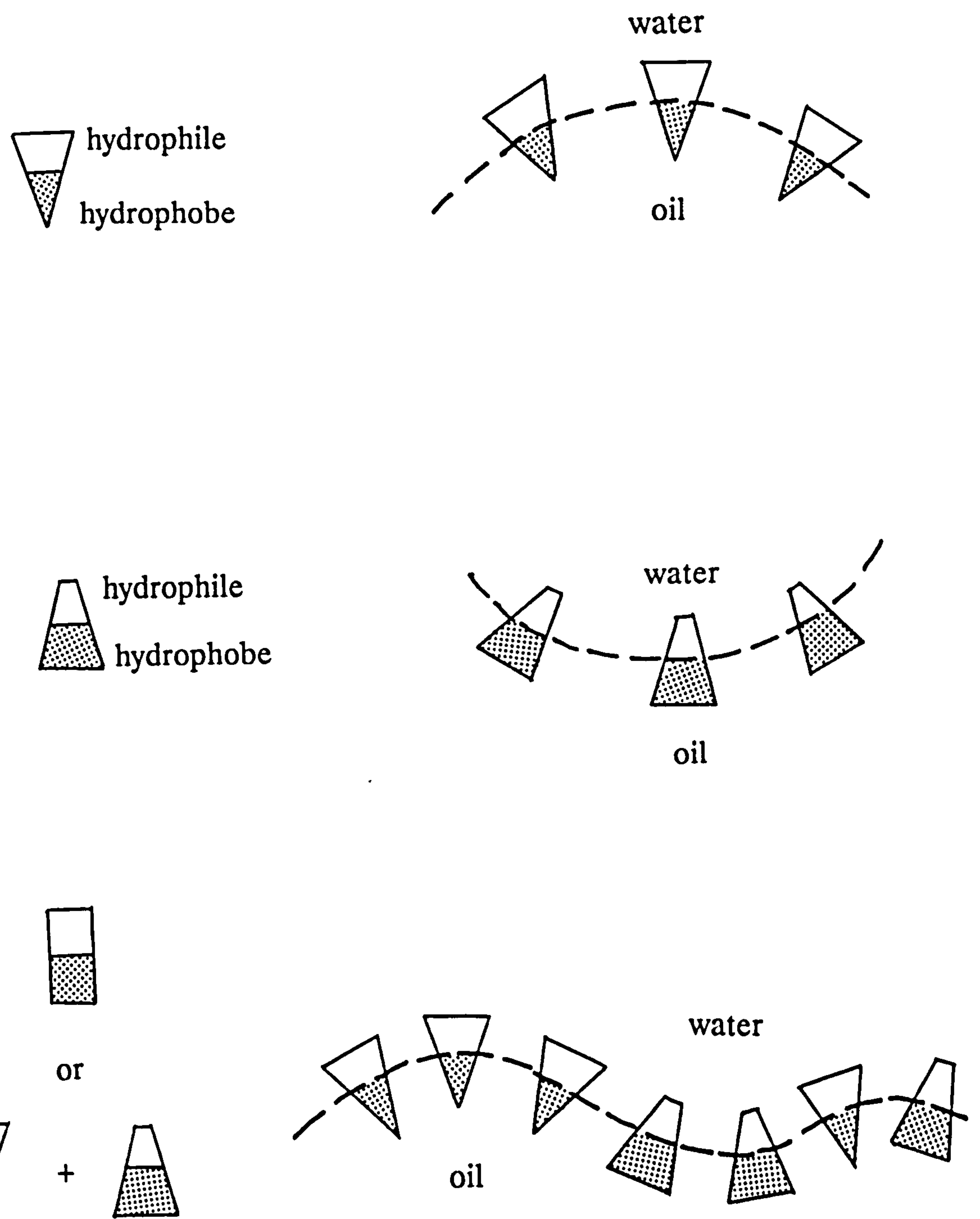


Figure 1.5: Variation of spontaneous surfactant film curvature with surfactant shape. Copied from reference 101.

curvatures (C_1 and C_2) may exist, resulting in a bending energy as described by Helrich [102];

$$F = 1/2K(C_1 + C_2 - 2C_0)^2 + \bar{K}C_1C_2 \quad \text{eqn.5}$$

where;

F = the bending energy

C_1 and C_2 = principle curvatures

= $1/R_1$ and $1/R_2$ respectively

C_0 = spontaneous curvature

K = elastic modulus (also called the rigidity)

\bar{K} = saddle splay (or gaussian) elastic modulus

The saddle splay elastic modulus, \bar{K} , is often assumed to be zero.

In droplet microemulsions $C_1 = C_2 = C = 1/R$, where C is the actual curvature, and R the radius of the droplet. When the amount of the dispersed phase is small, the droplet radius R is less than R_0 . Increasing the dispersed phase causes the droplets to swell until a maximum radius, R_{\max} , is achieved [103].

When the curvature of the surfactant film is small and close to zero (for example when the volume fraction of the oil and water are similar) bicontinuous or lamellar structures can occur. In bicontinuous microemulsion systems the surfactant film remains highly flexible, but with lamellar structures, long range order is present which does not exist in microemulsions [104].

In bicontinuous structures, thermal motion can however result in layer roughness and local curvature fluctuations of the surfactant film. The layer roughness may be characterised by the persistence length, ξ_k . ξ_k is the distance along which the layer remains flat. It is related to the rigidity by;

$$\xi_k = a \exp (2\pi K/kT) \quad \text{eqn.6}$$

where;

k = Boltzmann constant

T = temperature

a = molecular length

If the elastic modulus is greater than kT ($K = 10-100kT$ for phospholipid

bilayers) the surfactant layer is rigid, ξ_k is macroscopic, and the interface is flat over large distances. If however the bending elastic constant, K , is small and comparable to kT , ordered structures are not stable, ξ_k is microscopic, and bicontinuous microemulsions with characteristic size ξ_k exist [105]. This explains why structural inversion in microemulsions may occur via a lamellar phase, whereas sometimes the transition is a continuous one.

When K is too small, ξ_k is of the order of the molecular length (a), at which point the microemulsion structure begins to vanish into a molecular mixture in which well defined surfactant structures are unable to form [103].

Curvature effects can help to explain the role of cosurfactant in microemulsion formation. The cosurfactant can i) act to decrease the o/w interfacial tension compared to the surfactant alone, ii) contribute to the spontaneous curvature (and migrate to regions of strong curvature), and iii) act to lower the elastic moduli by disorganising the interfacial layers and hence favouring microemulsion, compared to liquid crystal, phases. For example, if the curvature modulus in a liquid crystal is in the region of $10^{-20}J$, and the molecular length is assumed to be 10\AA , then $2\pi K/kT \approx 15$, and ξ_k is about 1 million times the molecular length. As a result the interface is stiff, and the structure ordered. If however, by adding a short chain alcohol, K can be reduced by a factor of 5, $\xi_k \approx 20a$ ($\approx 200\text{\AA}$) and the interface is strongly wrinkled and flexible at scales larger than 200\AA [21].

Caution is however needed in comparing the rigidities of different monolayers. The uncertainties involved may be large, and the different methods used to estimate the rigidities are not directly comparable [106]. Direct experimental methods, such as ellipsometry [107] tend to measure the elastic modulus, K , only. Other methods use the relationship between the interfacial tension (γ) and the radius of spontaneous curvature (R_0) given by the equation [105];

$$\gamma = 2K / RR_0 \quad \text{eqn.7}$$

where R is the radius of a microemulsion drop in a two phase system (Winsor I or II), in which case the droplet radius is virtually equal to the spontaneous radius R_0 ($=1/C_0$). Hence [108];

$$\gamma \approx 2K / R^2 \quad \text{eqn.8}$$

However these equations neglect the contribution of the saddle splay modulus, \bar{K} . The significance of \bar{K} is less clear than K and C_0 , but it is postulated that a large negative value of \bar{K} encourages microemulsion droplet formation and decreases shape fluctuation, although it may also increase droplet size polydispersity [109, 110].

A modification of equation 8, to include the saddle splay modulus, has been suggested [104];

$$\gamma \approx (2K + \bar{K}) / R^2 \quad \text{eqn.9}$$

As a result some values of rigidity, calculated from interfacial tension and the measured size of microemulsion droplets, will not be values of K but of $K + \bar{K}/2$. An example of the variety of K values, determined by applying different techniques and equations, can be found in the much investigated AOT microemulsion systems. A large range of values from 0.5 - 5kT have been quoted by various workers [104].

Using the nonionic surfactant, $C_{12}E_5$ in three-component alkane/water microemulsion systems, Aveyard *et al* [106] have determined a $K + \bar{K}/2$ value of $1 \pm 0.5kT$ in heptane, and $2.3 \pm 0.9kT$ in tetradecane. In addition, using data of other workers, they obtained values of $K + \bar{K}/2$ of 0.7kT, 0.6kT and 0.3kT for AOT/water/n-heptane/NaCl, SDS/butanol/water/NaCl/toluene and sodium hexadecylbenzene sulphonate/butanol/water/NaCl/dodecane systems respectively.

In comparison Lee *et al* [111] have determined K by ellipsometry for C_mE_n /alkane/water systems in which the alkane used was varied in order to obtain a PIT of the system in the range of 20-30°C. They obtained values of 0.35kT for C_8E_3 /decane/water systems, and 0.76kT for $C_{10}E_4$ /octane/water.

The persistence length of the interface, ξ_k , calculated using equation 6, increases exponentially with increasing K . The value obtained will also depend on the method and accuracy with which K is determined. In addition, the molecular length, a , which should approximate the diameter of the surfactant molecule, is not known [111]. Choice of a is somewhat arbitrary,

usually between 5Å [104] and 10Å [100]. Experimenting with the surfactants C₆E₂, C₈E₃, C₁₀E₄ and C₁₂E₅, Lee *et al* [112] have found a rapid increase in the persistence length as the surfactant chain length varied. For instance assuming a molecular length of 7.5Å for both C₈E₃ and C₁₀E₄ resulted in calculated ξ_k values of 50 and 188Å respectively, which both compared well to the persistence lengths measured experimentally by SANS [111].

1.4.2 The models

1.4.2.1 Droplet model

The droplet model for microemulsions, as first proposed by Schulman, predicts a microstructure of o/w or w/o droplets. When the composition is known, the droplet radius can be predicted by the available interfacial area and the total volume of the dispersed phase;

$$R = \frac{3 \Phi_d}{C_s a_o} \quad \text{eqn.10}$$

where;

Φ_d = the dispersed phase volume fraction; either Φ_w or Φ_o

C_s = the number of surfactant molecules per unit volume

a_o = area per surfactant molecule at the interface

Although there will usually be some surfactant in the external phase this will be close to the critical micellar concentration (CMC) of the surfactant in pure oil or water [103]. Since R depends only on the amount of surfactant at the interface, in a few cases where the CMC may be large (for example some alkyl polyglycol ethers in oil) this concentration must be subtracted from C_s [103].

From equation 10, it follows that with a fixed concentration of surfactant (and hence an approximately constant interfacial area) R is expected to increase as the internal phase is added. This relationship assumes a hard sphere model in which there is no interaction between droplets. This assumption appears to hold for some microemulsion systems. For example, a linear increase in observed radius with dispersed water content has been found in AOT microemulsions with a w/o droplet structure [8]. Droplets swell until a

maximum radius R_{\max} is reached. Once R_{\max} is attained, if further dispersed phase is added, it will be rejected as an excess phase resulting in Winsor I or II systems [103].

In some cases however, the interactions between microemulsion droplets are attractive, and R_{\max} cannot be reached. In such cases droplets may collide, deform [113], their surfactant layers interpenetrate [114] and droplet aggregates may begin to occur at only a few percent of the dispersed phase [21]. Although the droplet model is useful in a number of microemulsion systems, when the assumption of spherical droplets does not predict sample scattering or other experimental properties, other models must be employed [115].

1.4.2.2 Talmon-Prager model

The Talmon-Prager model [116] represents microemulsion structure as a random geometry of interspersed oil and water domains generated by a Voronoi tessellation, with the surfactant adsorbed at the boundary [117, 118].

In order to construct the model; firstly a set of random points are generated around which associated Voronoi tessellating polygons are drawn. The cells are then filled with water or oil according to the available volume fractions (ϕ and $1-\phi$) of the microemulsion composition. Lastly, the interface (assumed to have negligible volume) is set between adjacent cells which have different contents. Typical results are shown in figure 1.6.

If ϕ_w is less than a certain critical value, ϕ_p , the systems will be oil continuous with isolated water polygons representing w/o microemulsion droplets. After ϕ_p , the model predicts a continuous path of water from one side of the sample to the other, ie. a bicontinuous system. A further transition occurs at $\phi_w = 1-\phi_p$, when the oil polygons are no longer connected, as in o/w microemulsion droplets. In this model ϕ_p (or the percolation threshold) is found to be approximately 0.18. Hence bicontinuous microemulsions are predicted for polar volume fractions between about 18-82%.

The success of the Talmon-Prager model is to generate an average size of oil and water domains which are of the same order of magnitude as the observed

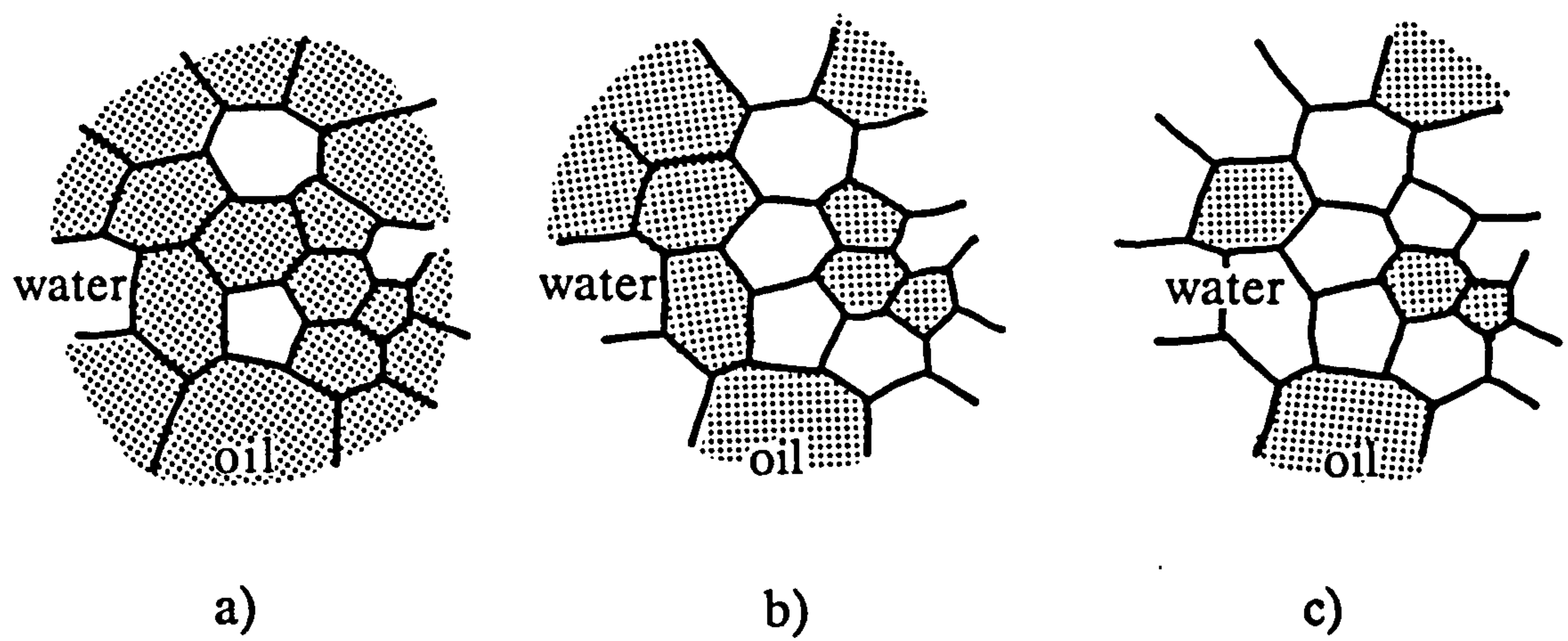


Figure 1.6: The Talmon-Prager model for microemulsion systems: Voronoi tessellation for systems with increasing water to oil ratio (a to c). Copied from reference 21.

size [8]. Although the first model to offer a continuous transition between w/o and o/w microemulsions via bicontinuous systems, scattering experiments so far have always been incompatible with the Talmon-Prager model [115].

1.4.2.3 Cubic random cell (CRC) model

DeGennes and Taupin [105] further developed the model postulated by Talmon and Prager. In this CRC model (also referred to as a lattice gas model) the random polygons of the Talmon-Prager model are made more simple by replacing them with a cubic lattice. It is from the model of DeGennes and Taupin that many of the relationships in section 1.4.1.3 (for example eqn.6) have been derived. In this model the sides of the cubes are set at the characteristic length, ξ , and the cubes (volume ξ^3) are filled at random with water or oil according to their volume fraction in the composition. The characteristic length, ξ , is assumed to be equal to the persistence length, ξ_k , which is given by;

$$\xi_k = \frac{6 \Phi_o \Phi_w}{C_s a_o} \quad \text{eqn.11}$$

or

$$\xi_k = \frac{6 \Phi_o \Phi_w}{\Sigma} \quad \text{eqn.12}$$

where;

C_s = the number of surfactant molecules per unit volume

a_o = interfacial area per surfactant molecule

Σ = total surfactant interfacial area

In cases of isolated oil or water droplets of dispersed phase volume fraction, Φ_d , equation 10 for droplet microemulsions applies.

In the DeGennes and Taupin model a single phase is expected when coupling between adjacent cubes ($\gamma \xi_k^2$) is weaker than kT [105]. That is;

$$\gamma \leq kT / \xi_k^2 \quad \text{eqn.13}$$

ξ_k will increase with Φ_o and Φ_w until a maximum, ξ_o , when the interfacial

tension becomes too high, and emulsion failure will occur. Applying equation 13 to a more general case; γ is in the order of kT/L^2 where L is the dispersion size ($L=2R$ for droplets, and ξ_k for middle phase microemulsions). However it has been found that the interfacial tension correlates only approximately with kT/L^2 ; the ratio $\gamma L^2/kT$ varying with salinity and the nature of the surfactant [100].

The model of DeGennes and Taupin however does not predict the experimentally observed three-phase equilibrium [119]. Hence the model has been extended by Widom [120, 121] to allow a variable cell size (ξ) and interfacial area per surfactant molecule. The Widom model does predict two- and three-phase equilibria, and postulates that ξ depends on the bending constant, K . The relationship between ξ and ξ_k however is not clear in this model [103].

In their model, Safran *et al* [119, 122] assumed the area per surfactant molecule remains fixed, and that the free energy consists of both bending energy and entropy of mixing [123]. They found that ξ in their model is closely related to the persistence length (ξ_k) of deGennes and Taupin.

1.4.2.4 Disordered open connected (DOC) model

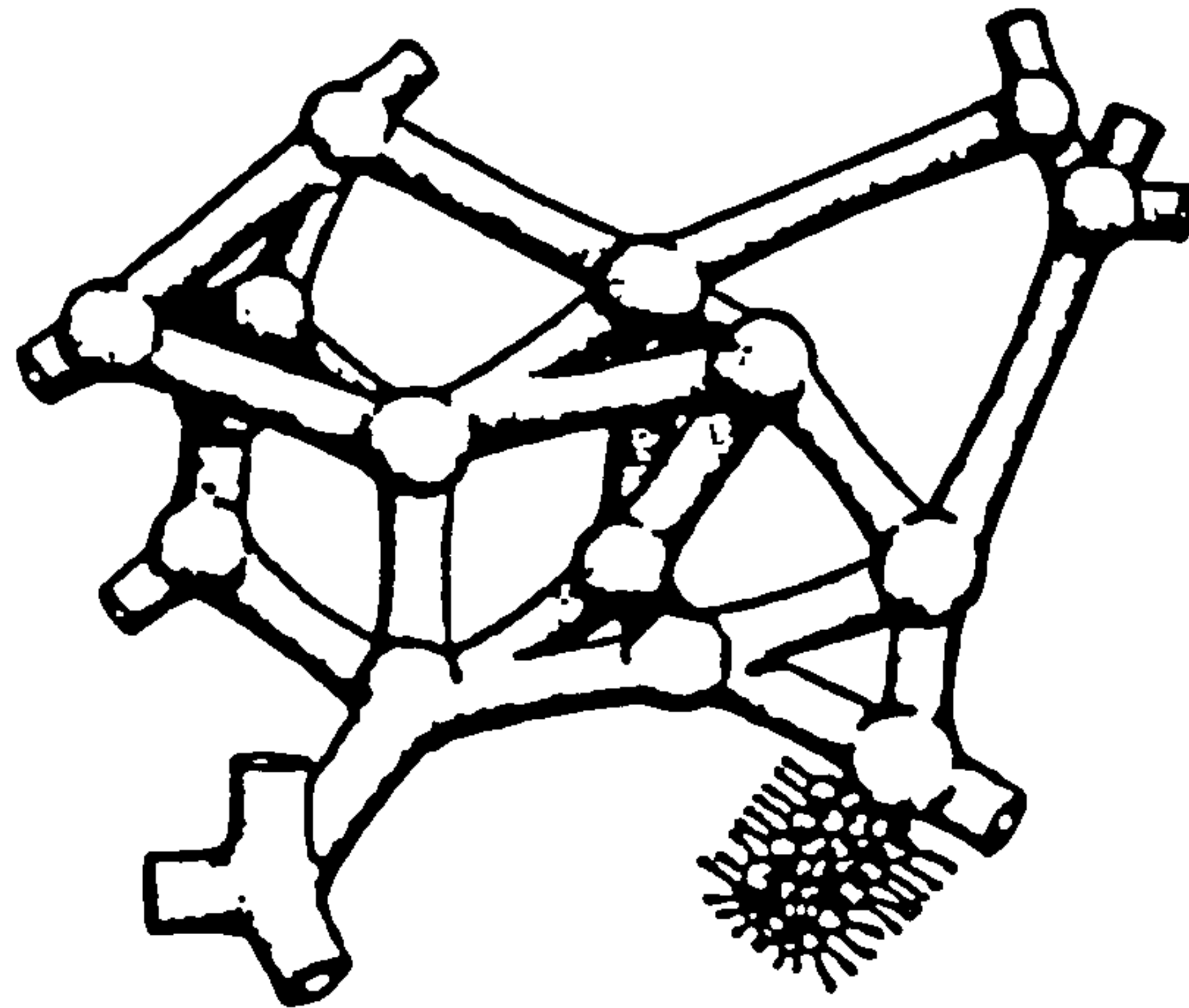
The Talmon-Prager and CRC models appear to be compatible with high self diffusion coefficients of oil and water in the same sample of a concentrated microemulsion. Light scattering studies may also be understood by these models [8]. However, both models fail to explain the presence and/or position of scattering peaks determined by SAXS [8, 124]. In contrast, the DOC model correlates well with SAXS experiments, predicting the scattering peak, and also the threshold conductivity phenomena found in 3-component ionic microemulsions [115, 124].

The DOC model [96, 124, 125] consists of a network of spherical droplets and connected cylinders as shown in figure 1.7. The model is specified by i) N ; the density of the spherical centres in space, ii) z ; the average coordination number, which is the number of cylinders at each sphere, iii) R ; the radius of the spheres, and iv) r ; the radius of the cylinders.

To maintain the same value of mean curvature on both the spherical and cylindrical parts of the interface the ratio R/r is fixed at 2 [125]. Hence the DOC model can be constructed for a given set of values for N , z and R . Firstly, a random set of points is generated with a minimum separation of $2R + 2l_c$. A sphere of radius R is placed at each of these points, and the nearest neighbours of each point are determined. Neighbouring spheres are then connected by cylinders of radius $r = R/2$, until the average coordination number for the structure is z . When $z = 0$ the hard sphere model for microemulsions exists. The DOC model predicts microemulsions between $z = 0$ and $z \approx 13.4$ [125].

The DOC model appears to predict the scattering behaviour of three-component ionic microemulsions in which the structure is set by the molecular packing. It does however have limitations, and is inadequate to describe AOT/water/oil systems in which $v/a_o l_c$ is not well fixed by composition, and tends to retain its droplet structure. Similarly the DOC model cannot adequately predict microemulsion structure when the geometrical constraints are relaxed and large bending radius variations are allowed, as is the case when a cosurfactant is added to a system containing single-chained surfactants [115].

a)



b)

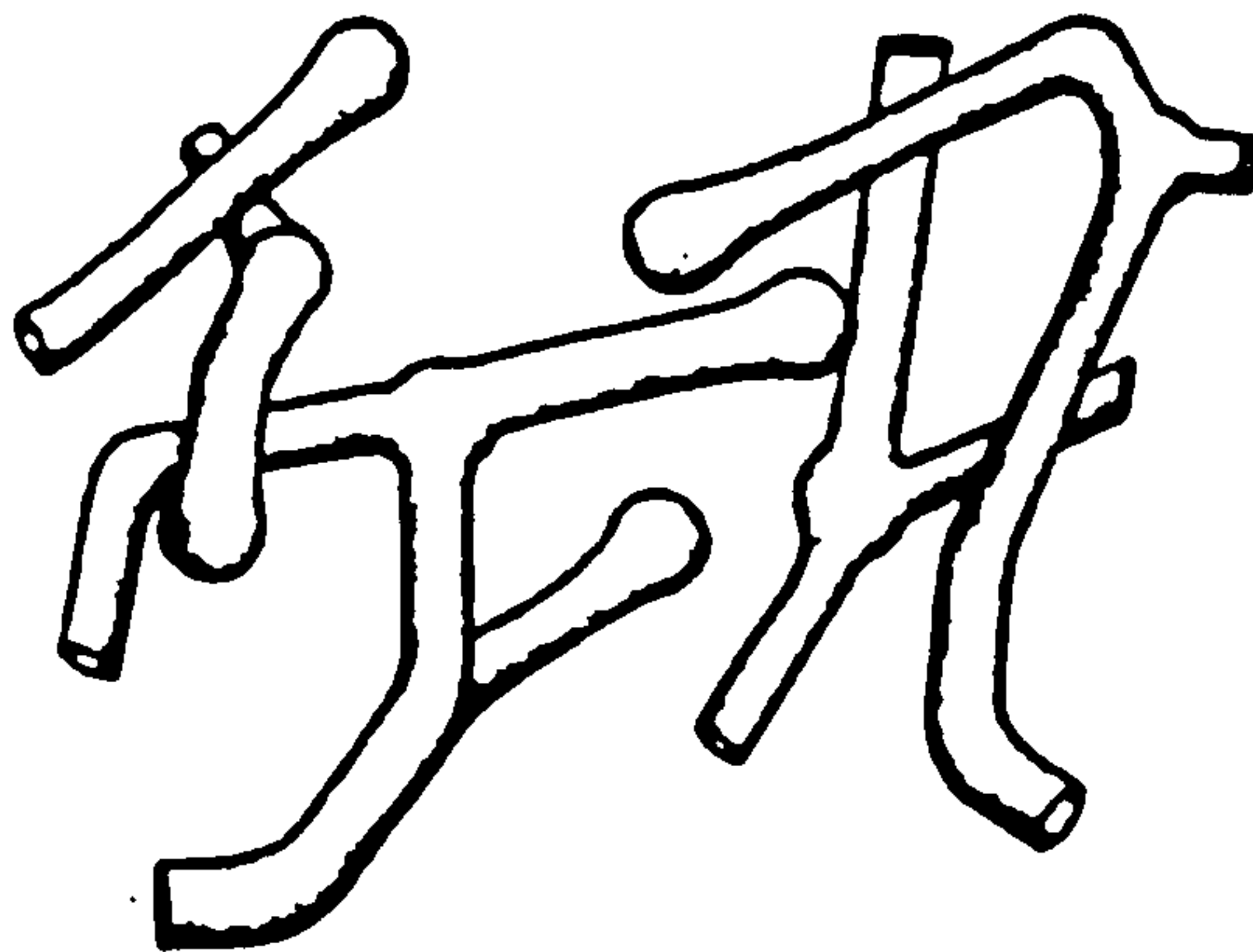


Figure 1.7: Schematic diagram of a DDAB/water/cyclohexane microemulsion according to the DOC model of microemulsion structure, with connectivity a) $Z = 4$, and b) $Z = 2$. Copied from reference 124.

1.5 Potential applications of microemulsions

1.5.1 Microemulsions in tertiary oil recovery.

After their initial discovery, much of the work on microemulsions has been stimulated by the potential of microemulsions in tertiary, or enhanced oil recovery. Oil recovery from a reservoir occurs in three stages. In the primary process, the presence of natural gases forces the oil through the wells. When this pressure is no longer capable of pushing any more oil out, water is injected to force out further oil (secondary oil recovery). After the first two stages up to 70% of the oil can still remain in the reservoir. Of this remaining oil, 20-30% is trapped in the pores of the rocks by capillary forces. Microemulsion theory is employed in tertiary oil recovery (or surfactant flooding) to decrease the interfacial tension between the oil and water, displace oil from the porous rock matrix, and thus improve oil recovery. The whole field of microemulsion potential in tertiary oil recovery is extensively covered by Bansal and Shah [126]. The environmental conditions that need to be considered are discussed by Neustadter [127].

1.5.2 Microemulsions as media for chemical reactions.

O/w, w/o and bicontinuous microemulsions have been employed as reaction media, solubilising a large number of different components, and providing a large internal interface [128]. Until recently use of microemulsions in this respect has not been studied in as much detail as micellar systems [129]. The reactions in microemulsions can however be very different from those in micelles [130], and the reaction rates found can be quite similar [131], or significantly greater [132].

The use of o/w microemulsions as reaction media has been reviewed by Pelizzetti *et al* [129]. Examples cited illustrate that microemulsions alter the microenvironment of the solubilised reactants, and so effect the product distribution, dissociation constants, redox potentials and reactivity. The separation of reducing and oxidizing agents in individual compartments in a

w/o microemulsion system has proved useful in studying the production of artificial solar power [133]. Microemulsions also provide the opportunity for organising polar and apolar molecules which is, for example, important for investigating the photochemical processes of chlorophyll [130, 134]. Chlorophyll contains both a polar and nonpolar region. Its average location is found to be in the interface region of ionic four-component o/w microemulsions where it undergoes photodegradation [135] and is able to participate in photosensitised redox reactions between water-soluble, oil-soluble or adsorbed substances [136]. Alternatively, photosynthetic activity has been investigated after the introduction of whole plant cells into AOT w/o microemulsions [137], although the size of the resulting cell-containing droplets is outside the usually accepted range for microemulsions.

Microemulsions have been shown to have interesting applications in the field of metal recovery by liquid-liquid solvent extraction processes. For example, anionic surfactant Winsor II microemulsion systems have been used to concentrate dilute aqueous solutions of metallic cations by an extraction-reextraction sequence [138]. Alternatively an industrial extractant may be added to, or used to replace, the oil component and a metal-extractant complexation reaction can occur [139, 140]. Microemulsions can improve the rate of extraction of the metal species [141]. The separation of different metal ions (for example Co^{2+} and Ni^{2+}) in an aqueous liquid may also be possible if a microemulsion system can be chosen in which the reaction rate can be slowed to the extent that it can be stopped at the moment most of the fast complexing metal (Co^{2+}) has reacted [142].

The composition of the microemulsion system used in chemical reactions is an important variable. For example, with many w/o microemulsions the reaction rate is found to increase as the ratio of water to surfactant decreases [132, 143]. Other important factors include the type of surfactant used (anionic, cationic or nonionic), although not necessarily the amount [143], the balance of the hydrophilic and lipophilic properties of the surfactant [144], and the type and quantity of cosurfactant added [129, 145]. Additionally, if nonionic microemulsion systems are employed, temperature becomes very important. The nonionic surfactant selected should be one which will give a one phase system at the temperature required for the desired reaction rate [128].

Barnickel *et al* [146] have reacted AgNO_3 and NaNH_4 using C_{12}E_4 w/o

microemulsions. They found that different diameters of silver particles could be achieved as the water/surfactant ratio (and hence the size of the w/o droplet) was varied. Microemulsion structure also appears to be an important determinant of reaction rate. For instance, in some reactions definite w/o droplets are required to increase the reactivity [147]. In other reactions, microemulsion compositions corresponding to the transition from o/w to bicontinuous, and from bicontinuous to w/o give enhanced reaction rates [148].

1.5.3 Microemulsions as a media for enzyme catalyzed reactions.

Reverse w/o microemulsions are of interest in the field of enzyme catalyzed reactions. These systems retain all the properties characteristic of microemulsions. They are therefore stable, optically transparent, easily prepared and do not require the high shear preparation of macroemulsions produced for similar purposes [149] or the employment of sonication which may inactivate the enzymes [150]. Compared to a purely aqueous medium, reverse microemulsions show a closer structural similarity with biomembranes, and hence may represent *in vivo* enzyme function more closely [150]. The water core of such microemulsion systems provide a microenvironment in which the enzyme is protected from the denaturing effect of the external organic solvent [151]. This aqueous microenvironment favours enzyme activity and in microemulsions is combined with an enormous interface through which lipophilic substrates can be catalyzed [152] and a highly dynamic nature which allows very rapid movement of products into and out of the water pool [153].

Variables which affect the catalytic activity and the rate of reaction include the amount of water present [150, 153], the volume fraction of oil present [154], the organic solvent used in the external phase [155] and the surfactant used [155, 156]. Based on previously published data, rate equations for the kinetics of enzyme-catalyzed reactions in w/o microemulsions have been suggested [157].

Initial biocatalysis investigations using w/o microemulsions tended to use ionic surfactants such as cetyltrimethylammonium bromide [151]. Commonly AOT [150] was employed so that the addition of an alcohol as cosurfactant

could be avoided. Three component nonionic microemulsions have more recently been studied. It is possible that higher stability of the enzyme protein can be achieved by employing less aggressive nonionic surfactants rather than charged surfactants [156]. In comparison to ionic systems such nonionic based reversed microemulsions have been found to both increase [155] and decrease [153] the reaction rate. The presence of terminal OH groups in many nonionic surfactants can however give rise to severe side reactions [155].

There has been considerable research into these w/o microemulsion reaction media, but as yet no industrial applications. This is mainly due to the practical and economic difficulties of product recovery from solvents with high concentrations of surfactant. Hence the use of w/o detergentless microemulsions has been advocated [158, 159]. Such systems, in which an alcohol acts as the surface active agent, still allow protection of the protein from the organic phase and are similar to surfactant-containing microemulsions in terms of their stability, transparency and ease of production. Although a range of structures may be expected throughout the clear region of a detergentless microemulsion, well defined microdroplets appear to be necessary for achieving high catalytic activity [159]. The disadvantage of such systems however is that the large amount of alcohol employed may act as a substrate and lead to side reactions [160].

Further investigations intended to increase the practicability of using o/w microemulsions as enzyme media, include the use of Winsor III microemulsion systems and microemulsion based organogels. In Winsor III systems it is postulated that the surfactant and enzyme should remain in the middle phase microemulsion with the products preferentially distributing into either the excess organic or aqueous phase [160]. Adding gelatin to AOT reverse microemulsions allows the production of an enzyme-containing gel which has advantages over conventional microemulsions in terms of the ease of product separation and the reuse of enzymes [161].

1.5.4 Microemulsions as liquid membrane carrier agents.

Microemulsion droplets have demonstrated the ability to transport substances which are insoluble (or very poorly soluble) in the continuous phase, which could lead to numerous approaches in techniques of separation, as possible

carriers of biomolecules or drugs [162] and as models used in the study of transport in biological membranes [141, 163]. As discussed in section 1.5.2, microemulsion systems containing an extractant have been used in the extraction of metals via a complexation reaction. Although those microemulsions containing an extractant have been shown to transport a higher flux of K^+ and Na^+ picrate, the microemulsions themselves also act as carriers [141].

In studies investigating microemulsions as transporting liquid membranes a U-tube is commonly employed, in which the microemulsion phase is placed in the bottom with the excess phase (donor and receiver) introduced into both arms [163]. The excess phase may be either oil (o/w microemulsions used) or water (w/o microemulsions used) so that Winsor I or II systems respectively exist when equilibrium is reached.

The flux of a solute transferred via these biphasic microemulsion systems has been found to depend on the initial concentration of the solute in the donor phase [163], the concentration of the dispersed phase [141, 163], the nature and amount of surfactant used [164], the alkyl chain length of any alcohol used as cosurfactant [164] and the structure of the microemulsion phase determined by its composition [165, 166]. Depending on the nature of the surfactant, different mechanisms of transfer (interfacial loading and unloading) appear to take place [166, 167].

1.5.5 Microemulsion gels.

Although microemulsions are by definition low viscosity systems, there are three categories of gels which have been described as microemulsions, or are based on microemulsion systems.

A large number of terms, including transparent oil-water (TOW) gels [168] and liquid crystal microemulsion gels [169] have been suggested for the first group of gels which, in common with liquid microemulsions, contain oil, water and surfactant, are thermodynamically stable, transparent, isotropic and non-birefringent. These systems are however semi-solid and may have a characteristic *ring* when the container is tapped. Such gels tend to occur at high surfactant concentrations [170] in a region which borders on the o/w

microemulsion area of the phase diagram [171].

Small angle neutron scattering, light scattering [171] and electron microscopy [172] investigations have supported the presence of spherical o/w microemulsion droplets within these gels, and suggests the mutual interaction of the droplets hinders free mobility [170, 172] and the possible formation of a cubic crystalline phase [168, 173]. The application of these clear, stable, oil- and water-containing gels as cosmetic and pharmaceutical vehicles is reviewed by Provost [168].

The other two categories of gels originate from w/o microemulsion systems. These gels are either lecithin based, or gelatin-containing gels both of which are referred to as microemulsion based gels or organogels [174].

Lecithin gels can be produced from an organic solvent, lecithin and water. Although some solvents, such as chloroform and benzene do not allow the formation of lecithin gels [175], at least fifty organic solvents have been shown to permit such gels to form [174]. The solvent used, the amount of water and the amount of lecithin present have large influences on the viscosity of the resulting gel. Also, lecithin of insufficient purity fails to produce these organogels [176].

The structural details of lecithin gels is still unknown [175]. Such gels are however non-birefringent (hence not a liquid crystal mesophase) and not a cubic crystalline phase [174]. NMR [175], SANS [177], rheological and light-scattering studies [174] have supported a hypothesis that the addition of water results in one dimensional aggregation of lecithin molecules into long and flexible cylindrical reverse micelles. At a threshold lecithin volume fraction these cylinders entangle forming a dynamic network, as suggested in figure 1.8, and also represented by the gel model illustrated in figure 1.9a.

The study of lecithin gels in organic solvent could be of direct biological importance. These gels are also biocompatible, and with their capacity of incorporating guest molecules may lead to important cosmetic and pharmaceutical applications [174], possibly allowing easier absorption of drugs or cosmetics through the intestine or skin [178].

Organogels which form due to the presence of gelatin tend to originate from

three-component w/o microemulsion systems with AOT as surfactant, although AOT systems in which the nonionic surfactant, Tween 85, has been added have also been used [174]. The variables involved in the formation of these gels depends on the composition of the parent microemulsion, particularly the ratio of water to surfactant and the concentration of gelatin used [179]. At low gelatin concentrations the systems remain liquid and transparent. Also, at low water/surfactant ratios gels are not possible. This is possibly because at low water content insufficient gelatin has been introduced into the system [174].

With gelatin based organogels, unlike lecithin gels, the selection of the organic phase is critical for gel formation. Gelatin based organogels have been found to form with parent w/o microemulsions composed of AOT, water and isooctane [174, 180, 181, 182, 183] or heptane [179, 184]. Some other organic solvents tested such as cyclohexane [179], isopropyl palmitate or hexadecane do not result in gel formation, although isopropyl palmitate microemulsions could be made to form gels if butanol is added to the system [174].

Partial phase diagrams, showing gelatin versus water content, have been produced by Petit *et al* [182] for the gelatin/AOT/isooctane/water system at room temperature, in which four regions have been identified; a clear liquid sol region, a two-phase area, a precipitate region (in which there is insufficient water to solubilise all the gelatin) and the gel phase. Gelation of the systems appears to occur only with significant gelatin concentrations ranging from 6-15% depending on the experimental conditions. The junction of the four regions is termed the *saturation point*.

Petit *et al* [182] have studied the structure of gels at the saturation point. At this point practically one molecule of gelatin per microemulsion droplet is found. Using conductivity, SANS and SAXS data they have suggested that at the saturation point about 30% of the gelatin content penetrates the water pools of the w/o microemulsions and 70% is in direct contact with the isooctane or the surfactant interface. A model of water spheres interconnected by gelatin rods that are free from surfactant as shown in figure 1.9c is proposed.

Also using the gelatin/AOT/isooctane system, Quellet and Eicke [181]

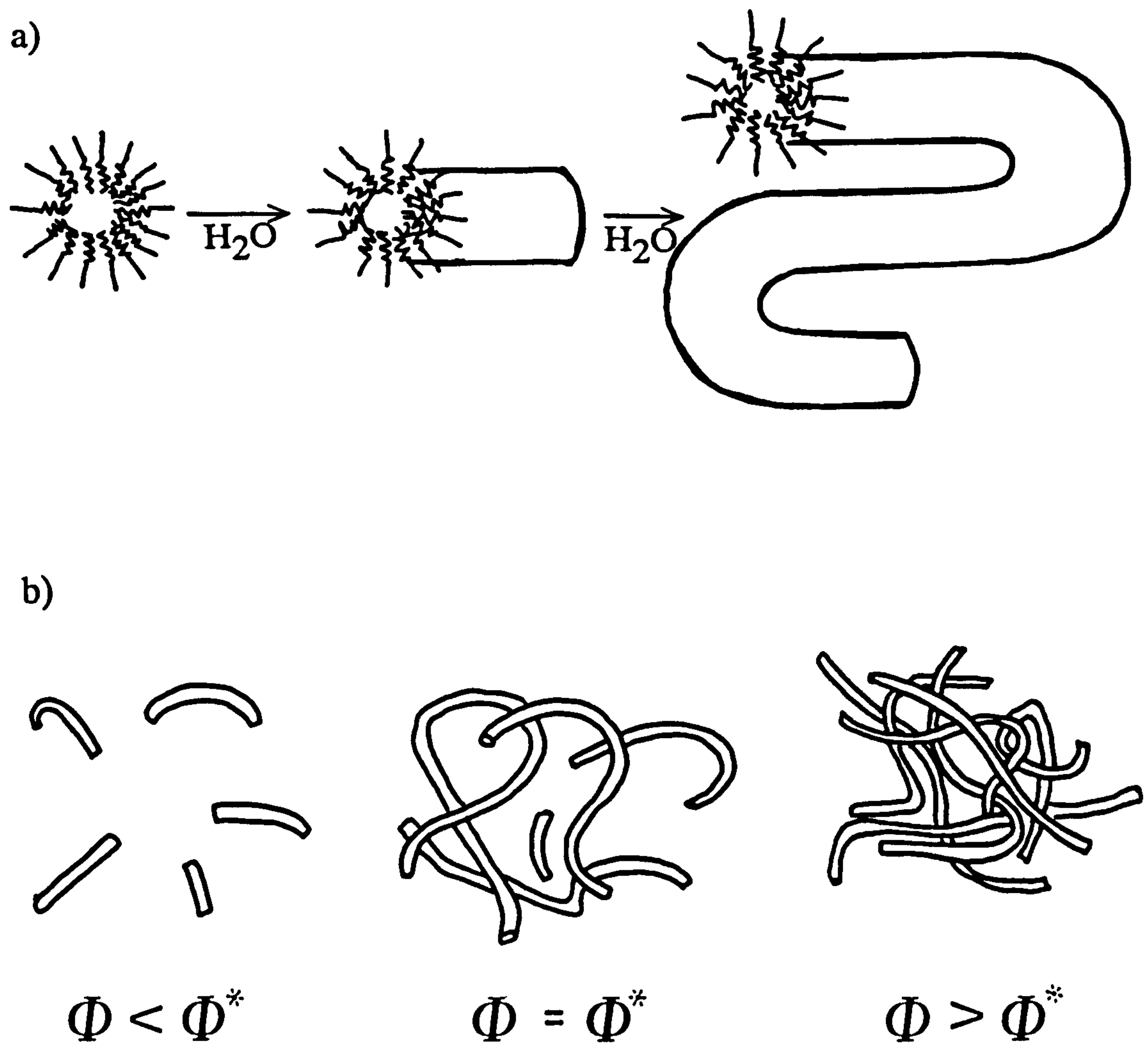


Figure 1.8: Model of reversed lecithin w/o microemulsions; a) addition of water increases one dimensional growth, and b) change in the entangled network as the lecithin volume fraction is increased. Copied from reference 174.

suggest gelation occurs in three stages. Firstly, *nanogels* form in which the gelatin is found inside the water pools, these nanodroplets then coagulate into infinite clusters, and thirdly, bulk gelation occurs, with crosslinking of the individual droplets due to helix formation of the gelatin polypeptide [183]. These workers expect the gelatin to be confined to the aqueous nanodroplets with some polar side chains adsorbed at the interface. This model may not however contradict that of Petit *et al* [182] who were only considering the specific case of the saturation point, where the highest gelatin concentration for the lowest amount of water is to be expected. Quellet *et al* [183] argue that few gelatin molecules would be expected in the apolar phase if there is enough water available for the solubilisation of their polar side groups.

Based on electrical conductivity and SANS data a further model is proposed by Atkinson *et al* [185] for the gelatin/AOT/heptane system of a rigid network of gelatin-water rods coexisting with microemulsion droplets (Fig 1.9b)

Organogels with gelatin have attracted interest due to a variety of potential applications. Such systems could be used to prepare gelatin films which are insoluble in organic solvents, but which swell in water, they could be used to solubilise a range of substances [174], including drugs for transdermal delivery [185]. Enzyme and bacteria can be entrapped into these gels without any loss of activity and hence their potential as a media for enzyme synthesis [174, 180, 185] (see section 1.5.3).

1.5.6 Microemulsions as blood substitutes

At present, blood transfusion is the only effective way of restoring oxygen to body organs and tissues in situations where supply is seriously impaired. The development of an artificial transporter of respiratory gases would be of considerable value, especially if such a formulation was free of immunological and infectious risks, chemically stable and easy to store and use [186]. Certain fluorocarbons, which are chemically and biologically stable, are able to store oxygen and release it in the presence of carbon dioxide [187].

The use of o/w microemulsions which contain these oxygen-carrying fluorocarbons as the dispersed phase would have the advantages of forming

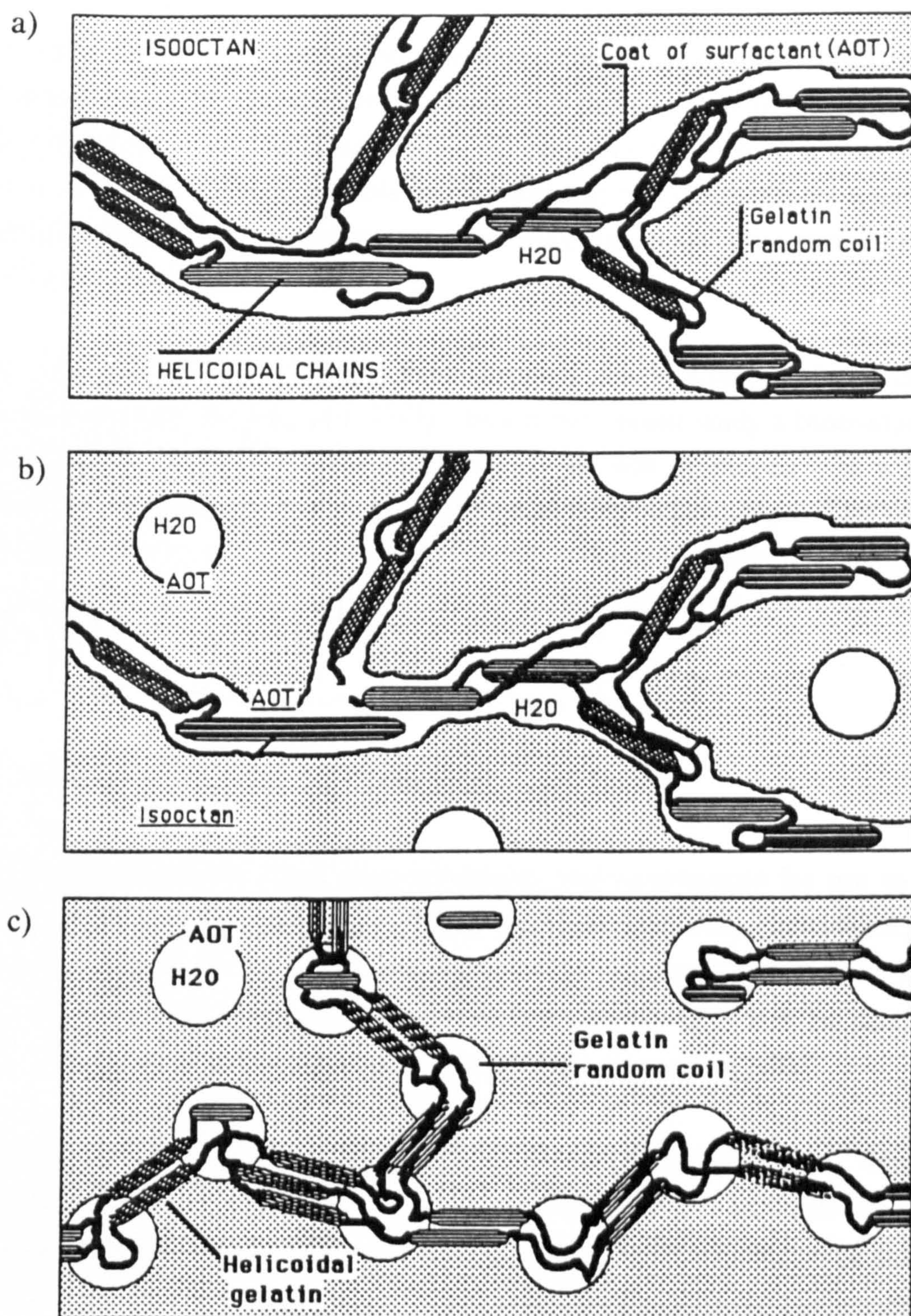


Figure 1.9: Three proposed models for microemulsion gels containing gelatin; a)cylindrical model, b)reverse droplets and cylindrical structure, and c)reverse droplets interconnected by gelatin rods. Copied from reference 182.

spontaneously, the ability to pass through capillaries because of their small particle size [188], and of remaining stable for periods of up to several years [189].

Generally, to prevent separation between the hydrocarbon chains of the surfactant and the fluorinated chains of the oil, the production of a microemulsion with a perfluorinated oil requires the use of a fluorinated surfactant [190]. Hence, possible microemulsion blood substitutes have been proposed which contain a fluorocarbon, a fluorinated nonionic surfactant and an aqueous phase [189].

Some fluorinated surfactants are however only slowly eliminated and can be degraded to toxic fluoride ions [191]. In a more recent study a biocompatible hydrogenated nonionic surfactant, Montanox 80, was employed with a mixed fluorinated and hydrogenated oil ($C_8F_{17}-CH_2CH=CH-C_4H_9$). The oil and surfactant appear to be compatible, and the microemulsions produced have been found to be well tolerated in rats and mice, giving oxygen absorbances comparable to that of blood [186].

1.5.7 Microemulsions for drug delivery.

Microemulsion systems have been proposed, and investigated for use as drug delivery systems [188]. Because of their small particle size, transparency and thermodynamic stability, microemulsions can be sterilised by filtration [192], easily inspected for bacterial contamination [193] and will be stable to transport vibrations and temperature fluctuations on storage [192].

Microemulsions offer the advantage of providing a vehicle for drugs of different lipophilicities in the same system [194]. In addition, o/w formulations provide a water-continuous dosage form which can be used to deliver water-insoluble drugs, and avoid the undesirability of the parenteral administration of suspensions, or the need to add cosolvents, or to chemically modify the drug molecule [193]. Conversely, w/o microemulsions provide a means of incorporating, protecting and increasing the bioavailability of some water-soluble moieties such as proteins [195]. Furthermore, microemulsions are interesting as possible therapeutic systems which may allow prolonged drug release, improve overall absorption of a drug [194] and possibly help to

reduce side effects and lower the dose required [196].

Microemulsion systems have been considered for use as topical preparations which could, for example, be used to include sunscreens [197, 198] or moisturisers [198]. They may also prove useful in the application of therapeutic agents for local (see fig. 1.10) [199, 200] or systemic delivery [201].

The flux of water through the skin is important for topical delivery. Hence the amount of water in a microemulsion formulation is important. Water flux from microemulsions, produced by dioctyl sodium sulphosuccinate (DSS) as surfactant and octanol as cosurfactant, have been investigated by Osborne *et al* [202]. These workers found that in microemulsions with only a low water content most of the water is bound to the surfactant head groups and not available for transport across the skin. Furthermore microemulsions containing little water may actively dehydrate the skin and increase the skin barrier. In high-water microemulsions (containing free, unbound water) water transport through the skin can in fact increase approximately six times (fig 1.11).

With the same microemulsion systems, and using glucose as a model drug, these workers suggest that free water is necessary for the significant transport of any hydrophilic drug, and that glucose delivery can increase thirty times by employing a microemulsion containing 35-68% water, compared to its delivery from the *in vitro* application to human skin of an equivalent amount of glucose in pure water [203].

The *in vitro* absorption of cetyl alcohol and octyldimethyl PABA from a microemulsion formulation (silicone fluid, water and polysorbate emulsifiers) applied to human and hairless mouse skin has been compared to the absorption from a cream and lotion. The microemulsion was found to increase the rate of penetration 2-6 times, and the total amount absorbed by more than twice, compared to the other two formulations. Pretreatment of the skin with the microemulsion preparation was also found to allow faster and deeper penetration of cetyl alcohol, and hence the possibility of the microemulsion itself, or the surfactant or cosurfactant it contains, compromising the barrier properties of the stratum corneum must be considered [198].

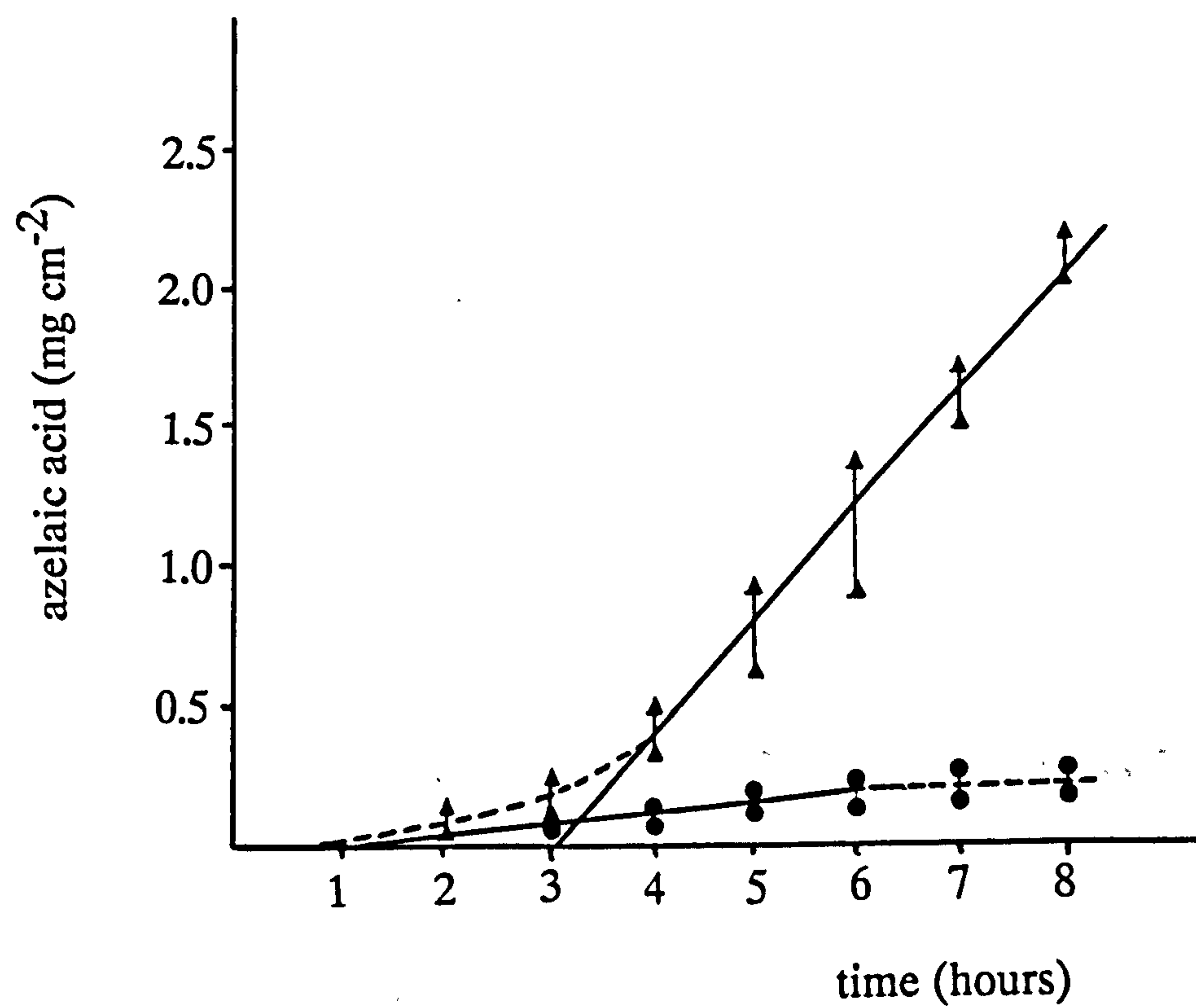


Figure 1.10: *In vitro* permeation of azelaic acid into hairless mouse abdominal skin vs time from a viscosized microemulsion (\blacktriangle) and from a gel (\bullet). Copied from reference 199.

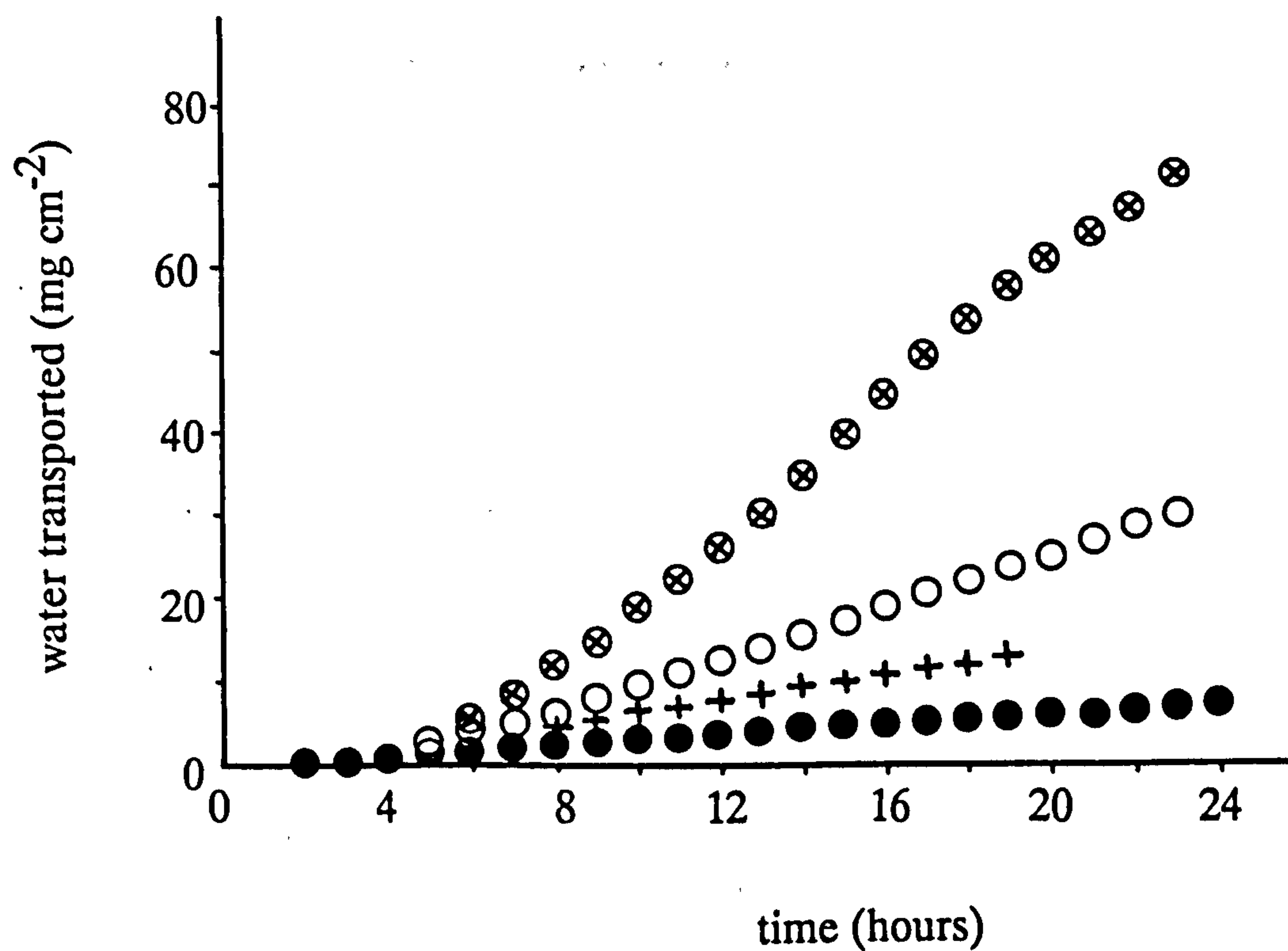


Figure 1.11: *In vitro* transdermal water transport through human cadaver skin for pure water (+) and microemulsions containing 15 (●), 35 (○) and 68 (⊗) % water and a 58:42 weight ratio of dioctyl sodium sulphosuccinate:octanol. Copied from reference 203.

A novel approach to the use of microemulsions has been applied to the transdermal administration of β -blockers by Kemken and coworkers [204]. A saturated water-free *microemulsion* is applied to the skin in an occlusive patch formulation. Water uptake from the skin is predicted to result in the production of a w/o microemulsion, thereby reducing the solubility of the drug in the patch. This reduction of solubility in the formulation encourages a high transdermal absorption rate. In rabbit studies, improved *in vivo* transdermal absorption of bupranolol and timolol was observed compared to the absorption from a transdermal matrix patch of the drugs [205].

1.5.7.1 Water-in-oil microemulsions.

The inclusion of hydrophilic drugs into w/o microemulsions has been investigated by a number of research groups. For example Jayakrishnan *et al* [206] found the incorporation of hydrocortisone by ionic four-component w/o microemulsions (using a combination of sodium stearate and sodium myristate as surfactant) decreased as the chain length of the alcohol increased from n-butanol to n-heptanol. Changes in the surfactant concentration, oil chain length and water-to-oil ratio did not however show any significant effect on the amount of drug incorporated. The formulation variables and the possibility of using alcohol-free w/o microemulsions with a combined surfactant (Span 20 and AOT) for pharmaceutical applications is discussed in reference 207.

In w/o microemulsions produced from water, hexanol and ethyl oleate, with lecithin as surfactant, Gasco *et al* [208] found the hydrophilic drug doxorubicine to be mainly present in the aqueous phase, but also partly dissolved in the oil phase due to lipophilic complexes with the lecithin. Comparing doxorubicine with the more lipophilic drug, 1-demethoxy-daunorubicine, it is suggested that variation of the lipophilicity of a drug and hence the strength of the drug-phospholipid complex can modify the reservoir effect of such microemulsions [209].

Gasco and coworkers have also investigated the production of nanoparticles resulting from the polymerization of monomers included in w/o microemulsions [210]. Extending this work, the incorporation of doxorubicine into nanoparticles obtained by the polymerization of

nonaqueous AOT/butanol/hexane microemulsions (in which ethylene glycol replaces water as the dispersed phase) has been reported [211].

Most investigations into w/o microemulsions for drug delivery appear to have concentrated on the use of such systems for peptide delivery. Many endocrinologic diseases and deficiency syndromes are caused by the reduced presence, or total absence, of peptides and polypeptides. Such conditions may require long-term (even life long) treatment. Due to advances in biotechnology, peptides and proteins are becoming more readily available in sufficient quantities at affordable costs.

The delivery of peptides is not, however, without problems. Most peptides have short elimination half lives which may be only a few minutes long. The large molecular size of such materials (1,000 - 100,000 Daltons) makes absorption generally poor, and they are susceptible to a range of peptidases present in the body.

In recent years new drug delivery systems and devices have been developed, and the feasibility of peptide delivery by a variety of routes has been investigated. In this context microemulsions, in particular w/o microemulsion systems, have attracted significant interest. Ritschel and coworkers have been particularly active in this regard. A review of their work using microemulsions to enhance the absorption of cyclosporin A, vasopressin and insulin from the gastrointestinal tract is given in reference 195. These workers studied three types of peptide-containing w/o microemulsions; clear liquid microemulsions for *in situ* studies using isolated rat intestine, gel microemulsions (formed by adding 6-10%w/w of a silicon-based stiffening agent Cab-O-Sil® to liquid microemulsions) for rectal bioavailability studies, and encapsulated gel microemulsions for use in oral absorption studies. A range of surfactants, cosurfactants and oils were used, with water or buffer employed as the dispersed aqueous phase.

Oral delivery by microemulsions of the peptide cyclosporin A (M_r 1203) was compared to a commercially available IV preparation and oral solution. The commercial oral preparation is an oily solution which must be diluted with water before use, after which it forms a fine emulsion of 2-4 μ m droplet size [212]. A more in depth study of one of the microemulsion-containing capsule formulations resulted in a similar extent of absolute and relative

bioavailability to that found with the oral solution when tested in beagle dogs [213].

Results of a similar study carried out using rats [214] showed a significant increase (over 400%) in the bioavailability of a w/o microemulsion capsule preparation (ME11) over that of the oral solution, and these workers attributed the increased bioavailability in part to the smaller particle size of the microemulsion formulation. The difference in droplet size alone however cannot be the complete explanation, as another microemulsion formulation, of similar particle size but with a different oil phase, did not improve oral absorption. It is also important to note that in comparison with the commercial IV preparation the rats given ME11 suffered an increased intensity of side effects, and in one case death.

The GIT absorption of insulin using microemulsions has been investigated by the Ritschel group [195, 215]. The rectal application of microemulsion gel preparations to rabbits resulted in the reduction of blood glucose levels to varying levels by six different formulations [195]. Experimenting with beagle dogs, an insulin-containing encapsulated microemulsion gel administered orally, was found to be superior in pharmacological action compared to the equivalent liquid microemulsion formulation. These workers thought this observation was due to the capsule delivery system allowing greater colonic insulin release, and hence increasing the absorption of the peptide 250-300% [195].

One of the six microemulsion formulations used in the above study [195] was further tested for its ability to deliver insulin by intraperitoneal administration to mice. The formulation chosen contained a commercially available oil; Cetiol V[®] (oleic acid decylester), Labrasol[®] (polyoxylated capryl-caprinic acid glycerides) as surfactant, Plurol isostearique[®] (polyglycerol isostearate) as cosurfactant and triethanolamine-HCl (7.4) buffer as the aqueous phase in a ratio of 0.66:1:0.86:0.84. The results suggested that the microemulsion formulation itself may have had a glucogenic effect, resulting in an increase in plasma glucose, and that, furthermore the potency of the insulin in the microemulsion appears to be lost in about 14-28 days. Hence, without further alteration in the formulation the insulin within these microemulsions would not withstand prolonged storage, even at 4°C [215].

Oral delivery of insulin via a microemulsion based dosage form has also been tried on three human, insulin-dependent-diabetes-melitus patients. The w/o microemulsions in this study consist of an aqueous phase (containing the insulin and the protease inhibitor aprotinin), lecithin, cholesterol and non-esterified fatty acids. The resulting microemulsion was sprayed onto an inert carrier (carboxymethylcellulose calcium) and placed in hard gelatin capsules. All three patients experienced a reduction in blood glucose, and their diabetes was subsequently controlled on oral insulin over a long term trial of six months [216].

Another peptide which has been incorporated into a w/o microemulsion, and administered by various routes, is salmon calcitonin. The calcitonin contained in the formulation was found to lower the serum calcium levels in rats after both injection and GIT administration [217].

Gasco *et al* [218] have produced a biocompatible lecithin-based w/o microemulsion which contains the luteinizing hormone-releasing hormone analogue, [D-Trp-6]LH-RH. *In vitro* experiments suggested the w/o microemulsion formulation could be utilised for a few weeks, as the peptide within the microemulsion appeared to be partially protected from biodegradation by the environment. *In vivo* rat studies showed that a single IM dose of the analogue in the microemulsion reduced the testosterone levels of the treated group compared to the controls, and that the suppression of testosterone production was maintained for over three weeks.

1.5.7.2 Oil-in-water microemulsions.

Oil-in-water microemulsions are generally considered interesting for the delivery of oil soluble pharmaceuticals and vitamins. To date most o/w systems investigated for their use as a vehicle tend to also include a medium chain alcohol, such as butanol, as cosurfactant. The removal of such a cosurfactant from these microemulsions would be preferred for pharmaceutical applications. However although naturally occurring, biocompatible amphiphiles such as lecithin, do form microemulsions with cosurfactants such as butanol [196, 208] the systems formed when the alcohol is replaced by cholesterol [219], or not included at all [193], tend to be of larger particle size and greater polydispersity [220], and hence usually appear

turbid [221] even when subjected to prolonged sonication [219] or microfluidization [193, 219]. Although such systems can be used to incorporate lipid soluble drugs [222] their description as microemulsions is very tenuous and such systems are not considered here as true microemulsions.

Gasco and coworkers [223, 224, 225, 226, 227, 228] have investigated the incorporation of a number of drugs into o/w microemulsion systems. The formulations used usually contain isopropyl myristate (IPM) as oil phase, AOT, lecithin or a nonionic Tween (Tween 60 or 80) as surfactant, and butanol as cosurfactant.

The presence of two drugs, menadione ($\log P=2.2$) and prednisone ($\log P=1.46$) did not influence the stability of o/w microemulsions produced from IPM/butanol/water and either AOT or egg lecithin. At maximum solubility of the drugs in each system no change in the microemulsion composition was required, and the minimum amount of cosurfactant necessary to obtain transparent systems did not vary as a consequence of the added drug [194, 223].

The release rates of five steroid drugs of varying lipophilicities from AOT microemulsions have been investigated [224]. In all cases the *in vitro* release rates from the microemulsions were lower than those from solutions. The different release rates between microemulsions and solutions have been attributed to the partition of drugs between the dispersed oily droplets and the continuous phase of the microemulsion. Hence drug release from the microemulsions appears to be governed both by the transfer of the drug from the dispersed phase to the continuous phase, and by the diffusion of the drug from the continuous phase [224]. The release rate was also influenced by the amount of cosurfactant present. Consequently, the percentage of cosurfactant added to a formulation can allow different release rates of the same drug.

A similar trend was found using the lipophilic drug prednisone in an IPM/butanol/lecithin o/w microemulsion. The permeability constant of the prednisone out of the microemulsion formulation was reduced 4-5 times, compared to that of a solution. Furthermore, it appeared that as the drug was removed from the continuous phase, drug molecules partitioned from the internal phase in order to maintain the equilibrium. The potential reservoir

effect of the dispersed phase could also be modified by the cosurfactant [225].

Less lipophilic drugs would be expected to have less partitioning into the dispersed phase of an o/w microemulsion, and hence use of o/w microemulsions for delivering such drugs would offer only limited value as a prolonged release formulation. The lipophilicity of hydrophilic drugs can however be enhanced by the formation of lipophilic ion-pairs [226]. Ion-pair formation and incorporation into microemulsions has been tried for the water soluble drugs propranolol, in a formulation intended for transdermal delivery [227], and timolol, for ocular administration [196]. The permeability constant of propranolol from an IPM/Tween 60/butanol/pH 6.5 buffer o/w microemulsion containing octanoic acid was up to 10 times lower than that found without the counterion. Prolonged release of propranolol (with a propranolol:octanoic acid molar ratio of 1:16.4) was found to follow pseudo zero order kinetics over 48 hours [227]. Similarly the lipophilicity of timolol has been increased by octanoic acid ion-pair formation. Incorporation of the ion-pair into an IPM/butanol/egg lecithin/pH 7.4 buffer microemulsion allowed the concentration of the drug in the dispersed phase to be modulated, and the timolol release to be prolonged *in vitro* [196].

The bioavailability of timolol from ion-pair microemulsions, a solution of the ion-pair, and a solution of timolol alone, was tested *in vivo* by instillation into the conjunctival sac of rabbits. The amount of drug transported to the aqueous humour was measured. No inflammatory effects were observed from the microemulsions with, or in the absence of, drug. Results showed greater absorption of timolol from the microemulsion preparation compared to the aqueous solution (AUC 3.5x greater), with a longer absorption time. Comparison of the ion-pair solution to the aqueous solution also showed that the AUC increased (4.2x), but without the prolongation of absorption experienced with the microemulsions. The ion-pair microemulsion appeared to both enhance the bioavailability of the timolol in the external phase, and allow a reservoir effect in the dispersed phase to prolong absorption [228].

It should however be noted that a variation in the release of a drug can also occur due to interaction with the surfactant, which can also modify the reservoir effect of the dispersed phase of the microemulsion. This was observed when doxorubicine ($P_{\text{oct}}=0.52$ at pH 7) was added to o/w microemulsions produced from AOT or Tween 80. Almost all of this

hydrophilic drug would be expected in the external aqueous phase, but no release was found from either microemulsion. Ion-pair or complexation interactions between the drug and surfactant are suggested to be the cause of this observation [208].

Although a number of microemulsion systems of both the o/w and w/o type have been investigated for their potential as formulations for various drugs, many of the examples quoted above include the use of ionic surfactants, such as AOT, or the addition of a medium chain alcohol as cosurfactant. Because of their toxicity, use of such surfactants and cosurfactants is pharmaceutically undesirable. In the present investigation, the ability of commercial nonionic surfactants to produce o/w microemulsions (generally without the addition of an alcohol) was investigated. The compositions over which microemulsion systems exist, some of their physicochemical properties, and their ability to incorporate poorly water soluble drugs was studied.

CHAPTER TWO: Experimental

2.1 Materials

All materials obtained commercially were used as received. Triple distilled water obtained from a well-seasoned all-glass still was used throughout.

2.1.1 Surfactants

A range of commercially available polyoxyethylene ether surfactants of the C_mE_n type were used. The Brij[®] surfactants were supplied by Sigma Chemical Company Ltd (Poole, Dorset) and those of the Volpo[®] series from Croda Chemicals Ltd (Goole, North Humberside). The surfactants used are given in table 2.1.

2.1.2 Oils

Various oils were employed as the organic phase of the microemulsion systems. These included a range of hydrocarbon oils; heptane (FSA Laboratory Supplies, Loughborough), 1-heptene, octadecane (Sigma Chemical Company Ltd, Poole, Dorset), 1-octadecene, 1-hexadecene, (Fluka, Glossop, Derbyshire), hexadecane (Fluka, Glossop, Derbyshire or Aldrich Chemical Company Ltd, Gillingham, Dorset). Isopropyl myristate (IPM) was obtained from Sigma Chemical Company Ltd (Poole, Dorset). The triglycerides used were commercially available soybean oil (Sigma Chemical Company Ltd), super-refined soybean oil (gift from Croda Inc., USA) and Miglyol[®] 812 (gift from Hüls AG, Germany).

Table 2.1: Composition of the polyoxyethylene surfactants used.

Surfactant	Abbreviation	Trade Name(s)
polyoxyethylene–10–oleyl ether	$C_{18-1}E_{10}$	Brij 96 Volpo N10
polyoxyethylene–10–stearyl ether	$C_{18}E_{10}$	Brij 76
polyoxyethylene–10–cetyl ether	$C_{16}E_{10}$	Brij 56
polyoxyethylene–10–lauryl ether	$C_{12}E_{10}$	–
polyoxyethylene–20–stearyl ether	$C_{18}E_{20}$	Brij 78
polyoxyethylene–20–oleyl ether	$C_{18-1}E_{20}$	Brij 99
polyoxyethylene–5–oleyl ether	$C_{18-1}E_5$	Volpo N5
polyoxyethylene–4–lauryl ether	$C_{12}E_4$	Brij 35

2.1.3 Cosurfactants

Cosurfactants used were short to medium straight-chained alcohols; methanol (FSA Laboratory Supplies, Loughborough), butanol (BDH Ltd, Poole, Dorset), pentanol (Aldrich Chemical Company Ltd, Gillingham, Dorset) and the polyols; glycerol, xylitol and sorbitol (Sigma Chemical Company Ltd, Poole, Dorset).

2.1.4 Drugs

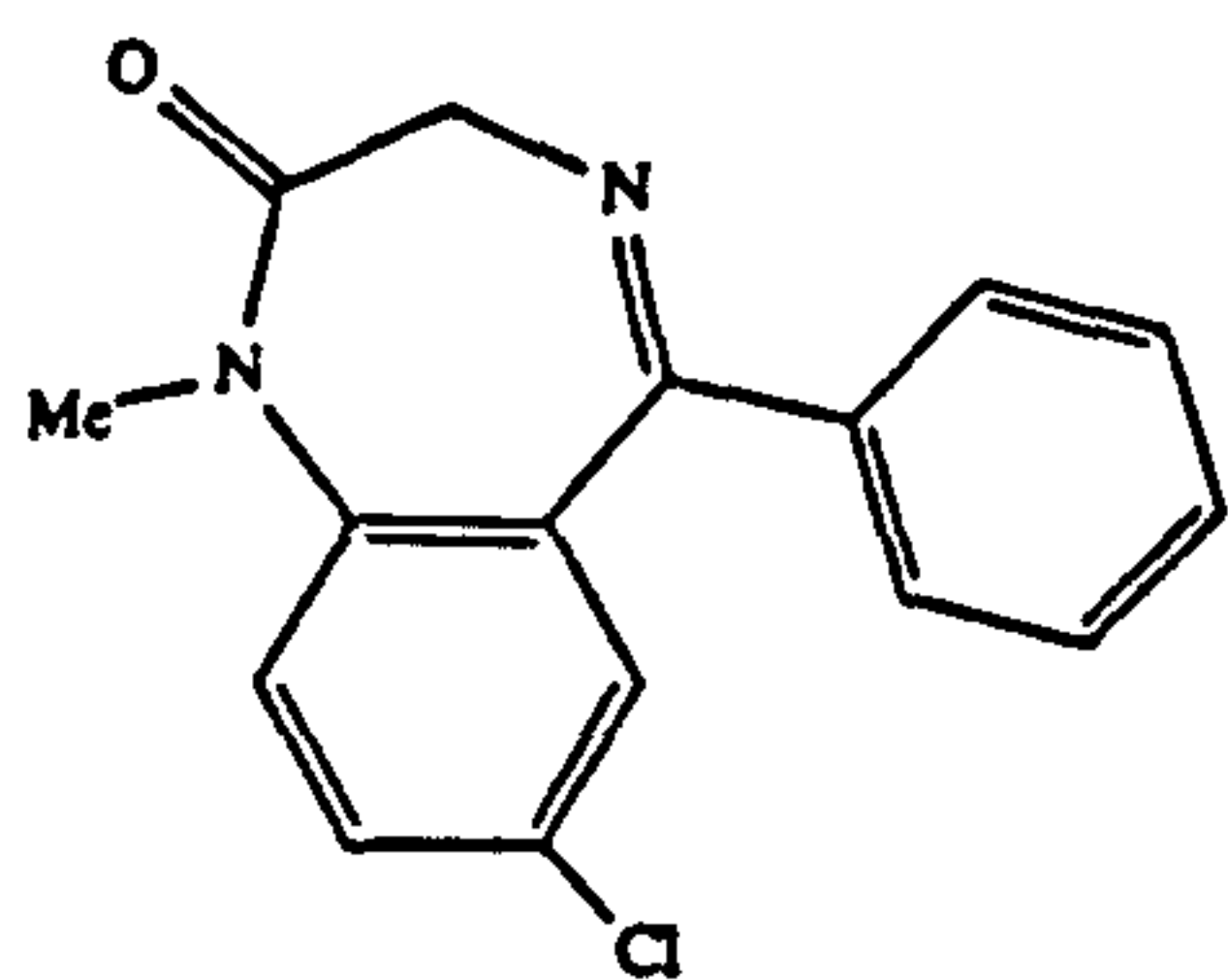
The incorporation of various drug molecules was tested in some microemulsion compositions. Drugs used were diazepam (gift from Roche Products Ltd, Welwyn Garden City), testosterone, testosterone propionate, testosterone enanthate (Sigma Chemical Company Ltd, Poole, Dorset), progesterone (gift from Cox Pharmaceuticals, Barnstaple, Devon) and medroxyprogesterone acetate (gift from Upjohn Ltd, Crawley, West Sussex). The structure and log P_{oct} values for each of these drugs is given in Table 2.1.

2.1.5 Miscellaneous chemicals

Dimethoxytetraethylene glycol (DMTG) was obtained from Sigma Chemical Company Ltd (Poole, Dorset) and sulphuric acid was from BDH Ltd (Poole, Dorset). Benzene (spectrophotometric grade) and toluene (spectrophotometric grade) were from Aldrich Chemical Company Ltd (Gillingham, Dorset).

Table 2.2: Drugs used in this study.

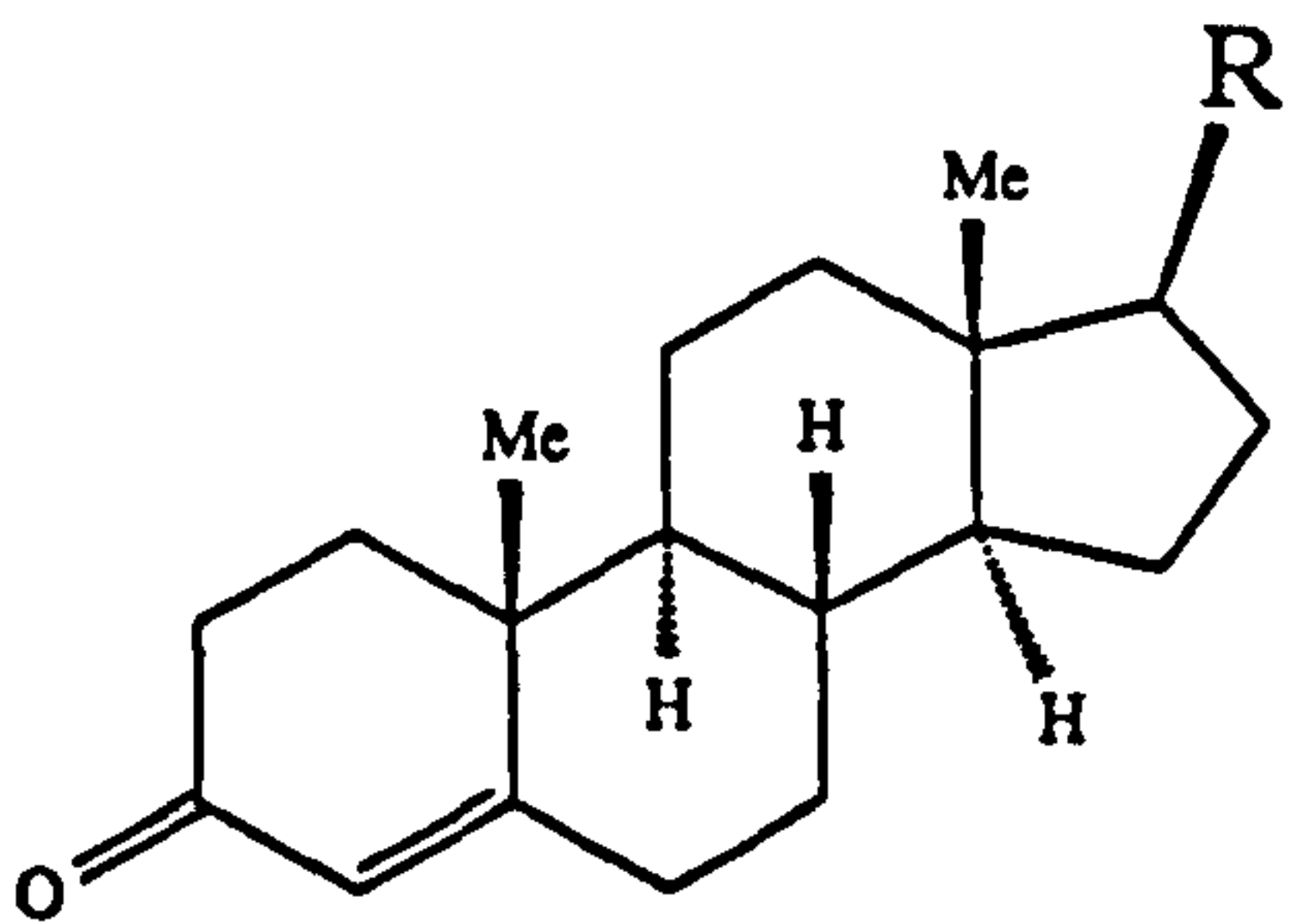
a: Diazepam



Mr	LogP _{Oct} *
284.8	3.18

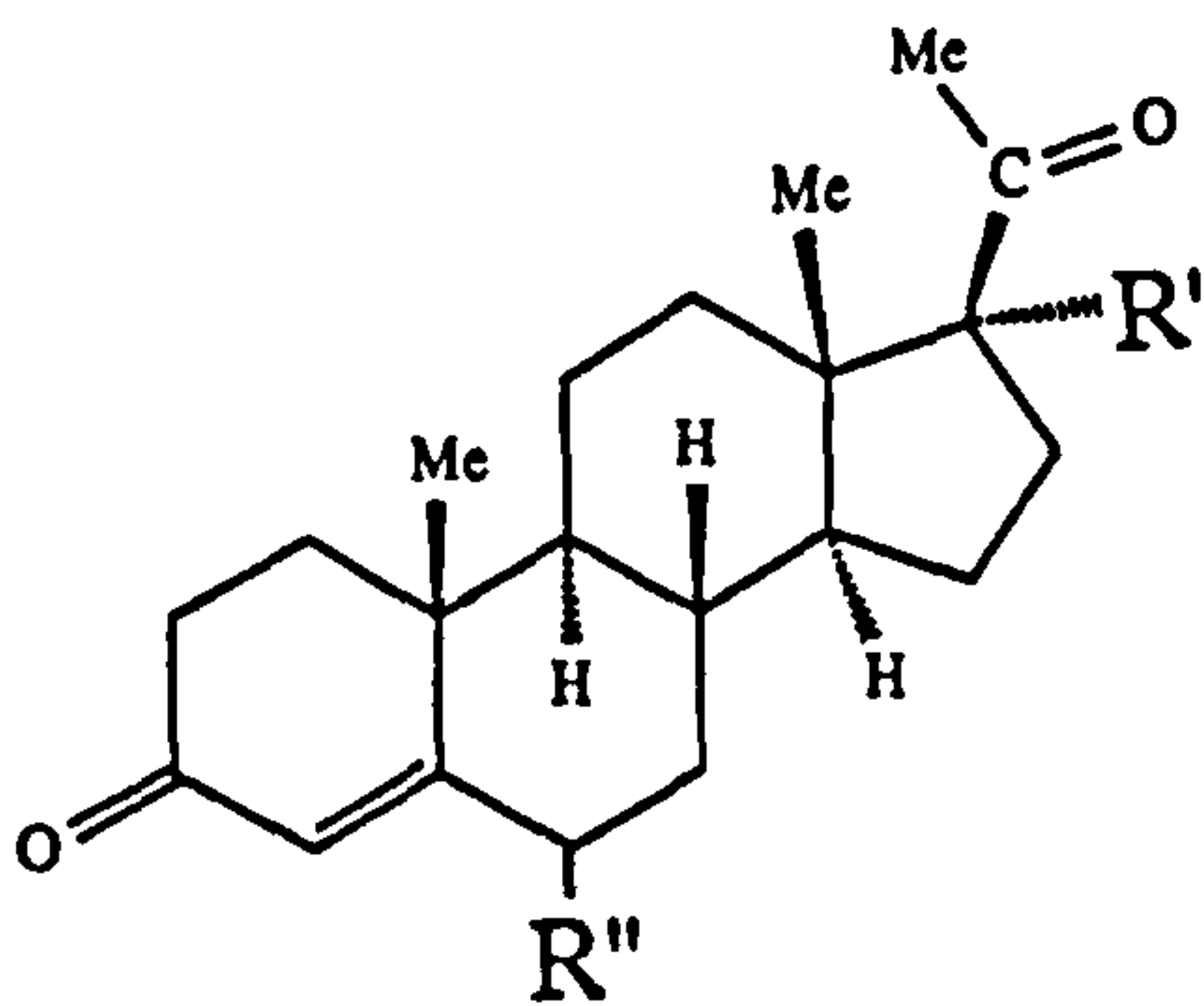
b: Steroids

i)



Drug	R	Mr	LogP _{Oct} *
testosterone	OH	288.4	3.35
testosterone propionate	OCOCH ₂ CH ₃	314.5	4.78
testosterone enanthate	OCO(CH ₂) ₅ CH ₃	400.6	6.90

ii)



Drug	R'	R''	Mr	LogP _{Oct} *
progesterone	H	H	314.5	3.85
medroxyprogesterone acetate	OCOCH ₃	CH ₃	386.5	4.27

* calculated values obtained from reference 229

2.2 Methods and apparatus

2.2.1 Microemulsion production

Samples were individually prepared by heating the required weight of oil, surfactant, water and, if required, cosurfactant or drug, in a closed container to 70°C with constant stirring for 5 minutes. Samples were then allowed to return to room temperature with constant stirring.

Compositions which appeared visibly clear, non-birefringent when observed through crossed polaroids, and liquid were classified as microemulsions.

2.2.2 Determination of phase diagrams

The areas of existence for microemulsion systems were determined by individually preparing a large number of compositions. Samples were inspected visually immediately, 24 hours, 7 days, and one month post-production and storage under ambient laboratory conditions.

Those samples which remained completely clear, isotropic, non-birefringent and liquid (ie Winsor IV systems discussed in section 1.2) after one month were included in the microemulsion area of existence. Samples which were turbid, exhibited phase separation or birefringence, or which formed clear or turbid gels were taken to lie outside the microemulsion area. This information was plotted on a triangular phase diagram, and the boundaries of the microemulsion domains drawn with an estimated accuracy of $\pm 1\%$ for each component. For the sake of clarity the experimental points tested have been omitted from some of the phase diagrams drawn.

Triangular phase diagrams were used to represent the areas of existence of both 3-component (oil/surfactant/water) microemulsions and 4-component systems (oil/surfactant/cosurfactant/water or drug/oil/surfactant/water).

In 3-component systems each apex of the triangular plot represents 100% of one of the three ingredients. Each point within the triangle represents

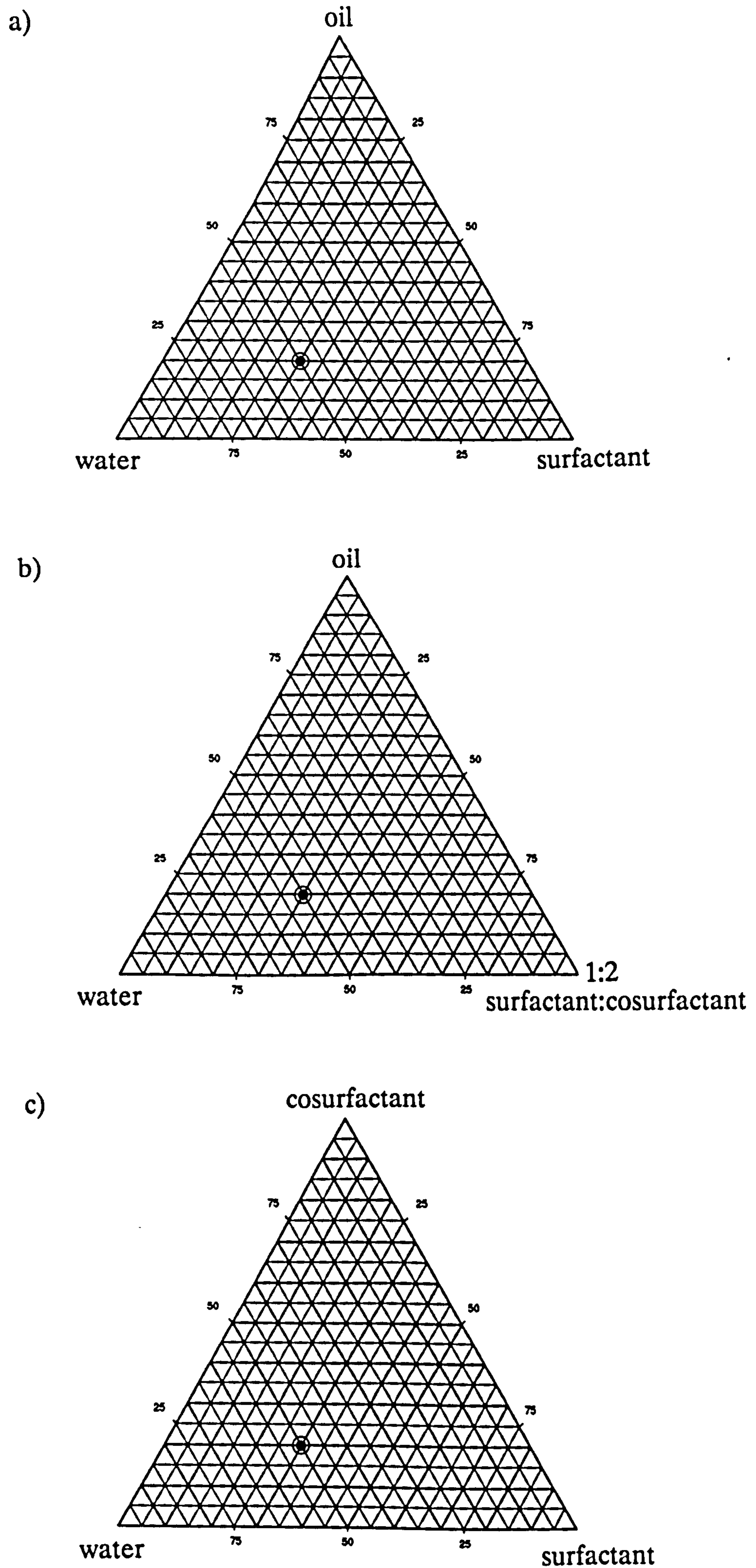


Figure 2.1: Alternative methods of constructing triangular phase diagrams; a) 3-component systems, b) 4-component systems with a fixed ratio of surfactant:cosurfactant (1:2) and c) 4-component systems with a constant percentage (5%w/w) of oil.

different combinations of the three components. Hence the point shown in figure 2.1a has a composition of 20% oil, 50% water and 30% surfactant.

In order to show the variation of four ingredients (ie oil, surfactant, cosurfactant and water) on a triangular plot, two different techniques are used. In the first method a triangular plot is constructed in which the ratio of surfactant to cosurfactant remains constant throughout the diagram. The surfactant apex of figure 2.1a then becomes a surfactant:cosurfactant apex. For example, in figure 2.1b a ratio of surfactant:cosurfactant of 1:2 has been chosen. Therefore the point drawn represents a composition of 20% oil, 50% water, 10% surfactant and 20% cosurfactant.

The alternative method which has been used to represent four components was to allow each triangular diagram to represent a constant percentage of oil phase throughout. The true proportion for any point on the triangle can be obtained for each of the other three components by multiplying the phase diagram proportion by $(100-x)/100$, where x is the percentage of oil for that particular phase diagram. Therefore in figure 2.1c, with 5% oil, the same point drawn represents a composition of 5% oil, 28.5% surfactant, 19% cosurfactant and 47.5% water.

Drug compounds were only added to 3-component microemulsion systems without cosurfactant. Hence these systems have been represented on triangular phase diagrams such as 2.1a in which an area of existence can be drawn for a particular concentration of drug. In making up these samples the amount of oil and surfactant was kept the same as in the corresponding drug-free microemulsion systems, and the amount of water was reduced to allow for the addition of drug.

2.2.3 Determination of maximum drug incorporation

The maximum incorporation of each drug was determined in both cosurfactant-free microemulsion systems and surfactant solutions within the same surfactant concentration range.

Samples were produced in the absence of drug as described in section 2.2.1. A known excess of drug was then added to each microemulsion or surfactant

solution. Each composition was tested in duplicate. The samples were allowed to equilibrate at $25\pm 1^{\circ}\text{C}$ in a shaking waterbath for eight days. After eight days excess drug was removed by filtration through a $0.22\mu\text{m}$ Millipore mixed cellulose ester (nitrate and acetate) filter, and appropriate dilution of samples carried out; diazepam-containing samples were diluted with 0.5% sulphuric acid in methanol, and steroid-containing samples with methanol only. After duplicate dilutions of each sample, the concentration of the resulting clear preparations were determined by ultraviolet analysis using a Perkin Elmer Lambda 5 spectrophotometer, employing blanks containing the equivalent concentration of surfactant and oil, and comparison with previously determined calibration curves for each drug. The resulting mean concentration ($n\geq 4$) of incorporated drug in surfactant solutions and microemulsions containing the same concentration of Brij 96 were compared using an unpaired t-test at a significance level of 95% ($P=0.05$).

Drug solubility was similarly determined in triple distilled water, various oil phases, and in varying concentrations (20-100%w/w) of DMTG in water. In contrast to aqueous samples, excess drug was removed from the oil and DMTG-containing samples by centrifugation.

2.2.4 Stability testing via temperature cycling

The stability of nine soybean oil/Brij 96/water microemulsions containing 0, 1, 2 and 4 %w/w testosterone enanthate were tested by temperature cycling. Samples were subjected to repeated cycles of exposure to a 30°C environment for 8 hours, followed by 16 hours in a 4°C environment for a total of 28 days.

Stability was assessed visually by the appearance of the microemulsion systems before and after treatment. In addition, PCS measurements were compared on day 1, 7, 14 and 28 for drug-free compositions, and on day 1 and 28 for drug-containing samples.

2.2.5 Determination of phase inversion temperature

The PIT of some of the microemulsions were determined using a thermometer inside a test-tube placed in a water bath. Samples were introduced into the

test-tube and heated fairly rapidly to get an approximation of the temperature at which turbidity occurred (ie the PIT). The temperature was then varied more slowly around the approximation of PIT at a rate of change of about 1°C per minute, until two temperature readings were obtained with increasing temperature (clarity to turbidity) and decreasing temperature (turbidity to clarity). The mean of these four temperatures was taken to be the PIT of the system.

2.2.6 Conductivity measurements

Conductivity was determined for test compositions across the area of existence of 4-component soybean oil/Brij 96/butanol/water microemulsions along selected tie-lines. Values were obtained as a consequence of a dielectric spectroscopy study in which readings of conductance, capacitance and dielectric loss were taken at frequencies between 0.01 and 10,000Hz, at 25°C. Each microemulsion sample was placed in a dielectric cell consisting of two metal electrodes of fixed separation distance. An alternating current was generated by a Frequency Response Analyser (FRA, Solatron) and passed through the sample via a Chelsea Interface (Chelsea Dielectrics Group). The signal was analysed by the FRA, and a printout of the data obtained. Readings of conductivity were extracted at three different frequencies (100, 1000 and 10,000Hz).

2.2.7 Density measurements

Measurements of density were required for interfacial tension (spinning drop tensiometer) determinations. They were obtained using a Paar DMA 35 density meter at the appropriate temperature if possible, by taking the mean of four separate readings. When the density of samples above 40°C were required, they were obtained by extrapolation of values gained at lower temperatures.

2.2.8 Interfacial tension measurements

Interfacial tension measurements were determined by two different

techniques. Tension values above $2\text{-}3\text{ mNm}^{-1}$ were collected using the du Nuoy ring method (fig.2.2a). This technique was used to test soybean oil/triple distilled water systems containing up to 10 %w/w Brij 96, and up to 10 %w/w of either butanol or glycerol as cosurfactant at room temperature. A spinning drop tensiometer technique [230] was used to determine the interfacial tension of soybean oil/water systems containing 20 %w/w Brij 96 and either 10 or 20 %w/w butanol, pentanol or glycerol, with increasing temperature.

The du Nouy platinum ring was attached to a digital multimeter (Intelligent multimeter, Thurlby 1905a, Radio Spares Co.). The system had been previously tested using the known surface tension of triple distilled water in order to obtain a calibration between voltage and tension for the meter. The multimeter was programmed to record the maximum, minimum and mean tension for each test. The maximum tension corresponds to the surface tension when the ring passes from liquid to air, or the interfacial tension when the ring passes from a lower aqueous phase to an upper oil phase.

Before each test the surface tension of triple distilled water in the test vessel was determined, and the vessel recleaned until a value of $72\pm0.5\text{mNm}^{-1}$ was obtained. Between readings the du Nuoy ring was cleaned by flaming. In order to avoid contamination of the ring, when determining the interfacial tension, the ring was lowered into position when only the lower aqueous phase (either water or surfactant solution) was present. The soybean oil phase (in which cosurfactant may have been previously added) was then carefully added on top of the water, the system was gently rotated, covered and allowed to equilibrate for five minutes, after which time an initial tension reading was taken. To determine the interfacial tension the ring was slowly drawn up through the lower aqueous phase, into the oil phase until it completely detached from the aqueous layer. The maximum tension was recorded, and the interfacial tension was taken as the maximum tension on the run minus the initial tension reading.

In order to determine the variation of lower interfacial tensions (generally $< 2\text{mNm}^{-1}$) with temperature, a Kruss spinning drop tensiometer Site 04 (Fig.2.2b) was used. Approximately 1mm^3 of soybean oil was injected into the horizontal capillary which was filled with aqueous phase (containing any surfactant and cosurfactant) and rotating about its long axis. Temperature

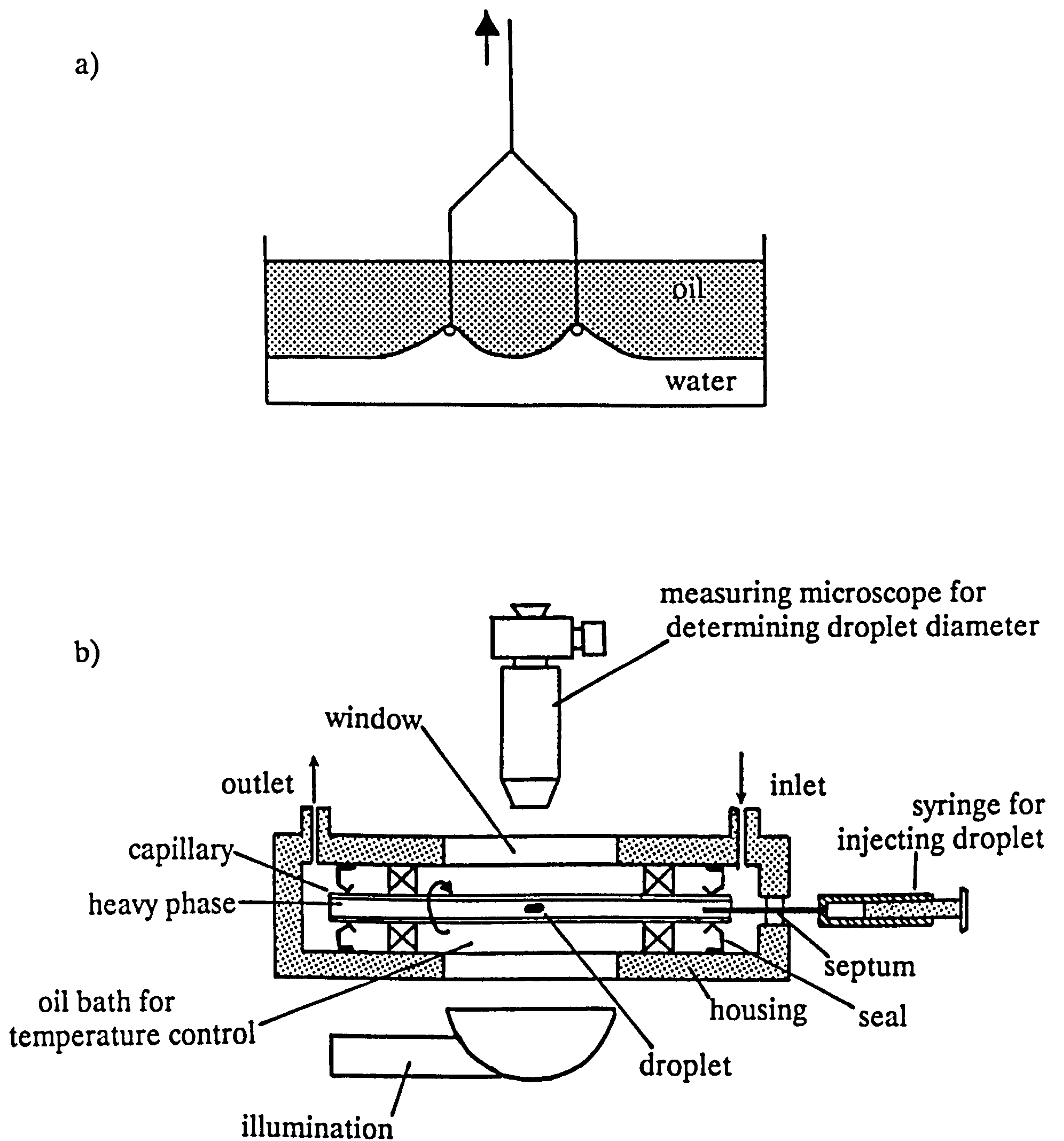


Figure 2.2: Apparatus used to determine interfacial tensions; a) du Nuoy tensiometer and b) Kruss spinning drop tensiometer.

was controlled by an attached oil bath, and the flow of the denser aqueous phase controlled so that a suitable drop of the soybean oil remained within the observation window. A few minutes was allowed for equilibrium at the selected temperature and rotation speed.

At a sufficiently high speed of rotation the droplet assumes the form of a cylinder with hemispherical ends. Provided the length of the droplet is greater than four times the diameter, interfacial tension, γ , is given by;

$$\gamma = \frac{1}{4} r_c^3 \Delta\rho \omega^2 \quad \text{eqn.14}$$

where;

r_c = cylinder radius of the droplet

$\Delta\rho$ = density difference between the 2 phases

ω = angular velocity

Equation 14 can be transferred to quantities measurable by the instrument;

$$\gamma = e (V d)^3 n_r^2 \Delta\rho \quad \text{eqn.15}$$

where;

V = magnification factor (mm/sdv)

sdv = scale division seen through microscope

d = diameter of the drop (sdv)

n_r = revolutions per minute (rpm)

e = specific machine constant of 3.427×10^{-7} (mN cm³ min²/m g mm³)

The density difference between the two phases was previously determined (see section 2.2.7), and the speed of rotation was displayed on the instrument. The magnification factor depends on the refractive index of the higher density liquid, the bath oil and the temperature. It was determined for each different aqueous phase and temperature using a calibrating wire of diameter 1.000mm (hence $V = 1.000/\text{sdv}$).

2.2.9 Refractive index measurements

Refractive index measurements were required for light scattering studies. For PCS investigations, the refractive index required is that of the external

phase. Samples tested were all cosurfactant-free 3-component microemulsions, in which the external phase was assumed to contain only water, and hence a value of 1.33 was used.

In TILS studies both absolute and differential values of refractive index were required. Experimental refractive index determinations were obtained using an Abbe 60/ED degree scale refractometer (Bellingham and Stanley, Sevenoaks). The experimental temperature of 30°C was maintained by circulating water from a temperature-controlled waterbath through the housing of the prism. The refractive index of each sample was determined at three different wavelengths (589.6, 546 and 436nm). Measurement at 589.6nm was obtained using a sodium light source, and at 546nm a mercury light source with an attached green filter was employed. A scale reading was obtained at these two wavelengths by manipulation of the mirror until the borderline between light and dark regions was positioned at the centre of the crosswires in the eyepiece. Under these conditions the scale reading in the other eyepiece was noted. The reading at 436nm was achieved using the blue spectral line of an unfiltered mercury light source, in which case the reading was taken when the blue line passed through the centre of the crosswires of the eyepiece. Three readings were taken from each of two aliquots of the same sample, and the mean of the six measurements converted directly to refractive index at each wavelength using relationships supplied with the instrument. The refractive index at 488nm was interpolated from plots of refractive index vs λ^{-2} for the three experimentally determined values, according to the Cauchy formula [231].

2.2.10 Light scattering studies

Light scattering studies (PCS and TILS) were carried out on undiluted microemulsion samples using a Malvern 4700c light scattering instrument (Malvern Instruments Ltd) equipped with a 75mW Argon ion laser operating at a wavelength of 488nm.

The apparatus was set up as shown in figure 2.3. Light scattered by the sample was detected by a photomultiplier (PM) mounted on a turntable which could be adjusted by a stepper motor control unit to allow measurement between 10 and 170° to the incident beam. Temperature

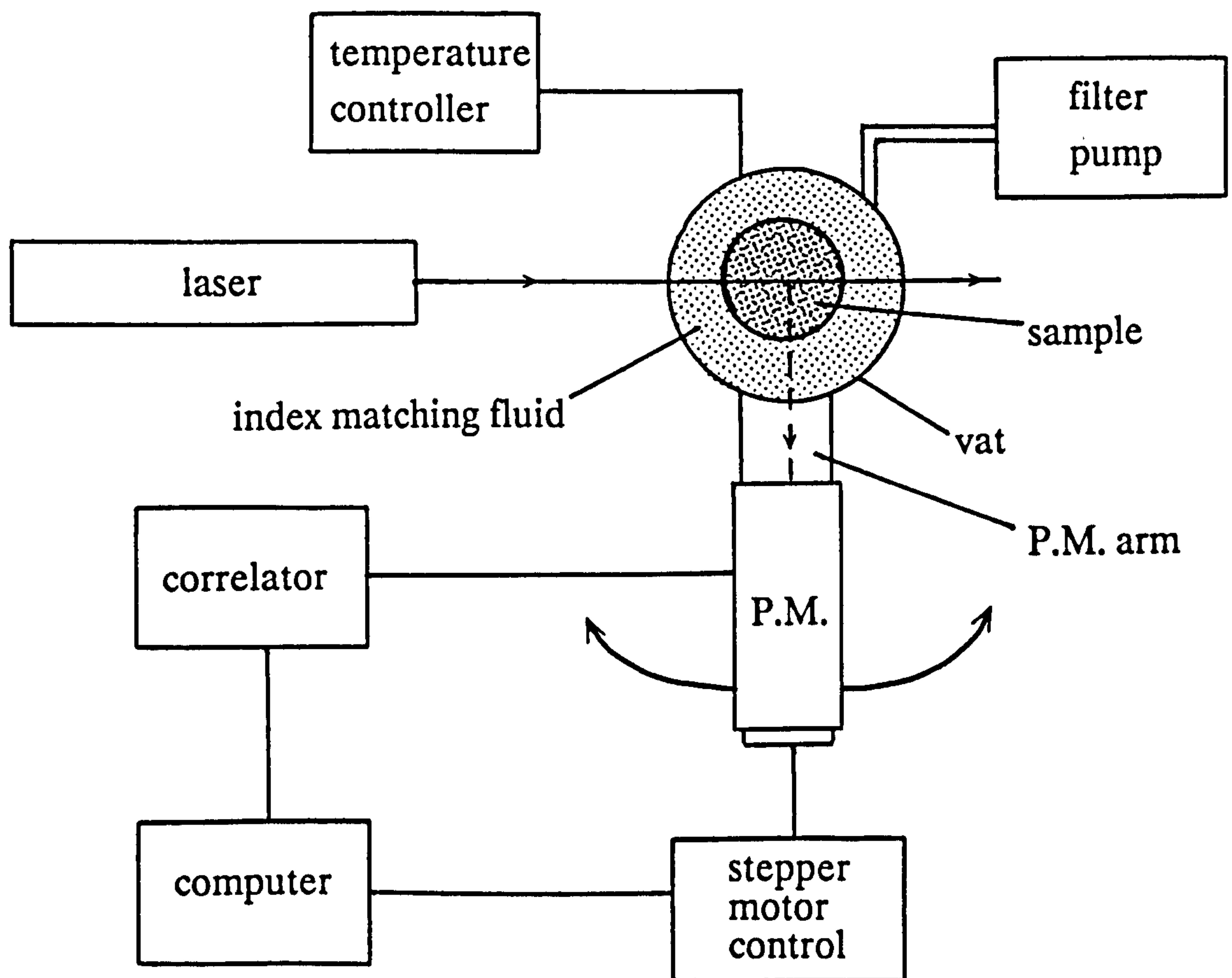


Figure 2.3: Schematic diagram of Malvern 4700c laser light scatter

control (accurate to 0.1°C) was obtained by the temperature control unit and an attached waterbath. The index matching fluid employed was triple distilled water which was refiltered, via the attached filter pump, through a $0.45\mu\text{m}$ filter after the addition of each new sample. The count rate (photons per second) measured by the PM could be altered by adjustment of the intensity of the laser and by the aperture of the PM tube and was displayed on the visual display unit of the attached computer. The attached 128-channel correlator allowed PCS measurements to be conducted, which were initiated and analysed by the Malvern software in the computer unit.

2.2.10.1 Photon correlation spectroscopy

PCS was employed to investigate the size distribution of o/w cosurfactant-free microemulsion samples containing soybean oil, Brij 96 and triple distilled water of varying composition within the area of existence found. The values found were compared to samples when the nature of the oil phase was varied, and when the drug, testosterone enanthate, was added.

Samples were analysed (most usually at a scattering angle of 90°) using the auto-sizing function of the Malvern 4700 in intensity mode. Except for those samples tested as part of the stability study, all samples had been prepared the previous day. Each was filtered three times through a $0.22\mu\text{m}$ Millipore cellulose acetate/nitrate filter and generally tested in disposable 4-clear sided fluorimeter cells (used once only) with plastic stoppers. Compositions containing heptane and 1-heptene were tested in clear sided quartz cells. Samples tested at 45 and 135° in order to investigate the possibility of angular dependence, or which were tested in the same experimental session by both TILS and PCS, were contained within glass Buchard cells with teflon stoppers. In all cases 10-15 minutes was allowed before analysis for the sample to equilibrate at the testing temperature. The intensity of the incident laser beam and PM tube aperture was adjusted so that each sample was tested at a photon count rate of approximately 200,000 counts per second.

Photon correlation spectroscopy (PCS) is also known as quasielastic light scattering (QELS or QLS) and dynamic light scattering (DLS). Brownian motion of particles causes the scattering of light, and causes the intensity of the scattered light to vary with time. Large particles will move more slowly

and hence result in slower intensity fluctuations. PCS employs the rate of change of light fluctuations to determine the size distribution of the particles scattering light. Each of the 128 channels of the correlator measures the change in light fluctuation over a particular sample time. For particles of a single size, a plot of counts per correlator channel against delay time produces a single exponentially decreasing function. Where more than one size of particle is present the correlation function is a sum of many different exponentials. Analysis of the autocorrelation function is obtained over a period of time and with sufficient data points the diffusion coefficient of the particles can be determined.

The correlation function is determined by;

$$G(t) = \langle N' \rangle^2 \{1 + B \exp (-t/t_c)\} \quad \text{eqn.16}$$

where;

N' = average intensity measured in photons per unit time

B = a constant, less than 1, which depends on the optics

t = delay time

t_c = characteristic decay time

In the simplest case of identical spheres diffusing freely, t_c is related to the diffusion coefficient of the scattering particles by;

$$t_c = (DK_s^2)^{-1} \quad \text{eqn.17}$$

where;

D = diffusion coefficient of the scatterers

K_s = the light scattering vector

$$= \left(\frac{4 \pi RI}{\lambda_0} \right) \sin \left(\frac{\theta}{2} \right) \quad \text{eqn.18}$$

RI = the refractive index of the liquid in which the scatterers are suspended

λ_0 = wavelength of light in a vacuum

θ = scattering angle of observation

The software used with the Malvern 4700c analyses the correlation function by taking its log and fitting a power series;

$$Y(t) = A + Bt + Ct^2 \quad \text{eqn.19}$$

where;

$Y(t)$ = log of the correlation function

t = delay time

A, B & C are constants fitted by analysis

A is the intercept on the y-axis, related to the signal-to-noise ratio. B represents the *Z-average mean* size, used by Malvern to give the mean of the particles weighted by the amount of scattered light. C is related to the width of the size distribution. C/B^2 gives the polydispersity.

To achieve a Z-average mean diameter the Rayleigh-Gans-Debye (RGD) theory is used. This theory assumes all the droplets are spherical, and does not require the refractive index of the scattering particles. The viscosity of the external phase is required. In all microemulsions tested by PCS the external phase was assumed to be water. The corresponding viscosity of water at experimental temperature was automatically selected and applied by the Malvern software accompanying the light scattering instrument.

Assuming interactions between particles can be neglected (ie the existence of non-interacting spheres) the hydrodynamic diameter of the spheres can be obtained from the Stokes-Einstein equation;

$$d = \frac{kT}{3 \pi D \eta} \quad \text{eqn.20}$$

where;

d = diameter of spheres

k = Boltzmann constant

T = absolute temperature

D = diffusion coefficient

η = viscosity of the suspending fluid

2.2.10.2 Total intensity light scattering

A range of o/w microemulsions of the soybean oil/Brij 96/triple distilled water type, both with and without drug, were investigated using TILS. Each sample was filtered three times through two 0.22 μ m Millipore mixed cellulose ester filters, followed by at least two filterings through a lower 0.1 μ m and

upper 0.22 μ m filter. Samples were tested in a glass Buchard cell with a teflon stopper and allowed to equilibrate to temperature for 10-15 minutes in the sample chamber before testing.

The intensity of scattered light (for the same laser strength and PM aperture) at 45 $^{\circ}$ and 135 $^{\circ}$ was determined to check for dust. Samples with a ratio of scatter for these two angles greater than 1.1, or in which there was a large variation in the intensity readings at 45 $^{\circ}$ were refiltered.

The TILS measurements were taken at 90 $^{\circ}$. The intensity of the incident laser beam and PM aperture were adjusted to give a photon count of between 1,000,000 - 1,500,000 counts per second, allowing the highest possible counts for the low scatter of the toluene standard, while still maintaining linearity of the PM tube. Manipulation of beam intensity and aperture also allowed more than one reading to be taken within this range of count rate.

In order to avoid the continued use of benzene, the relative scatter of toluene to benzene at 488nm and 30 $^{\circ}$ C over a range of intensity and aperture settings was determined. A mean ratio of the scatter of benzene/scatter of toluene of 0.88 was found. The scattering intensity of each microemulsion sample was calibrated against benzene by taking the count rate of a filtered sample of toluene (spectrophotometric grade) at identical incident beam intensity and PM tube aperture, and multiplying the toluene scatter by 0.88. The resulting ratio of scatter by the microemulsion to scatter by benzene was corrected for solvent scatter by subtracting the ratio of scatter of water to benzene (0.1875). Hence the corrected value for the scattering intensity of the microemulsion, or micellar sample, (S_{90}) was obtained.

The Rayleigh ratio, at 90 $^{\circ}$, of each sample relative to benzene was then calculated by;

$$R_{90}(\text{microemulsion}) = S_{90}(\text{microemulsion}) \times R_{90}\text{benzene} \quad \text{eqn.21}$$

where a value of $R_{90}\text{benzene}$ at 30 $^{\circ}$ C and 488nm of $3.259 \times 10^{-5} \text{ cm}^{-1}$ was used [232].

2.2.10.3 Analysis of TILS data

The molecular weight of a Brij 96 micelle, and the area occupied by a Brij 96 head group (a_0) were determined by analysis of TILS data for concentrations of surfactant of up to 2% using the relationship;

$$\frac{K_1 c}{R_{90}} = \frac{1}{M} + 2B c \quad \text{eqn.22}$$

where;

K_1 = an optical constant

c = concentration

R_{90} = Rayleigh ratio of sample relative to benzene

M = molecular weight of the scattering unit

B = second virial coefficient

At very low concentrations, the virial coefficient can be ignored and equation 22 may be simplified to;

$$\frac{K_1 c}{R_{90}} = \frac{1}{M} \quad \text{eqn.23}$$

and hence;

$$M = \frac{R_{90}}{K_1 c} = \frac{S_{90} \times R_{90}(\text{benzene})}{K_1 c} \quad \text{eqn.24}$$

For vertically polarized incident, and unpolarized scattered light [233];

$$K_1 = \frac{4 \pi^2 R_{I_0}^2}{\lambda_0^4 N_A} \left(\frac{dRI}{dc} \right)^2 \frac{R_{I_{\text{benzene}}}^2}{R_{I_0}^2} \quad \text{eqn.25}$$

where;

R_{I_0} = RI of the solvent

$R_{I_{\text{benzene}}}$ = RI of benzene

λ_0 = wavelength of light *in vacuo*

N_A = Avogadro number

$\left(\frac{dRI}{dc} \right)$ = change of refractive index of the surfactant solution with concentration

c = concentration

Hence;

$$M = \frac{R_{90}(\text{benzene}) \lambda_0^4 N_A}{4 \pi^2 RI_{\text{benzene}}^2} \frac{1}{(dRI/dc)^2} \frac{S_{90}}{c} \quad \text{eqn.26}$$

=>

$$M = A \frac{1}{(dRI/dc)^2} \frac{S_{90}}{c} \quad \text{eqn.27}$$

where A is a temperature-dependent constant, having a value of 1.2375 cm³mol⁻¹ at 30°C. S₉₀/c was obtained from the slope of the initially linear portion of the plot of S₉₀ against concentration of Brij 96, and (dRI/dc) was obtained from the slope of the plot of refractive indices of Brij 96 solutions versus surfactant concentration for measurements taken using a sodium lamp (589.6nm).

The aggregation number of the surfactant micelle was therefore obtained by dividing the molecular weight of the aggregate (M) by the molecular weight of one surfactant molecule.

The volume of the micelle was estimated by multiplying the aggregation number by the volume of the surfactant hydrophobe, v, and assuming the existence of spherical micelles, a radius and total surface area was obtained. Division of the total surface area of the micelle by the aggregation number allowed an estimation of a₀.

Data from TILS studies of microemulsions was analysed by a procedure based on the use of the Percus and Yevick hard sphere model for interparticulate interaction previously used by Attwood and Ktistis [234] for o/w microemulsions produced from IPM, polysorbate 60, sorbitol and water. In this model the microemulsion structure is assumed to consist of spherical oil droplets surrounded by a surfactant interface, and it is necessary to initially attain a first approximation of the size of these droplets.

In the present study the assumption was made that all the oil (soybean oil) and all the surfactant (Brij 96) in the composition was present in the

monodisperse, spherical microemulsion droplets, and that the external phase consisted only of water. Based on this spherical droplet model two radii were defined. The first, r_1 , constitutes the radius of the hydrocarbon core of the microemulsion droplet which consists of both the soybean oil and the hydrophobic portions of the surfactant molecules. The second radius, r_2 , is that of the entire anhydrous microemulsion particle; that is, the central oil core and all of the surfactant molecule including both the inner hydrophobic chain and the outer ethylene oxide hydrophilic group.

The surface area of the inner droplet defined by r_1 will be the product of the area occupied by one surfactant molecule (a_o) and the number of surfactant molecules in one microemulsion droplet (n_s).

Hence;

$$4 \pi r_1^2 = n_s a_o \quad \text{eqn.28}$$

The volume of the inner droplet will be the sum of the volume of all the oil molecules and the hydrophobic portions of all the surfactant molecules present in one droplet, ie;

$$\frac{4 \pi r_1^3}{3} = n_o v_o + n_s v \quad \text{eqn.29}$$

where;

n_o = number of oil molecules in one microemulsion droplet

v_o = volume of the oil molecule

v = volume of the surfactant molecule hydrophobe

The relative numbers of oil and surfactant molecules per droplet depends on the molar ratio, f , of these two components in the formulation, hence;

$$f = \frac{n_o}{n_s} = \frac{\text{weight oil}}{\text{weight surfactant}} \times \frac{M_r \text{ surfactant}}{M_r \text{ oil}} \quad \text{eqn.30}$$

and so

$$n_o = f n_s \quad \text{eqn.31}$$

Therefore r_1 can be calculated by combining equations 28, 29 and 31;

$$\frac{4/3 \pi r_1^3}{4 \pi r_1^2} = \frac{f n_s v_o + n_s v}{n_s a_o} \quad \text{eqn.32}$$

=>

$$r_1 = \frac{3(fv_o + v)}{a_o} \quad \text{eqn.33}$$

Once r_1 is known the number of surfactant molecules per droplet (n_s) can be calculated from equation 28, and the larger radius, r_2 derived as follows:

If V_x is the volume of the surfactant headgroup shell, then;

$$V_x = n_s v_h \quad \text{eqn.34}$$

where v_h is the volume of the hydrophilic group of the surfactant, calculated by multiplying the number of ethylene oxide groups by the molecular volume of a single ethylene oxide, 65.7\AA^3 [235].

V_x is also the difference in the volumes of the sphere defined by the radii r_1 and r_2 , ie;

$$V_x = \frac{4 \pi r_2^3}{3} - \frac{4 \pi r_1^3}{3} \quad \text{eqn.35}$$

Combination of equations 34 and 35 shows that r_2 can be calculated from the equation;

$$r_2 = \left[\frac{3 n_s v_h}{4 \pi} + r_1^3 \right]^{1/3} \quad \text{eqn.36}$$

and the volume of the total anhydrous droplet, V_{r2} given by;

$$V_{r2} = \frac{4 \pi r_2^3}{3} \quad \text{eqn.37}$$

The volume fraction of the microemulsion droplets in a water external phase (ϕ_{r2}) was estimated from V_{r2} and the volume of the bulk water phase per microemulsion droplet (V_w). The number of water molecules associated with each microemulsion droplet was calculated according to the molar ratio of total water to total surfactant present in the composition, and the number of surfactant molecules per droplet (n_s) previously calculated using equation 28. So;

$$n_w = n_s \times \frac{\text{weight water}}{\text{weight surfactant}} \times \frac{M_r \text{ surfactant}}{M_r \text{ water}} \quad \text{eqn.38}$$

where;

n_w = the number of water molecules associated with each droplet

Hence V_w can be calculated by;

$$V_w = n_w \times 29.9 \quad \text{eqn.39}$$

where 29.9\AA^3 is the molecular volume of one water molecule [236].

Therefore ϕ_{r2} can be obtained by;

$$\phi_{r2} = \frac{V_{r2}}{V_{r2} + V_w} \quad \text{eqn.40}$$

With model values of r_2 and V_{r2} , the interpretation of TILS results was carried out according to the method previously used to interpret w/o [237, 238] and o/w [234] microemulsion scattering data. The Rayleigh ratio R_θ at a scattering angle, θ , for unpolarised light is given by the equation;

$$R_\theta = K_O (1 + \cos^2 \theta) M c P(Q) S(Q) \quad \text{eqn.41}$$

where;

M = molecular mass of the scattering units

c = concentration

K_O = an optical constant

$P(Q)$ = the particle scattering form factor

$S(Q)$ = the structure factor

and Q is the scattering vector for a sample with refractive index RI given by;

$$Q = \frac{4 \pi RI \sin(\theta/2)}{\lambda_0} \quad \text{eqn.42}$$

K_O is an optical constant defined by;

$$K_O = \left[\frac{9 \pi^2 RI^4}{2 N_A \lambda_0^4 \rho_s} \right] \left[\frac{RI_s^2 - RI^2}{RI_s^2 + 2RI^2} \right]^2 \quad \text{eqn.43}$$

where;

RI_s = refractive index of the scattering units

ρ_s = density of scattering units

The particle scattering form factor, $P(Q)$, is given by;

$$P(Q) = [3(\sin QR - QR \cos QR) / (Q^3 R^3)]^2 \quad \text{eqn.44}$$

where R is the radius of the scattering particles.

The structure factor, $S(Q)$, is included to allow for interparticle interactions in concentrated systems and has the form;

$$S(Q) = 1 + \frac{4 \pi N_s}{Q} \int_0^\infty [g(r_s) - 1] r_s \sin Q r_s dr_s \quad \text{eqn.45}$$

where;

N_s = the number of scattering units per unit volume ($= 1/\Phi_{r2}$)

r_s = the distance between the centres of the scattering units

$g(r_s)$ = the particle radial distribution function

In this model the scattering units are assumed to be spheres of radius r_2 with a volume fraction in the sample of Φ_{r2} , hence the molecular mass and concentration of scattering units can be represented by;

$$M = \frac{4 \pi r_2^3}{3} \rho_s N_A \quad \text{eqn.46}$$

and

$$c = \Phi_{r2} \rho_s \quad \text{eqn.47}$$

Furthermore, all scattering measurements were carried out at 90° , and so equation 41 can be rewritten as;

$$R_{90} = K_2 \Phi_{r2} r_2^3 S(90) P(90) \quad \text{eqn.48}$$

where;

$$K_2 = \frac{6 \pi^3 R I^4}{\lambda_o^4} \left[\frac{R I_s^2 - R I^2}{R I_s^2 + 2 R I^2} \right]^2 \quad \text{eqn.49}$$

The interparticle interactions between the scattering units, $S(Q)$, was estimated using the relationship;

$$S(Q) = [1 - N_s c (2QR_{HS})]^{-1} \quad \text{eqn.50}$$

with

$$c(2QR_{HS}) = -32 \pi R_{HS}^3 \int_0^1 \frac{\sin(2sQR_{HS})}{2sQR_{HS}} \times \frac{(\alpha + \beta s + \gamma s^3)}{s^2} ds \quad \text{eqn.51}$$

where R_{HS} is the hard sphere radius.

R_{HS} was taken to be the calculated anhydrous radius of the o/w microemulsion droplet (r_2) plus a thickness, t_1 . That is;

$$R_{HS} = r_2 + t_1 \quad \text{eqn.52}$$

By supplying the calculated values of r_2 and Φ_{r2} , and assuming that the refractive index of the scattering units at 488nm ($R I_s$) was that of the soybean oil, an iterative method of calculation was used which altered the values of t_1 (and hence R_{HS}) to give the best fit between the calculated R_{90} (from eqn.48) and the experimentally determined R_{90} .

The volume fraction of spheres of radius R_{HS} (ϕ_{HS}), was then calculated from;

$$\phi_{HS} = \frac{R_{HS}^3}{r_2^3} \phi_{r2} \quad \text{eqn.53}$$

and the coefficients α , β and γ , in equation 51, defined by;

$$\alpha = (1 + 2\phi_{HS})^2 / (1 - \phi_{HS})^4 \quad \text{eqn.54}$$

$$\beta = -6 \phi_{HS} (1 + 0.5 \phi_{HS})^2 / (1 - \phi_{HS})^4 \quad \text{eqn.55}$$

$$\gamma = 0.5 \phi_{HS} (1 + 2 \phi_{HS})^2 / (1 - \phi_{HS})^4 \quad \text{eqn.56}$$

CHAPTER THREE: Soybean oil/Brij 96/water microemulsions

3.1 Area of existence

Three component microemulsion systems were found to form (and remain stable under ambient laboratory conditions) with commercially available soybean oil, Brij 96 and triple distilled water. Initially two regions were observed, one at lower surfactant concentration, and another, much smaller region, close to the Brij 96 apex. Samples within this latter region remained clear for 7 days, after which time, however, they became increasingly turbid and took on the appearance of a macroemulsion system (Fig.3.1). The area found at lower surfactant concentrations was determined by the appearance of the individual microemulsion samples after one month at ambient conditions. Those samples stable after one month appeared to remain clear for time periods in excess of one year, and were therefore presumed to represent the region containing indefinitely stable microemulsion systems.

The stable microemulsion area found at lower surfactant concentrations (Fig.3.2) is in contrast to that found by Kale and Allen [239] who could not produce microemulsions using light liquid paraffin, Brij 96 and water in the absence of cosurfactant. The region found in this study does however cover a similar concentration range to that found for the isotropic water-continuous phase, L_1 , for paraffin/Brij 96/water systems found by Gradzielski *et al* [171], the mineral oil/Brij 96/water systems of Orecchioni *et al* [240] and the L_1 phases observed by Lo *et al* [241] using ten different oils. Although, unlike these three studies [171, 240, 241], the area observed here does not extend to the water apex. This difference could however be explained by the larger number of compositions concentrated around this area of existence

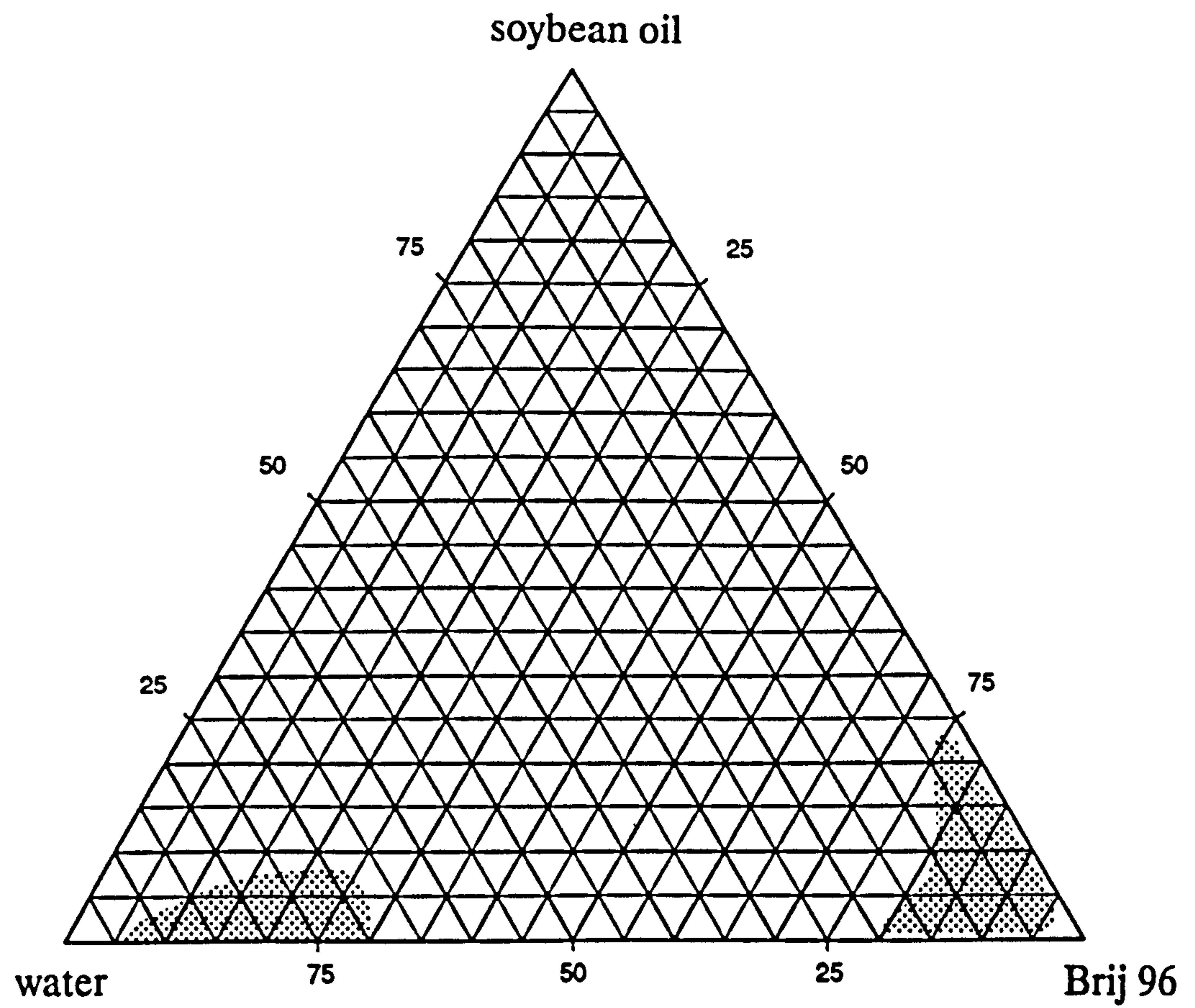


Figure 3.1: Triangular phase diagram showing the initial regions of clear liquid compositions occuring for soybean oil/Brij 96/water systems.

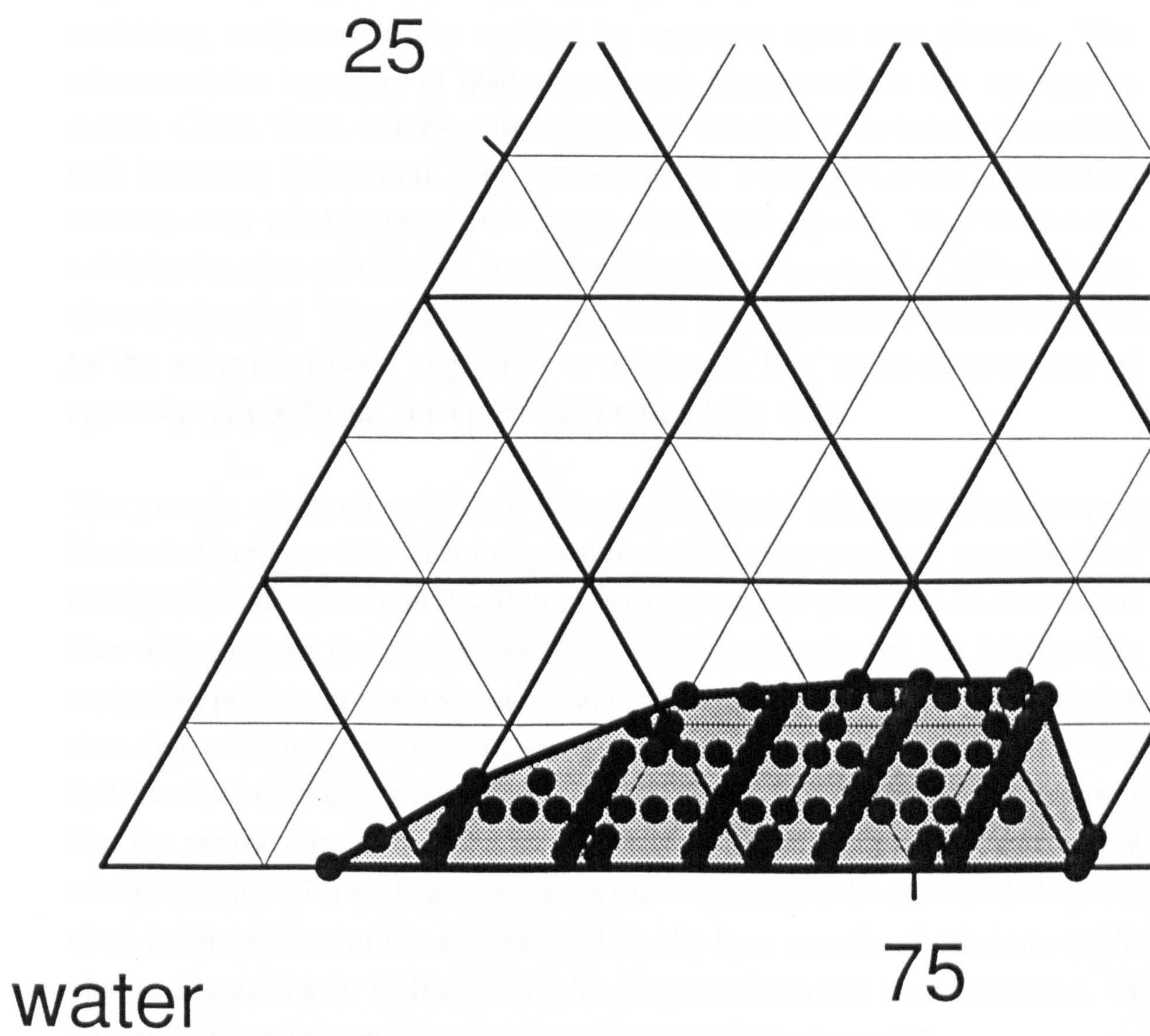


Figure 3.2: Partial phase diagram showing the area of o/w microemulsion existence for soybean oil/Brij 96/water systems.

that were produced in this study, allowing the region to be more closely defined. It was also observed that the microemulsion compositions individually produced within the shaded area shown in figure 3.2 could be diluted with water to compositions closer to the water apex which, although outside the microemulsion region, remained clear.

The area of microemulsion existence shown in figure 3.2 lies between 8-28 %w/w Brij 96, with a maximum incorporation of about 6.5 %w/w soybean oil occurring at approximately 20-22 %w/w surfactant. Compositions outside this region of existence towards the water apex, exhibited varying degrees of turbidity, and eventually tended to separate into two phases. The microemulsion boundary at higher surfactant concentrations was not easy to define. Clear, fluid, microemulsion systems tended to increase in viscosity with increasing Brij 96 until gel systems formed. These gels could also form in initially clear fluid systems after some time had elapsed. They sometimes exhibited a ring on tapping, and birefringence was usually (although not always) observed. The appearance of a clear gel region immediately adjacent to the microemulsion region at a minimum Brij 96 concentration of approximately 30% has been previously noted [170, 171].

The present study concentrated around the liquid microemulsion systems illustrated in figure 3.2. This fairly water-rich, oil-poor region is most likely to consist of oil droplets stabilised in an external water phase by an interfacial film of surfactant molecules [85, 242]. Due to the size of the triglyceride molecules present in the soybean oil and the length of the hydrocarbon chains that they contain, the oil is not expected to significantly penetrate into the hydrocarbon chains of the surfactant [243, 244]. It is therefore anticipated that the central core of the o/w microemulsion droplet will consist exclusively of soybean oil. This soybean oil core is then expected to be surrounded by the oleyl hydrocarbons of the Brij 96, and finally by a mantle of ethylene oxide chains, increasing in hydration as the distance from the core increases. A model for the microemulsion droplets is postulated in figure 3.3.

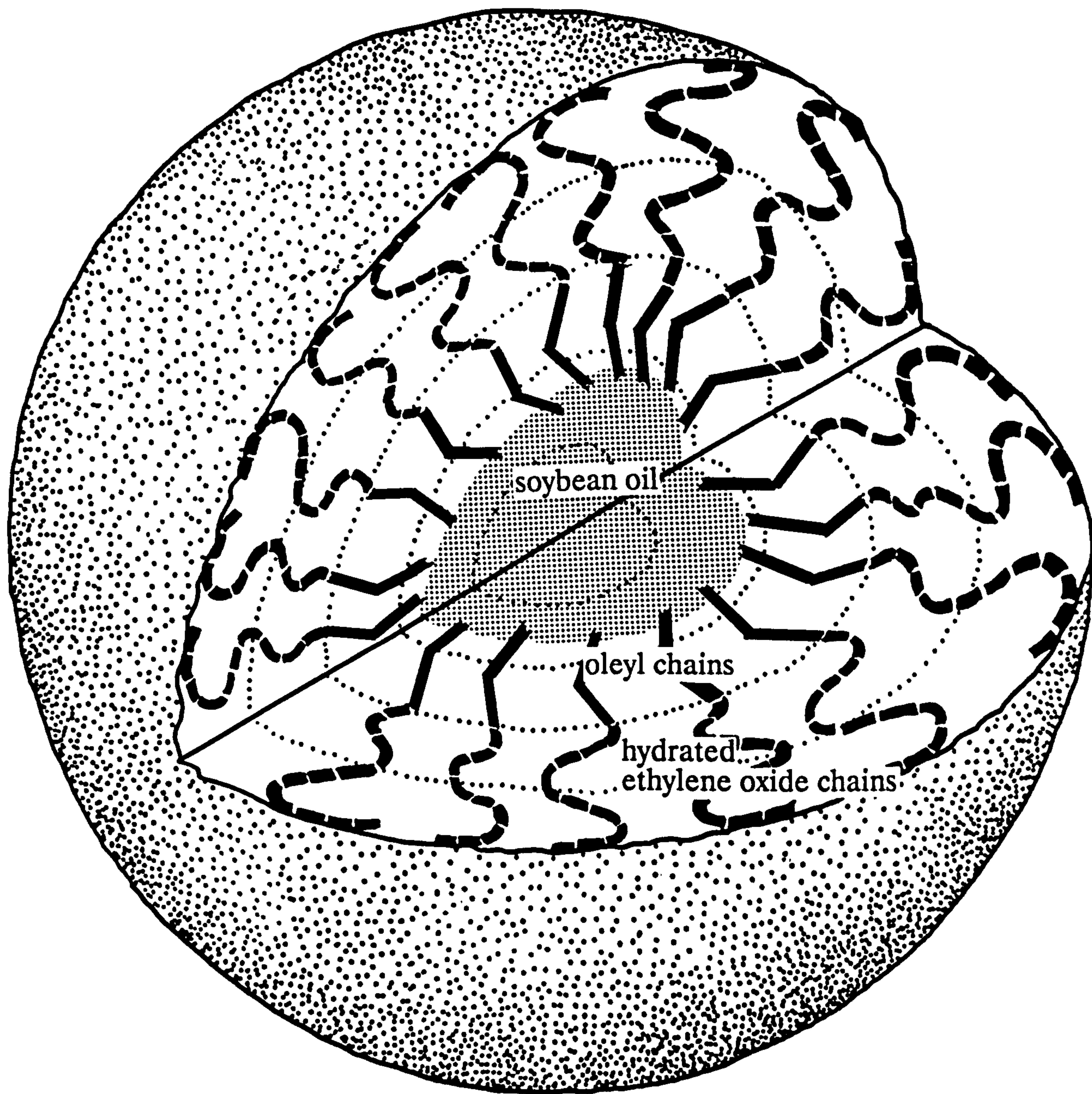


Figure 3.3: Proposed model for soybean oil/Brij 96/water o/w droplet microemulsion.

3.2 Effect of temperature on the area of existence

The effect of temperature on the area of existence of this 3-component microemulsion system has been studied. Microemulsion systems throughout the phase diagram were observed after one month at 4⁰, 25⁰, 37⁰ and 50⁰C.

No completely clear microemulsion systems were found at 4⁰C. The microemulsion region shown in figures 3.1 and 3.2 was replaced by systems which initially appeared turbid, and which with time separated into 2-phase Winsor I systems consisting of a lower clear and upper turbid phase. At 25⁰C the microemulsion area observed was the same as described above for ambient conditions. At 37⁰C the clear microemulsion region at lower surfactant concentrations remained essentially the same, but the previously unstable clear region near the surfactant apex became stable for at least one month, and extended along the soybean oil/Brij 96 axis, as shown in figure 3.4. The two clear areas were separated from each other along the water-surfactant axis by gel-like compositions. The areas observed at 50⁰C were similar to those at 37⁰C, with a possibly slightly extended clear surfactant-rich region.

3.3 Phase inversion temperatures

The cloud point (CP) of a nonionic surfactant system is the temperature at which the total effective force between micelles changes from being repulsive (lower temperatures) to attractive (higher temperatures). This change is generally considered to be due either to an increase in the attractive forces (due to van der Waals forces and hydrophobic interactions between hydrophobic surfaces) or to a decrease in repulsive forces (due to hydration forces), or a combination of the two effects [245] in addition to interrelated changes in micelle size and shape [246]. With ethylene oxide surfactants in particular, an increase in temperature results in dehydration of the ethylene oxide chains [247, 248] causing a reduction of a_0 , hence an increase in the CPP, and the formation of more elongated aggregates of reduced curvature and a higher aggregation number [246, 248].

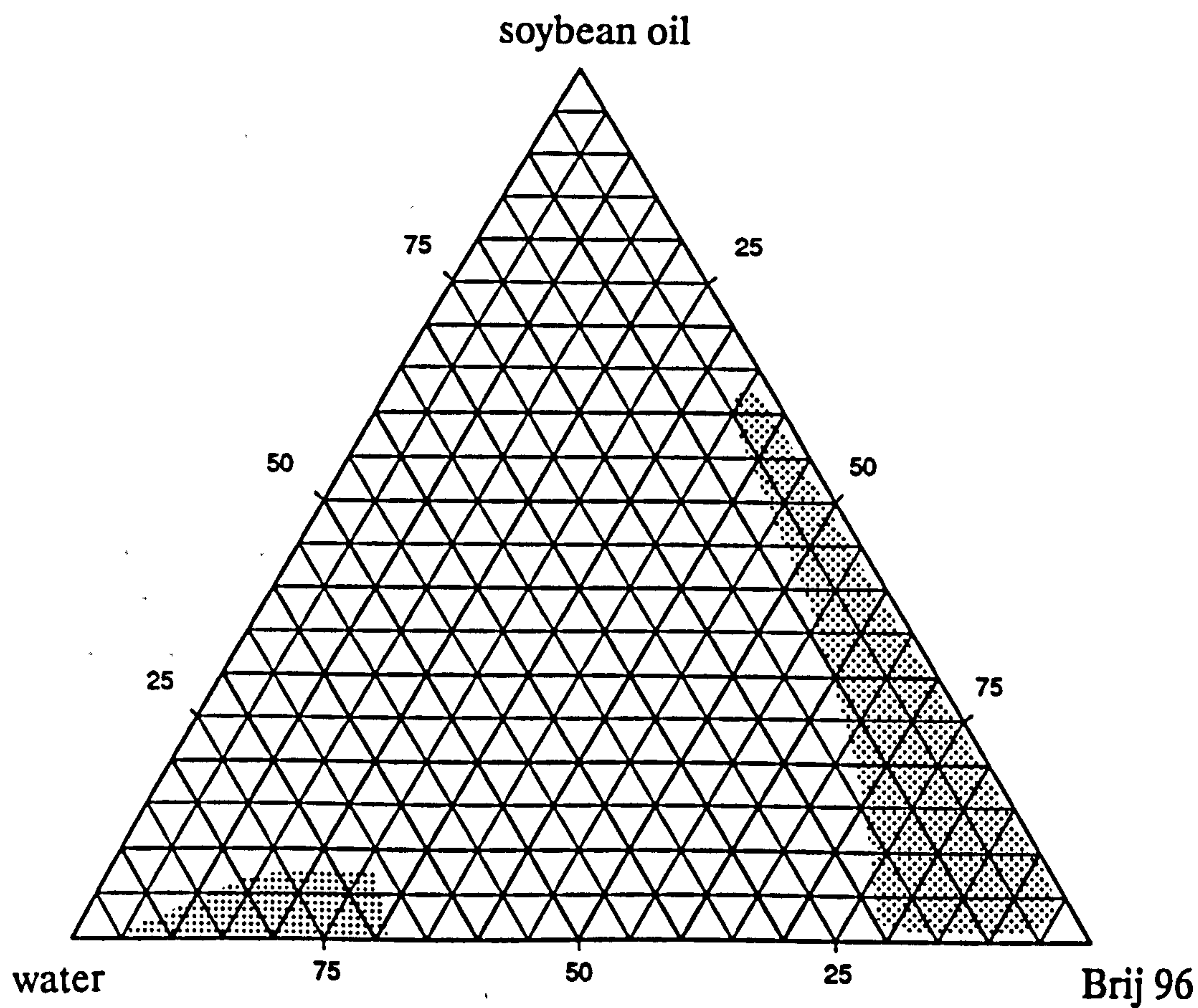


Figure 3.4: Triangular phase diagram showing the area of existence of clear, liquid compositions found in soybean oil/Brij 96/water systems after storage at 37°C for 1 month.

The CP of a surfactant solution may be raised or lowered by the presence of various additives including a number of oils; the corresponding temperature of emulsions (or microemulsions) is called the phase inversion temperature (PIT) [249]. Results of the CP found for Brij 96/water systems, and the PIT of a number of soybean oil/Brij 96/water microemulsions are shown in table 3.1 and figure 3.5.

The results found in this study show the expected increase in CP with increasing nonionic surfactant concentration at concentrations above the CMC [245]. The values of PIT found illustrate the complex and concentration-dependent way in which the addition of oil affects the CP. For microemulsions containing the same soybean oil content a decrease in the PIT was observed with increasing Brij 96 content. At lower surfactant concentrations (for example less than about 20 %w/w Brij 96 for microemulsions containing 2 %w/w soybean oil) the PIT was higher than the corresponding CP. At higher surfactant concentrations however, the PIT of the microemulsion systems was lower than a solution of the same Brij 96 concentration. Microemulsion systems containing 5 %w/w soybean oil, and either 20 or 25 %w/w Brij 96 showed an increased PIT compared to the corresponding microemulsion containing only 2 %w/w soybean oil.

A possible explanation for the varying effect of the soybean oil on CP is based on the shape of the aggregates formed. Transformation of rodlike micelles into globular structures by solubilisation of hydrocarbon has been suggested for some ionic surfactants [250]. For nonionic surfactants it has been postulated that if the hydrocarbon forms a *core* in the micelle interior, and if the micelles are originally asymmetrical and the addition of the oil phase results in a more spherical shape, the CP will be raised [246]. The high concentration of surfactant used to form these microemulsions means that surfactant solutions of the same Brij 96 concentration range are likely to be in close proximity to the phase boundary with liquid crystalline phases [251]. Hence these systems will be fairly densely packed, and tending away from discrete micellar units. The addition of 2 %w/w soybean oil at Brij 96 concentrations lower than 20 %w/w may encourage a more spherical shape and discourage the tendency to pack into hexagonal structures. At the same temperature, the attractive forces for systems with the same concentration of Brij 96 may therefore be less in microemulsion systems compared to micellar

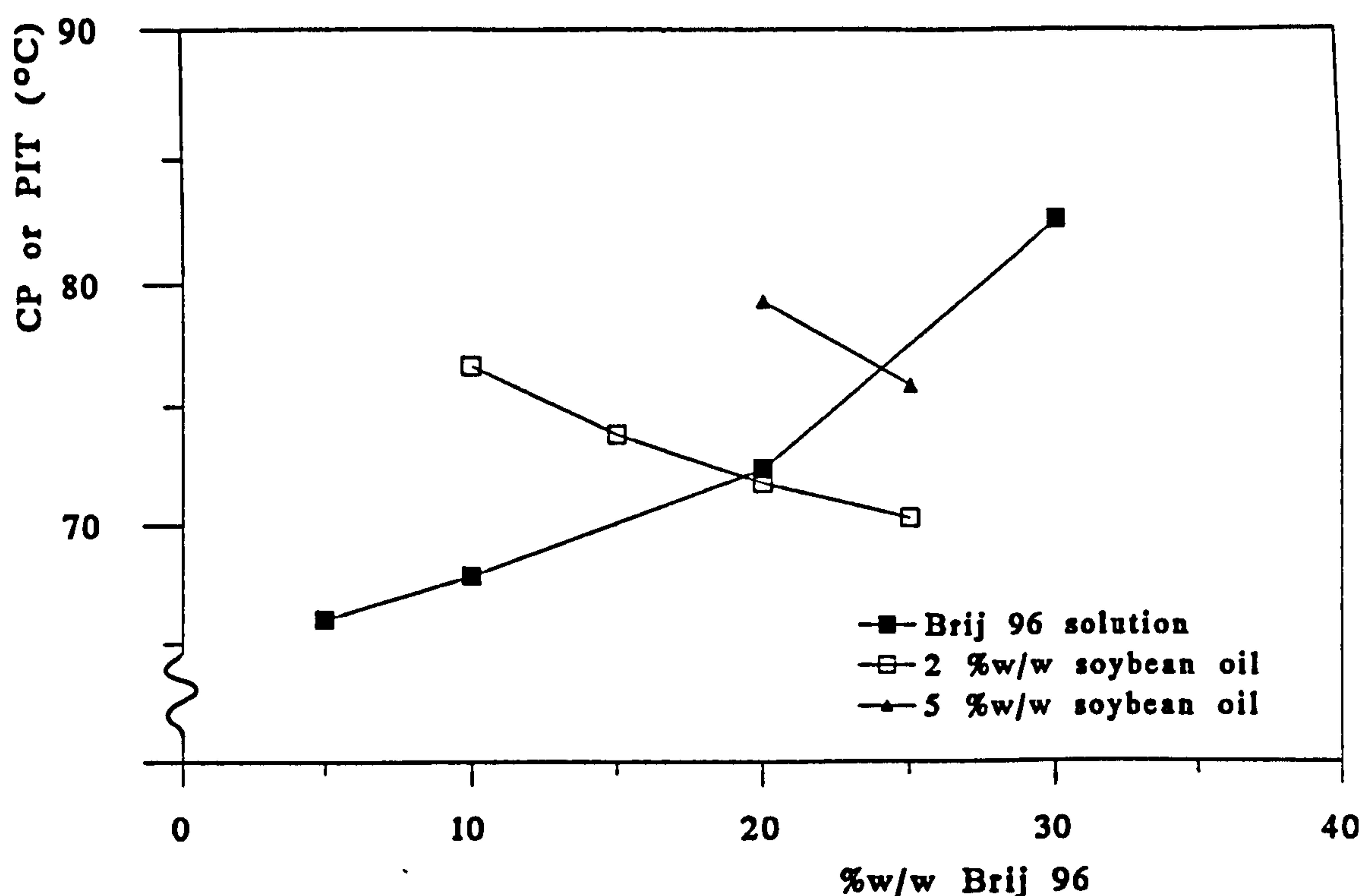


Figure 3.5: Cloud point or phase inversion temperature as a function of Brij 96 concentration for surfactant solutions, and 2 or 5 %w/w soybean oil microemulsions.

Table 3.1: Cloud point or phase inversion temperature (°C) of Brij 96 surfactant solutions, and microemulsions containing 2 and 5%w/w soybean oil.

%w/w Brij 96	%w/w soybean oil		
	0	2	5
5	66.0	—	—
10	67.8	76.6	—
15	—	73.8	—
20	72.4	71.8	79.3
25	—	70.3	75.8
30	82.6	—	—

ones, so that a higher temperature is required before the attractive forces balance the repulsive forces of the system (ie. the CP is reached). From the limited data with 5 %w/w soybean oil microemulsions this effect appears to be extended to higher surfactant concentrations (approximately 25 %w/w Brij 96). The addition of a greater amount of soybean oil (5 %w/w compared to 2 %w/w) for the two Brij 96 concentrations tested resulted in higher PITs. This observation may similarly be due to the formation of a larger oil core which encourages sphericity more strongly.

For those microemulsions with higher concentrations of surfactant, the PIT of microemulsion systems were found to be lower than the CP of the corresponding surfactant solution. It is possible with these concentrations of Brij 96 the tendency for the surfactant solution towards forming a liquid crystalline structure is much stronger. Subsequently, the amount of oil added is insufficient to alter the shape of the surfactant aggregates towards that of a spherical droplet with an oil core. The presence of the oil may in fact encourage aggregation of the surfactant systems by either increasing the attractive forces and/or decreasing the repulsive forces of the systems. The effect of other oils on the CP is discussed in chapter 4 (4.2.1.1.1).

3.4 Light scattering investigations

3.4.1 Photon correlation spectroscopy

In PCS the calculation of hydrodynamic radius from the diffusion coefficient is only strictly valid for very dilute systems. Highly concentrated dispersed systems result in measuring faults due to both multiple scattering of the laser beam, and the interaction between individual particles [252, 253]. The overall effect is to result in a higher apparent diffusion coefficient, and consequently an underestimate of particle size [252, 254]. Hence systems which are examined by PCS are often diluted in order to increase the distance between droplets and therefore decrease the interparticulate forces [255].

In microemulsion systems however, dilution would alter the interfacial

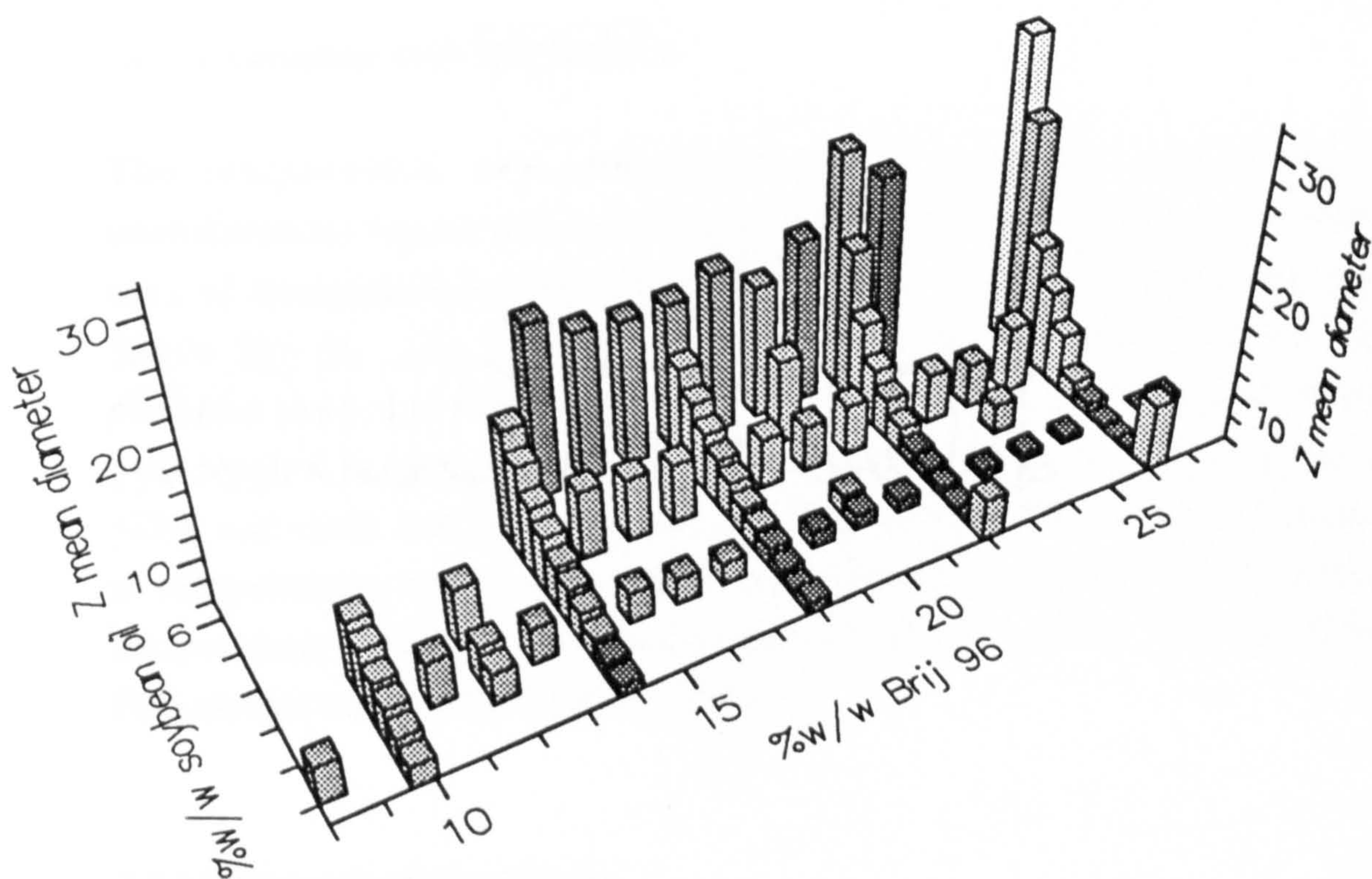


Figure 3.6: Apparent Z mean diameters (nm) determined within the area of o/w microemulsion existence for soybean oil/Brij 96/water systems.

composition of droplets, resulting in a change of structure or stability of the system [256] and the possible disappearance of the microemulsion phase altogether [257, 258]. In this study therefore all PCS measurements were conducted on undiluted microemulsion samples. The possible errors in the resulting Z mean diameter which is calculated are acknowledged, and the diameters generated are therefore referred to as the *apparent Z mean diameter*. The apparent Z mean diameter found for the compositions tested over the microemulsion area of existence for soybean oil/Brij 96/water systems is shown in figure 3.6.

3.4.1.1 Variation with temperature

The temperature dependence of the PCS results within the o/w microemulsion region was tested on a composition which was well within the area of microemulsion existence; containing 2 %w/w soybean oil and 14 %w/w Brij 96. The apparent Z mean diameter and polydispersity values obtained were not significantly altered between temperatures of 25-40°C. This result is in agreement with similar studies using both nonionic micelles [259] and other nonionic microemulsion systems [106] which conclude that at temperatures well below the PIT the intensity of scatter varies little with temperature, indicating only fairly weak interactions exist. All the following PCS studies were carried out at 30±0.1°C.

3.4.1.2 Reproducibility of data

All the apparent Z mean diameters generated from the scatter of the microemulsion systems detected at 90° are the average of at least five repeat measurements of each individually prepared sample. The variation found with separately prepared samples, produced and tested on different days was also investigated. The apparent Z mean diameter and polydispersity of thirteen such repeated measurements are listed in table 3.2.

For microemulsion samples well within the o/w microemulsion area, the difference in size found between two samples of the same nominal composition was small. The diameters tended to be within 1nm of each other. Those samples nearer the extremities of the area of existence, particularly at

Table 3.2: Reproducibility of PCS data: The apparent Z mean diameter (nm) and polydispersity determined for different samples (1 and 2) of the same composition, and the ratio of diffusion coefficients at 45^oC and 135^o.

Microemulsion Composition	Z mean diameter		Polydispersity		$\frac{D_{45^{\circ}}}{D_{135^{\circ}}}$
	1	2	1	2	
2% soybean oil / 10% Brij 96	10.0	10.5	0.141	0.136	1.009
2% soybean oil / 14% Brij 96	8.4	8.6	0.133	0.146	0.986
2% soybean oil / 18% Brij 96	7.1	7.9	0.153	0.211	0.999
2% soybean oil / 22% Brij 96	6.0	6.9	0.299	0.235	1.001
2% soybean oil / 26% Brij 96	6.1	6.1	0.300	0.291	0.982
4% soybean oil / 14% Brij 96	12.2	13.0	0.321	0.275	1.029
4% soybean oil / 18% Brij 96	9.7	10.4	0.318	0.332	0.998
4% soybean oil / 22% Brij 96	9.2	9.8	0.350	0.364	0.985
4% soybean oil / 26% Brij 96	13.1	13.9	0.344	0.332	—
6% soybean oil / 14% Brij 96	25.6	21.0	0.692	0.401	—
6% soybean oil / 18% Brij 96	18.8	21.2	0.724	0.467	1.024
6% soybean oil / 22% Brij 96	22.2	22.7	0.443	0.446	—
6% soybean oil / 26% Brij 96	37.9	56.3	0.503	0.592	—

higher oil concentrations (6 %w/w) show both a high degree of polydispersity and larger variation between the size of the two samples.

In addition, the diffusion coefficients of a range of samples within the microemulsion region were determined at angles other than 90° to investigate if there was any angular dependence of the PCS data. The ratio of the diffusion coefficient at 45° to the diffusion coefficient at 135° ($D_{45^\circ}/D_{135^\circ}$) were in all cases found to be between 0.9 and 1.1. Hence, no significant asymmetry appeared to be present, and the existence of large linear aggregates, composed of strings of microemulsion droplets, unlikely.

3.4.1.3 Changes with increasing soybean oil content

The variation in size and polydispersity with increasing soybean oil concentration was investigated for five concentrations of Brij 96 (10, 14, 18, 22 & 26 %w/w). Results are shown in figures 3.7 - 3.11.

It is interesting to note that at lower concentrations of Brij 96 (10, 14 & 18 %w/w) the presence of only a small amount of soybean oil resulted in a microemulsion of smaller apparent Z mean diameter than the corresponding surfactant solution containing no oil phase. At 22 %w/w Brij 96 the initial decrease in apparent Z mean diameter with the addition of up to 4 %w/w soybean oil was only slight. At 26 %w/w Brij 96 there was in fact a small increase in size with the addition of 0.5 %w/w soybean, although smaller sizes were observed at 1-3 %w/w soybean oil levels. A possible explanation is found in the log/log plots of scattering intensity vs diameter for each series. In all the surfactant solution samples of 10 %w/w Brij 96 or above, a bimodal distribution was found. Similar trends have been observed for micelles produced with the nonionic surfactants $C_{14}E_8$ [260] and Triton X-100 [261]. In these cases, the bimodal distributions observed at higher surfactant concentrations were thought to be due to the coexistence of spherical micelles with aggregates of loose clusters.

Although the addition of small amounts of oil may act to increase the size of individual droplets, it also appeared to discourage the formation of larger aggregate clusters, and as a result a decrease in the overall apparent Z mean diameter was noticed. With the assumption that all the surfactant present is

contained within the microemulsion aggregates, this observation may be because less interdroplet interactions are present in systems with a smaller number of larger droplets. As a result of smaller aggregate clusters forming, the intensity plots of those microemulsions systems containing only a few percent soybean oil, and with 10, 14 or 18 %w/w Brij 96, appear monomodal.

With 10 %w/w Brij 96 (fig.3.7) although polydispersity does increase with increasing soybean oil content, the scattered intensity plots remain monomodal until the phase boundary for microemulsion existence is reached. There is an essentially linear increase in the apparent Z mean diameter with a soybean oil content up to 3 %w/w.

At 14 %w/w Brij 96 (fig.3.8) there also appears to be a linear increase in size with increasing soybean oil content between 0.5 and 3 %w/w. At oil contents greater than 3 %w/w however, polydispersity appears to increase more rapidly, and a more exponential increase in Z mean diameter was observed. At 2.5 % w/w soybean oil a bimodal distribution begins to emerge in the log/log intensity vs diameter plots, which becomes quite pronounced at 3 %w/w soybean oil levels and above. The increase in the apparent Z mean diameter of the 14 %w/w Brij 96 microemulsion droplets at soybean oil contents of 3 %w/w soybean oil or more appears to be due, not only to an increase in individual droplet size, but also (possibly because of the increased size of the droplets) an increase in the interaction between droplets and the formation of cluster aggregates. These clusters seem to increase in both size and predominance as more oil is added.

Figure 3.9 shows the results for systems containing 18 %w/w Brij 96. As observed with 14 %w/w surfactant, while the distribution of intensity vs size remained essentially monomodal, and individual microemulsion droplets exist, a linear increase of apparent Z mean diameter was found with increasing soybean oil content. The polydispersity and range of sizes within a sample also increased with increasing oil content until, at about 5 %w/w soybean oil, the intensity plots are distinctly bimodal. Further addition of soybean oil then resulted in a increase in both the size of the individual microemulsion droplets (shown by the position of the first intensity population) and in the size and extent of the larger clusters. At this stage, the corresponding increase in the apparent Z mean diameter becomes non-linear with increasing oil content.

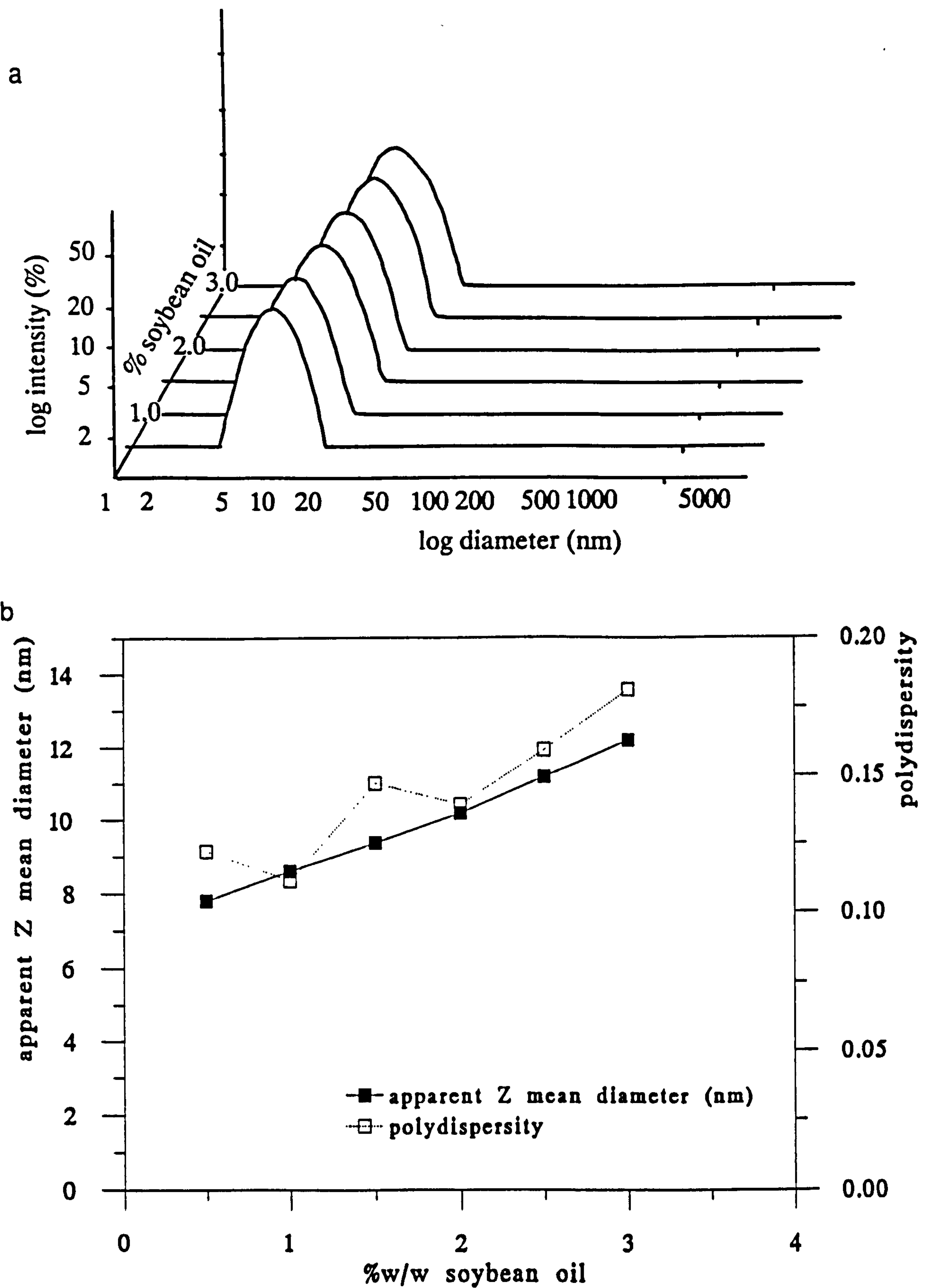


Figure 3.7: PCS results found for microemulsion systems containing 10 %w/w Brij 96 with increasing soybean oil content; a) log intensity vs log diameter plots, and b) graph of apparent Z mean diameter and polydispersity vs %w/w soybean oil.

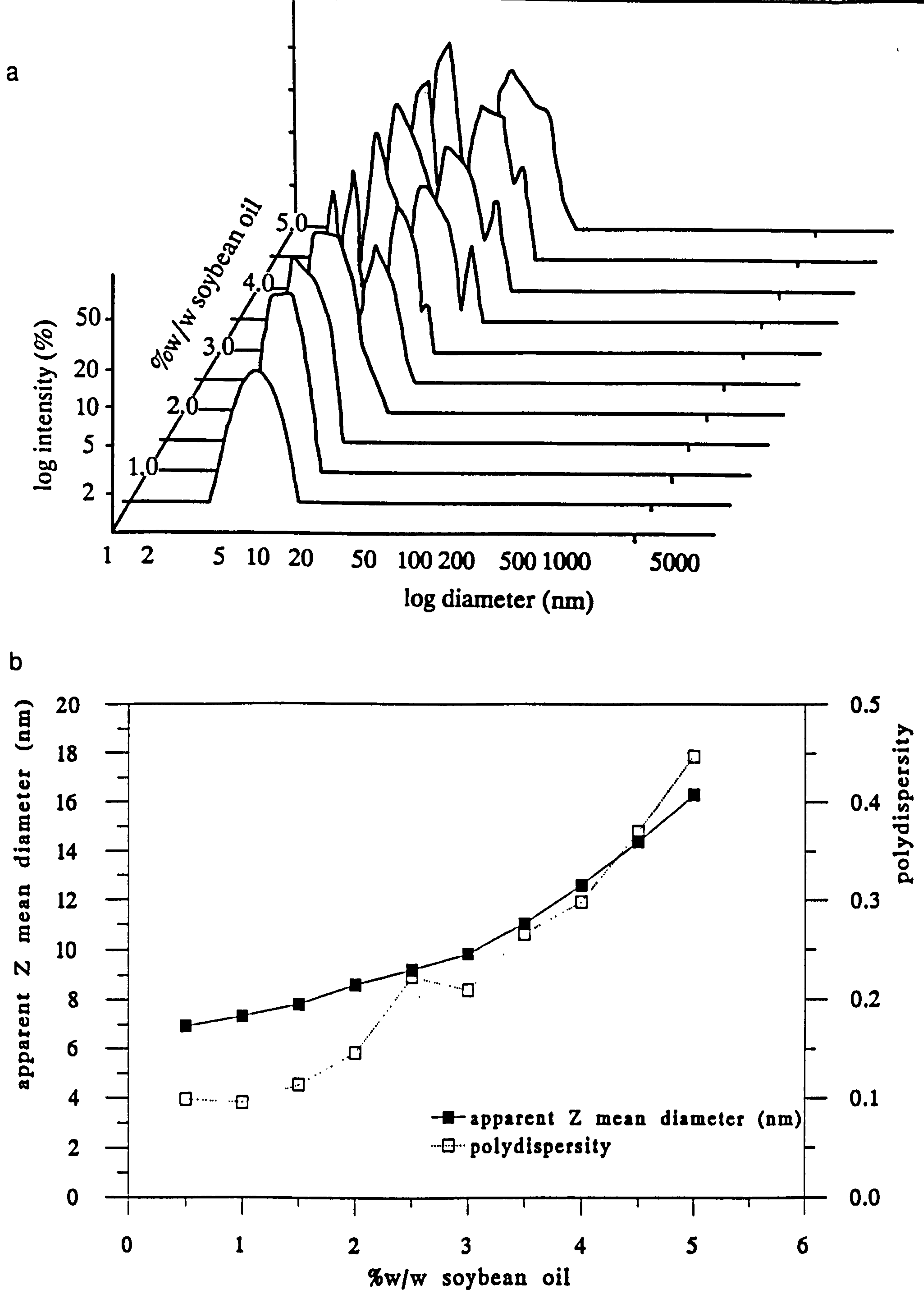


Figure 3.8: PCS results found for microemulsion systems containing 14 %w/w Brij 96 with increasing soybean oil content; a)log intensity vs log diameter plots, and b)graph of apparent Z mean diameter and polydispersity vs %w/w soybean oil.

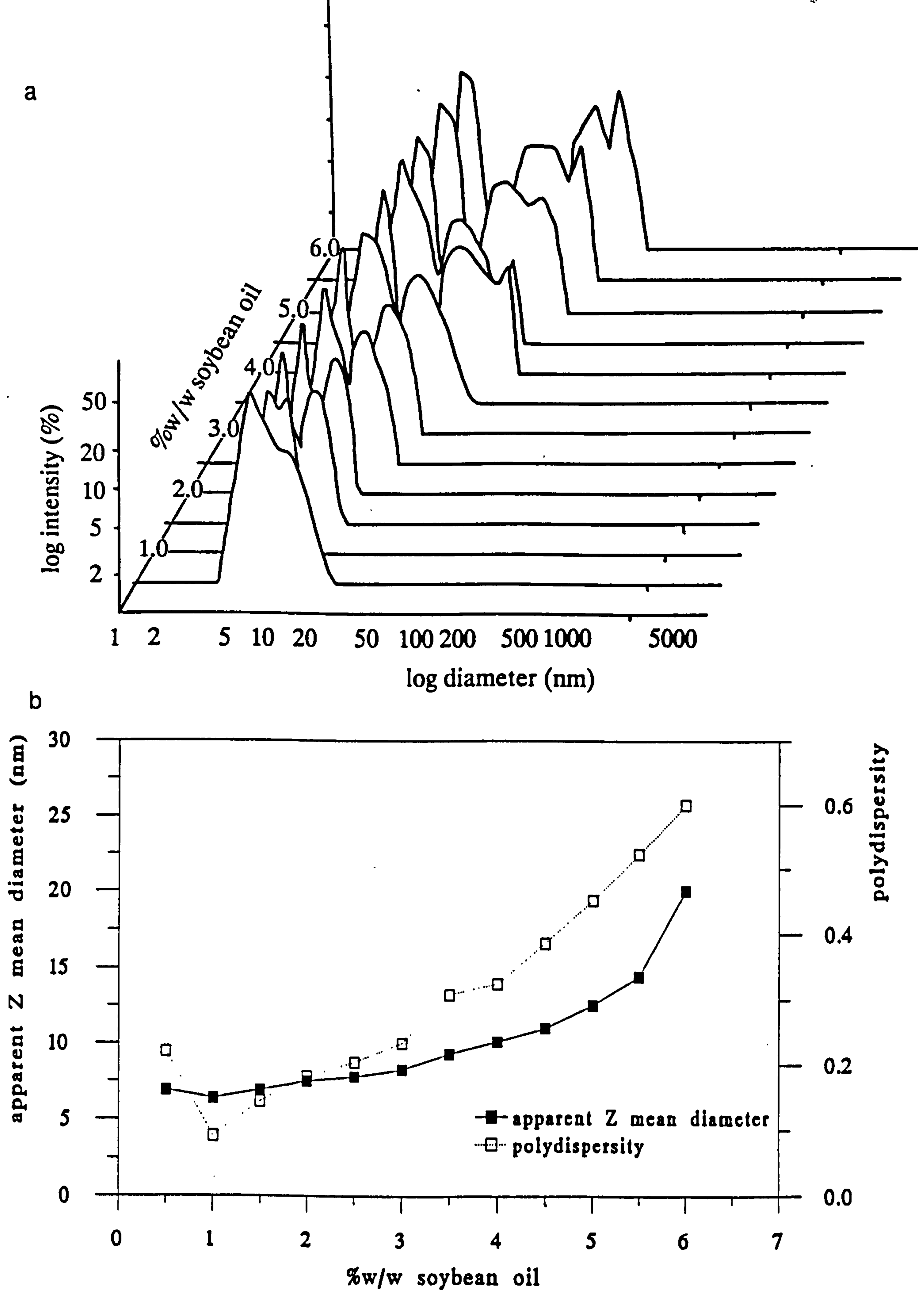


Figure 3.9: PCS results found for microemulsion systems containing 18 %w/w Brij 96 with increasing soybean oil content; a) log intensity vs log diameter plots, and b) graph of apparent Z mean diameter and polydispersity vs %w/w soybean oil.

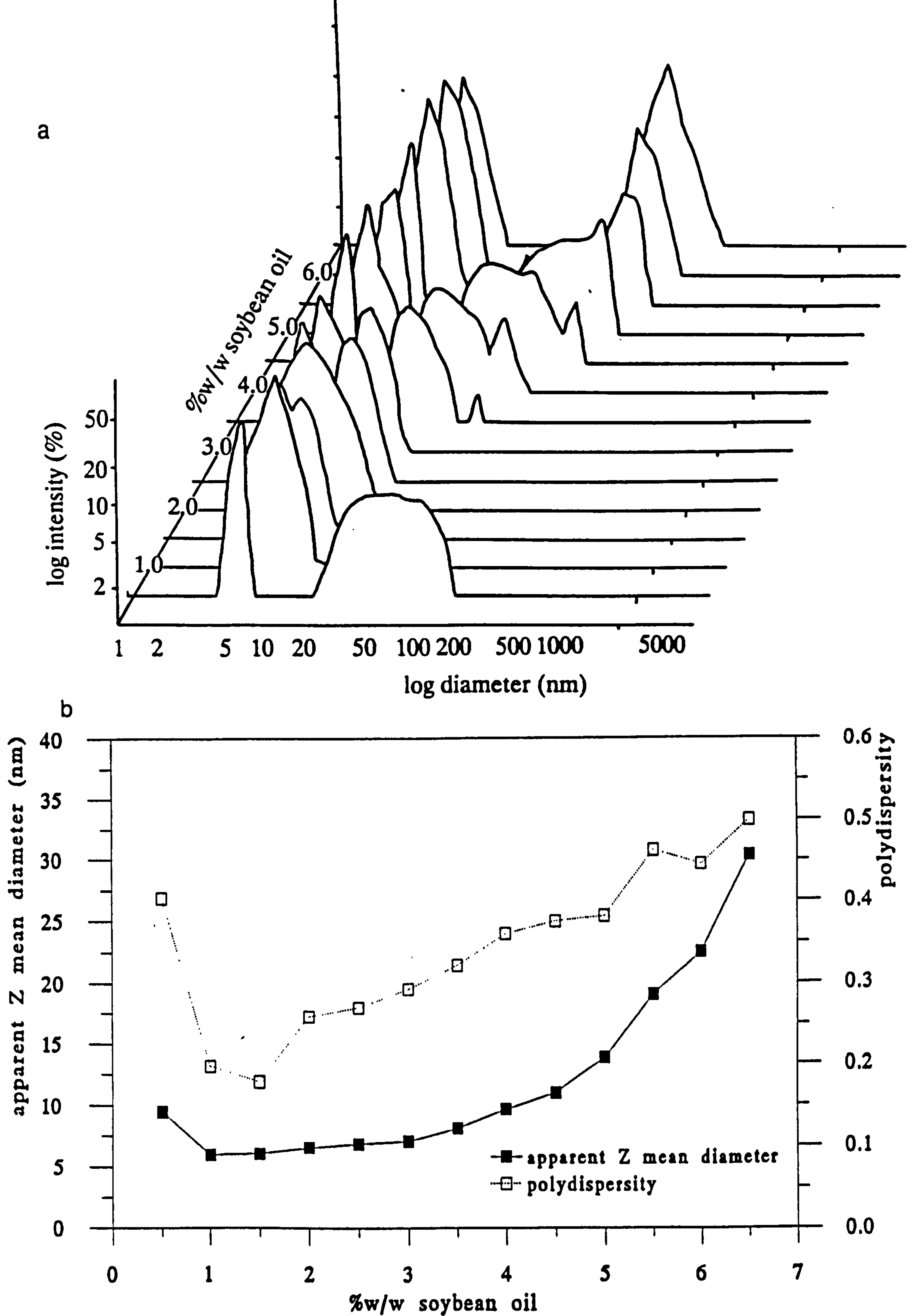


Figure 3.10: PCS results found for microemulsion systems containing 22 %w/w Brij 96 with increasing soybean oil content; a) log intensity vs log diameter plots, and b) graph of apparent Z mean diameter and polydispersity vs %w/w soybean oil.

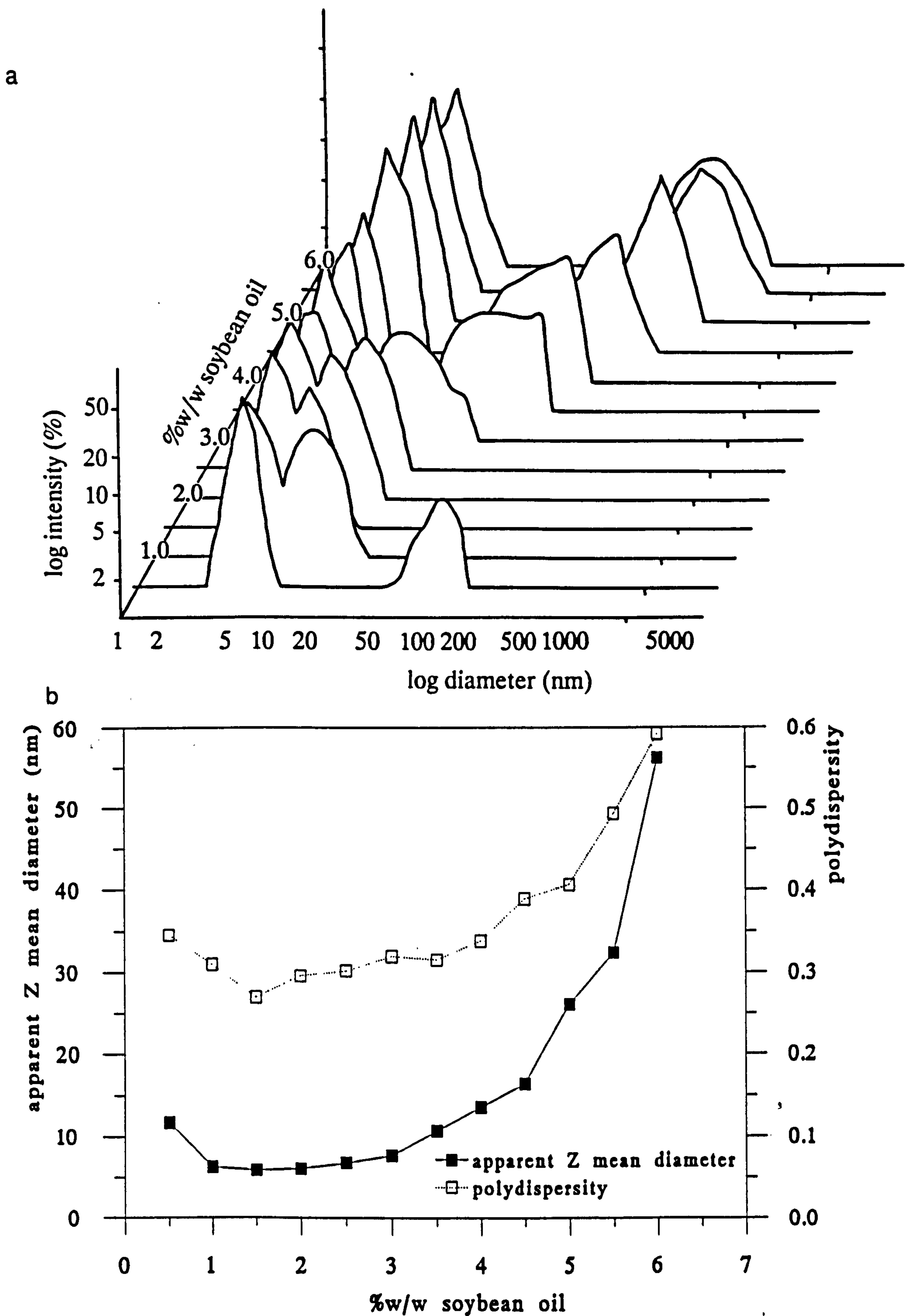


Figure 3.11: PCS results found for microemulsion systems containing 26 %w/w Brij 96 with increasing soybean oil content; a) log intensity vs log diameter plots, and b) graph of apparent Z mean diameter and polydispersity vs %w/w soybean oil.

With 22 and 26 %w/w Brij 96 (figs.3.10 & 3.11) the observed trends were similar to those above. For these two surfactant concentrations there is however very little growth in size found up to 3 %w/w soybean oil. Above 3-4 %w/w soybean oil the distribution becomes increasingly bimodal, and the second peak (corresponding to the population of droplet clusters) became completely separate from the individual droplet peak, moving towards much higher diameters with each addition of oil and with correspondingly high values of polydispersity. Above 6.5 %w/w oil, systems containing either 22 or 26 %w/w Brij 96 began to appear turbid. Those in the 26 %w/w Brij 96 series also exhibited a marked increase in viscosity.

3.4.1.4 Changes with increasing Brij 96 content

The effect on microemulsion size and distribution with increasing surfactant concentration was investigated with fixed soybean oil contents of 2, 4 and 6 %w/w. Brij 96 solutions without any added oil were also examined by PCS and the results are shown in figure 3.12. For Brij 96 surfactant solutions, the size of the micelles found was fairly constant (9.7 or 9.8nm) up to a surfactant concentration of 2 %w/w Brij 96. This constant size would be expected if the micelles were acting as non-interacting spheres at low concentrations. However, above 2 %w/w Brij 96 the droplets do appear to be interacting and the resulting apparent Z mean diameters increased to 11.2nm for both 5 and 10 %w/w Brij 96. The addition of still more surfactant resulted in a lower apparent Z mean diameter, but an increase in the polydispersity as two populations begin to diverge in the log intensity distribution plots.

The decrease in the observed diameter at higher concentrations of Brij 96 was probably the result of interactions due to crowding and the subsequent failure of the Stokes-Einstein equation (eqn.20) to calculate the diameter of individual droplets from the observed diffusion coefficient. Certainly the log distribution plots (fig.3.12a) indicate an increase in predominance of a larger sized population with increasing Brij 96 concentration. It has been suggested that the larger-sized population, probably arising from clusters of smaller micelles, is a precursor stage of the liquid crystalline phase occurring at higher surfactant concentrations [261].

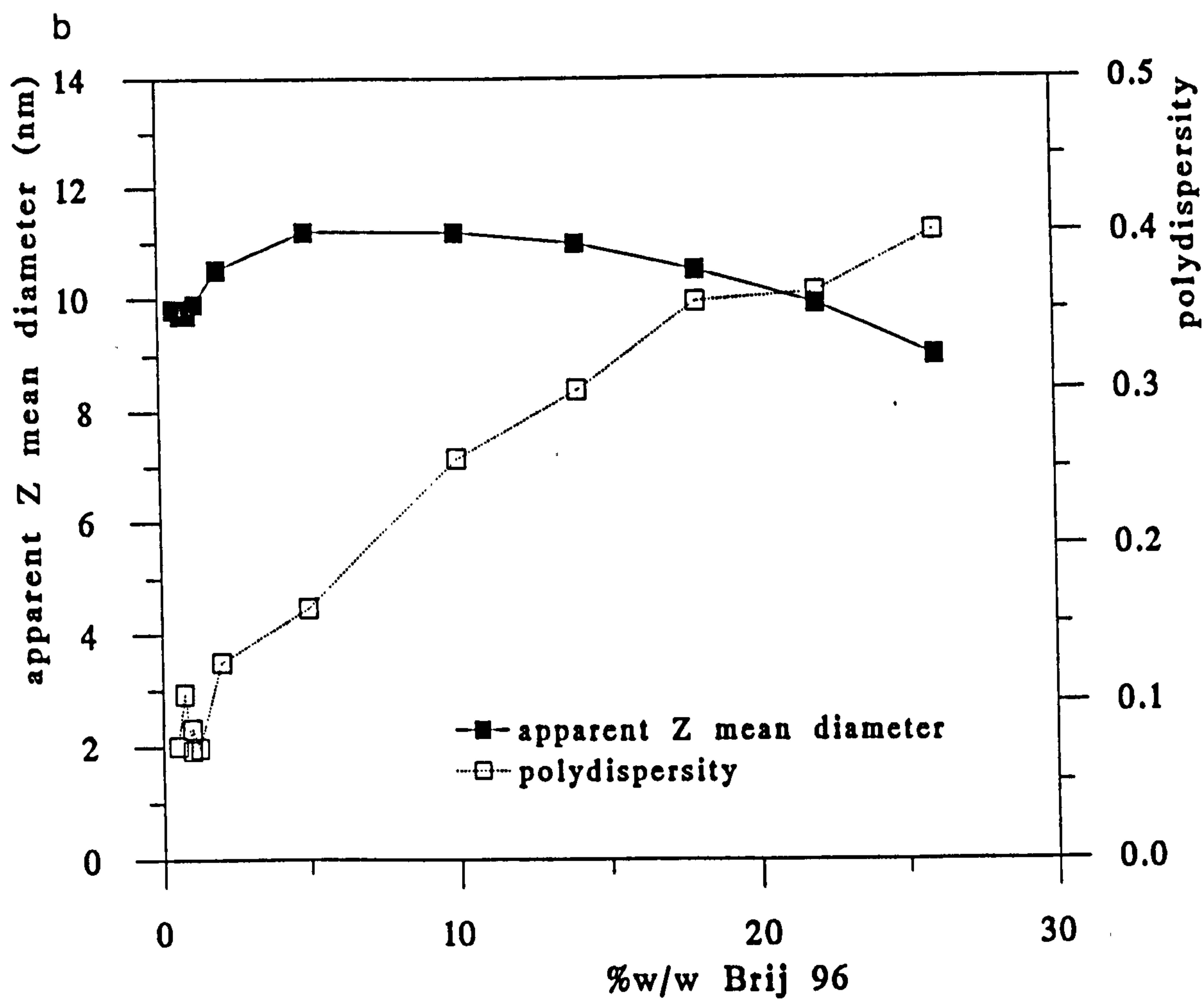
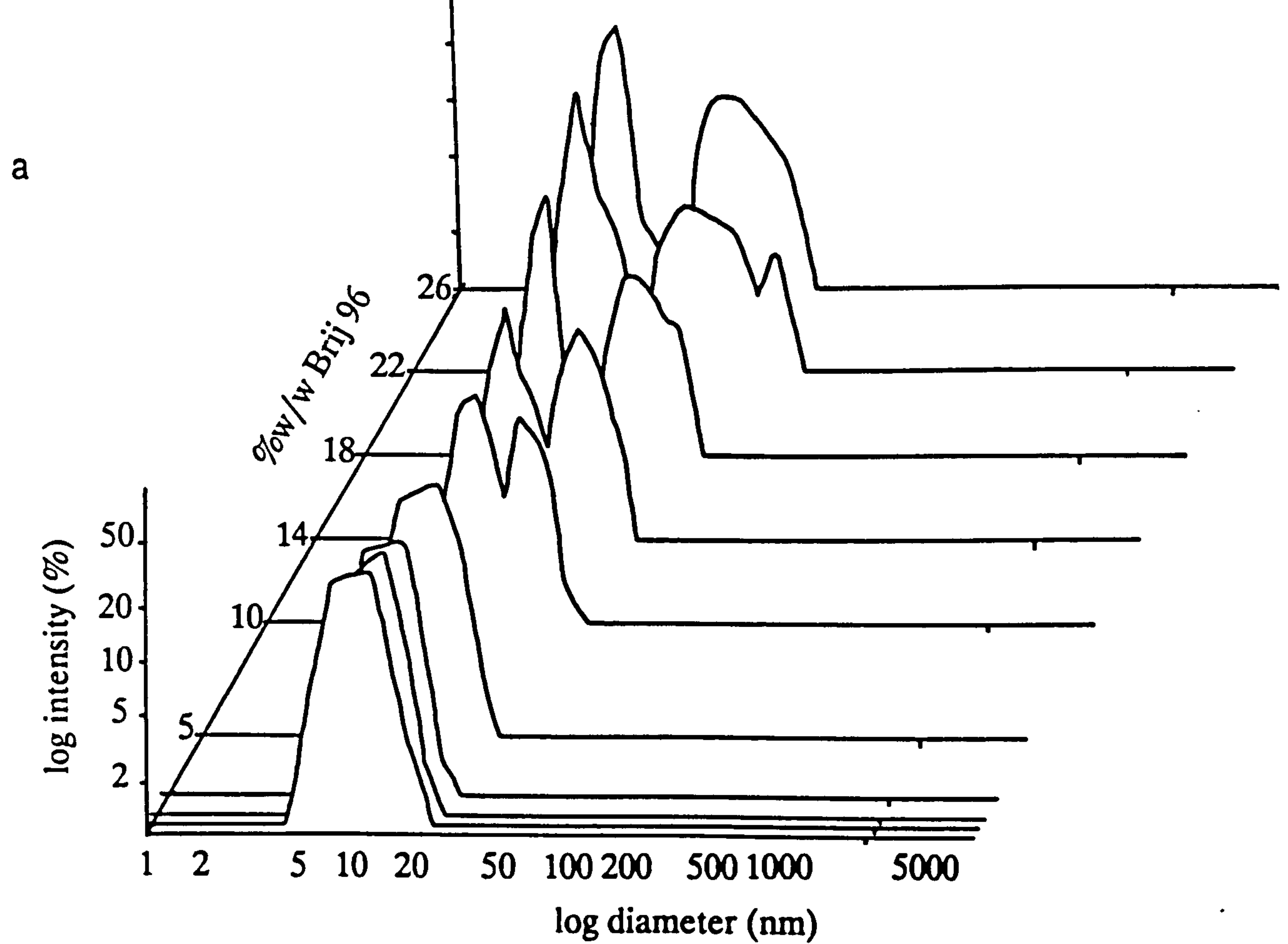


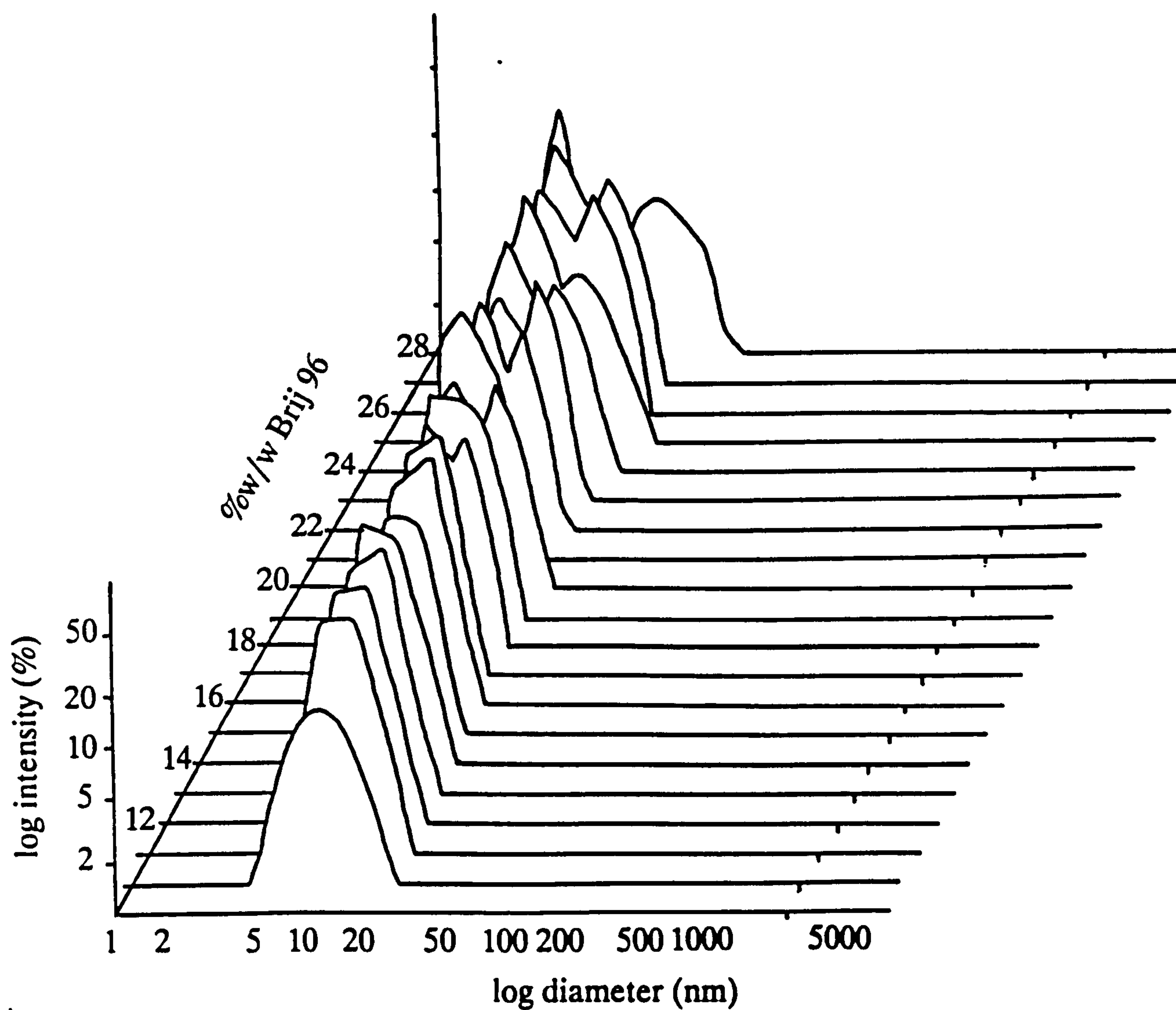
Figure 3.12: PCS results found for surfactant solutions with increasing Brij 96 content; a) log intensity vs log diameter plots, and b) graph of apparent Z mean diameter and polydispersity vs %w/w Brij 96.

In the presence of 2 %w/w soybean oil, microemulsion compositions containing between 10 and 28 %w/w Brij 96 were tested. Results showed (fig.3.13) a fairly linear decrease in calculated droplet size with increasing Brij 96 concentrations of between 10-26 %w/w. Above 26 %w/w surfactant there was a slight increase in mean diameter. This upturn at higher concentrations corresponded with the emergence of bimodal intensity distributions. It is interesting to note that with equivalent concentrations of Brij 96 the microemulsion compositions containing 2 %w/w soybean oil were smaller in size than the corresponding surfactant solution. The emergence of bimodal intensity plots also appeared to begin at higher concentrations of Brij 96 when soybean oil was present. At 2 %w/w soybean oil the oil appeared to discourage the attractive interdroplet interactions that result in cluster formation and thereby caused a decrease in the apparent Z mean diameter compared to micelles. This was not however the case when more oil was added.

In samples containing 4 %w/w soybean oil (as found with microemulsions containing 2 %w/w soybean oil) the initial trend observed was a decrease in the apparent Z mean diameter with increasing surfactant concentration (fig.3.14). This decrease appeared to be fairly linear up to 18 %w/w Brij 96, after which concentration the apparent Z mean diameter remained at a fairly constant 10nm until quite a dramatic increase in size began at 24 %w/w Brij 96. The results for samples with 27 and 28 %w/w Brij 96 are not shown in figure 3.14b, but apparent Z mean diameter values of 126 and 252nm, and polydispersity indices of 0.900 and 0.987 respectively were found. All the log intensity plots with 4 %w/w soybean oil exhibited bimodal distributions; the larger diameter population increasing in dominance and diameter with increasing surfactant concentration. This is particularly true for surfactant concentrations greater than 24 %w/w. The composition containing 4 %w/w soybean oil with 28 %w/w Brij 96, although remaining clear was very viscous, and the intensity plot corresponding to this sample showed that no individual microemulsion droplets were present, and in fact this composition is probably better classified as an oil-containing liquid crystalline, or possibly cubic, phase.

In order to incorporate 6 %w/w soybean oil into microemulsion systems, fairly high concentrations of Brij 96 (between 15 and 26 %w/w) were

a



b

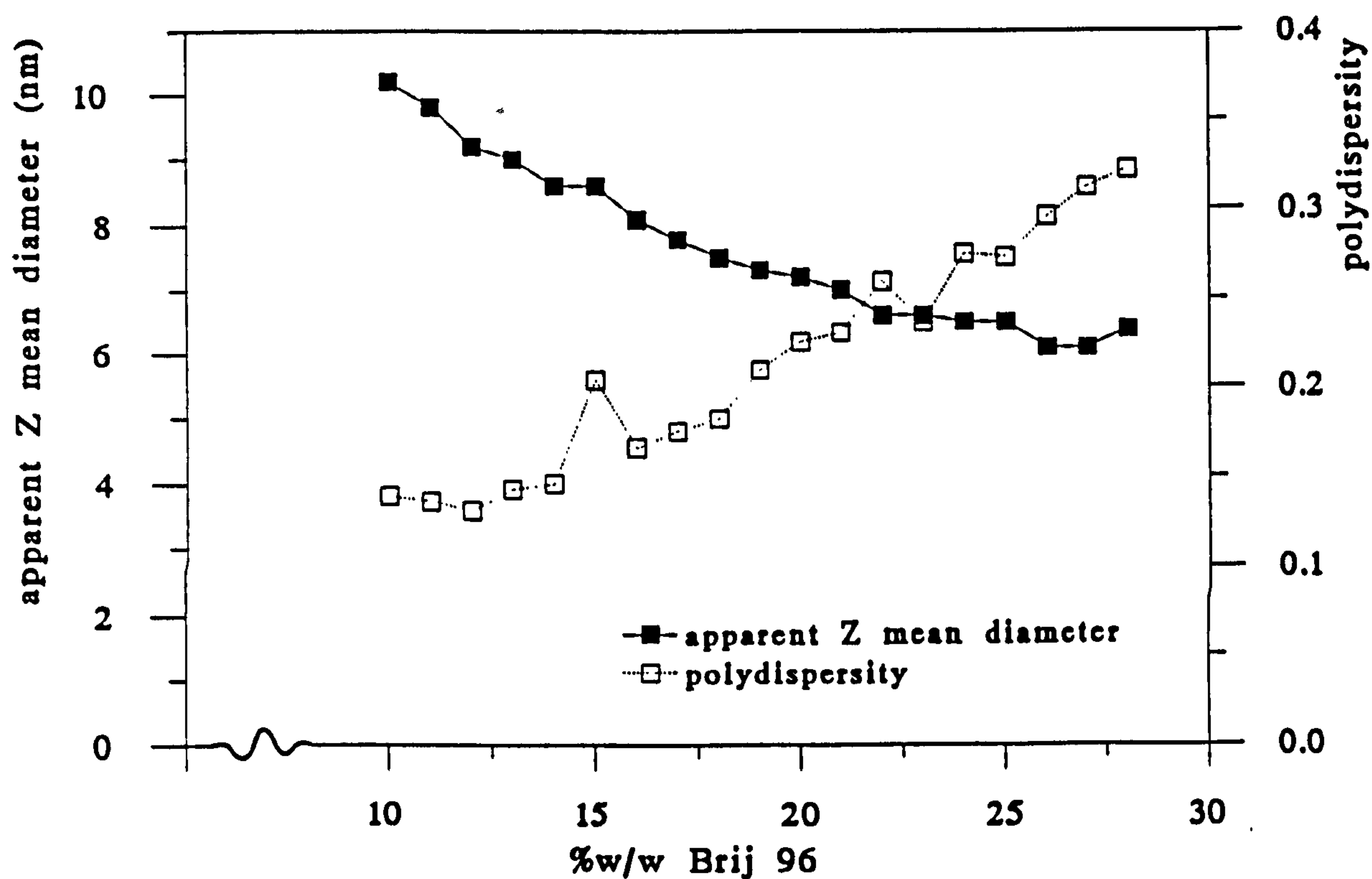


Figure 3.13: PCS results found for microemulsion systems containing 2 %w/w soybean oil with increasing Brij 96 content; a) log intensity vs log diameter plots, and b) graph of apparent Z mean diameter and polydispersity vs %w/w Brij 96.

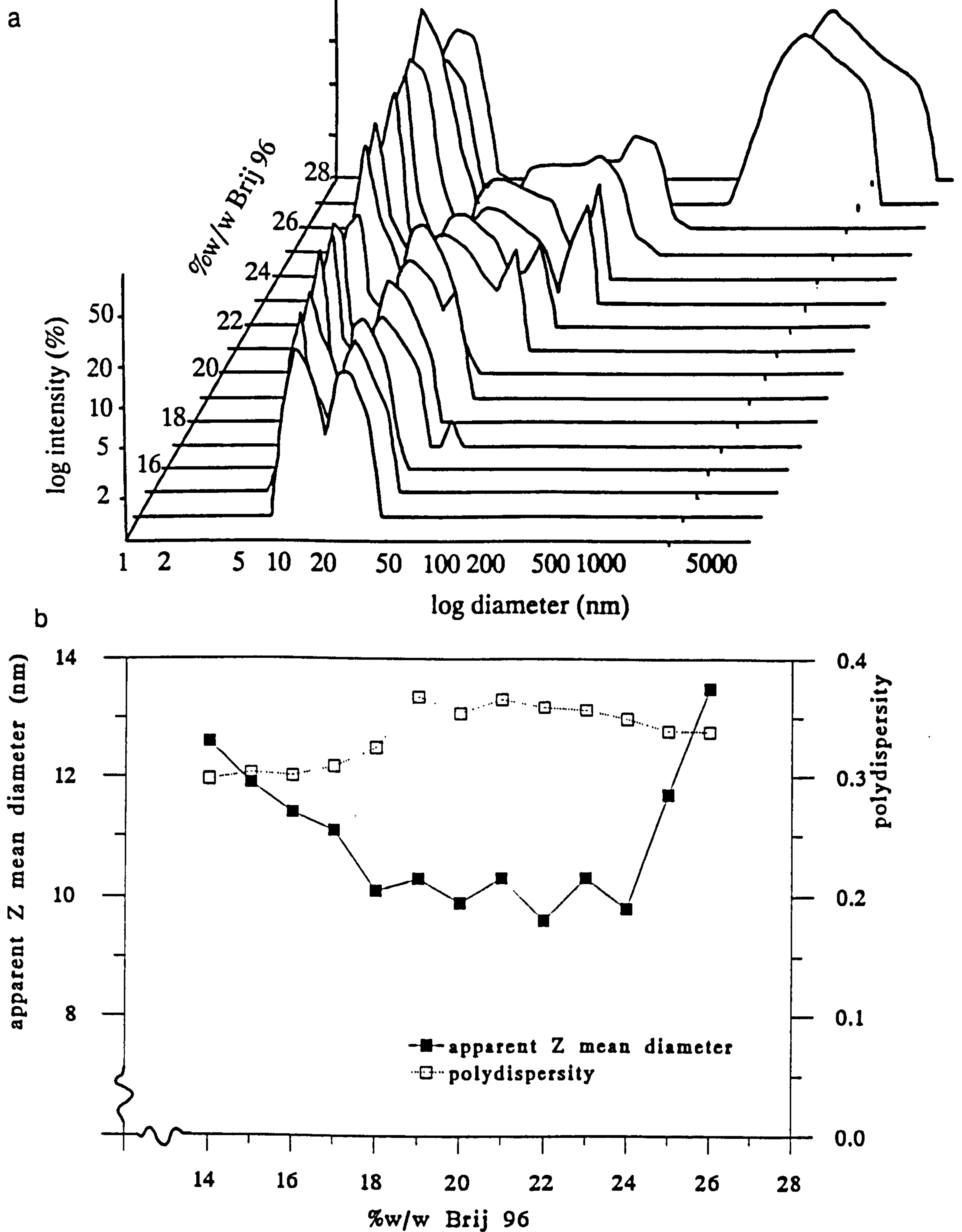


Figure 3.14: PCS results found for microemulsion systems containing 4 %w/w soybean oil with increasing Brij 96 content; a) log intensity vs log diameter plots, and b) graph of apparent Z mean diameter and polydispersity vs %w/w Brij 96.

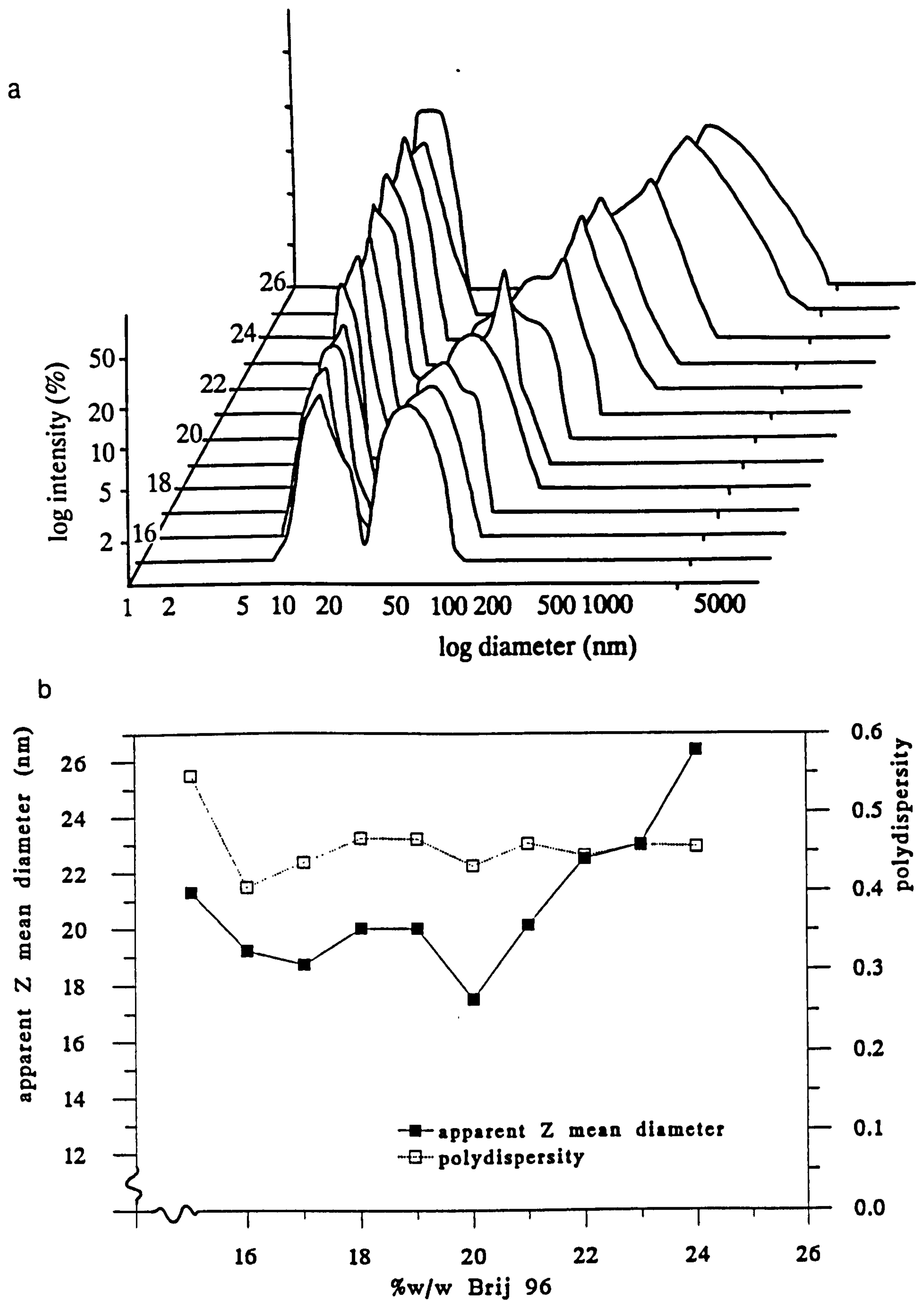


Figure 3.15: PCS results found for microemulsion systems containing 6 %w/w soybean oil with increasing Brij 96 content; a)log intensity vs log diameter plots, and b)graph of apparent Z mean diameter and polydispersity vs %w/w Brij 96.

required. As found with 4 %w/w soybean oil, the apparent Z mean diameter showed an initial decrease with increasing surfactant concentration, a reasonably level region around 16-21 %w/w Brij 96, and then a large increase (fig.3.15). Again, these results were consistent with the increasing dominance of the population of larger sized clusters as the surfactant concentration increased.

3.4.1.5 Changes with a fixed weight ratio of Brij 96:soybean oil

Compositions in the area of microemulsion existence along two fixed weight ratios of Brij 96:soybean oil (4:1 and 8:1) were investigated by PCS. Samples were made either individually, or by dilution along the tie line. Comparison of the apparent Z mean diameters for the same composition, produced by either method showed no difference in size. When producing samples by dilution however, it was possible to achieve clear liquid compositions which lie outside the previously determined area of microemulsion existence. Results are shown in figures 3.16 and 3.17, in which the weight fraction of the microemulsion is defined as the weight of the surfactant and oil divided by the total weight of the microemulsion ingredients (ie. $\frac{g[\text{Brij 96} + \text{soybean oil}]}{g[\text{Brij 96} + \text{soybean oil} + \text{water}]}$).

There was little difference in the apparent Z mean diameter of microemulsions with a fixed ratio of Brij 96:soybean oil of 8:1. The most concentrated member of the series (and from which the dilutions were made) was a microemulsion containing 24 %w/w Brij 96 and 3 %w/w soybean oil. The next possible composition of the series, containing 28 %w/w Brij 96 and 3.5 %w/w soybean oil (weight fraction 0.315) was turbid and very viscous, therefore outside the area of microemulsion existence, and not tested. The size of the microemulsion droplets changed little over the area of existence along the 8:1 tie line (fig.3.17) although there was a distinct bimodal distribution and hence evidence of aggregation found at a weight fraction of 0.27. It is interesting to note that although a microemulsion could not be individually prepared with a composition of 4 %w/w Brij 96 and 0.5 %w/w soybean oil, the same composition achieved by dilution still appeared to contain individual microemulsion droplets. The apparent Z mean diameter for this sample was however larger than the other members of the series.

In comparison, a fixed Brij 96:soybean oil ratio of 4:1 gave higher apparent Z mean diameters than all compositions with a ratio of 8:1. This is to be expected from the results of increasing oil content as previously described (3.4.1.3). Although not included in the graph of figure 3.17 the sample containing 24 %w/w Brij 96 and 6 %w/w soybean oil (weight fraction = 0.3) also fell into the classification of a microemulsion and was the original composition from which the diluted samples were obtained. For this sample an apparent Z mean diameter of 50.9nm was found. The same composition, previously tested had however resulted in an apparent Z mean diameter of 26.4nm (3.4.1.4). As can be seen in the log intensity vs log diameter plots of both samples (figs.3.15 & 3.16b) although this composition also contained individual microemulsion droplets, there was a significant larger-sized population which contributed to the high mean diameter, and to the difference in the apparent Z mean diameter for two samples of the same composition (3.4.1.2).

Distinct bimodal distributions were also seen for microemulsions with a weight fraction greater than 0.2. The appearance of bimodal distributions corresponded to the increased apparent Z mean diameter found with increasing weight fractions above 0.2 shown in figure 3.17. Weight fractions of between 0.1 and 0.2 exhibited essentially monomodal distributions of scattered intensity and showed no change in the size of the microemulsion droplets. As observed with a Brij 96:soybean oil weight ratio of 8:1, samples which were normally outside the microemulsion region, but which were obtained by dilution, did contain droplets, and also exhibited an increase in the apparent Z mean diameter compared to microemulsions produced inside the microemulsion region.

The results obtained from these two ratios of surfactant to oil therefore indicate that in the inner regions of the microemulsion area (below concentrations of both oil and surfactant at which individual microemulsion droplets begin to aggregate) the size of the o/w microemulsion droplet remains almost constant if the ratio of surfactant to oil remains the same. Large changes are again seen closer to the border of microemulsion existence.

These results are also interesting from the point of view of using PCS to study microemulsions. The different compositions tested for each ratio of surfactant to oil were all obtained from varying degrees of dilution of one original

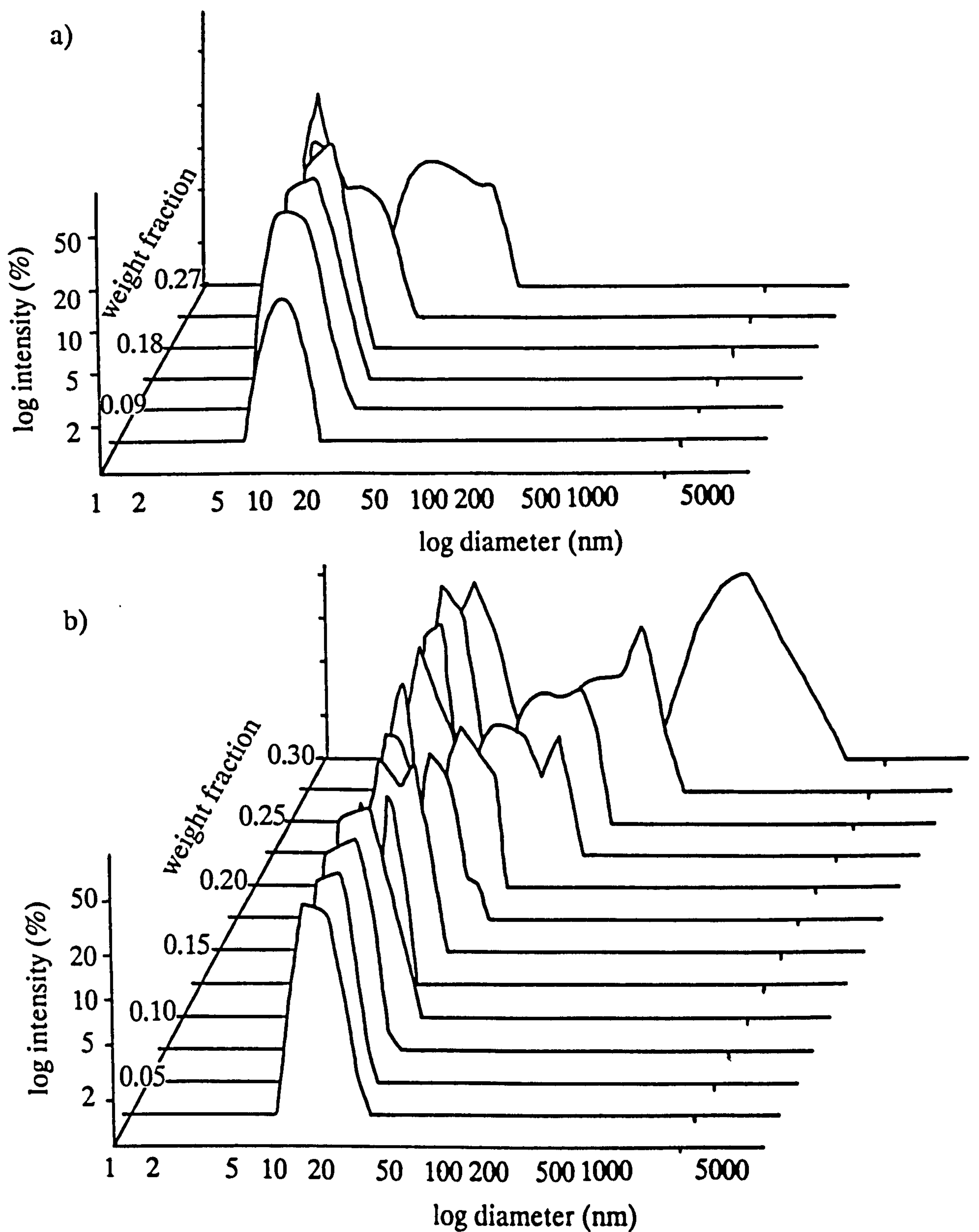


Figure 3.16: Log intensity vs log diameter plots for diluted microemulsion systems with increasing weight fraction ($\text{g}[\text{oil} + \text{Brij } 96] / \text{g}[\text{oil} + \text{Brij } 96 + \text{water}]$) with a constant weight ratio of Brij 96:soybean oil of a) 8:1, and b) 4:1.

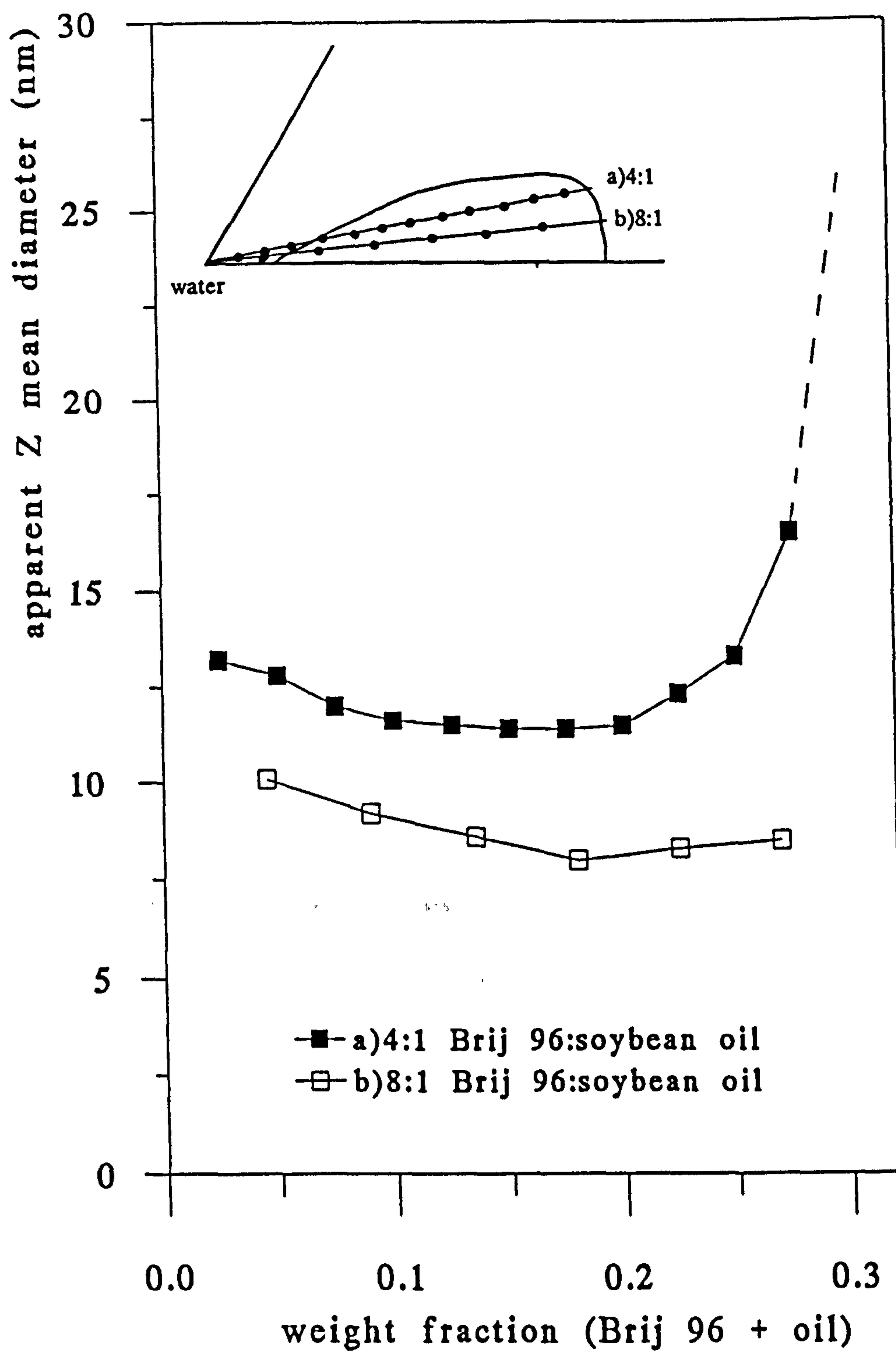


Figure 3.17: Apparent Z mean diameter and polydispersity as a function of weight fraction for microemulsions with a fixed ratio of Brij 96:soybean oil of a)4:1 and b)8:1.

sample. A range of apparent Z mean diameter values were obtained. Whilst diluting a microemulsion system to a composition outside the area of microemulsion existence indicated the presence of droplets, the observed apparent Z mean diameter was greater than that found for those compositions within the area. If the increase was due only to the reduction of interactions, and subsequent measuring errors observed at higher concentrations (resulting in an underestimation of droplet size) it might be expected that a change of apparent Z mean diameter would also be seen with those diluted samples still within the area of existence. This however was not the case, and may therefore support the premise that dilution of microemulsion systems in order to reduce multiple scattering and interdroplet interactions is inappropriate. Although the droplet sizes obtained by PCS from undiluted samples cannot be used without correction, the apparent values and the scattered intensity distribution obtained from each sample are useful in order to appreciate changes that are occurring across the microemulsion area of existence.

3.4.2 Total intensity light scattering

3.4.2.1 Brij 96 micellar systems

Plots of the Rayleigh ratio, and the reduced scattered intensity (c/R_{90}), as a function of Brij 96 concentration observed for micellar systems is shown in figure 3.18. As previously reported for micelles of Triton X-100 [261], the present study shows that at Brij 96 concentrations up to 2 %w/w the Rayleigh ratio increases linearly, as would be expected from independent, spherical particles. A peak of R_{90} occurred between 5 and 10 %w/w surfactant, and then the observed values decreased in a non-linear fashion.

Analysis of this TILS data for Brij 96 solutions up to 2%w/w was carried out as described in chapter 2 (2.2.10.3) using equation 27. The resulting molecular weight of the Brij 96 aggregate was calculated to be 79301 gmol^{-1} , and hence (using a molecular weight of 708 gmol^{-1} for Brij 96) an aggregation number of the aggregate of 112 was determined.

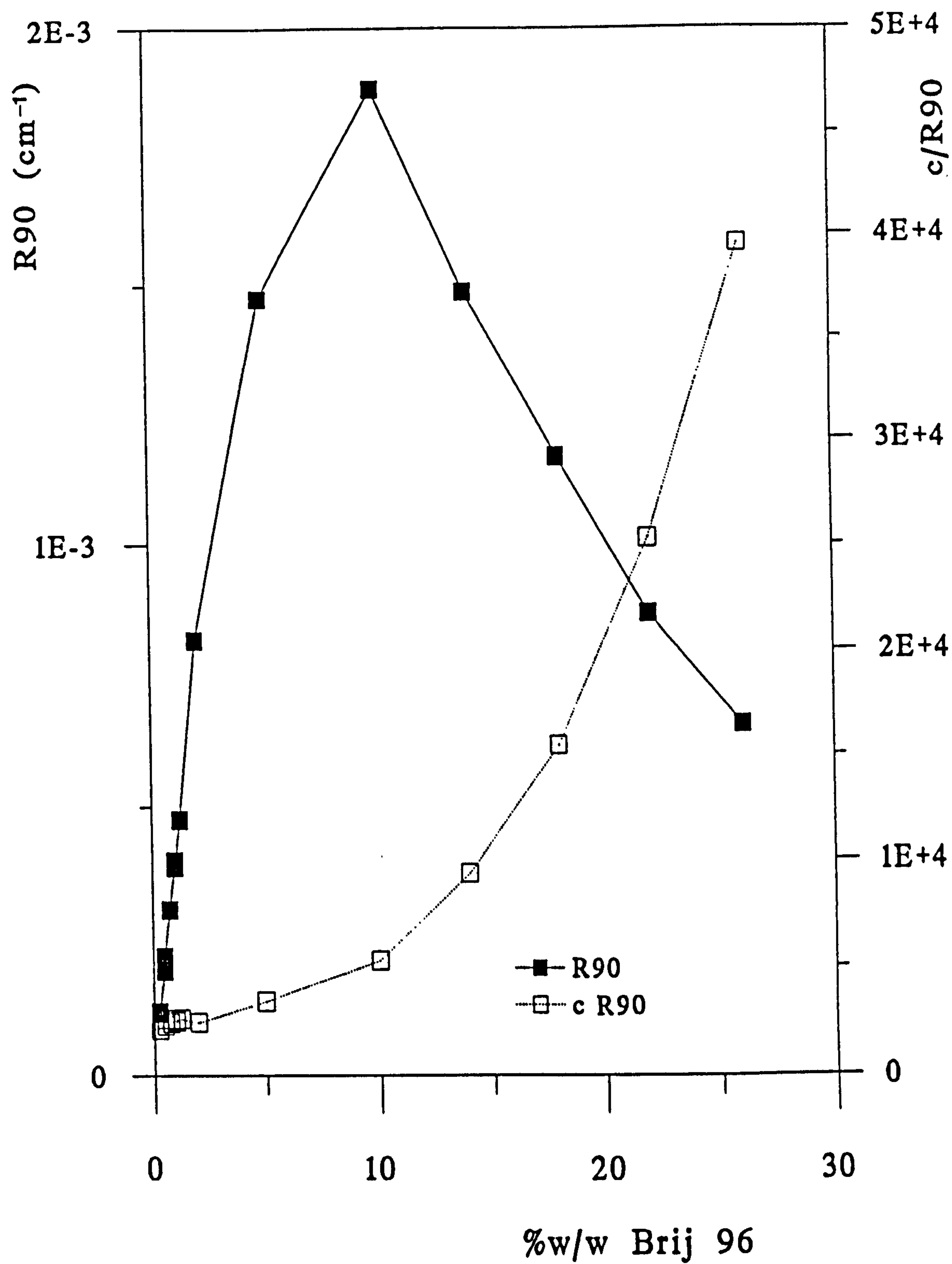


Figure 3.18: TILS results of Brij 96 micellar systems; R_{90} and c/R_{90} , as a function of Brij 96 concentration.

The volume of the oleyl hydrophobe of Brij 96, calculated by summing the volume contributions of the chemical groups it contains, was estimated to be 500Å. Assuming a spherical micelle with aggregation number 112, the volume and radius of the hydrocarbon core were subsequently calculated to be 56000Å³ and 23.7Å respectively. An average a_o of 63Å² for each surfactant molecule was also obtained.

It has however been suggested for C_mE_n surfactants where $m=12$, that spherical micelles are not possible [262]. In order to determine if spherical micelles were possible, based on the TILS results observed with $C_{18-1}E_{10}$ in this study, the maximum extended alkyl chain length (l_{ext}) for the unsaturated oleyl hydrocarbon was estimated from equation 3 [92] and model building studies (using a cis double bond angle of 150°, a cis double bond length of 1.35Å, and a value of 1.5Å for the terminal hydrogen). A value of l_{ext} of 21.6Å was calculated. As the l_{ext} calculated was less than the radius derived from experimental TILS data assuming the Brij 96 micelle to be spherical, it appears unlikely that they do form spheres, and more likely that an ellipsoidal model used by Tanford *et al* [93] for C_mE_n surfactants applies.

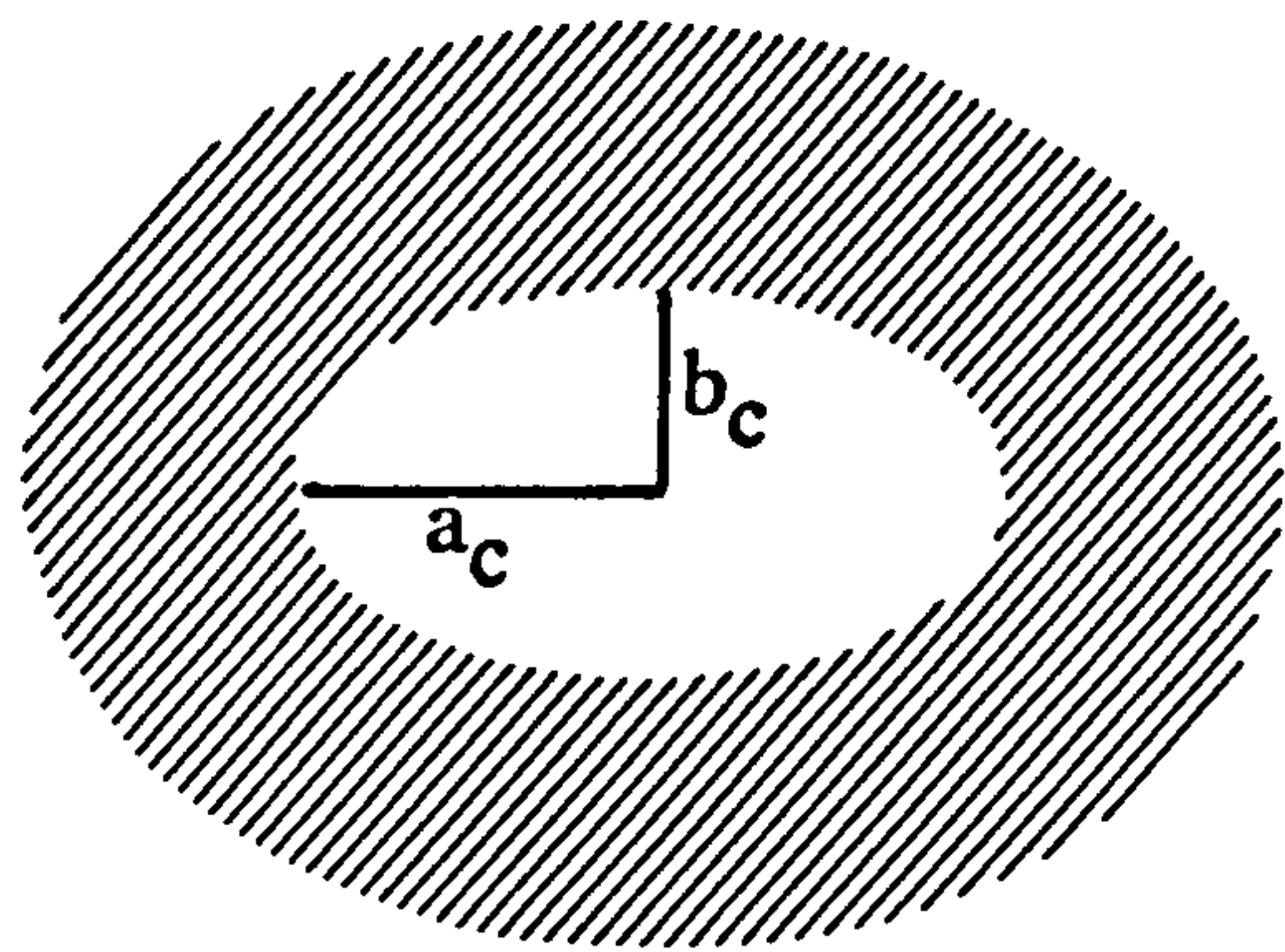
Assuming a prolate ellipse, the volume of the hydrophobic core can be described by;

$$V_c = \frac{4\pi}{3} a_c b_c^2 \quad \text{eqn.57}$$

where $b_c < a_c$, and b_c is less than or equal to the length of the surfactant alkyl chain. Calculations of various ratios of a_c and b_c for a Brij 96 micelle with an aggregation number of 112 are given in table 3.3.

It can be seen from table 3.3 that for the extended alkyl chain length (21.6Å) to be less than b_c the ratio of $a_c:b_c$ must be greater than about 1.3:1. However, as previously pointed out (1.4.1.1) the actual surfactant hydrocarbon chain length (l_c) in a micelle will be in a liquid rather than an extended state, and values of 75-80% of l_{max} have been proposed as realistic [93, 94]. If however b_c is set to a value of 75% l_{ext} (16.2Å) the calculated dimensions of a_c and b_c will be in the order of 3:1, which would represent the shape of a distinctly non-spherical micelle.

Table 3.3: Calculated dimensions for spherical and prolate ellipsoidal Brij 96 micelles with an aggregation number of 112.



$a_c:b_c$	a_c (Å)	b_c (Å)
sphere		
1 : 1	23.7	23.7
prolate ellipsoid		
1.25 : 1	27.5	22.0
1.3 : 1	28.3	21.7
1.5 : 1	31.1	20.7
2 : 1	37.7	18.8
2.5 : 1	43.7	17.5
3 : 1	49.4	16.5
3.5 : 1	54.7	15.6
4 : 1	59.8	15.0

To obtain the dimensions of the complete micelle (ie hydrocarbon core plus ethylene oxide chains) the expected length of the ten attached ethylene oxide units must be added. This value will however depend on the conformation of the polyoxyethylene chains, and would be expected to range from a maximum of 35Å for chains in fully extended or zig-zag formation, down to approximately 15Å for a random coil configuration [93]. Assuming the ratio of a_c to b_c of 3:1, dimensions of the micelle of between 64.4-84.4Å and 31.5-51.5Å for the major and minor semi axes respectively would be expected.

Also assuming the ratio of a_c to b_c in the hydrocarbon core of 3:1 and a random coil configuration of the ethylene oxide chains (15Å) the ratio of the major and minor semi axes (a:b), including ethylene oxide chains of length 15Å, becomes 2.05:1. The constant diffusion coefficient observed with concentrations of Brij 96 in water of up to 2 %w/w (section 3.4.1.4) was used to calculate the values of a and b (using a ratio of 2.05:1) according to the adapted Stokes Einstein relationship for solvated ellipsoidal micelles [263];

$$D = \frac{k T}{6 \pi \eta a} G(p) \quad \text{eqn.58}$$

where $G(p)$ is the shape factor, related to the axial ratio, p ($p=b/a$) for prolate ellipsoids ($p < 1$) by;

$$G(p) = (1-p^2)^{-1/2} \ln \left[\frac{1 + (1-p^2)^{1/2}}{p} \right] \quad \text{eqn.59}$$

Values for a and b of 57 and 28Å respectively were obtained. These values are smaller than those obtained from TILS data, even when assuming a random coil conformation of the hydrophilic chains (64.4 and 31.5Å). The values of a and b compare to a hydrodynamic radius obtained by PCS, assuming spherical micelles, of 48.5Å. A hydrodynamic radius of 48.5Å is, however, in reasonable agreement to an anhydrous radius, determined by TILS, of 38.7Å which can be obtained by assuming the existence of a spherical hydrocarbon core (23.7Å) and a random coil conformation of the ethylene oxide chains (15Å).

3.4.2.2 Microemulsion systems

TILS investigations were carried out for some of those microemulsion compositions studied by PCS (3.4.1.3 and 3.4.1.4). The resulting Rayleigh ratio as a function of soybean oil concentration for microemulsion systems containing 10 and 14 %w/w Brij 96 are shown in figure 3.19a. The curves show a non-linear increase as the amount of soybean oil in the microemulsion was increased. Similar trends have been obtained for increasing volume fractions of IPM in o/w microemulsion systems containing IPM, sorbitol, water and either polysorbate 60 [234, 264] or polysorbate 80 [264].

When the soybean oil content was held constant, at either 2 or 4 %w/w, and the Brij 96 content was increased, plots of R_{90} against concentration of Brij 96 showed a non-linear decrease (fig.3.19b).

In order to derive radii (corrected for interparticle interactions) from the Rayleigh ratio values obtained by TILS, analysis of the results were carried out according to the method described in section 2.2.10.3 (eqns.28-56). The refractive index of the scattering unit (RI_s) was taken to be that of soybean oil at 488nm and 30°C (1.479). A molecular weight for this triglyceride oil, calculated based on the percentage distribution of the saturated and unsaturated free fatty acids attached to a glycerol backbone, of 870 gmol⁻¹ was used. A molecular volume of one oil molecule (v_o), based on this molecular weight and the density of the oil at 30°C, of 1563Å³ was calculated and employed. A molecular weight of 708 gmol⁻¹ was used for Brij 96, and 500Å³ was taken as the volume of the surfactant hydrophobe (see section 4.1.1.2).

One important parameter in the modelling calculations which is not however known, is the area occupied by the surfactant polar headgroup at the interface (a_o). Hence analysis of the TILS data was initially carried out using four values of a_o ; namely 48, 55, 63 and 70Å². A value of 48Å² was obtained by interpolation of the plot of a_o against number of ethylene oxide units for eight C_mE_n surfactants [251, 265, 266]. Similarly, 55Å² was the interpolated value obtained using the data of Tanford [93] assuming ellipsoidal C_mE_n micelles. Data from TILS results of Brij 96 solutions, assuming spherical micelles (3.4.2.1), had indicated the value for a_o of 63Å². However, the above TILS results also suggested that the Brij 96 micelles may in fact be non-

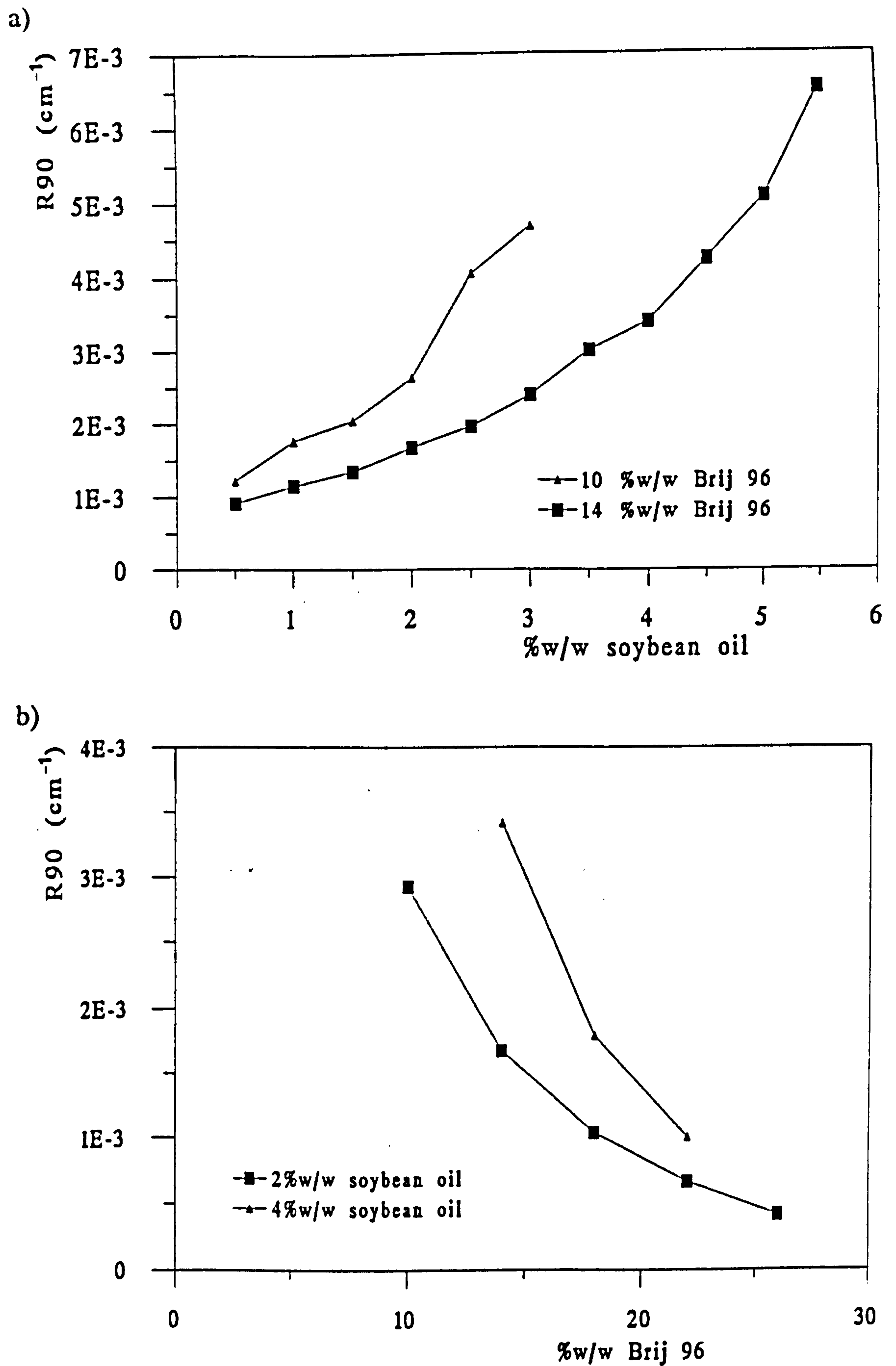


Figure 3.19: TILS results for microemulsion systems; a) R_{90} as a function of soybean oil concentration for microemulsions containing either 10 or 14 %w/w Brij 96, and b) R_{90} as a function of Brij 96 concentration for systems containing either 2 or 4 %w/w soybean oil.

spherical, in which case because a sphere represents the situation in which the surfactants will be most tightly packed, an a_o of some value greater than 63\AA^2 might be expected, and hence a value of 70\AA^2 was also tried.

The resulting calculated values of the anhydrous radii of the microemulsion droplet, r_2 , and the thickness of the outer layer, t_1 (to the nearest 0.5\AA), for all four values of a_o are given in tables 3.4 and 3.5.

Tables 3.4a and 3.4b show the change in microemulsion droplet size with increasing soybean oil content for systems containing 10 and 14 %w/w Brij 96 respectively. For all values of a_o , the observed trends for systems with the same surfactant content and increasing soybean oil concentration, was for r_2 to increase and for t_1 to decrease. The calculated size does however vary greatly depending on the value of a_o selected. The smaller the value of a_o , the larger the resulting calculated value of r_2 , and the more positive the value of t_1 .

Results in table 3.5 show the calculated values of r_2 and t_1 for the microemulsion compositions tested containing 2, 4 and 6 %w/w soybean oil. It can be seen that for the same soybean oil concentration the values of r_2 decreased with increasing surfactant concentration, and that the values of t_1 also tended to decrease. As already seen in table 3.4, values of r_2 and t_1 both decrease with an increase in the a_o selected.

Interpretation of TILS data by this method depends on the interpretation of the value t_1 . Previous applications of this model [234, 236, 237, 264] have assumed a fixed value, or values, of t_1 . In the case of o/w microemulsions calculations were carried out for several values of a_o and t_1 , in which t_1 was thought to correspond to the expected thickness of the hydrophilic polyoxyethylene outer shell [234, 264]. In the model employed in the present study, r_2 was calculated based on the oil and all the surfactant (including the polyoxyethylene shell) expected in one microemulsion droplet and t_1 was allowed to vary.

When a fixed concentration of surfactant was used and the amount of soybean oil in the microemulsion composition increased (table 3.4), it was found that t_1 decreased with increasing volume fraction (ϕ_{r_2}) and size (r_2) of the microemulsion droplet. For the three values of a_o greater than 48\AA , many

Table 3.4: Analysis of TILS results with increasing soybean content in microemulsions containing a)10 %w/w and b)14 %w/w Brij 96; microemulsion volume fraction, r_2 and t_1 determined for four values of a_0 .

a)

microemulsion composition	Φr_2	area occupied by the surfactant											
		$a_0=48\text{\AA}^2$				$a_0=55\text{\AA}^2$				$a_0=63\text{\AA}^2$			
		r_2		t_1		r_2		t_1		r_2		t_1	
		r_2	t_1	r_2	t_1	r_2	t_1	r_2	t_1	r_2	t_1	r_2	t_1
0.5% soybean oil / 10% Brij 96	0.104	45.5	7.0	39.7	0.5	34.6	-6.5	31.1	-4.5	34.6	-10.0	31.1	-14.5
1% soybean oil / 10% Brij 96	0.109	49.7	5.5	43.3	-1.5	37.8	-8.0	34.0	-16.0	37.8	-8.5	34.0	-17.5
1.5% soybean oil / 10% Brij 96	0.115	53.9	7.0	47.1	0	41.0	-16.0	36.9	-28.0	41.0	-14.5	36.9	-26.5
2% soybean oil / 10% Brij 96	0.120	58.1	7.0	50.6	-1.0	44.2	-5.0	39.7	-14.5	44.2	-11.0	39.7	-16.5
2.5% soybean oil / 10% Brij 96	0.125	62.2	2.5	54.3	-6.0	47.4	-11.0	42.6	-16.5	47.4	-14.5	42.6	-28.0
3% soybean oil / 10% Brij 96	0.131	66.3	3.5	57.8	-5.0	50.5	-11.0	45.4	-16.5	50.5	-14.5	45.4	-28.0

b)

microemulsion composition	Φr_2	area occupied by the surfactant											
		$a_0=48\text{\AA}^2$				$a_0=55\text{\AA}^2$				$a_0=63\text{\AA}^2$			
		r_2		t_1		r_2		t_1		r_2		t_1	
		r_2	t_1	r_2	t_1	r_2	t_1	r_2	t_1	r_2	t_1	r_2	t_1
0.5% soybean oil / 14% Brij 96	0.143	44.3	6.5	38.6	1.5	33.7	-2.5	30.3	-7.0	33.7	-7.0	30.3	-16.5
1% soybean oil / 14% Brij 96	0.148	47.3	6.0	41.3	1.0	36.0	-3.5	32.4	-7.0	36.0	-4.5	32.4	-12.0
1.5% soybean oil / 14% Brij 96	0.154	50.3	6.5	44.0	1.5	38.3	-4.5	33.4	-8.5	38.3	-6.0	33.4	-12.5
2% soybean oil / 14% Brij 96	0.159	53.3	6.0	46.5	0.5	40.5	-4.5	36.5	-9.0	40.5	-7.5	36.5	-14.5
2.5% soybean oil / 14% Brij 96	0.165	56.3	6.0	49.1	0.5	42.8	-6.0	38.5	-10.0	42.8	-7.5	38.5	-16.5
3% soybean oil / 14% Brij 96	0.170	59.2	5.0	51.7	-0.5	45.1	-7.5	40.5	-12.0	45.1	-9.5	40.5	-16.5
3.5% soybean oil / 14% Brij 96	0.175	62.2	4.0	54.3	-2.0	47.3	-9.5	42.6	-12.5	47.3	-11.0	42.6	-16.5
4% soybean oil / 14% Brij 96	0.181	65.1	3.5	56.8	-2.0	49.5	-11.0	44.6	-14.5	49.5	-14.5	44.6	-16.5
4.5% soybean oil / 14% Brij 96	0.186	68.0	2.5	59.4	-4.0	51.8	-16.5	46.6	-28.0	51.8	-14.5	46.6	-28.0
5% soybean oil / 14% Brij 96	0.191	71.0	1.0	61.9	-5.0	54.1	-11.0	48.6	-16.5	54.1	-14.5	48.6	-28.0

Table 3.5: Analysis of TILS results for microemulsions with increasing Brij 96 concentration; microemulsion volume fraction, r_2 and t_1 determined for four values of a_0 .

microemulsion composition	Φr_2	area occupied by the surfactant											
		$a_0=48\text{\AA}^2$		$a_0=55\text{\AA}^2$		$a_0=63\text{\AA}^2$		$a_0=70\text{\AA}^2$					
		r_2	t_1	r_2	t_1	r_2	t_1	r_2	t_1	r_2	t_1	r_2	t_1
2% soybean oil / 10% Brij 96	0.120	58.1	7.0	50.6	-1.0	44.2	-8.5	39.7	-17.5				
2% soybean oil / 14% Brij 96	0.159	53.3	6.0	46.5	0.5	40.5	-4.5	36.5	-8.5				
2% soybean oil / 18% Brij 96	0.199	50.6	6.0	44.2	2.0	38.5	-1.5	34.7	-4.0				
2% soybean oil / 22% Brij 96	0.238	49.0	5.5	42.7	2.5	37.2	-0.5	33.6	-2.5				
2% soybean oil / 26% Brij 96	0.278	47.8	5.5	41.7	2.5	36.3	0.5	32.7	-1.0				
4% soybean oil / 14% Brij 96	0.181	65.1	3.5	56.8	-2.0	49.5	-7.5	44.6	-12.5				
4% soybean oil / 18% Brij 96	0.220	59.9	5.0	52.3	0.5	45.6	-3.5	41.0	-6.0				
4% soybean oil / 22% Brij 96	0.259	56.5	5.0	49.3	1.5	43.0	-1.5	38.7	-3.5				
6% soybean oil / 18% Brij 96	0.241	69.0	0	60.2	-5.0	52.5	-9.0	47.2	-12.5				

of the values of t_1 were negative. As observed with PCS investigations of the same microemulsion systems, it is certainly likely that interactions within the system would increase with increasing volume fraction. Hence the interpretation of R_{HS} ($r_2 + t_1$) used here was that of the radius that would be required before interaction between droplets occurred, and t_1 was interpreted as some relative measure of how close the droplets are, and how likely they are to interact. Negative values of t_1 may therefore indicate interaction, and possible interpenetration of the ethylene oxide chains of neighbouring droplets. The results obtained with constant soybean oil content and increasing concentration of Brij 96 (table 3.5) are more difficult to interpret because the size of the droplets was decreasing with increasing volume fraction, and hence a greater number of smaller droplets were present per unit volume. Possibly as a result of this situation, a less clear cut trend is observed in the values of t_1 .

Inspection of tables 3.4 and 3.5 suggested, that based on this view of t_1 , that of the four values of a_0 used, a value of 48\AA^2 seems to be the most likely for the systems considered in this study. Using this value for the interfacial area of the surfactant, the region of microemulsion existence may be approximated by those microemulsion compositions which have a positive value of t_1 and as a result of which the outer ethylene oxide chains of a microemulsion droplet are not thought to interpenetrate with the chains of its neighbours. With a value of a_0 of 48\AA^2 a value of zero was obtained for the t_1 found with the composition consisting of 18 %w/w Brij 96 and 6 %w/w soybean oil. This sample is close to the boundary of microemulsion existence and, as will be seen in the following section (3.5), was not stable to temperature cycling. In figures 3.20 and 3.21, in order to define t_1 more closely, the best fit between the calculated and observed values of R_{90} , assuming the value of a_0 to be 48\AA , was determined using iterative steps in t_1 of 0.1.

Results plotted in figure 3.20a show the variation of r_2 and $r_2 + t_1$ (when $a_0 = 48\text{\AA}$) with increasing soybean oil content for microemulsions containing 10 and 14 %w/w Brij 96. As found with PCS, the size of the droplet increased with increasing oil content. For systems containing the equivalent concentration of soybean oil, the size of the microemulsion droplets produced with 14 %w/w Brij 96 was less than that of microemulsions containing 10 %w/w Brij 96. As shown more clearly with the series containing 14 %w/w Brij 96; as oil was added the microemulsion droplets increase in size (and so

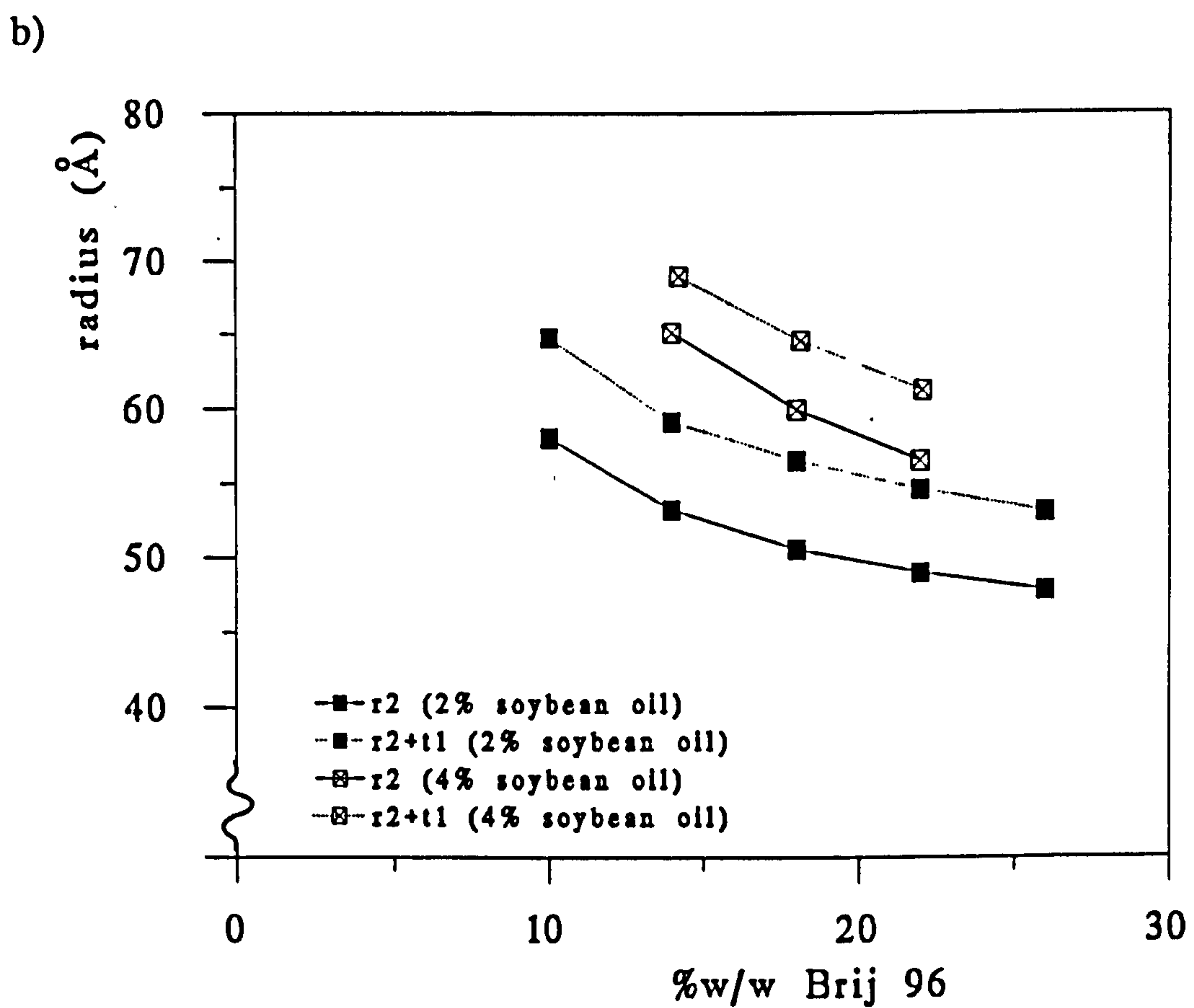
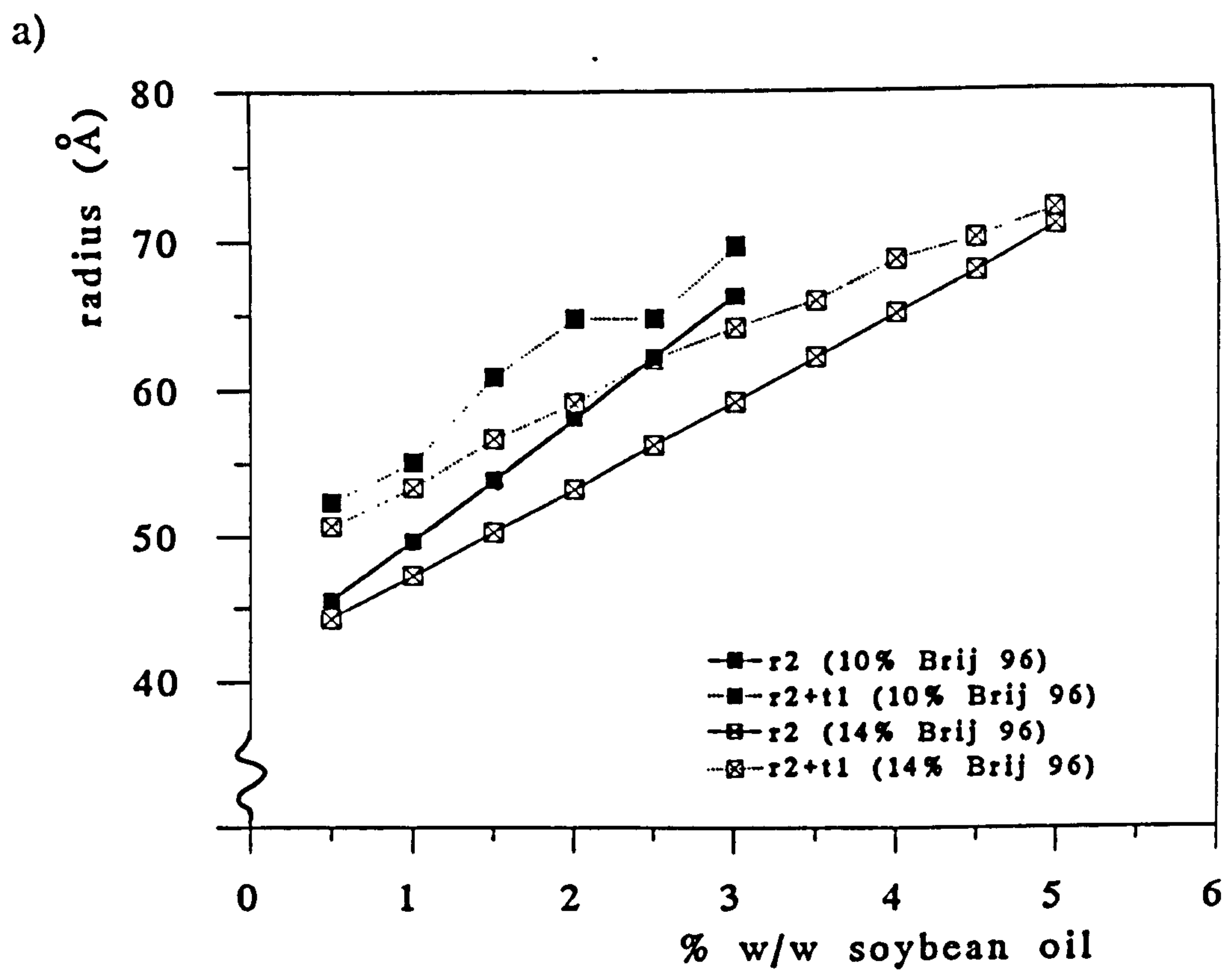


Figure 3.20: Values of r_2 and r_2+t_1 (Å) obtained by analysis of TILS data for microemulsions containing a) 10 or 14 %w/w Brij 96 as a function of Brij 96 content, and b) 2 or 4 %w/w soybean oil with increasing Brij 96 concentration.

become closer to the upper boundary of microemulsion existence) the value of t_1 was reduced.

The results of microemulsions containing a fixed soybean oil content with increasing Brij 96 concentration (assuming an a_o of 48Å) are shown in figure 3.20b. With both 2 and 4 %w/w soybean oil, the calculated size of the modelled droplet (r_2) became smaller with increasing concentration of Brij 96. The values of t_1 showed a less distinct trend. Similar values of t_1 were found for all concentrations containing 2 %w/w soybean oil. This observation may be because all the compositions containing 2 %w/w soybean oil are well within the boundary of the area of microemulsion existence. For the corresponding microemulsions containing the same concentration of Brij 96, but with 4 %w/w (rather than 2 %w/w) dispersed soybean oil, a reduced value of t_1 was seen, as might be expected because both the droplet size (r_2) and corresponding droplet volume fraction (Φ_{r_2}) were increased with increasing oil content.

3.4.2.3 Comparison of photon correlation spectroscopy and total intensity light scattering data

Using undiluted microemulsion systems, both PCS and TILS analysis suffer from the same limitations of having to interpret the degree, and correct for the occurrence of, interparticulate interactions. In the present study, no correction of PCS data was attempted. The observed values of R_{90} obtained by TILS were however interpreted by a model intended to compensate for interparticulate interactions.

In both PCS and TILS the values of droplet size obtained showed the same trends, namely; i) increasing size of the microemulsion droplets was seen with increasing soybean oil content in systems containing the same concentration of surfactant, and ii) a decrease in size was found when the soybean oil content was held constant and the surfactant concentration increased. These results are in agreement with previous investigations into the size of 4-component nonionic o/w microemulsions (containing a polyol cosurfactant such as glycerol or sorbitol in addition to the oil, nonionic surfactant and water of 3-component systems) obtained by TILS [234, 257, 264, 267].

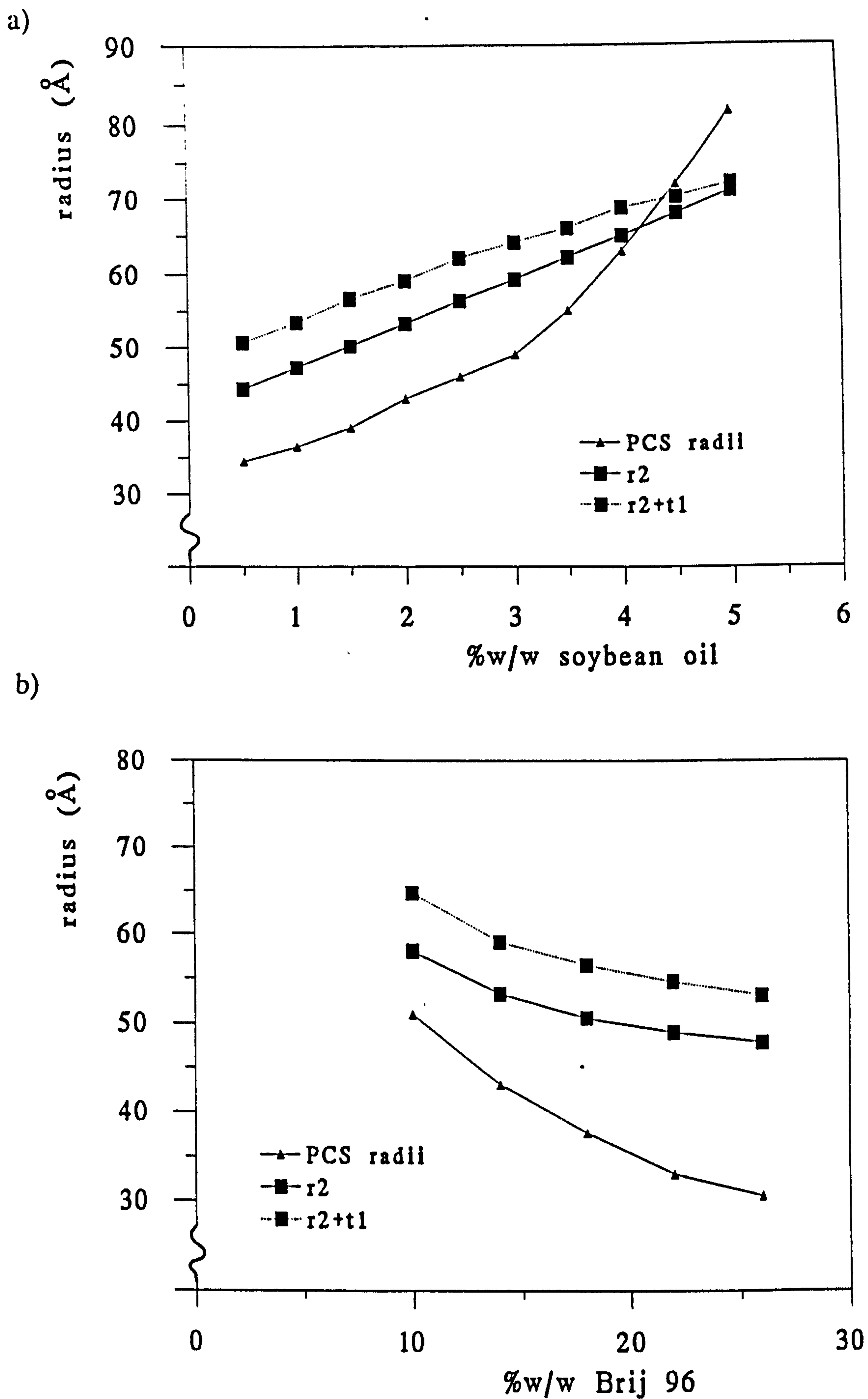


Figure 3.21: A comparison between radii obtained by PCS and TILS (r_2 and r_2+t_1) for microemulsion systems with a) 14 %w/w Brij 96 with increasing soybean oil concentration; and b) 2 %w/w soybean oil with increasing surfactant concentration.

The absolute values determined in this investigation by PCS and TILS techniques do however disagree. It might be expected that the hydrodynamic radius of a droplet determined by PCS should be greater than the anhydrous droplet size determined by TILS. In fact the results found show that greater values of size were determined by application of TILS. A comparison of the radii obtained by both techniques is given in figure 3.21a for microemulsions with 14 %w/w Brij 96, as a function of soybean oil concentration, and in figure 3.21b for microemulsions containing 2 %w/w soybean oil with increasing Brij 96 concentration. The differences found are expected to be due, at least in part, to the limitation of using the PCS data without any correction being made for interdroplet interactions and hence resulting in an underestimation of the droplet size [252]. Contributions to the disparity between the two techniques could however also arise due to the uncertainties and assumptions used in the interpretation of the TILS data. For example, the model used depended on the assumption that all of the oil and surfactant present in the composition was present only in the microemulsion droplets. The accuracy of the resulting values of r_2 obtained will depend on whether or not this assumption is reasonable. Furthermore, until reliable values of a_0 are determined for these systems, confidence in the absolute values of anhydrous radii obtained by this technique will remain low.

3.5 Stability of soybean oil/Brij 96/water microemulsions

A range of compositions over the microemulsion area of existence were examined for any physical change after subjecting the samples to successive cycles of 4°C (16 hours) and 30°C (8 hours) for 21 days. Only composition I (6 %w/w soybean oil/18 %w/w Brij 96) became turbid (therefore by definition no longer a microemulsion) over the period.

The samples were also examined by PCS over the 21 days. A graph of apparent Z mean diameter vs time is shown in figure 3.22. The mean diameter of samples containing 2 %w/w soybean oil (with 10, 14, 18, 22 and 26 %w/w Brij 96) remained fairly constant over the 21 days. There was however an increase in the size of compositions with 4 %w/w soybean oil. Examination of the log/log intensity vs diameter plots reveal that the change

in apparent Z mean diameter was due to an increase in the diameter and/or dominance of the larger-sized population within the size distribution, and hence could be due to an increase in aggregation of individual droplets with time. The increase in overall apparent Z mean diameter was not too large for samples with 14 and 18 %w/w Brij 96, but was very dramatic for the composition containing 22 %w/w and 4 %w/w soybean oil (H in figure 3.22). The apparent Z mean diameter of sample H remained fairly constant up to 14 days. When examined again at 21 days an increase in viscosity of the sample was noted, and the apparent Z mean diameter increased from 10 to 85nm. Examination of the log intensity plot at 21 days showed that this system still contained a population of small droplets, but the diameter of the larger-sized population had increased to between 200 and 1000nm.

Results of the PCS analysis of sample I, which becomes turbid between 7 and 14 days, appears rather unexpected. The initial size was similar to that found previously for the same composition (3.4.1.2) and it has already been shown (3.4.1.3) that this sample has a distinctly bimodal distribution. The apparent Z mean diameter was however reduced on days 7-21, even though the sample appears turbid on days 14 and 21. A proposed explanation for the observed decrease is that either the size or permanence of the larger-sized aggregates increased over the period of the test to the extent that a significant proportion of this population was removed during the filtering process carried out before each analysis.

In addition to testing the stability of the systems by temperature cycling, a portion of each composition was also held at 30°C for the entire 21 days. The apparent Z mean diameter for systems after this treatment is compared to that of the sample after 21 days of temperature cycling and the initial size found in table 3.6.

For samples containing 2 %w/w soybean oil there is not a large difference between the initial size, and the two temperature treatments for microemulsions with 10, 14 and 18 %w/w Brij 96. At 22 %w/w Brij 96 (sample D) however an apparent Z mean diameter of 11.4nm was found in comparison to 6.7 and 7.5nm for the initial and temperature-cycled samples respectively. The log intensity distributions showed that whereas the sizes within the temperature cycled sample remained monomodal over 21 days, a distinctly bimodal distribution was observed after the sample was held at

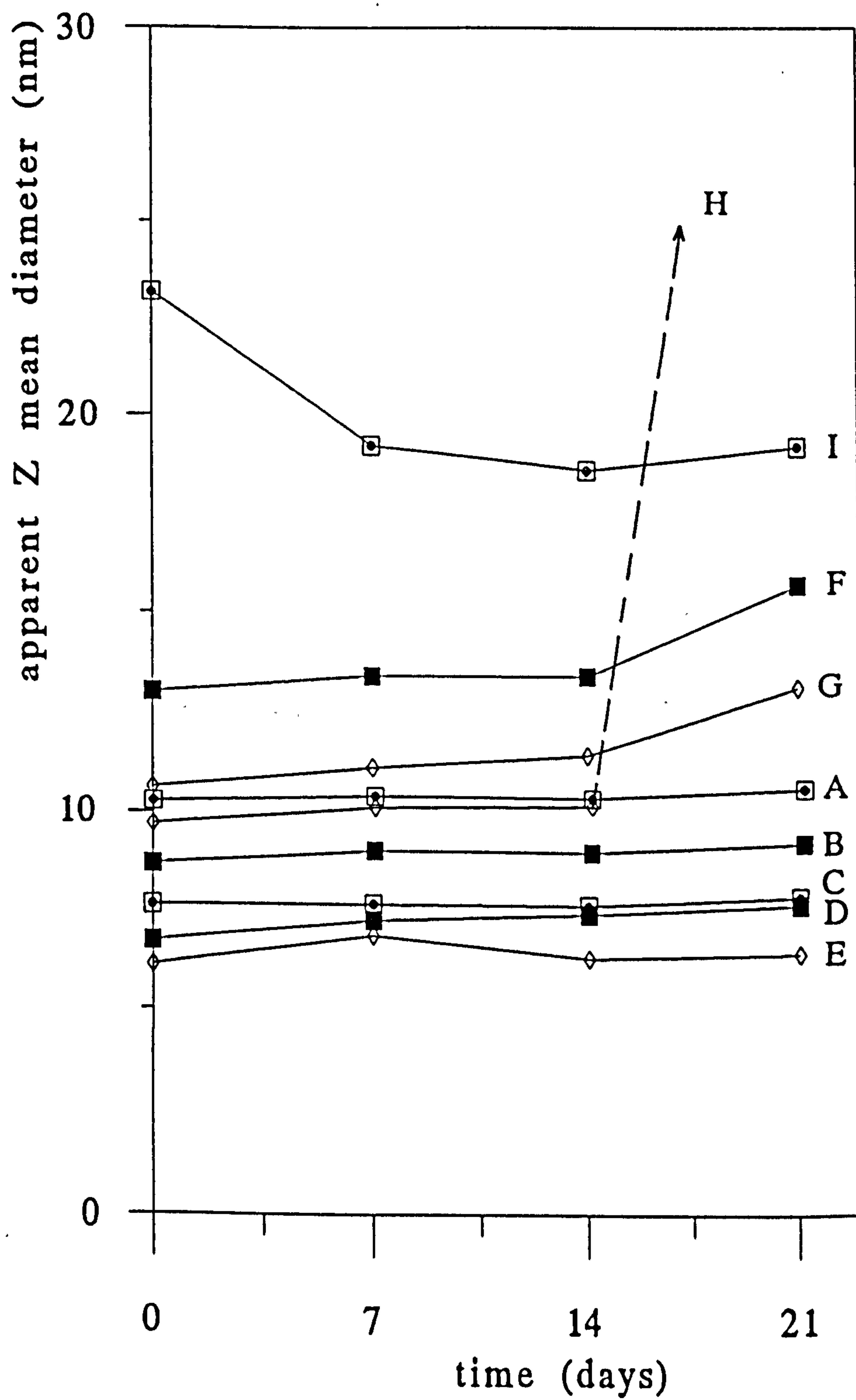


Figure 3.22: Apparent Z mean diameter vs time (days) for microemulsions undergoing temperature cycling stability testing.

Table 3.6: The apparent Z mean diameter (nm) of microemulsion samples before and after stability testing.

Sample	Microemulsion Composition	Apparent Z mean diameter		
		Initial	After 21 days	
			cycling 4/30 C	30 C
A	2% soybean oil / 10% Brij 96	10.3	10.8	12.2
B	2% soybean oil / 14% Brij 96	8.7	9.4	8.8
C	2% soybean oil / 18% Brij 96	7.6	7.7	8.0
D	2% soybean oil / 22% Brij 96	6.7	7.5	11.4
E	2% soybean oil / 26% Brij 96	6.1	6.3	gel
F	4% soybean oil / 14% Brij 96	13.0	15.7	17.6
G	4% soybean oil / 18% Brij 96	10.6	13.1	22.1
H	4% soybean oil / 22% Brij 96	9.7	84.5	137
I	6% soybean oil / 18% Brij 96	23.2	(T) 19.2	(T) 24.4

T = Turbid before filtering / size determined after filtering

30°C for 21 days. With composition E (2 %w/w soybean oil/26 %w/w Brij 96) after 21 days at 30°C the system was no longer a microemulsion, but has the appearance of a solid gel.

With microemulsions containing 4 %w/w soybean oil, all the apparent Z mean diameters found for samples subjected to 30°C, for 21 days were significantly greater than those found after temperature cycling. The most extreme example of this was composition H which gave an apparent Z mean diameter of 137nm following 21 days at 30°C compared to 84.5nm if exposed to temperature cycling. As found when subjected to temperature cycling, sample I became turbid with constant exposure to 30°C, although once again the apparent Z mean diameter was not as high as expected for a turbid sample.

It appears that microemulsion compositions in which PCS analysis indicates the formation of droplet clusters, if subjected to cycles of 30°C and 4°C exhibit a reduced tendency to aggregate compared to those kept at 30°C. In order to improve stability, prolonged storage at elevated temperatures would therefore appear to be inappropriate for these systems.

Interpretation of these stability testing results suggest that the droplet size of compositions within the o/w area of existence with lower oil and surfactant concentrations (which exhibit monomodal size distributions) remain relatively unchanged when subjected to temperature variations for 21 days. This would be expected from truly thermodynamically stable systems. It also appears that those microemulsions with higher surfactant and oil concentrations (which have been shown to aggregate and exhibit bimodal PCS intensity distributions) tend to increase in size with time. Even though these samples may appear to remain as microemulsions, their long term stability may be questionable, particularly if exposed to higher temperatures for extended periods. Similarly, instability in compositions located at the edge of the w/o microemulsion region produced with potassium oleate and various alcohol cosurfactants has also been reported by Müller and Müller [268].

CHAPTER FOUR: Other 3-component nonionic microemulsion systems

4.1 The influence of the surfactant

4.1.1 The surfactants used

4.1.1.1 Polydispersity of polyoxyethylene ether surfactants

It is necessary to note that all the C_mE_n surfactants used in this investigation were commercially available and not purified or dried before use. Most commercial surfactants consist of polydisperse materials with a distribution of ethylene oxide and alkyl chains [269]. In practice it is more common to encounter surfactants with polydisperse ethylene oxide groups [270]. For instance, up to twenty distinct peaks (thought to correspond to oleyl hydrophobes ether-linked to ethylene oxide chains of varying length) have been detected in a commercial sample of Brij 96 ($C_{18-1}E_{10}$) using HPLC techniques [271]. The average ethylene oxide content per hydrophobe can be determined by NMR techniques [272, 273].

The surfactants used here were not routinely screened by NMR but five surfactant samples tested did show reasonable agreement with the ethylene oxide content stated by the manufacturers, applying the method of analysis used by Lawrence [274], and assuming no variation in the alkyl chain length. Results are shown in table 4.1.

The effect of polydisperse ethylene oxide groups on surfactant/water mixtures has been reported to result in mesophases corresponding to single component surfactants of smaller ethylene oxide numbers [270]. Polydisperse surfactants

may therefore be considered effectively less hydrophilic in water than their corresponding monodisperse surfactant, with the CP occurring at lower temperatures [275].

The same relationship does not necessarily hold for microemulsions however. Using equal amounts of oil and water Wormuth and Geissler [275] found microemulsion phases occurred at higher temperatures when polydisperse surfactants with an average structure of $C_{12}E_n$ (with $n=4,5,6$ or 7) were used. Hence the polydisperse surfactants appeared to be effectively more hydrophilic than the corresponding monodisperse surfactants. These authors thought the difference was due to the significant amounts of unreacted alcohol and molecules with short ethylene oxide chains within the surfactant distribution which preferentially partitioned into the oil, and were consequently inactive in mixing the oil and water.

In contrast, because of the variation of surfactant chain length, commercial polyoxyethylene surfactants used in the production of microemulsions may be considered as already containing their own cosurfactant, which may result in an advantage in the formation of 3-component microemulsion systems.

As a result of polydispersity, caution needs to be applied in describing commercial surfactants by mole averages or average HLB values [275]. The possibility of batch to batch variation in ethylene oxide distribution and extent of polyoxyethylene hydration due to varying amounts of water present also exists. Variation in quality has been previously noted for surfactant/water systems containing different batches of commercially available Brij 96 [251]. During the course of the present study a number of batches of Brij 96 were employed. No gross changes in the area of 3-component soybean oil microemulsion existence shown in figure 3.2 were observed. In comparison, variation in CP values between different batches was noted. The cloud points of two different batches of Brij 96 (one of which, batch 23F-0780, was used to compare the cloud point of surfactant solutions and microemulsions shown in figure 3.5) and of another brand of $C_{18-1}E_{10}$; Volpo N10, are shown for comparison in figure 4.1. Hence the CP appears to be more sensitive, compared to the resulting area of microemulsion existence found, to the batch or brand of $C_{18-1}E_{10}$ used.

Table 4.1: Mean ethylene oxide units found for five of the surfactants used in this study, determined by NMR.

Surfactant		mean ethylene oxide units found by NMR
Brij 96*	C ₁₈₋₁ E ₁₀	10.2
Brij 99	C ₁₈₋₁ E ₂₀	19.1
Volpo N5	C ₁₈₋₁ E ₅	4.9
Brij 76	C ₁₈ E ₁₀	9.6
	C ₁₂ E ₁₀	9.3

* For ease of comparison between surfactants, Brij 96 is identified as C₁₈₋₁E₁₀ for the rest of this chapter.

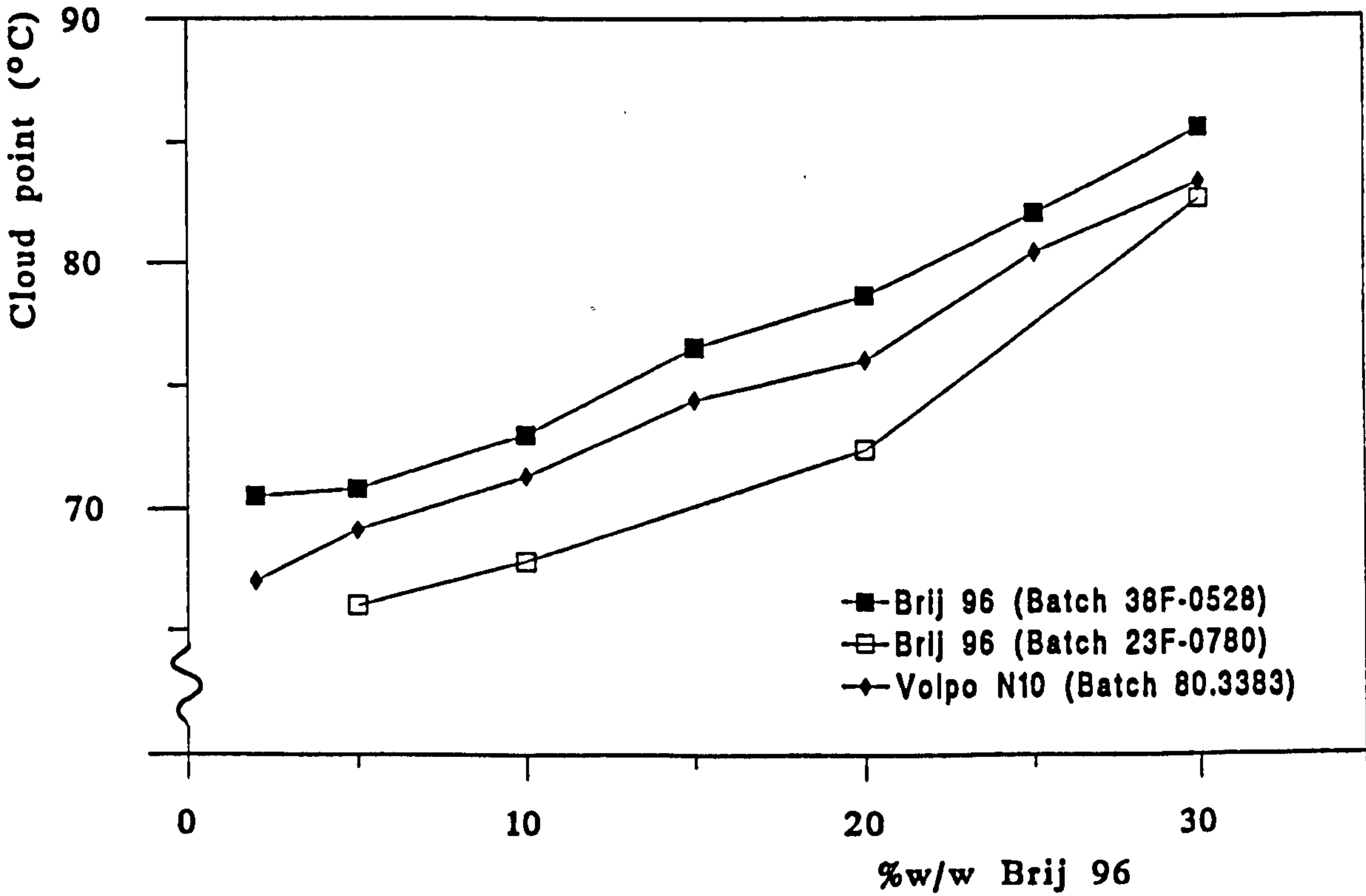


Figure 4.1: Variation of cloud point temperature vs Brij 96 concentration for different batches or brands of C₁₈₋₁E₁₀.

4.1.1.2 The HLB and CPP of the surfactants used

Eight C_mE_n surfactants were tested for their ability to form o/w microemulsion systems with soybean oil and water. The properties of this family of surfactants can be varied by alteration of the hydrocarbon chain length and saturation, and the number of attached ethylene oxide units. Hence the effect of changing the hydrophilic and hydrophobic portions of the surfactant on microemulsion formation at room temperature was observed. The HLB values quoted in table 4.2 were supplied by the manufacturers. The CPP (v/a_0l_c) was calculated (see 1.4.1.1) for each surfactant tested, based on the average structure claimed by the manufacturer. The values obtained are given in table 4.2.

The volume of the hydrocarbon chain (v) was calculated by summing the volume contributions (estimated from liquid density data) of the chemical groups it contains. Given that the volume of CH_3 -, $-CH_2$ - and $-CH=CH$ - groups are 55, 27 and 40\AA^3 respectively [8] the volume of the hydrophobic moiety, based on a chain length of one less than the number of carbon atoms (m), was calculated using;

$$v = 27(m-1-[2n_{cis}]) + 55 + 40n_{cis} \quad \text{eqn.60}$$

where;

n_{cis} = number of cis double bonds.

The length of the hydrocarbon chain, l_c , was taken to be 80% of the extended hydrocarbon chain length (l_{ext}). For saturated hydrocarbon moieties l_{ext} was calculated using equation 3 [92], in which n_c was taken to be a value of one less than the number of carbon atoms in the chain. For the unsaturated oleyl hydrocarbon l_{ext} was estimated from model building studies using a cis double bond length of 1.35\AA and bond angle of 150° and a value of 1.5\AA for the terminal hydrogen.

To determine the area occupied by the polar headgroup at the interface (a_0) a plot of a_0 against number of ethylene oxide units was drawn using literature values of a_0 for eight C_mE_n surfactants [251, 265, 266]. The linear relationship found was described by the equation;

Table 4.2: CPP and HLB values of the surfactants used in this study.

Surfactant	$V (\text{\AA}^3)$	$l_c (\text{\AA})$	$a_o (\text{\AA}^2)$	CPP	HLB
$C_{18-1}E_5$	500	17.3	41.1	0.70	9.0
$C_{18-1}E_{10}$	500	17.3	48.9	0.59	12.4
$C_{18-1}E_{20}$	500	17.3	64.5	0.45	15.3
$C_{18}E_{10}$	514	18.4	48.9	0.57	12.4
$C_{18}E_{20}$	514	18.4	64.5	0.43	15.3
$C_{12}E_{10}$	352	12.3	48.9	0.59	14.0
$C_{12}E_4$	352	12.3	39.5	0.72	9.7
$C_{16}E_{10}$	460	16.4	48.9	0.57	12.9

$$a_o = 1.56n + 33.3 \quad (r=0.993) \quad \text{eqn.61}$$

where;

n = number of ethylene oxide units in the headgroup.

4.1.2 The areas of microemulsion existence found with soybean oil

Of the surfactants used, only C₁₈₋₁E₁₀ and C₁₂E₁₀ resulted in the formation of Winsor IV o/w microemulsion systems at room temperature when soybean oil was used as the dispersed phase. The triangular phase diagram for C₁₈₋₁E₁₀ (Brij 96) has been shown (fig.3.1) and discussed in the last chapter (3.1). The phase diagram for C₁₂E₁₀ is given in figure 4.2. The microemulsions produced with this surfactant formed a smaller region than that obtained with C₁₈₋₁E₁₀. As found with C₁₈₋₁E₁₀, the maximum surfactant concentration that allowed the formation of clear liquid systems remained about 30 %w/w, but the minimum C₁₂E₁₀ concentration required for microemulsions was increased to about 22 %w/w. The amount of soybean oil that could be incorporated was also significantly reduced, with maximum incorporation of only 2 %w/w soybean oil found using C₁₂E₁₀.

It is not however claimed that microemulsions containing soybean oil are not formed with the other surfactants. In this study o/w microemulsions in particular were being sought, and hence compositions within the phase diagram far from the water apex were less extensively studied. In addition, compositions classified as microemulsions were only those which formed completely clear Winsor IV systems. Other multiphase systems may have contained microemulsion phase(s) in equilibrium with non-microemulsion excess phases.

The effect of temperature was also not considered. Classification of microemulsion existence was made at ambient temperature only. The existence and structure of microemulsion systems, as well as the hydrophilic-lipophilic properties of nonionic surfactants is highly dependent on temperature (1.3.3) and the possibility of o/w microemulsion systems at other temperatures is not discounted. For example in this investigation C₁₂E₄ was found to have a large w/o region at high surfactant and soybean oil concentrations, but no o/w systems were found. This is consistent with

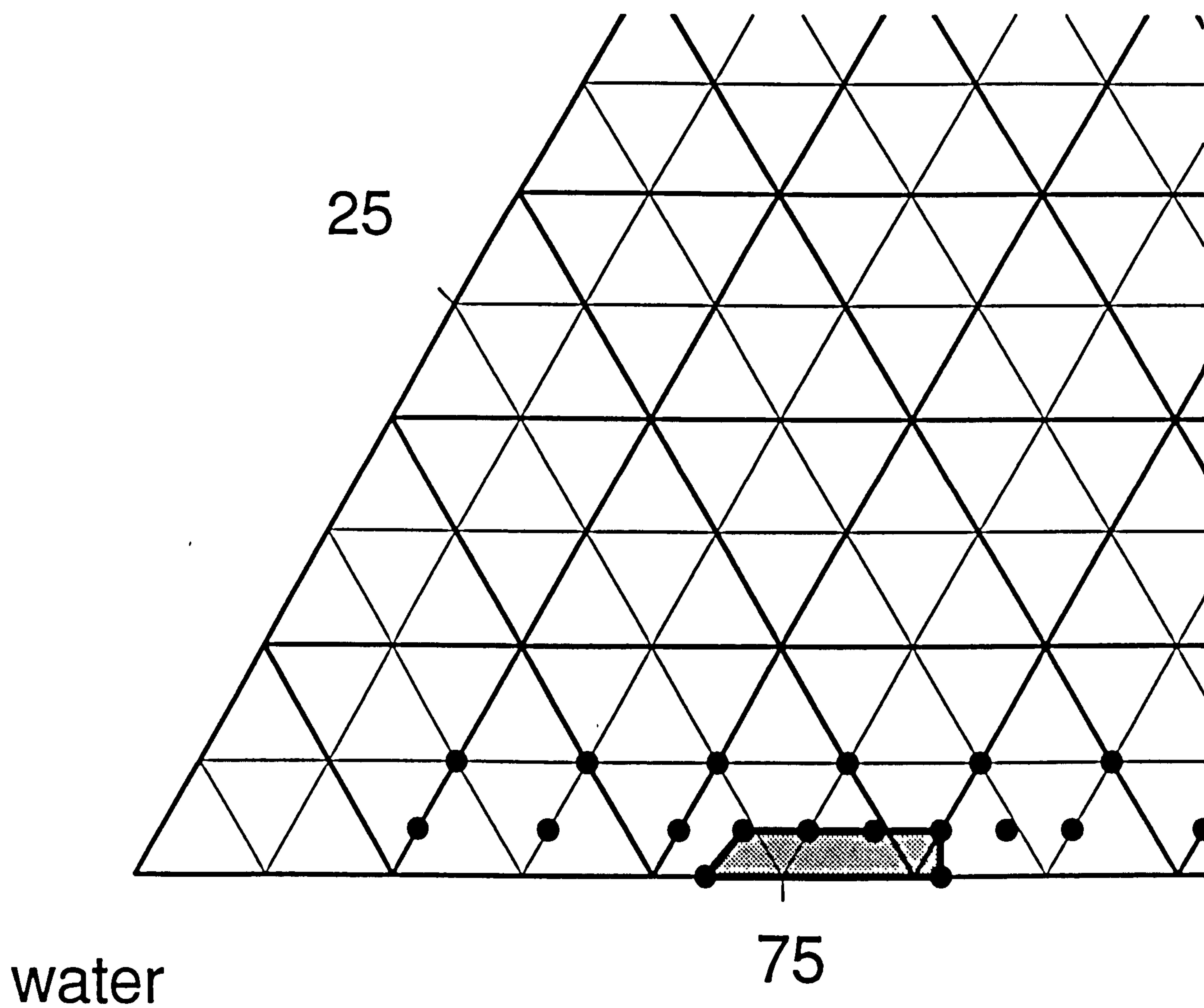


Figure 4.2: Partial triangular phase diagram for o/w microemulsions formed with $C_{12}E_{10}$, soybean oil and water.

other studies using $C_{12}E_4$ in which two clear regions were possible at lower temperatures, but at temperatures in excess of 20°C only w/o systems were found for heptane [276], decane [277], dodecane [278] and hexadecane [279].

The results of this study indicate the difficulty of predicting which nonionic surfactants can form o/w microemulsions at room temperature based on either HLB or CPP classifications. Three surfactants with oleyl hydrophobes were compared ($C_{18-1}E_5$, $C_{18-1}E_{10}$ and $C_{18-1}E_{20}$). Because of large differences in the average ethylene oxide content, there is a spread in values of both HLB and CPP for the three. Only $C_{18-1}E_{10}$ was found to produce microemulsions at room temperature, hence it might be expected that other surfactants of similar HLB and/or CPP (12.4 and 0.59 respectively) may also produce microemulsions with soybean oil.

Most significantly however, in contrast to using $C_{18-1}E_{10}$ as surfactant, soybean oil microemulsions could not be formed with $C_{18}E_{10}$ which has the same HLB value, and a very similar CPP (0.57). It therefore appears that structural considerations such as the presence of a cis double bond, which is assumed to introduce some degree of disorder and hence fluidity of the interface, are important in predicting which surfactants can be used for 3-component microemulsion formation.

The limitations of the HLB system are well documented. The system does not take into account the surfactant concentration, the oil:water ratio or the temperature [280, 281] and lacks sensitivity to the structure of the surfactant hydrophobe [282].

The geometric theory of surfactant aggregates (1.4.1.1) predicts o/w microemulsion formation when the surfactant structural properties result in a CPP of between 0.5 and 1, with higher oil encapsulation occurring after the ratio exceeds 0.8 [283]. Although amendment of the CPP to $(v/a_o l_c)_{\text{eff}}$ due to the interpenetration of the oil into the hydrophobic region of the surfactant film is advocated [284], due to the size of the triglyceride molecules present, soybean oil was not expected to alter the CPP values calculated in table 4.2.

It appears significant that the two surfactants which do form clear systems both have a CPP of 0.57, although surprising that surfactants with similar

values ($C_{18}E_{10}$, $C_{16}E_{10}$) did not therefore form microemulsions. Use of the CPP as a predictive tool also fails to explain why the polyoxyethylene ether surfactants with higher values of CPP failed to produce clear o/w microemulsion systems.

Whereas HLB and CPP are assigned to the surfactant molecule, other relationships have been suggested for particular microemulsion systems. These include the hydrophile lipophile index, HLK (ratio of water uptake to oil uptake by a particular microemulsion system at a specific temperature) [285] and use of the HLB temperature (1.3.3). Although the HLB temperature and HLK are useful for evaluating the hydrophilic-lipophilic properties of a nonionic surfactant in a given system, they would be of limited use in predicting which surfactants would form microemulsions until a large volume of experimental results were gained for different surfactant and oil combinations.

Hence results of this investigation suggest that, other than the possible advantage of a cis double bond (or other group which introduces disorder) the selection of C_mE_n nonionic surfactant for microemulsion production at room temperature appears to remain largely empirical.

4.2 The influence of the oil

4.2.1 The effect of different oils on $C_{18-1}E_{10}$ systems

4.2.1.1 One component oils

The effect of size and structure of the employed oil phase on the level of incorporation into nonionic surfactant films, and their subsequent effect on phase diagrams and microemulsion formation, has been studied by a number of workers. Many investigators have studied differences in the PIT of oil/surfactant/water systems, which may change widely depending on the oil phase used [286].

Microemulsion regions may also be shifted, and tend to occur at higher temperatures as the hydrocarbon chain length of the oil increases [269, 279]. Therefore at least one difficulty that arises from studying different microemulsions at only one temperature, is that the temperature selected may be above or below the PIT for a particular surfactant and oil. Oil incorporation increases as the PIT is approached, but if the temperature is above the PIT for the system o/w microemulsions will not occur [85].

4.2.1.1.1 The effect on phase inversion temperature

The PITs of microemulsions containing 10, 15 or 20 %w/w C₁₈₋₁E₁₀ and 2 %w/w of various dispersed oil phases are shown in table.4.3. It has already been shown in chapter 3 (3.3) that the presence of soybean oil resulted in an increase in the cloud point of an equivalent solution of surfactant for concentrations of C₁₈₋₁E₁₀ below about 20 %w/w, but at higher surfactant concentrations the PIT was reduced. In contrast, the PIT of systems containing heptane, 1-heptene, hexadecane and 1-hexadecene were less than the corresponding cloud point observed for 10, 15 and 20 %w/w surfactant, and for the equivalent microemulsion system produced with soybean oil. In general the PIT of the 1-alkene hydrocarbons was found to be lower than that of an alkane of the same chain length. The PIT of the longer octadecane and 1-octadecene systems were only compared at 10 and 20 %w/w surfactant concentration. 1-Octadecene was observed to reduce the CP, relative to a micellar system, and the PIT relative to the equivalent soybean oil microemulsion. This depression was only small at 10 %w/w/ C₁₈₋₁E₁₀, but more pronounced at 20 %w/w C₁₈₋₁E₁₀. The PIT behaviour of microemulsions containing 2 %w/w of the C₁₈ alkane, octadecane, exhibited a similar trend to that observed with 2 %w/w soybean oil microemulsions (section 3.3); a PIT higher than the CP of a 10 %w/w surfactant solution, and lower than the CP at 20 %w/w C₁₈₋₁E₁₀.

The depression of PIT found was however significantly greater with the shorter heptane and 1-heptene than the longer C₁₆ hydrocarbons. Other workers have also reported that for the same nonionic surfactant, the PIT tends to increase with the chain length of the oil [248, 249, 287] and decrease with aromaticity and polarity [288, 289]. The hypothesis of Aveyard *et al* [246] discussed in section 3.3 suggests that the CP of a micellar system is

Table 4.3: Cloud point and phase inversion temperatures of micellar and o/w microemulsion systems containing 2 %w/w of various dispersed oil phases.

oil	Temperature (°C)		
	%w/w C ₁₈ –1E ₁₀		
	10	15	20
no oil (micellar)	67.8	72.1	72.4
2 %w/w oil			
soybean oil	76.6	73.8	71.8
Miglyol 812	66.5	64.0	63.3
isopropyl myristate	52.8	—	53.3
heptane	44.9	44.0	46.0
1-heptene	43.3	46.5	46.5
hexadecane	68.0	66.5	67.5
1-hexadecene	61.9	59.5	66.0
octadecane	71.6	—	71.9
1-octadecene	66.4	—	66.1

raised if the added oil forms a core and encourages a more spherical shape. It may therefore follow that systems containing the shorter hydrocarbons, in particular heptane and 1-heptene, are more asymmetrical.

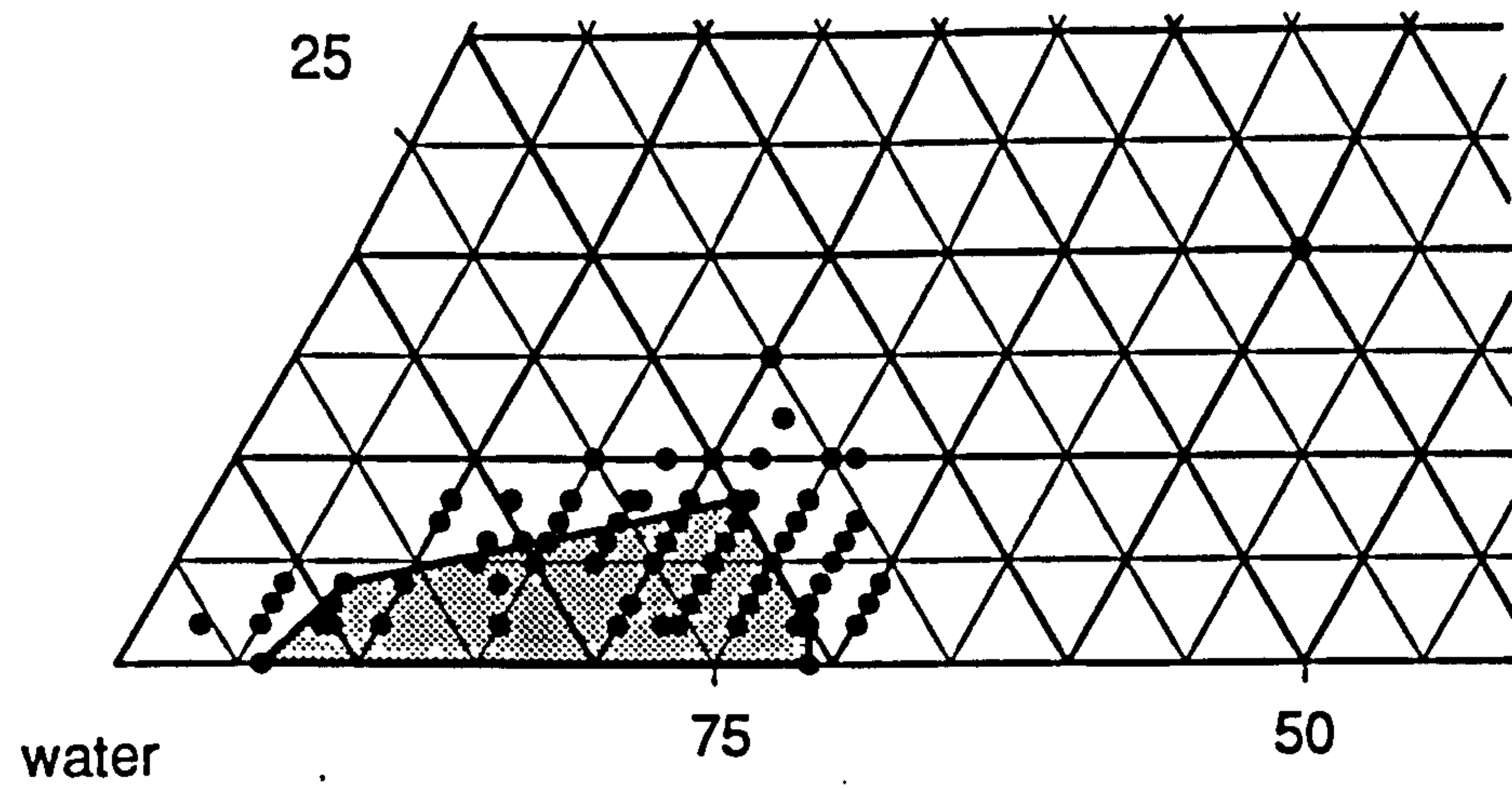
Work on alkane uptake in bilayers [290, 291, 292] and microemulsion systems [243] suggests that alkanes with a hydrocarbon chain length less than that of the surfactant, penetrate much more than those with greater chain length. Penetration of the oil into the hydrophobic region of the interface would tend to increase the effective CPP by increasing the hydrocarbon volume of the surfactant molecule at the interface (v), although this may to some extent be balanced by the effect of increasing the interfacial area (a_o). An increase in the CPP discourages the formation of spherical o/w droplets and encourages the w/o microemulsion formation [284, 293]. As a result of the structural changes arising from oil penetration into the surfactant interface the temperature at which the o/w systems begin to invert to w/o systems, and hence the PIT, will be lowered.

4.2.1.1.2 The effect on the area of existence

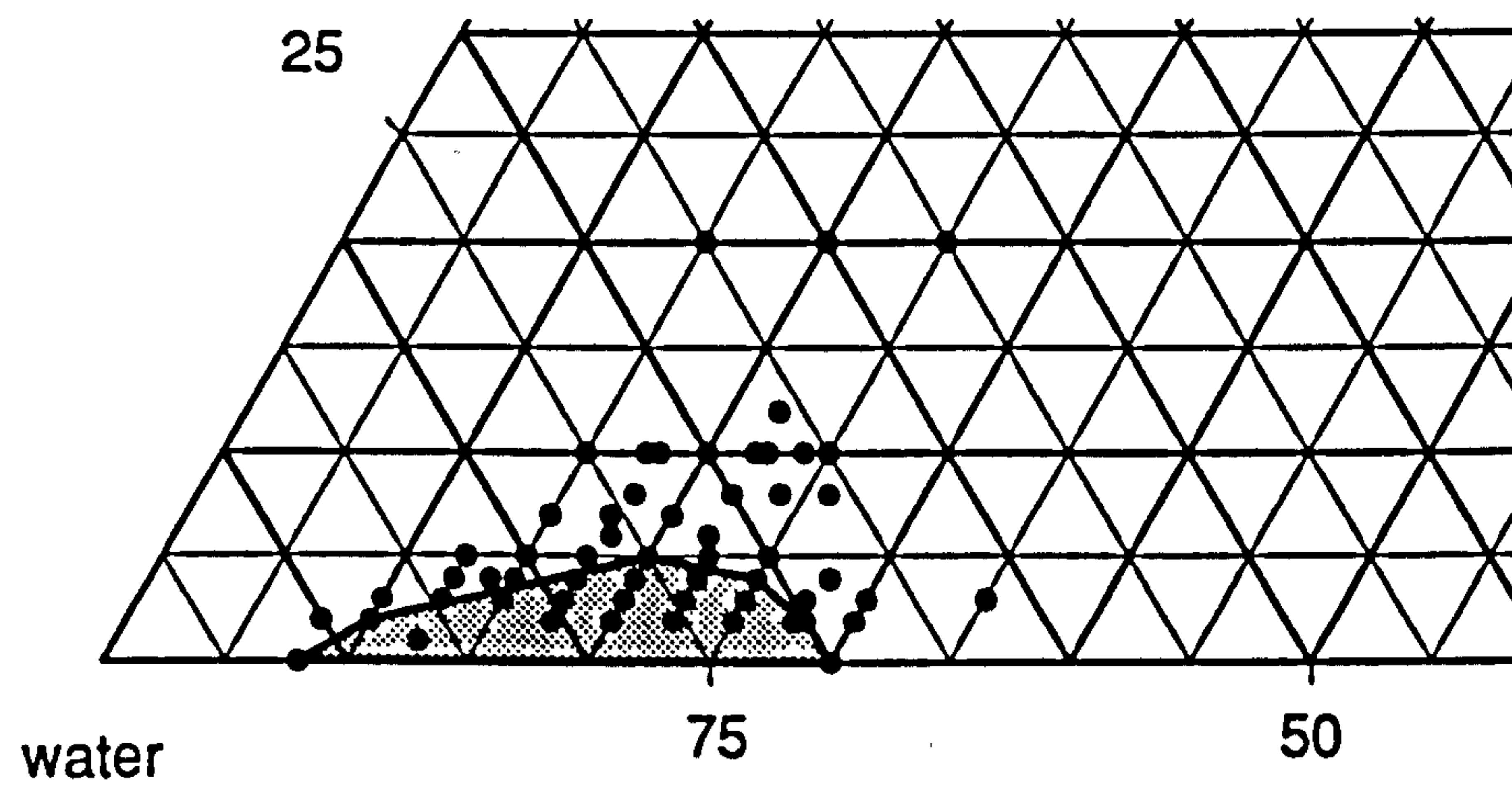
As the oil phase used alters the PIT of the $C_{18-1}E_{10}$ microemulsion systems, and is therefore thought to affect the structure, it is anticipated that the area of existence of o/w microemulsions within the triangular phase diagram may also be altered. The L_1 region (ie o/w microemulsions) of ten different oils studied by Lo *et al* [241] were all found at a $C_{18-1}E_{10}$ concentration less than 25 %w/v. The amount of oil incorporated, and hence the extent of the area of existence, varied with the oil phase used. Of the oils tested, the largest region and highest uptake was found for cyclohexanone. For example 19.36 %w/v cyclohexanone could be incorporated when 10 %w/v $C_{18-1}E_{10}$ was present. This very high uptake was explained by these workers to be a reflection of the high polarity and water solubility of this oil phase. Two alkanes were also among the oils tested; hexane and dodecane. Hexane gave an o/w area of existence approaching that of cyclohexanone with 14.95 %w/v incorporation in 10 %w/w $C_{18-1}E_{10}$. In comparison, a maximum of 1.27 %w/v of the longer-chained dodecane was found at 10 %w/v $C_{18-1}E_{10}$.

In this investigation three alkanes and three 1-alkenes of carbon chain length 7, 16 and 18 were tested for their ability to form o/w microemulsion systems

a) heptane



b) hexadecane



c) octadecane

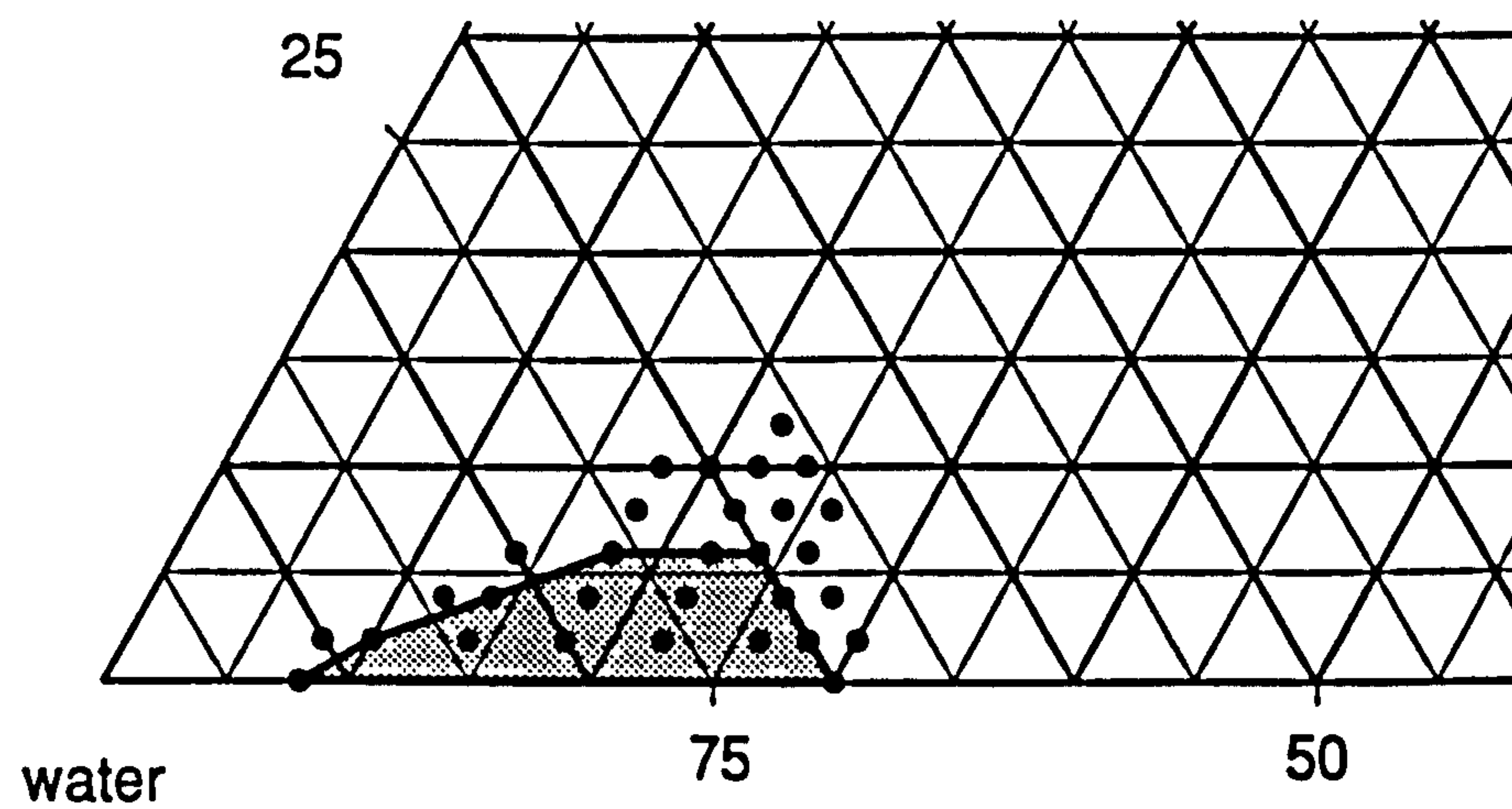
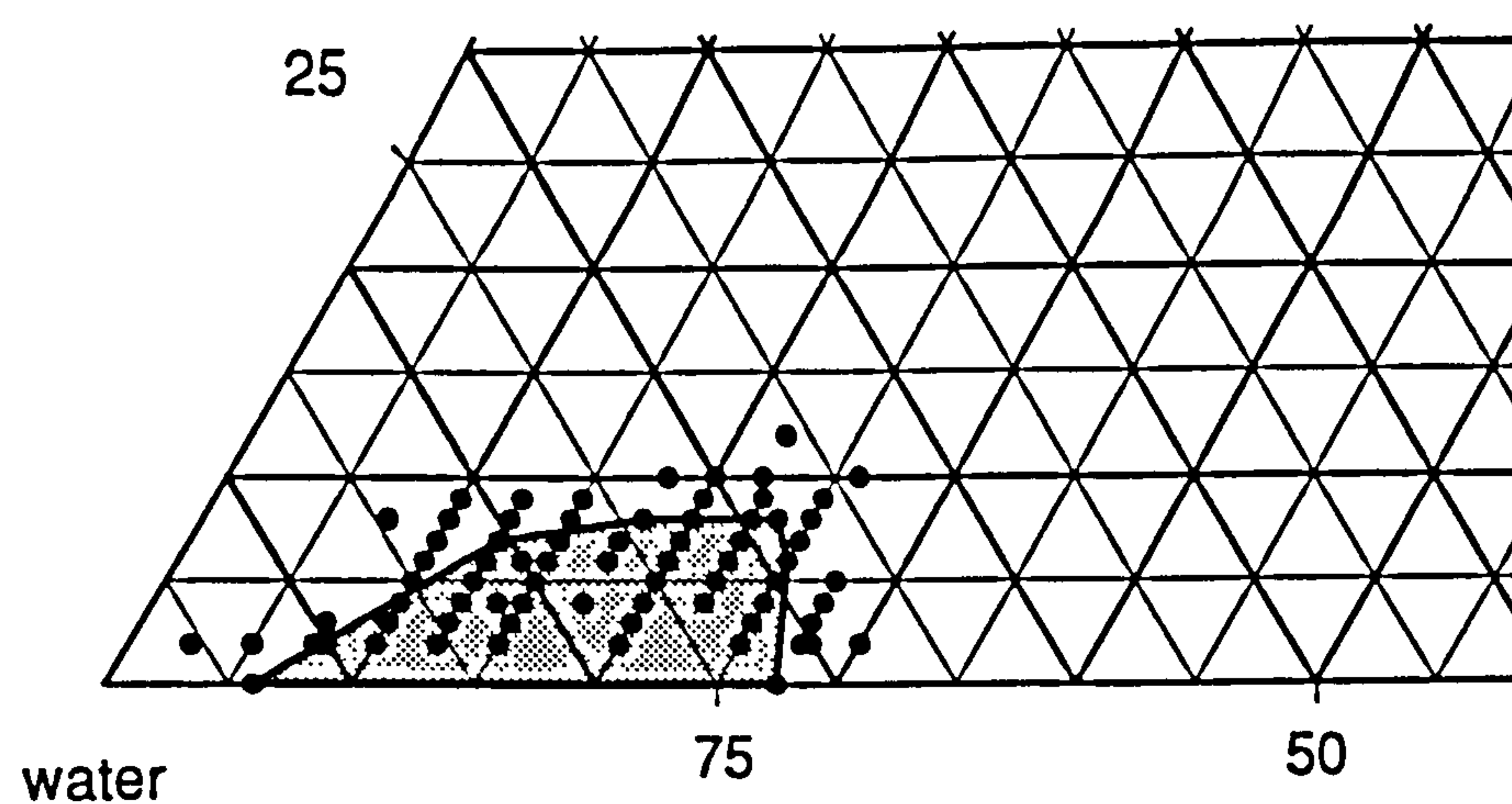
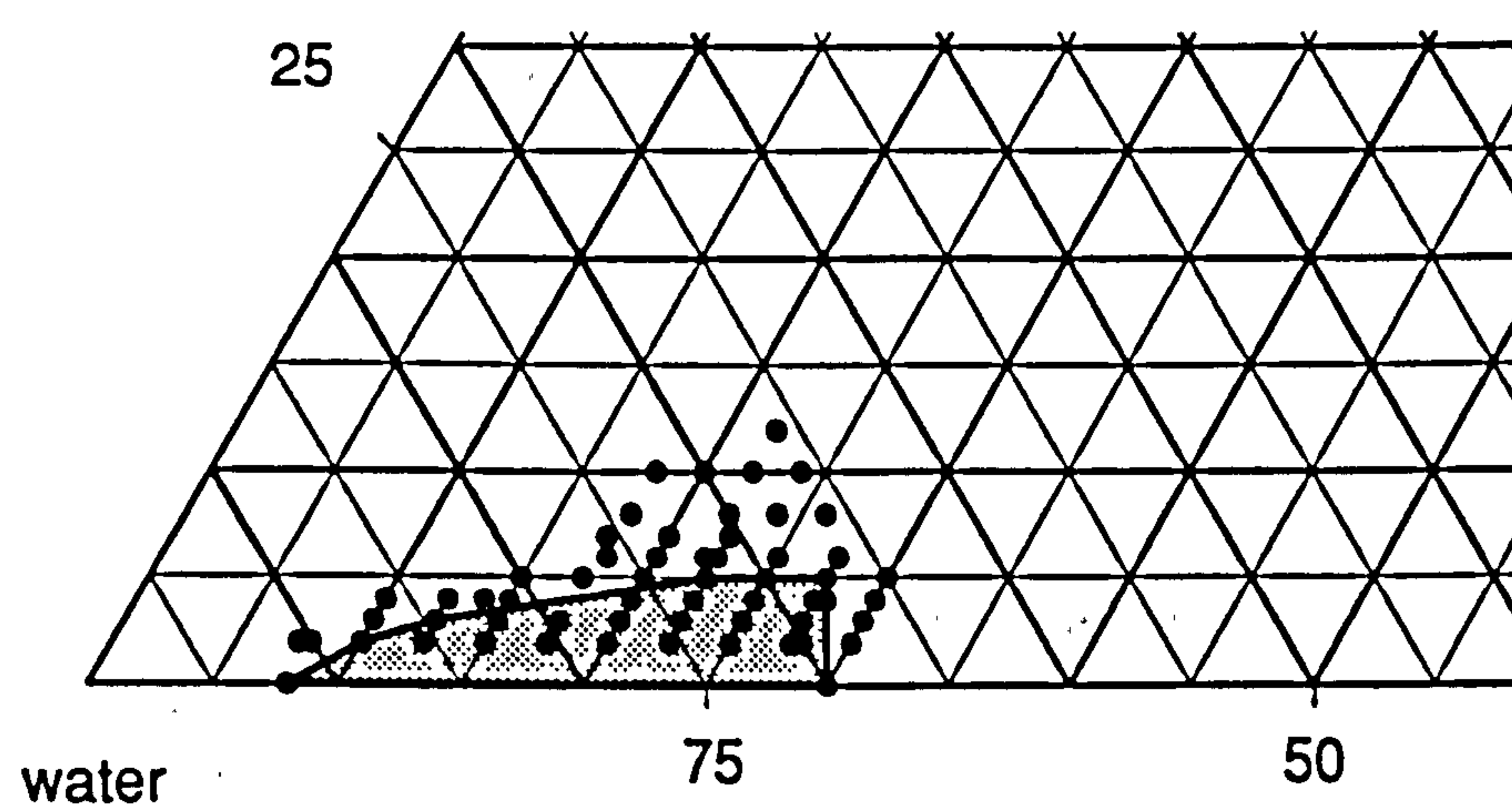


Figure 4.3: Partial triangular phase diagrams for o/w microemulsion systems formed with $C_{18-1}E_{10}$, water and a)heptane, b)hexadecane and c)octadecane.

a) 1-heptene



b) 1-hexadecene



c) 1-octadecene

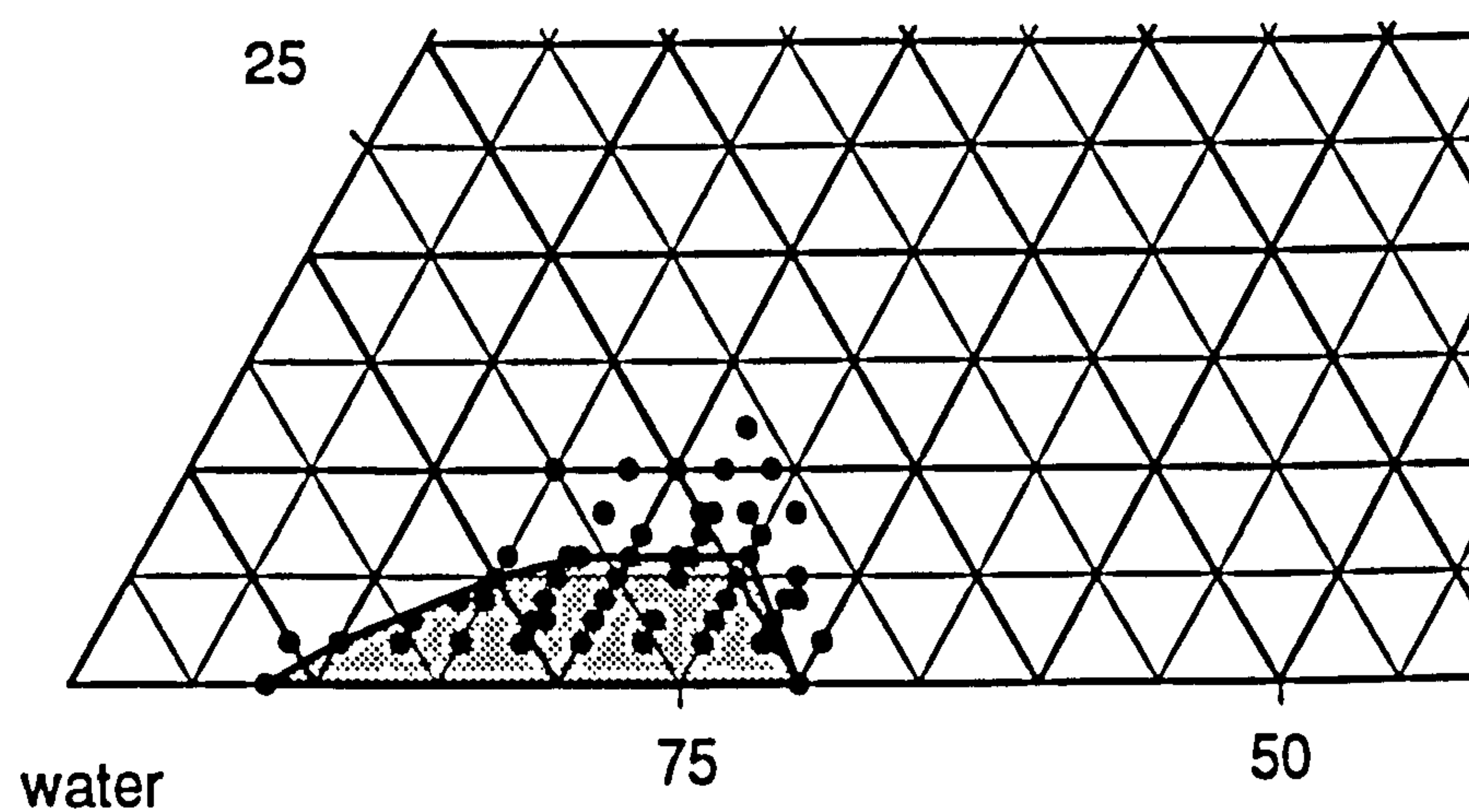


Figure 4.4: Partial triangular phase diagrams for o/w microemulsion systems found with $C_{18-1}E_{10}$, water and a)1-heptene, b)1-hexadecene and c)1-octadecene.

with $C_{18-1}E_{10}$. The area of existence found for the six oils are shown in figures 4.3 and 4.4. While on a molar basis, oils with a smaller molecular volume were solubilised to a greater extent, on a weight basis, the areas found for all six hydrocarbons were similar in position and maximum oil incorporation.

Of the three alkanes tested, heptane has the shortest chain length and would be expected to penetrate the surfactant interface to the largest extent [284]. Its presence caused a substantial decrease in the PIT compared to the CP of a surfactant solution with no oil. Hence at room temperature, the systems containing heptane are closer to their PIT than systems containing other oils. A maximum of 8 %w/w heptane was found to be incorporated at approximately 20 - 22 %w/w surfactant, with microemulsion formation requiring a minimum $C_{18-1}E_{10}$ concentration of about 6 %w/w.

When the alkane chain length was increased to 16, the corresponding area of microemulsion existence decreased slightly. Maximum incorporation of 5 %w/w hexadecane was found, and at least 8 %w/w $C_{18-1}E_{10}$ was required in order for microemulsions to form. Similarly with the 18 carbon octadecane, microemulsions were formed over a surfactant concentration range between 8 and 30 %w/w, with a 6 %w/w maximum incorporation of the oil occurring between 18 and 24 %w/w.

For the corresponding 1-alkene series, use of 1-heptene resulted in a greater maximum hydrocarbon incorporation compared to higher members of the series. As found with heptane, this maximum was about 8 %w/w and occurred with 18 - 24 %w/w surfactant, with a similar range of $C_{18-1}E_{10}$ concentration allowing microemulsion formation. As in the alkane series, the alkenes of longer chain length than 1-heptene resulted in an increase in the PIT and a reduction in the maximum amount of oil incorporated. 1-Hexadecene and 1-octadecene had maximum solubilisation levels of 5 and 6 %w/w respectively. Although alkenes have been found to penetrate the interface of a number of microemulsion systems to a greater extent than the corresponding alkane [293], if greater penetration was occurring with the alkenes used in the $C_{18-1}E_{10}$ systems investigated in this study, no subsequent differences in the area of existence were revealed.

These results show that at room temperature, when the shorter hydrocarbons

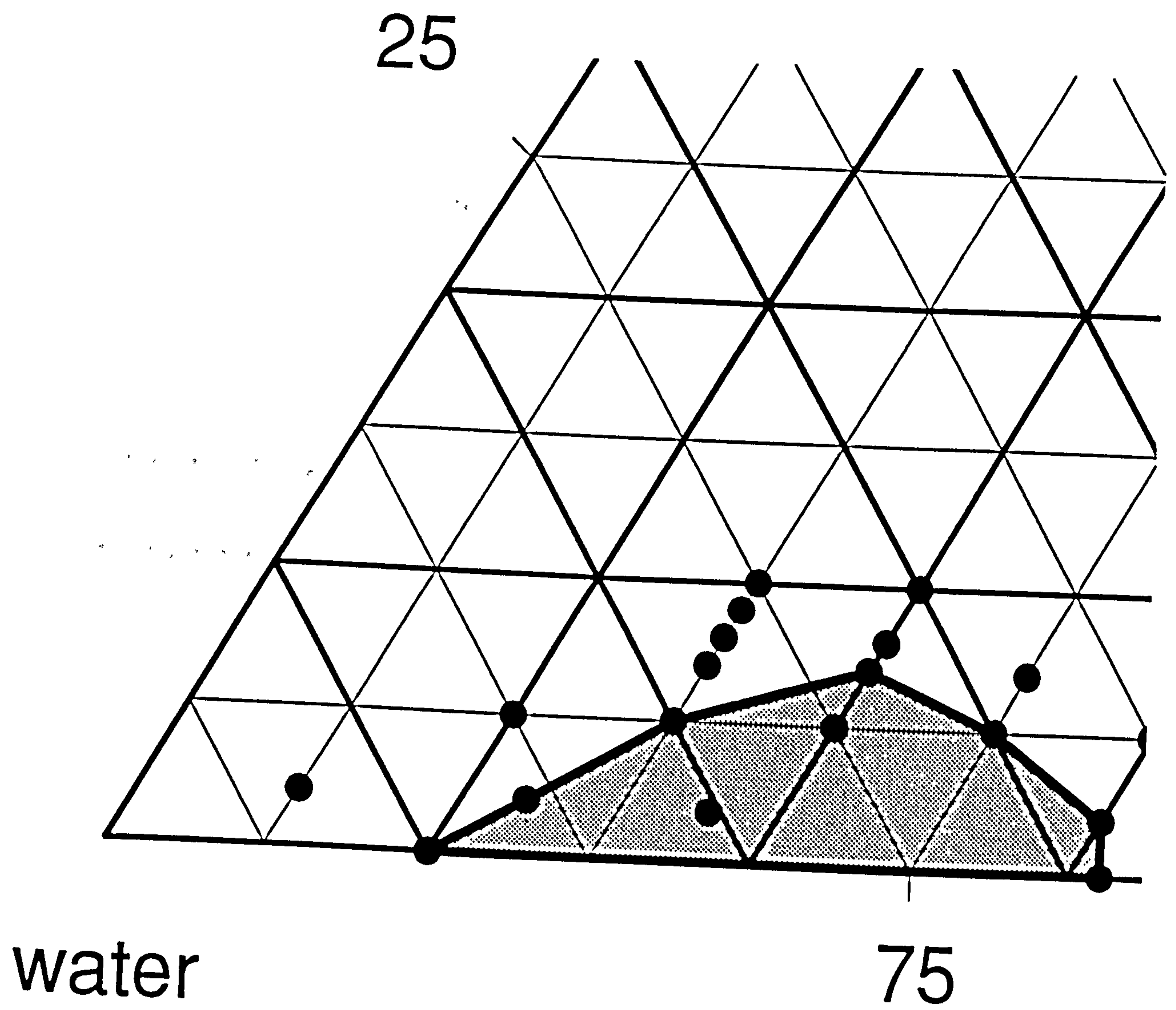


Figure 4.5: Partial triangular phase diagram for o/w microemulsions formed with $C_{18-1}E_{10}$, water and isopropyl myristate.

(heptane and 1-heptene) were employed as the dispersed phase, the area of microemulsion existence was extended into regions of lower surfactant concentration, and showed slightly higher oil incorporations. This increased area of existence could be a consequence of the ability of the smaller hydrocarbons to penetrate into the surfactant hydrophobic region, and hence allow more flexible structures. The larger area found with shorter oil phases could also be because the oils with longer hydrocarbon chains require a higher temperature for maximum solubilisation to occur [269].

In addition to the hydrocarbons, the ester; isopropyl myristate (IPM) was tested for its effect on microemulsion formation. The bulkier isopropyl ester group did not appear to significantly hinder the formation of clear systems at room temperature (fig.4.5). Microemulsion production was possible with a minimum of 10 %w/w surfactant, and a maximum of 7 %w/w oil was found at about 20 %w/w C₁₈₋₁E₁₀. The PIT of a microemulsion containing 2 %w/w IPM and 20 %w/w C₁₈₋₁E₁₀ was however reduced to 53.3°C.

4.2.1.2. Oil mixtures

4.2.1.2.1 Triglyceride oils

Soybean oil, used for most of the microemulsion studies in this research, is a multicomponent oil consisting of triglyceride molecules containing three fatty acid chains of varying length and saturation. Typical distribution of soybean oil shows that it consists of saturated and unsaturated fatty acids of C₁₆ - C₁₈ chain length, with linoleic acid (C₁₈₋₂) constituting about 50 % of the fatty acid content [294]. The solubilisation pattern of triglyceride oils by nonionic surfactants can be quite different from hydrocarbon oils [295]. As well as triglyceride molecules, commercial soybean oil also contains a percentage of unknown substances, and often about 1.5 to 4% phospholipids and other miscellaneous surface active impurities. Surface active impurities present in commercial soybean oil can alter the interfacial properties and adsorption behaviour of any surfactant under investigation [294].

In this study the area of three component microemulsions formed with C₁₈₋₁E₁₀ as surfactant, and either commercially available soybean oil, or soybean

oil super-refined by chromatographic purification, were compared to test if the impurities have any effect. Due to the lack of colour in the purified soybean oil, its substitution in place of commercial soybean oil resulted in clear, colourless o/w microemulsions compared with the slight yellow colour normally observed. The area of existence was not however found to change significantly, and remained the same as that shown in figure 3.2.

Another commercially available triglyceride used in this study was Miglyol 812. In comparison to the fatty acid distribution found in soybean oil, Miglyol 812 consists mainly of shorter $C_8 - C_{10}$ hydrocarbon chains. Due to this difference in the fatty acid chain lengths, Miglyol 812 has a reduced average molecular volume and increased polarity compared to soybean oil. As found with shorter hydrocarbon oils, the PIT found with Miglyol 812 systems was lower than that observed with soybean oil microemulsions (table 4.3). The area of existence found for Miglyol 812/ $C_{18-1}E_{10}$ /water o/w microemulsions is shown in figure 4.6. The area found extended over a similar range of surfactant concentrations as that found for soybean oil, although the minimum $C_{18-1}E_{10}$ required before microemulsion formation occurred was slightly reduced. The maximum oil incorporation was however lower than that found with the soybean oil systems. Whereas 6.5 %w/w soybean oil was incorporated at 20 %w/w $C_{18-1}E_{10}$, with Miglyol 812 a maximum of 5 %w/w was found.

4.2.1.2.2 Binary hydrocarbon oils

Selective solubilisation of one molecule over another in binary oil phases have been considered for some micellar systems [296, 297, 298]. In some cases the presence of small amounts of one oil was found to have a synergistic effect, causing an increased solubilisation of a second oil (for example benzene and hexane) due to the difference in location within the micelle of the molecules of the two oil phases [296]. Chen *et al* [284] found that whereas hexadecane did not form microemulsions with DDAB at 25°C, w/o or bicontinuous microemulsions were formed after the addition of a shorter chain oil such as hexane. These workers explain the results in terms of the shorter hexane penetrating the surfactant interface and acting in a similar fashion to a cosurfactant, swelling the effective chain volume (increasing CPP) and making it possible for microemulsions to form with non-penetrating

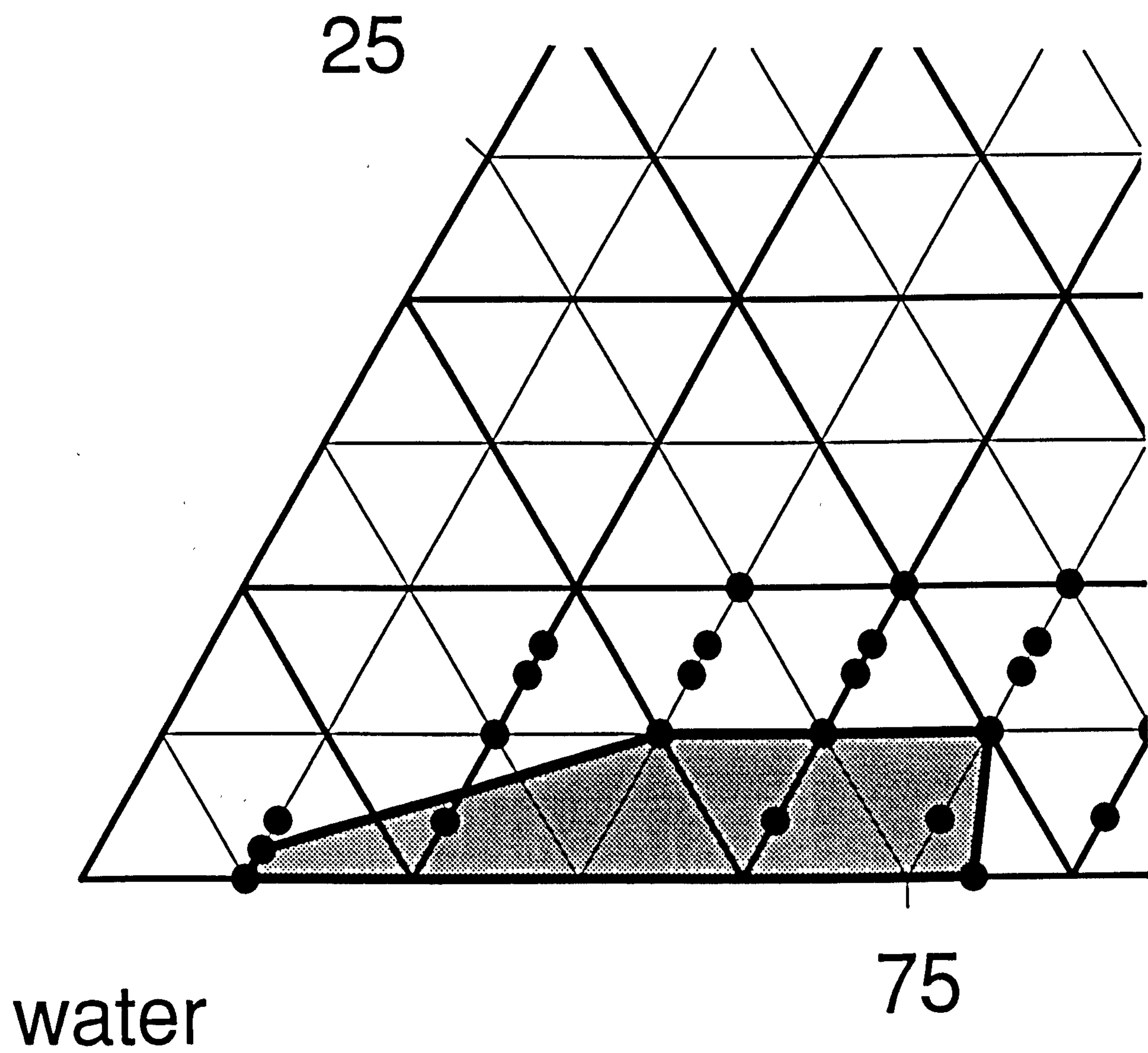


Figure 4.6: Partial triangular phase diagram for o/w microemulsions formed with $C_{18-1}E_{10}$, water and Miglyol 812.

hexadecane.

In this study binary mixtures of short- and long-chained alkanes and 1-alkenes were used to determine if there was any change in the extent or position of the o/w microemulsion region. The combinations heptane:hexadecane, heptane:1-hexadecene, 1-heptene:hexadecane and 1-heptene:1-hexadecene were used in a 1:1 weight ratio. There was little difference found between all four regions of microemulsion existence. All four microemulsion regions extended over a very similar range of $C_{18-1}E_{10}$ concentration, and the maximum oil phase incorporation was either 5 or 6 %w/w in all cases.

In order to try to accentuate any differences, binary mixtures of heptane and hexadecane were employed at weight ratios of 1:2.25 and 2.25:1. The weight ratio of heptane:hexadecane 1:2.25 is equal to a 1:1 molar ratio of the two oils. The weight ratio 2.25:1 gives a molar ratio of approximately 5:1. When a greater weight of the longer chained alkane was present in the mixture, the region of existence was not distinguishable from that found with hexadecane alone. When the combination was dominated by the shorter alkane, the area appeared to be intermediate between that of pure heptane and pure hexadecane. Hence no synergistic effect was noticed when the two oils of varying lengths were used in combination, however the presence of some hexadecane did appear to slightly reduce the area of existence compared to that found for pure heptane.

4.2.1.3 Photon correlation spectroscopy studies

The apparent Z mean diameters obtained from PCS results of four $C_{18-1}E_{10}$ microemulsion compositions with nine different oils are shown in table 4.4. There did not appear to be any significant difference in the size, at 30°C, of microemulsion droplets containing 2 %w/w oil and 10, 14 or 18 %w/w $C_{18-1}E_{10}$ when soybean oil, super-refined soybean oil, Miglyol 812, hexadecane, 1-hexadecene, octadecane and 1-octadecene were used as the dispersed phase (table 4.4).

The apparent Z mean diameters found for systems with 14 %w/w $C_{18-1}E_{10}$ and 4 %w/w oil were more variable, depending on the polydispersity found in the intensity distribution. Samples containing hexadecane, 1-hexadecene,

Table 4.4: Variation of apparent Z mean diameter found in o/w C₁₈₋₁E₁₀ microemulsions produced with different oils (nm).

Oil	Microemulsion composition							
	10% Brij 96 2% oil		14 % Brij 2% oil		18 % Brij 2% oil		14 % Brij 4% oil	
	Z mean diameter	polydispersity	Z mean diameter	polydispersity	Z mean diameter	polydispersity	Z mean diameter	polydispersiy
soybean oil	10.2	0.139	8.6	0.146	7.5	0.182	12.6	0.298
super –refined SBO	10.1	0.115	8.7	0.141	7.6	0.196	12.6	0.297
Miglyol 812	9.6	0.127	8.1	0.144	7.1	0.168	11.3	0.261
heptane	9.4	0.070	12.0	0.353	12.7	0.366	9.6	0.127
1 –heptene	17.0	0.343	13.9	0.285	11.4	0.267	12.3	0.315
hexadecane	10.0	0.073	8.4	0.090	7.3	0.124	11.3	0.207
1 –hexadecene	9.8	0.066	8.4	0.084	7.3	0.150	10.4	0.151
octadecane	9.8	0.084	8.5	0.095	7.4	0.125	10.8	0.162
1 –octadecene	10.0	0.090	8.4	0.128	7.3	0.133	10.9	0.175

octadecane, 1-octadecene and Miglyol 812 exhibited low polydispersity indices and monomodal log/log intensity vs diameter plots. Microemulsions with soybean oil (3.4.1) and super refined soybean oil both exhibited bimodal distributions with corresponding higher values of polydispersity. The position of the first intensity peak in the log intensity vs log diameter plots, indicated that the size of the individual microemulsion droplets in soybean oil systems was not significantly different from the size of droplets found in microemulsions produced from the five oils with monomodal distributions. However the presence of a bimodal population indicates that a degree of aggregation was occurring (3.4.1.3) and hence larger apparent Z mean diameters were calculated for these two oils.

The same microemulsion compositions containing heptane and 1-heptene however appeared to behave differently from the other oils. In most instances the apparent Z mean diameter was larger for these two oils than for the corresponding systems produced with the larger oils. The trends in size do not however follow those previously found for soybean oil with increasing surfactant and/or oil across the microemulsion area of existence (3.4.1). This is probably because, except for the composition with 10 %w/w C₁₈₋₁E₁₀ and 2 % heptane, all samples containing heptane or heptene showed bimodal intensity plots and high polydispersity.

The increase in polydispersity observed with heptane and 1-heptene as the oil phase, could arise because of the penetration of these smaller oils into the surfactant layer. Spherical droplets are implicitly assumed in PCS results, but because these oils are likely to result in more flexible and possibly elongated structures (4.2.1.1.1) a greater variation in the apparent Z mean diameter may be seen. Furthermore, the proximity of the test temperature (30°C) to the PIT for these systems could also be responsible for the high polydispersity. PCS results of nonionic surfactant systems can be unreliable in the region close to the PIT. In this temperature region (typically within 20°C of the cloud point) it is debated that increased growth observed in micellar systems occurs due to interactions and aggregation [299, 300, 301] or that the true situation is masked by perturbations due to critical phenomena [262, 302, 303, 304].

4.2.2 The effect of different oils on $C_{12}E_{10}$ systems

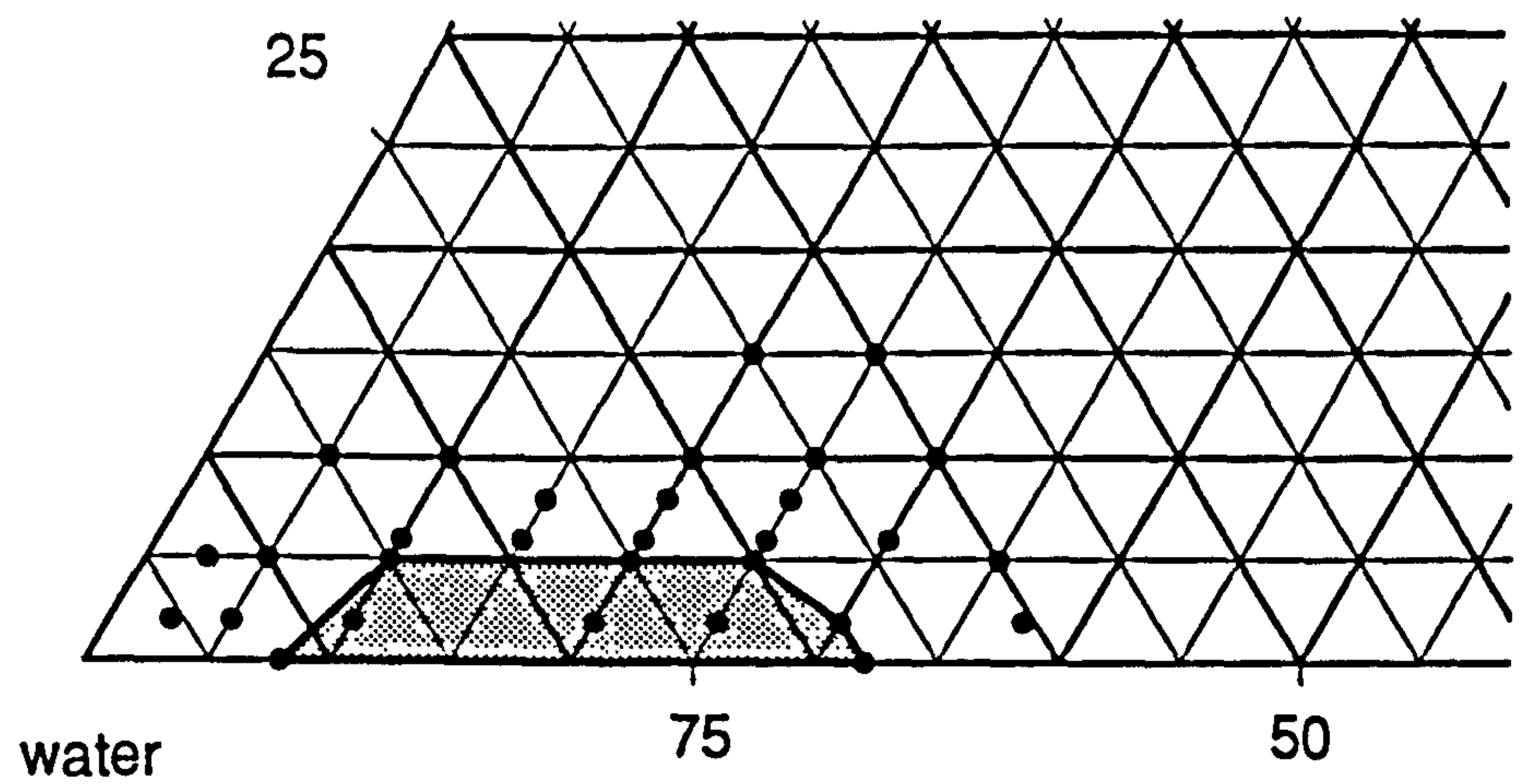
As discussed in section 4.1.2, with $C_{12}E_{10}$ as surfactant only a small o/w microemulsion region was found when soybean oil (fig.4.2) was used as the oil phase. Furthermore, this area was shifted towards higher surfactant concentrations than those found using $C_{18-1}E_{10}$. Results for other oils are given in figure 4.7 and 4.8.

The effect of the shorter hydrophobe in $C_{12}E_{10}$ compared to $C_{18-1}E_{10}$ appears to make the formation of microemulsion systems, at room temperature, more susceptible to the oil phase used. Whereas the areas and maximum oil incorporation found with $C_{18-1}E_{10}$ were similar for all the oils tested, with $C_{12}E_{10}$ the oil phase employed had a significant effect, which appeared to depend on the chain length of the oil used.

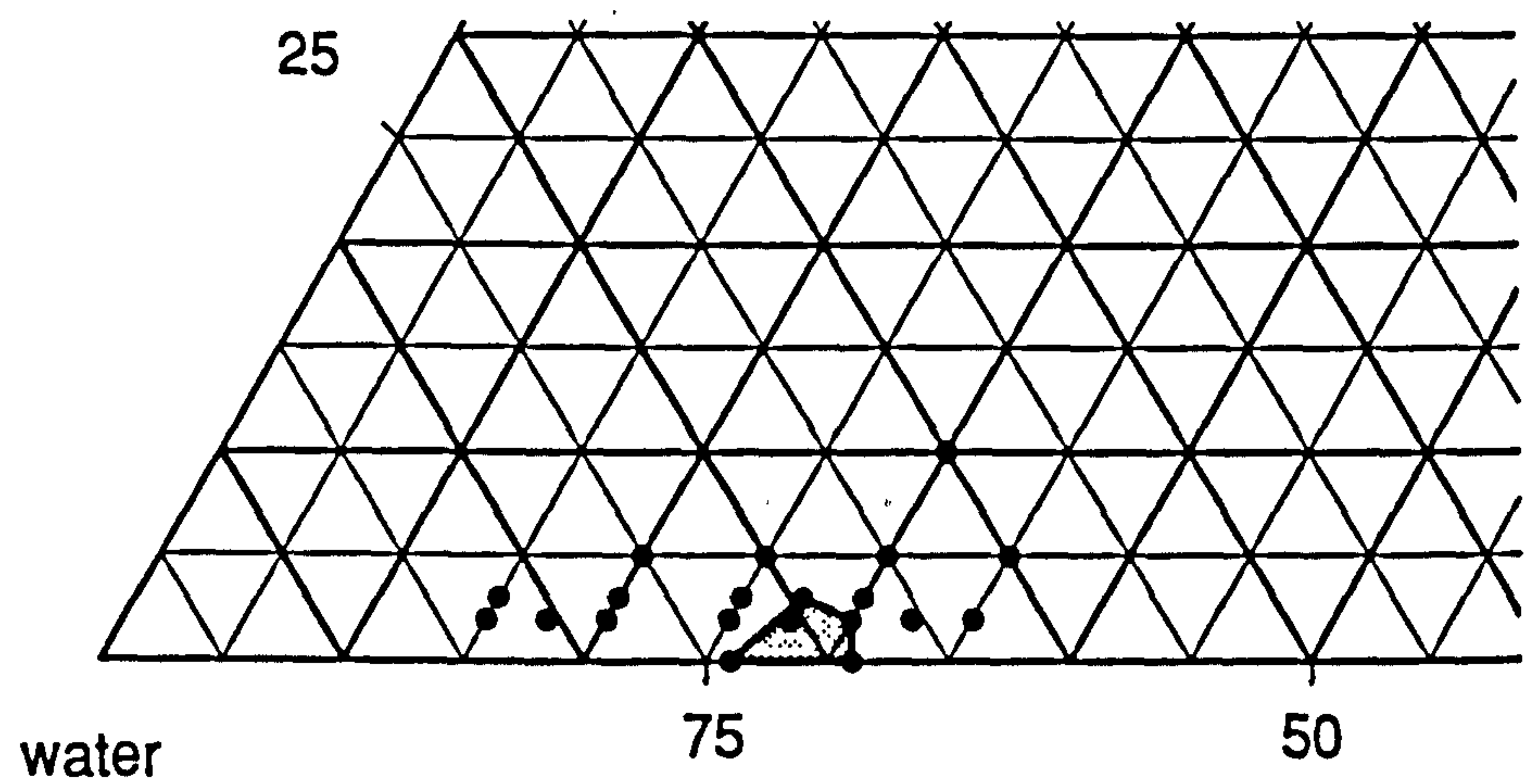
The 16 and 18 carbon alkanes and alkenes (hexadecane, 1-hexadecene, octadecane and 1-octadecene) resulted in the formation of very limited o/w microemulsion regions, with a maximum incorporation (typically at about 25 %w/w $C_{12}E_{10}$) of only 2-3 %w/w. Isopropyl myristate, with a carbon chain of 14, is closer in size to the hydrophobic portion of the surfactant. It appears that as a consequence of this reduced molecular size of IPM, a larger area than that seen with the C_{16} and C_{18} hydrocarbons was observed (fig.4.8a). The minimum $C_{12}E_{10}$ concentration required was about 14 %w/w, and systems remained clear and fluid until about 36 %w/w surfactant. Maximum incorporation of IPM of 5 %w/w occurred between 25-30 %w/w $C_{12}E_{10}$. Reducing the size of the oil to that of heptane and 1-heptene had an even more dramatic effect on the area. As found with IPM, the maximum incorporation was about 5-6 %w/w, but the region extended over a range of $C_{12}E_{10}$ concentrations between 5-34 %w/w.

Hence it appears that at room temperature larger areas of o/w $C_{12}E_{10}$ microemulsion systems are seen with oils of shorter chain length. This does not discount the possibility of more extensive regions occurring at other temperatures. With other C_mE_n surfactants it has been found that the longer the hydrocarbon chain of the oil, the higher the PIT [248], and the higher the temperature needed for maximum solubilisation to occur [269].

a) heptane



b) hexadecane



c) octadecane

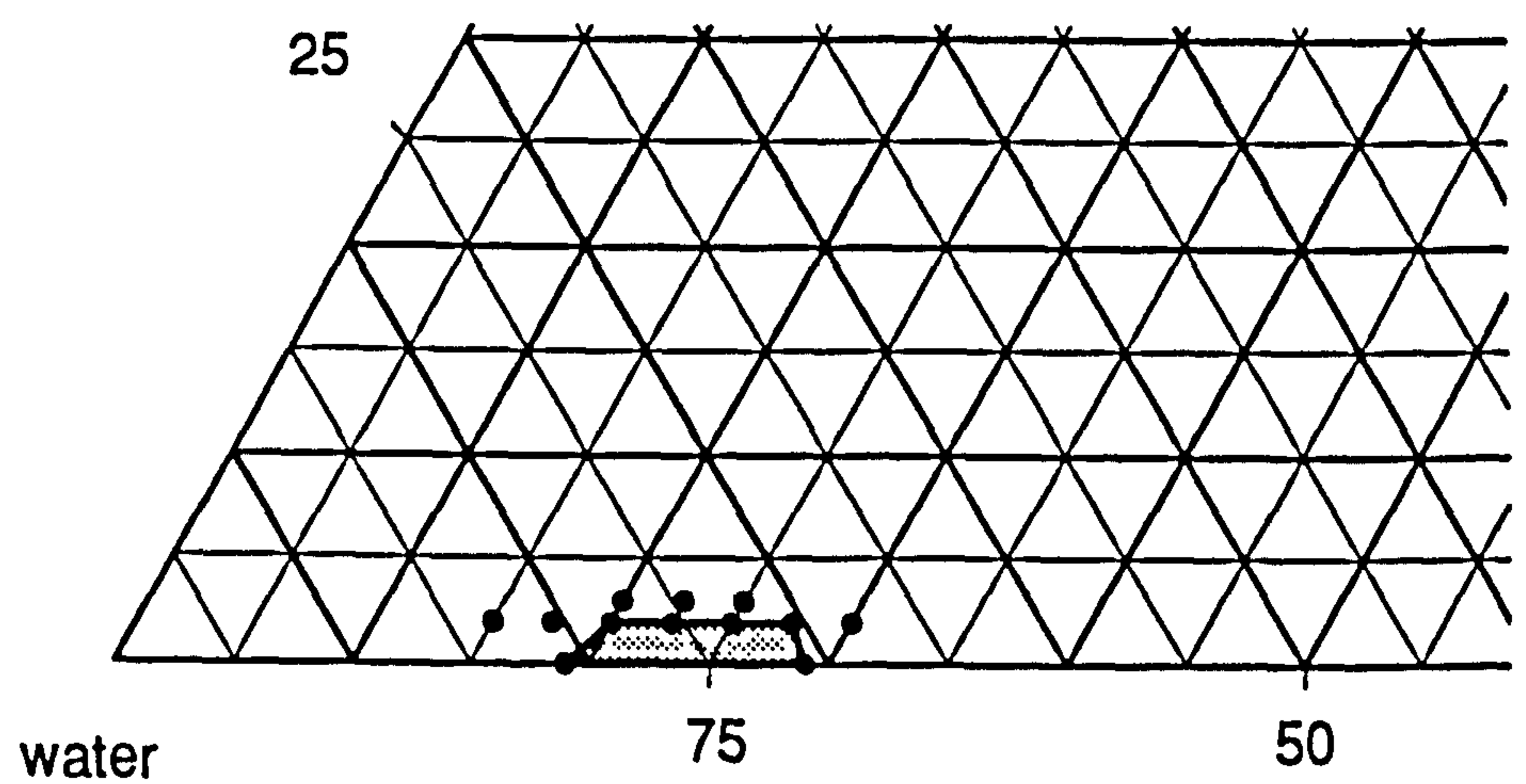


Figure 4.7: Partial triangular phase diagrams for o/w microemulsions formed with $C_{12}E_{10}$, water and a)heptane, b)hexadecane and c)octadecane.

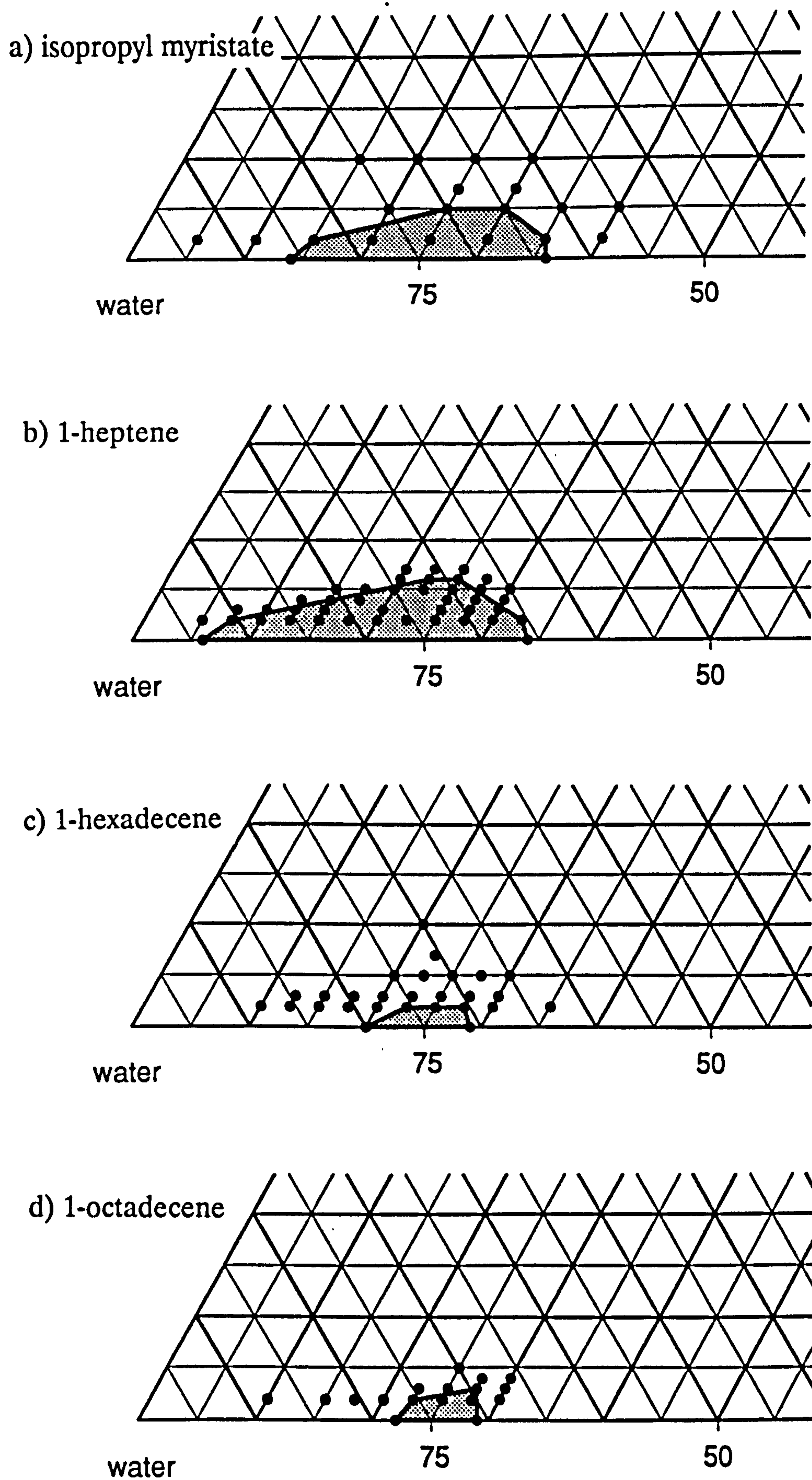


Figure 4.8: Partial triangular phase diagrams for o/w microemulsions formed with $C_{12}E_{10}$, water and a) isopropyl myristate, b) 1-heptene, c) 1-hexadecene and d) 1-octadecene.

4.2.3 The effect of oil on other surfactant systems

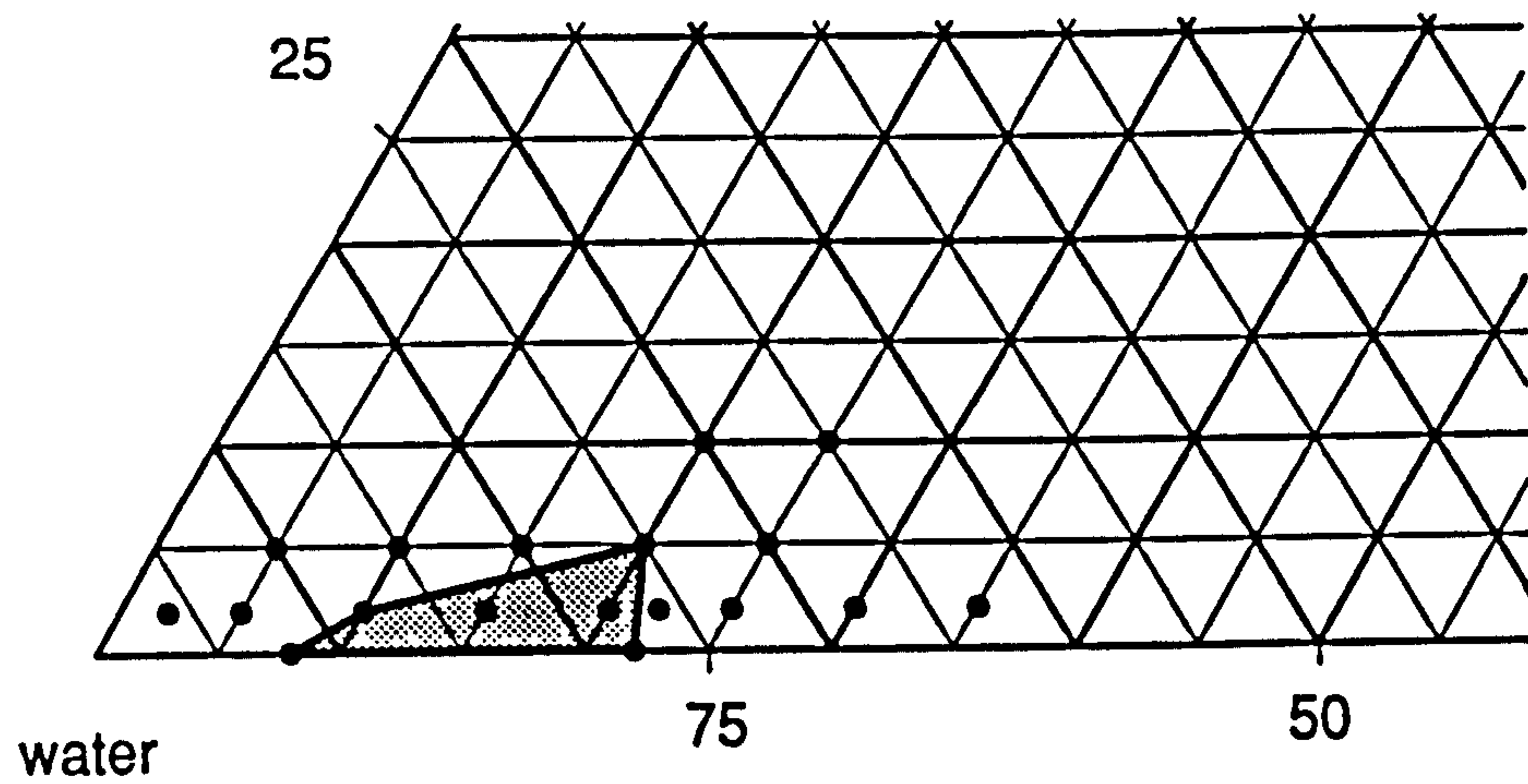
In addition to their ability to form o/w microemulsions with soybean oil (4.1.2) the eight C_mE_n surfactants used in this study were all tested with heptane and IPM. As found when using soybean oil, no o/w systems were observed using these two oils at room temperature for $C_{18-1}E_5$, $C_{18}E_{10}$, $C_{16}E_{10}$ or $C_{12}E_4$. Although not allowing the formation of o/w microemulsions with soybean oil, the surfactant $C_{18}E_{20}$ could produce microemulsions with heptane. Further study showed $C_{18}E_{20}$ also formed microemulsions incorporating 1-heptene, but not IPM, hexadecane, 1-hexadecene, octadecane or 1-octadecene. $C_{18-1}E_{20}$ was found to form clear o/w systems with heptane, 1-heptene, and a very small area with IPM, but not with the four longer chain hydrocarbons. The areas of microemulsion existence found for $C_{18}E_{20}$ and $C_{18-1}E_{20}$ are shown in figure 4.9 and 4.10.

A summary of all systems investigated is given in table 4.5. It appears that when attached to an average ten ethylene oxide units, the 18-carbon hydrophobe with the cis double bond is able to form microemulsions at room temperature, but the straight chained C_{18} or C_{16} is not. The area of existence and extent of oil solubilisation found for $C_{18-1}E_{10}$ was relatively insensitive to large changes in the properties of the oil phase (4.2.1). In contrast, microemulsion systems formed with the straight chain surfactant $C_{12}E_{10}$ (which has a smaller hydrophobe) are more sensitive to the size of the oil molecules, and o/w microemulsion formation is favoured with oils of smaller chain lengths.

It has however been previously reported that in order to solubilise some oils efficiently at a specific temperature, an optimum hydrophilic chain length of the surfactant is also required [288]. Surfactants with shorter ethylene oxide portions may have greater affinity for an oil phase, but will be unable to incorporate the oil into an o/w microemulsion unless the surfactant molecules are still able to form droplets in a water external phase. The need for a hydrophilic moiety of minimum size may explain the failure of $C_{18-1}E_5$ and $C_{12}E_4$ to form microemulsions.

Increasing the ethylene oxide content of the surfactant and increasing the hydrocarbon chain length of the oil both shift the solubility regions towards higher temperatures [248, 269]. In the cases of $C_{18-1}E_{20}$ and $C_{18}E_{20}$, o/w

a) heptane



b) 1-heptene

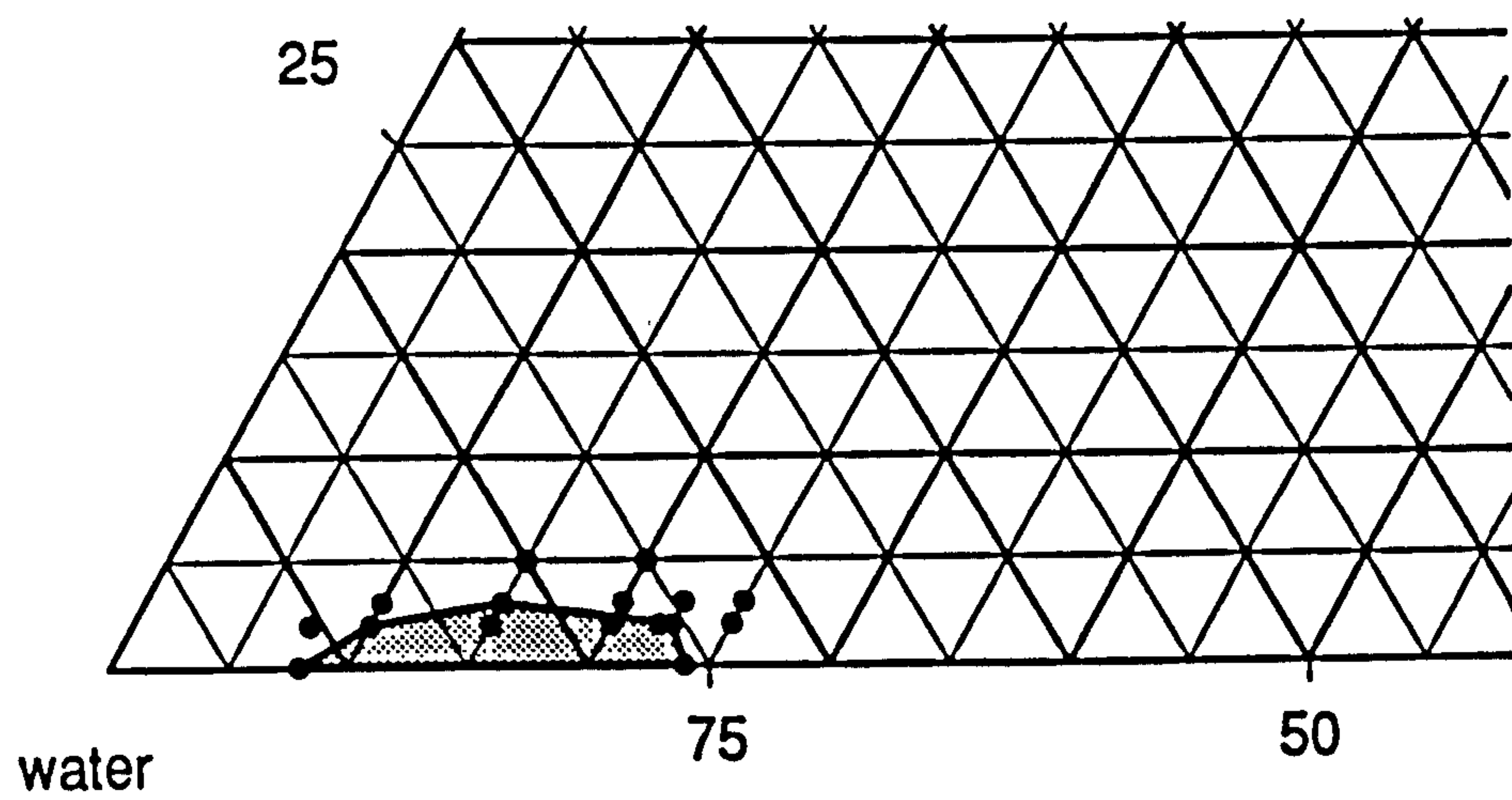
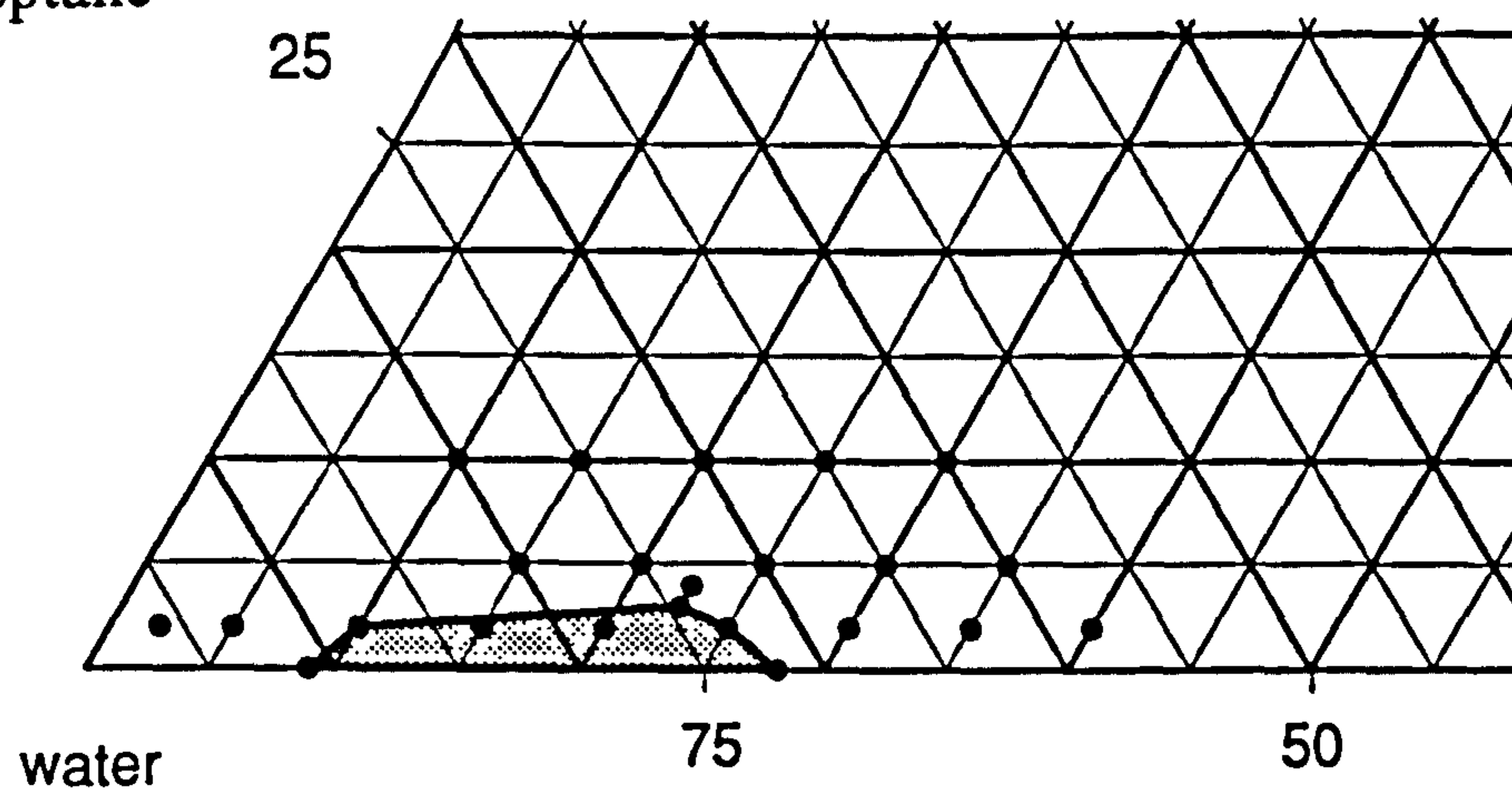
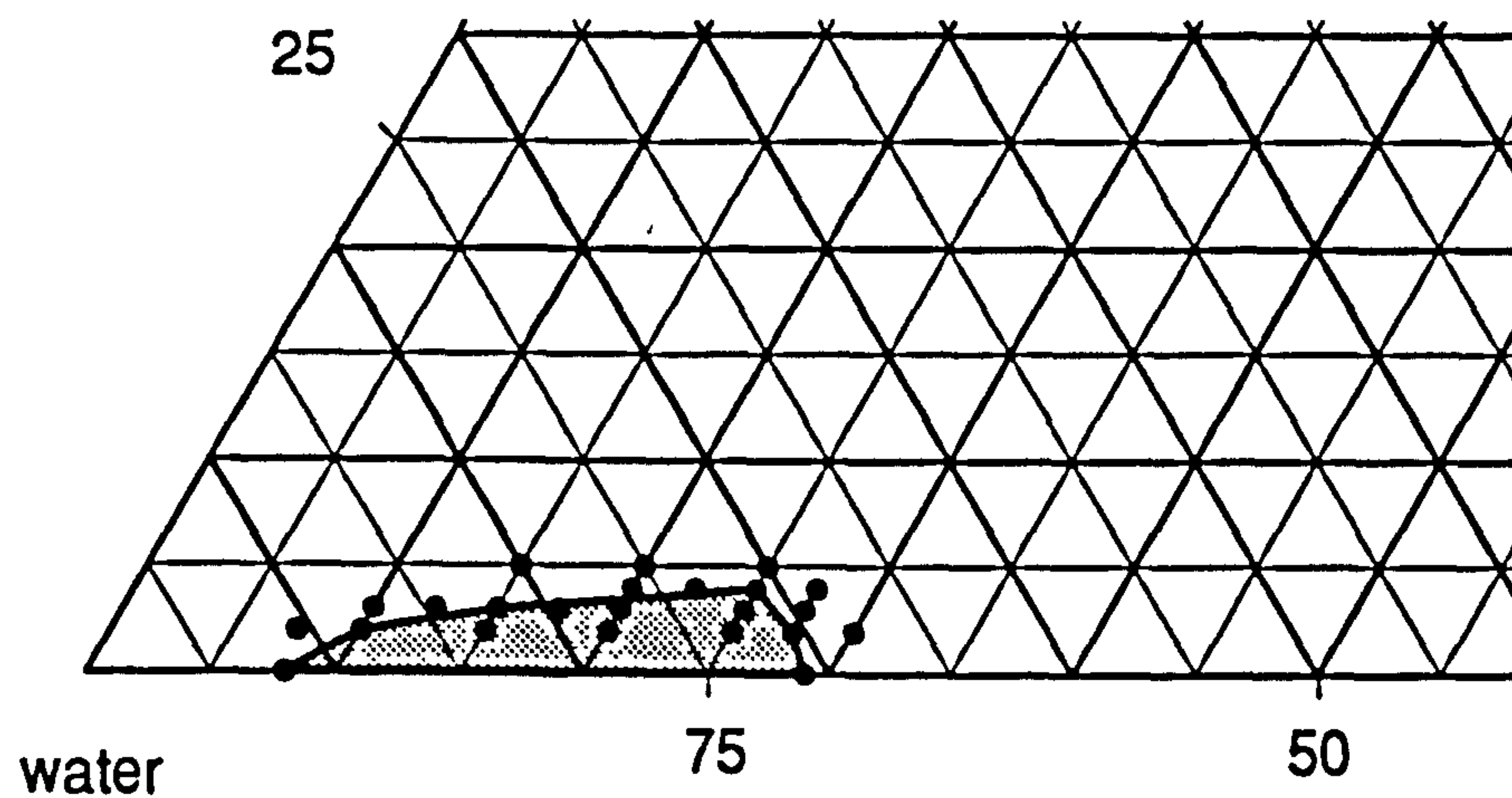


Figure 4.9: Partial triangular phase diagrams for o/w microemulsions formed with $C_{18}E_{20}$, water and a) heptane and b) 1-heptene.

a) heptane



b) 1-heptene



c) isopropyl myristate

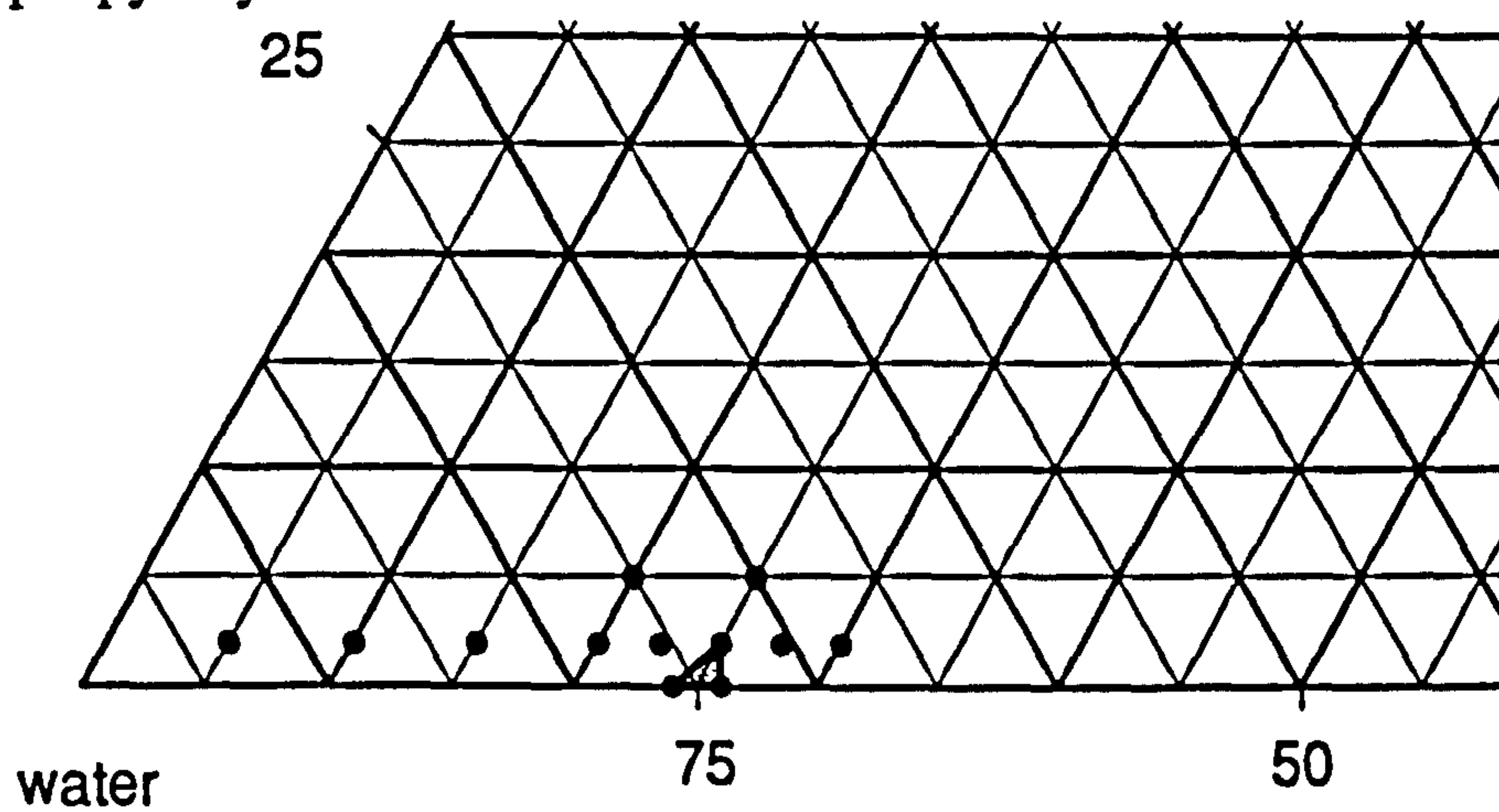


Figure 4.10: Partial triangular phase diagrams for o/w microemulsions formed with $C_{18-1}E_{20}$ and a)heptane, b)1-heptene and c)isopropyl myristate.

microemulsions were possible with shorter hydrocarbons at room temperature, but may only be possible with larger oils at higher temperatures.

This investigation has therefore illustrated that, at a set temperature, modification of 3-component oil/ C_mE_n surfactant/water systems alters microemulsion formation in a complex way which depends on the relative size and structure of the surfactant hydrophobe, the attached ethylene oxide chain and the oil phase to be incorporated.

Table 4.5: Ability of the surfactants and oils used in this study to form 3-component o/w microemulsions at room temperature.

Oil	Surfactant							
	C ₁₈₋₁ E ₁₀	C ₁₈₋₁ E ₂₀	C ₁₈₋₁ E ₅	C ₁₈ E ₁₀	C ₁₈ E ₂₀	C ₁₂ E ₁₀	C ₁₂ E ₄	C ₁₆ E ₁₀
soybean oil	Y	X	X	X	X	Y	X	X
isopropyl myristate	Y	Y	X	X	X	Y	X	X
heptane	Y	Y	X	X	Y	Y	X	X
1–heptene	Y	Y	–	–	Y	Y	–	–
hexadecane	Y	X	–	–	X	Y	–	–
1–hexadecene	Y	X	–	–	X	Y	–	–
octadecane	Y	X	–	–	X	Y	–	–
1–octadecene	Y	X	–	–	X	Y	–	–
light liquid paraffin	Y	–	–	–	–	–	–	–
Miglyol 812	Y	–	–	–	–	–	–	–

Y = does form microemulsions
X = does not form microemulsions
– = not tested

CHAPTER FIVE: Soybean oil / Brij 96 microemulsion systems with added cosurfactant

It has already been shown in chapter 3 that systems containing soybean oil, Brij 96 and water can form o/w microemulsions without the addition of a cosurfactant. The presence of cosurfactant is however vital for the formation of many microemulsion systems. These compounds (usually alcohols) can play a direct role in microemulsion formation due to their effect on the elasticity and spontaneous curvature of the interface [305], their ability to destroy liquid crystalline structures [306] and their effect on interfacial tension between the oil and water phases [12]. The cosurfactant may also act indirectly by modifying the environment of the surfactant and increasing its interfacial activity [307]. In this study the effect of the addition of three straight-chained alcohols, as well as more pharmaceutically acceptable polyols, on the phase behaviour of soybean oil/Brij 96/water microemulsions was investigated.

5.1 The addition of straight chain alcohols

5.1.1 The effect of alcohols on the area of existence

5.1.1.1 Methanol as cosurfactant

The effect of adding increasing amounts of methanol to soybean oil/Brij 96/water systems is shown in figure 5.1. The phase diagram for the 3-component system is represented by the triangular plot of figure 5.1a. When

the Brij 96 was replaced by a Brij 96:methanol mix of 4:1 (by weight), the original o/w microemulsion region remained, although the maximum incorporation of soybean oil was reduced from 6.5 to 5 %w/w, and that maximum occurred at a value of about 30 %w/w Brij 96(4):methanol(1). Another clear region was observed close to the Brij 96:methanol apex in a similar position to the surfactant-rich, clear region found at higher temperatures with the additive-free system (3.2). This region included compositions containing a maximum of 22 %w/w soybean oil when only 2-4 %w/w water was present, the remainder consisting of Brij 96 and methanol.

Increasing the amount of methanol to a Brij 96:methanol ratio of 2:1 further reduced the maximum soybean incorporation in the o/w region to 3 %w/w, occurring between 30-36 %w/w combined surfactant, with a shift in the region towards the Brij 96:methanol apex. When an equal weight ratio of Brij 96:methanol was employed as surfactant, no o/w microemulsion region was found at all.

The clear, surfactant-rich region observed with a combined surfactant of Brij 96:methanol of 4:1 was also present, although reduced, when a Brij 96:methanol ratio of 2:1 was employed. Further increase in the methanol content to a surfactant:cosurfactant ratio of 1:1 resulted in only a very small region of existence, close to the combined surfactant apex.

The observed shift in the o/w region of existence towards the combined surfactant apex with an increase in the amount of methanol is in line with the reduced Brij 96 content of the combined surfactant. For instance, the peak soybean oil incorporation using a combined surfactant of Brij 96(2):methanol(1) represents a Brij 96 concentration of 20-24 %w/w, the same as that found for the 3-component microemulsion system. The methanol does not therefore appear to be assisting the Brij 96 to form o/w microemulsions. In addition the presence of methanol resulted in a reduction in the amount of oil which could be incorporated.

Figure 5.2 represents the compositions of water, Brij 96 and methanol that allow microemulsions to form containing either 2 or 5 %w/w soybean oil (fig.5.2a and fig.5.2b respectively). It can be seen from these diagrams that in the low Brij 96/water-rich region, thought to consist of o/w microemulsion droplets, methanol was poorly tolerated. A Brij 96 concentration of 25 %w/w

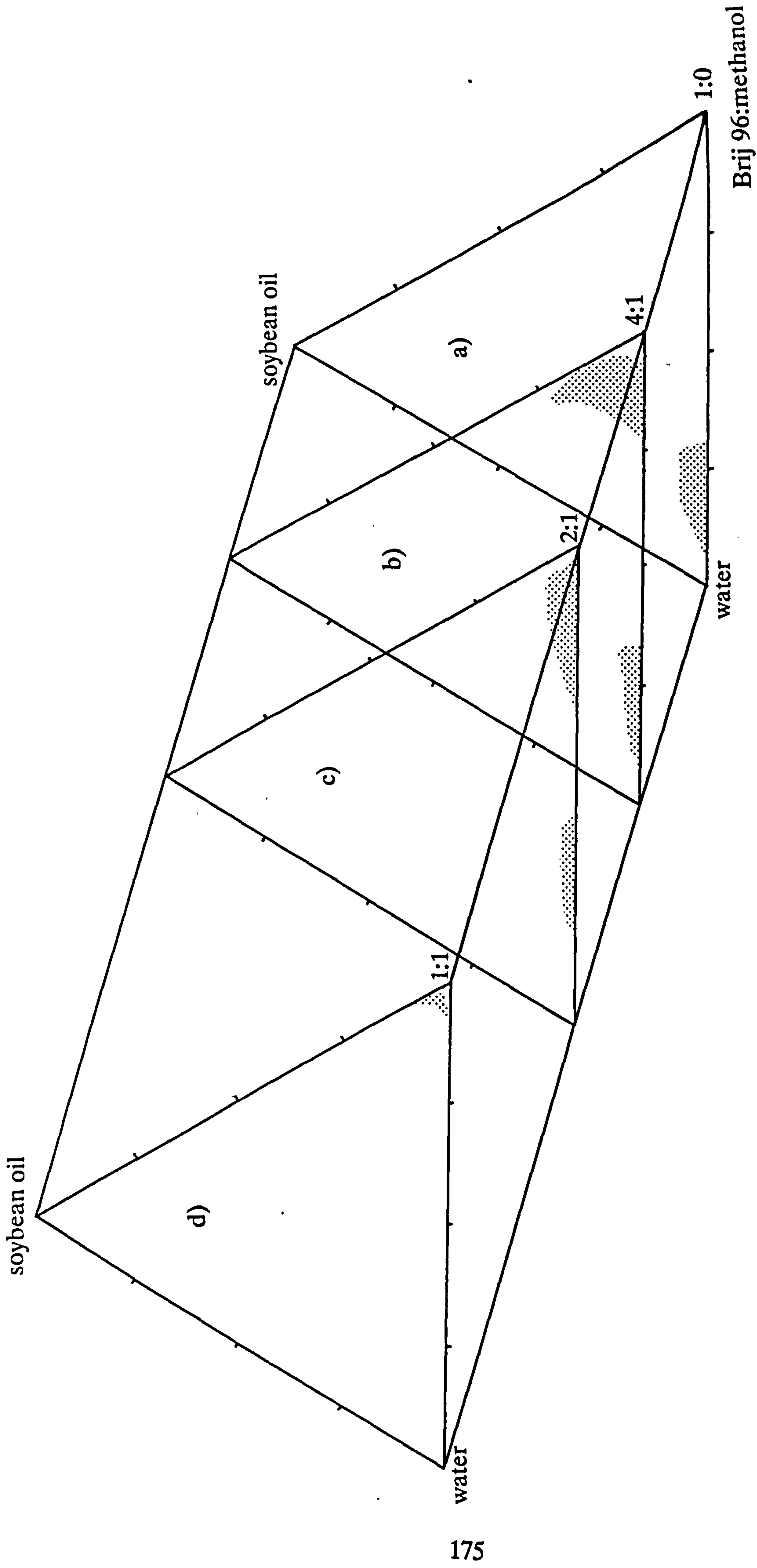


Figure 5.1: Triangular phase diagrams showing the change in microemulsion area of existence with changing weight ratio of Brij 96:methanol; a) 1:0, b) 4:1, c) 2:1 and d) 1:1.

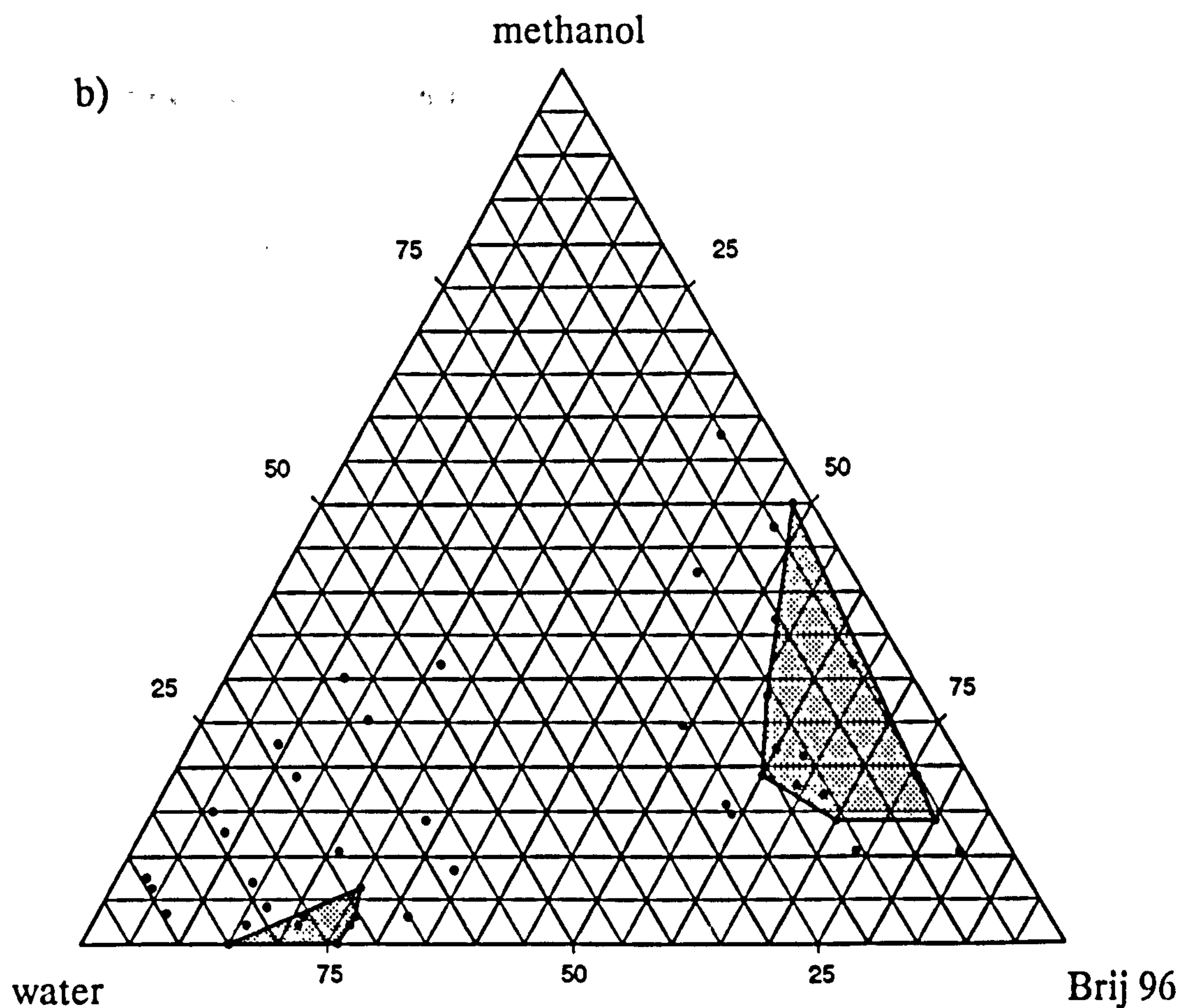
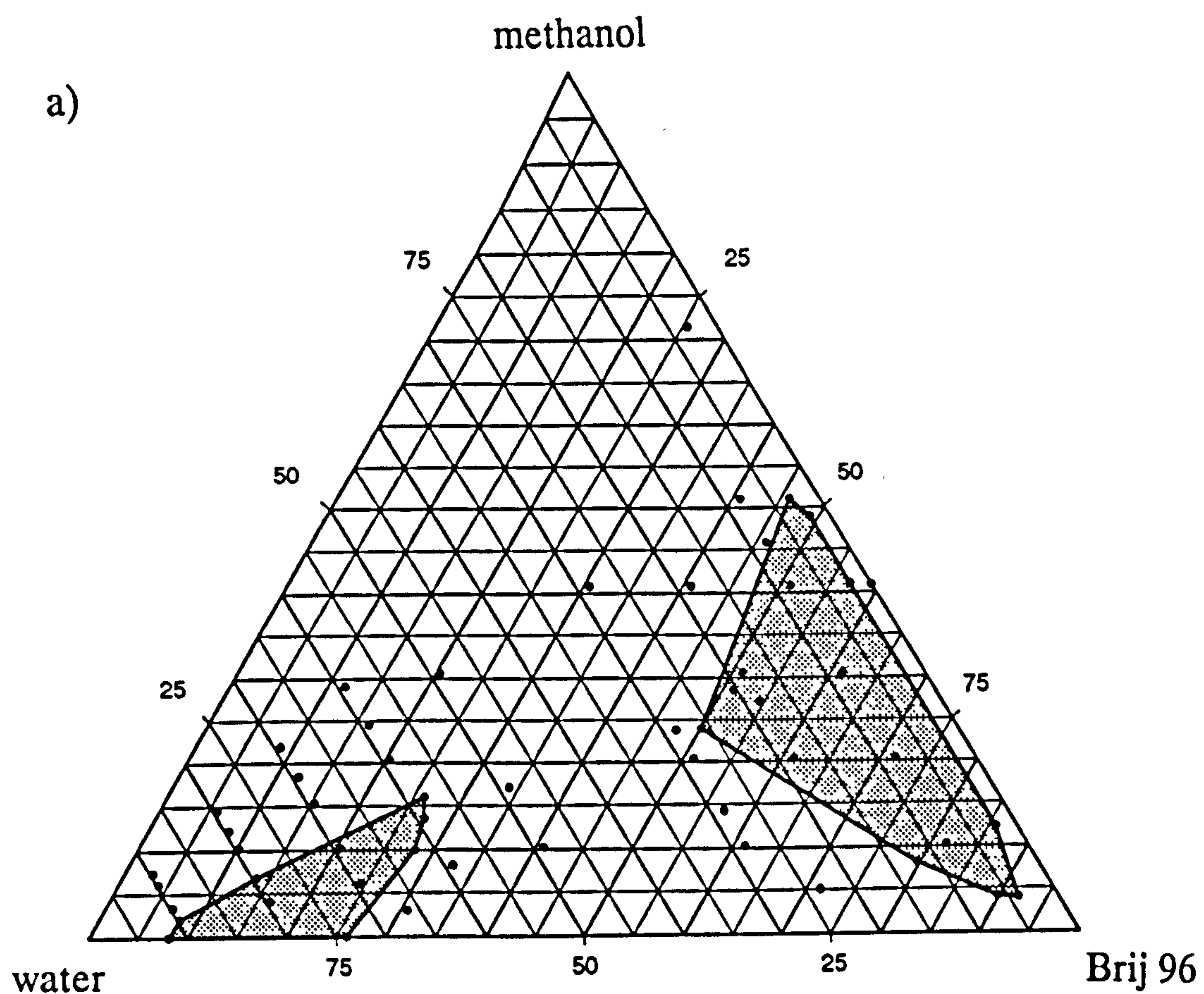


Figure 5.2: Pseudo-ternary phase diagrams showing the area of microemulsion existence in systems containing Brij 96/methanol/water and a) 2 %w/w soybean oil, and b) 5 %w/w soybean oil.

allowed a maximum of 16 and 6 %w/w methanol in microemulsions containing 2 and 5 %w/w soybean oil respectively. The effect on the area of o/w microemulsion existence suggests that the presence of methanol restricts o/w microemulsion formation, just as it has been reported to reduce micellisation (or in high concentration destroy the micelles) of other ethylene oxide surfactants [308, 309].

It can be seen from figures 5.1 and 5.2 that the presence of a small amount of methanol did however stabilise a clear, surfactant-rich area of low water content, and varying soybean oil content between 0 and 22 % w/w. It is not clear how this occurs. Methanol is not likely to be acting as a solvent for the oil, as it mixes poorly with soybean oil [310]. In addition, soybean oil incorporation also decreased with higher methanol contents (above a ratio of 4:1 Brij 96:methanol). Methanol is however highly soluble in water, and would normally partition almost exclusively into the aqueous phase. Hence it may be significant that the water content in this region is very low which might therefore suggest that the partitioning characteristics of the alcohol could be altered in these microemulsion systems.

5.1.1.2 Butanol as cosurfactant

The effect of the addition of 1-butanol to soybean oil/Brij 96/water systems is shown in figures 5.3 and 5.4. In contrast to the areas of existence seen with methanol, only one clear region was found, and no discrete o/w microemulsion region was observed. In addition, the region of microemulsion existence previously seen in 3-component systems was reduced when a combined surfactant of Brij 96:butanol of 4:1 or 2:1 was employed, and was not observed at all at a ratio of 2:3 Brij 96:butanol. Although microemulsions containing 2 %w/w soybean oil could still be produced in this region it can be seen in figure 5.4b that concentrations of Brij 96 (approximately 15-28 %w/w) which had previously allowed the formation of microemulsions containing 5 %w/w soybean oil, no longer resulted in the production of clear systems once butanol was added. With a ratio of Brij 96:butanol of 4:1 (which gave the largest area of existence in figure 5.3) the clear region did not begin until at least 25 %w/w of the combined surfactant was present. This corresponds to a Brij 96 content of 20 %w/w. Without cosurfactant, o/w microemulsion systems could be formed with a minimum of about 8 %w/w Brij 96. The

region found appears to approximately centre about the 50:50 soybean oil:water tie line, with a longer arm pointing towards the water apex. The opposite arm of the region, extending towards the soybean oil apex, allowed the formation of clear 4-component systems with a maximum of 46 %w/w soybean oil possible with 4 %w/w water and 50 % w/w Brij 96(4):butanol(1).

Increasing the butanol content to a ratio of Brij 96:butanol of 2:1 reduced the area of existence, although the area still remained near the mixed surfactant apex. The region extended from a maximum water content of 55 %w/w, curving around the surfactant apex to a maximum soybean oil content of about 32 %w/w. With further increases in butanol content (ratios of Brij 96:butanol of 2:3, 2:5 and 2:7) the arm extending to the water apex withdrew further towards the combined surfactant apex. A maximum water content of 35 %w/w was found with a combined surfactant of 2:3 Brij 96:butanol, and only 25 %w/w at ratios of Brij 96:butanol of 2:5 and 2:7. Similarly, the arm extending towards the soybean oil apex also reduced with increased butanol in the combined surfactant, until a maximum soybean oil incorporation of 24 %w/w was found with a Brij 96:butanol ratio of 2:7.

1-Butanol is a proven and effective cosurfactant used in many microemulsion systems. Due to its solubility characteristics, it has affinity for both the oil and water phase, and can act as a surfactant between such phases in the absence of more traditional amphiphiles [311, 312]. In 4-component microemulsion systems butanol tends to partition between the oil, water and surfactant regions, encouraging the formation of bicontinuous microemulsion structures [313, 314], increasing the total interfacial area and hence contributing to an increase in solubilisation [305].

In this study butanol has been shown to discourage the formation of o/w microemulsions, but on the other hand to encourage the formation of microemulsions over a wide range of compositions, particularly those compositions of high Brij 96 content. In its presence it was possible to produce clear systems with 10 %w/w soybean oil (and over), as is illustrated by the large area in figure 5.4c. This level of oil incorporation was not seen with soybean oil/Brij 96 systems without added cosurfactant, or over such a range of surfactant and cosurfactant concentrations in systems containing added methanol. It is also apparent from figures 5.3 and 5.4 that in the presence of butanol, the area of microemulsion existence had shifted towards

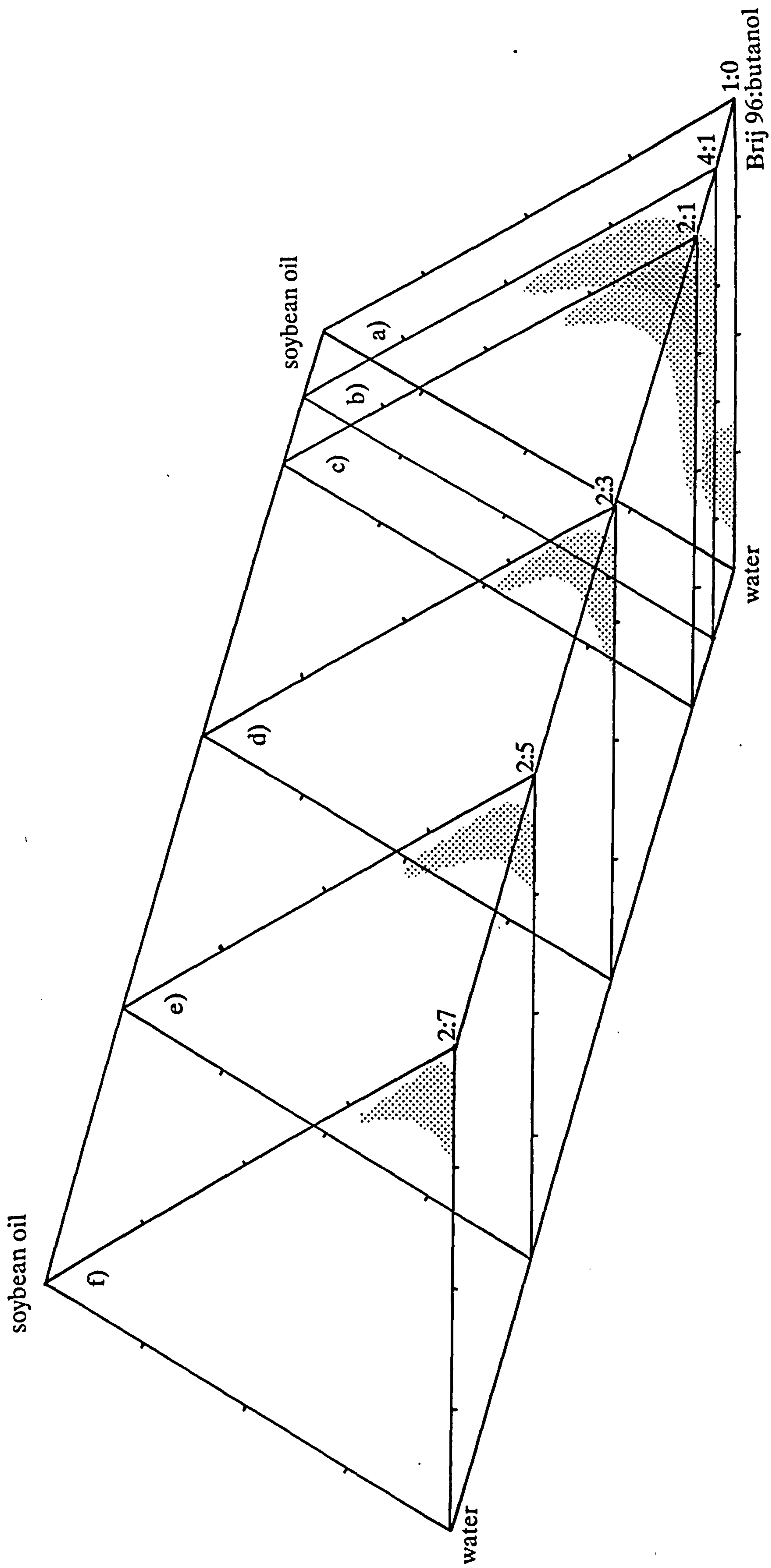


Figure 5.3: Triangular phase diagrams showing the change in microemulsion area of existence with changing weight ratio of Brij 96:1-butanol; a)1:0, b)4:1, c)2:1, d)2:3, e)2:5 and f)2:7.

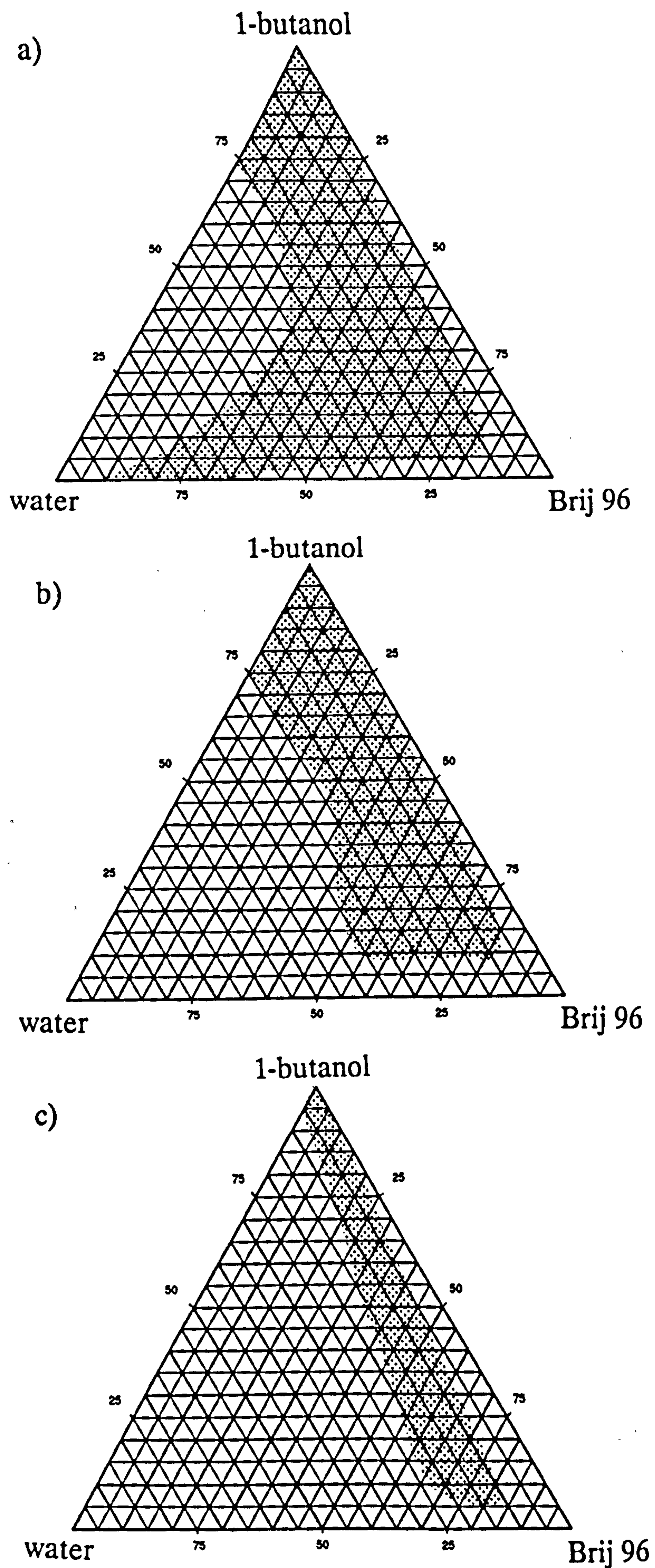


Figure 5.4: Pseudo-ternary phase diagrams showing the area of existence of microemulsion systems containing Brij 96/1-butanol/water and a) 2 %w/w soybean oil, b) 5 %w/w soybean oil and c) 10 %w/w soybean oil.

higher surfactant/cosurfactant concentrations (and lower water contents) compared to the 3-component, Brij 96-only systems. This shifted area of microemulsion existence extended through the gel region observed in 3-component systems.

5.1.1.3 Pentanol as cosurfactant

The effect of the addition of 1-pentanol to soybean oil/Brij 96/water systems on the area of microemulsion existence is shown in the triangular plots of figures 5.5 and 5.6. The areas found follow, with only small differences, the same trend as those described for butanol. With lower concentrations of pentanol (Brij 96:pentanol ratios of 4:1 and 2:1) the areas of existence extended further towards the water apex compared to the same ratios using butanol. For example, with a combined surfactant:cosurfactant ratio of 4:1, microemulsion existence began at a minimum combined surfactant concentration of about 15 %w/w for pentanol, compared to 25 %w/w for butanol. At a surfactant:cosurfactant ratio of 2:3 however, the arm extending to the water apex was shorter for pentanol than for butanol. Again, large regions of microemulsion existence incorporating higher levels of soybean oil (for example 10 %w/w) were possible with 4-component systems containing pentanol (fig.5.6c). For systems containing 1-pentanol, as also found using butanol as cosurfactant, a large area existed in which 5 %w/w soybean oil could be incorporated (fig.5.6b) but no microemulsions were possible for the same Brij 96/water concentrations in which o/w microemulsions had been formed without cosurfactant.

Like butanol, pentanol partitions between water and oil domains, and tends to form bicontinuous structures [315]. Because of its increased hydrophobicity, relative to butanol, less pentanol is expected in the water phase [316]. In systems of SDS, styrene and water, 60% of 1-pentanol was found in the surfactant interface [317], hence increasing the surface area and fluidity of the interface [318]. Due to the increased hydrophobic nature of pentanol compared to butanol, different distributions within the system would be expected for the two alcohols, and these are thought to result in the small changes in the phase domains that were observed in the present study.

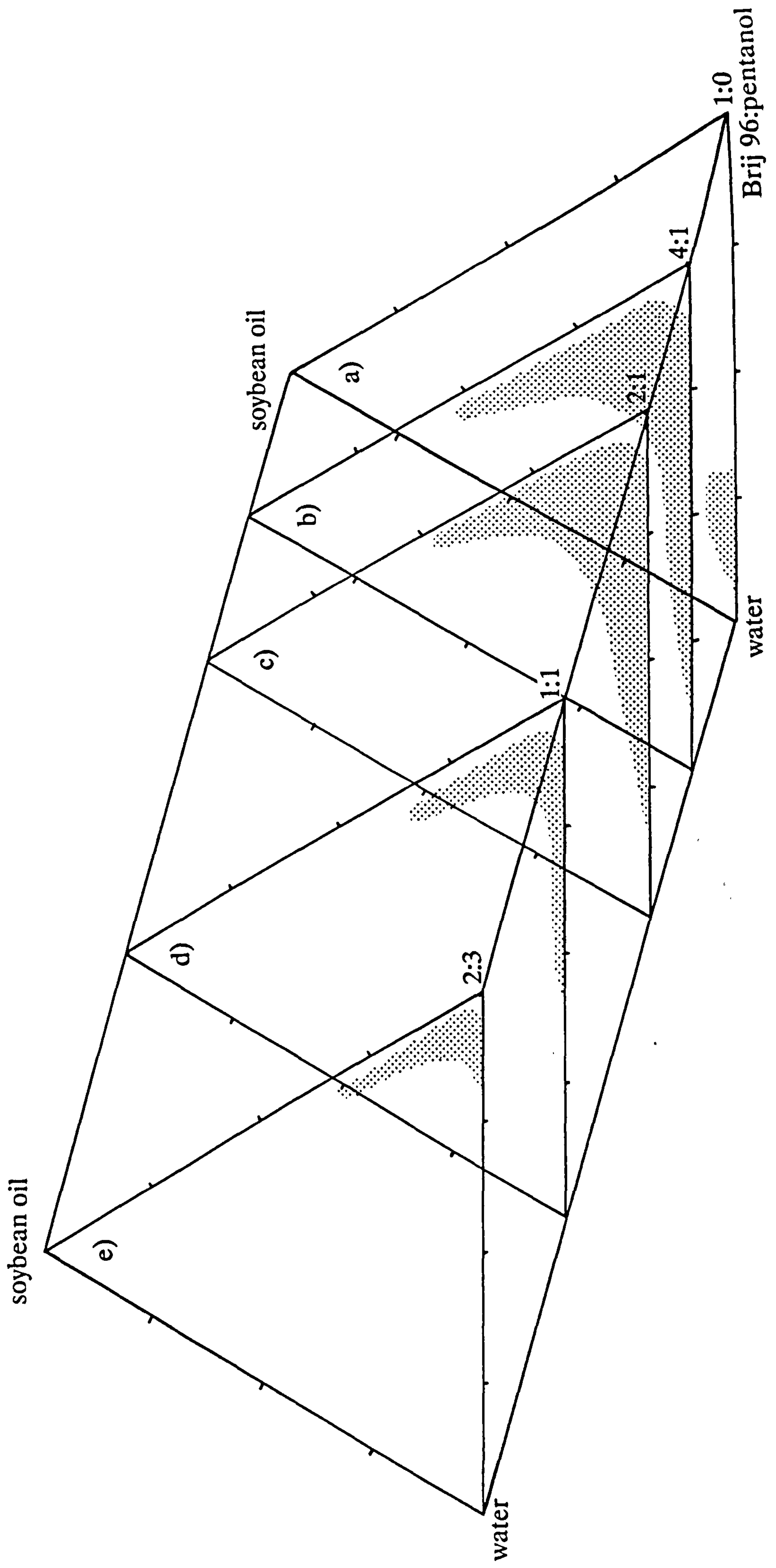


Figure 5.5: Triangular phase diagrams showing the change in microemulsion area of existence with changing weight ratio of Brij 96:1-pentanol; a) 1:0, b) 4:1, c) 2:1, d) 1:1 and e) 2:3.

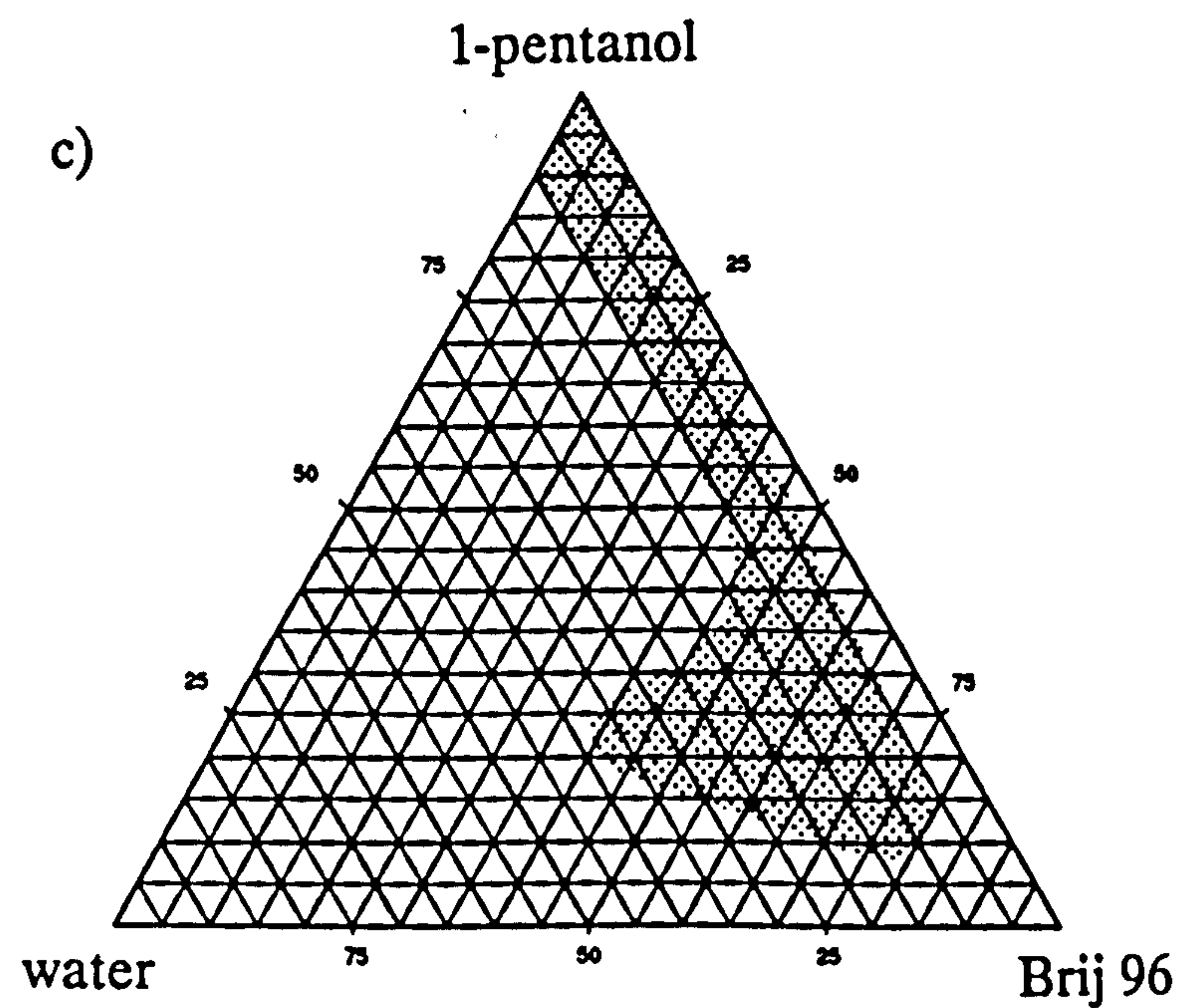
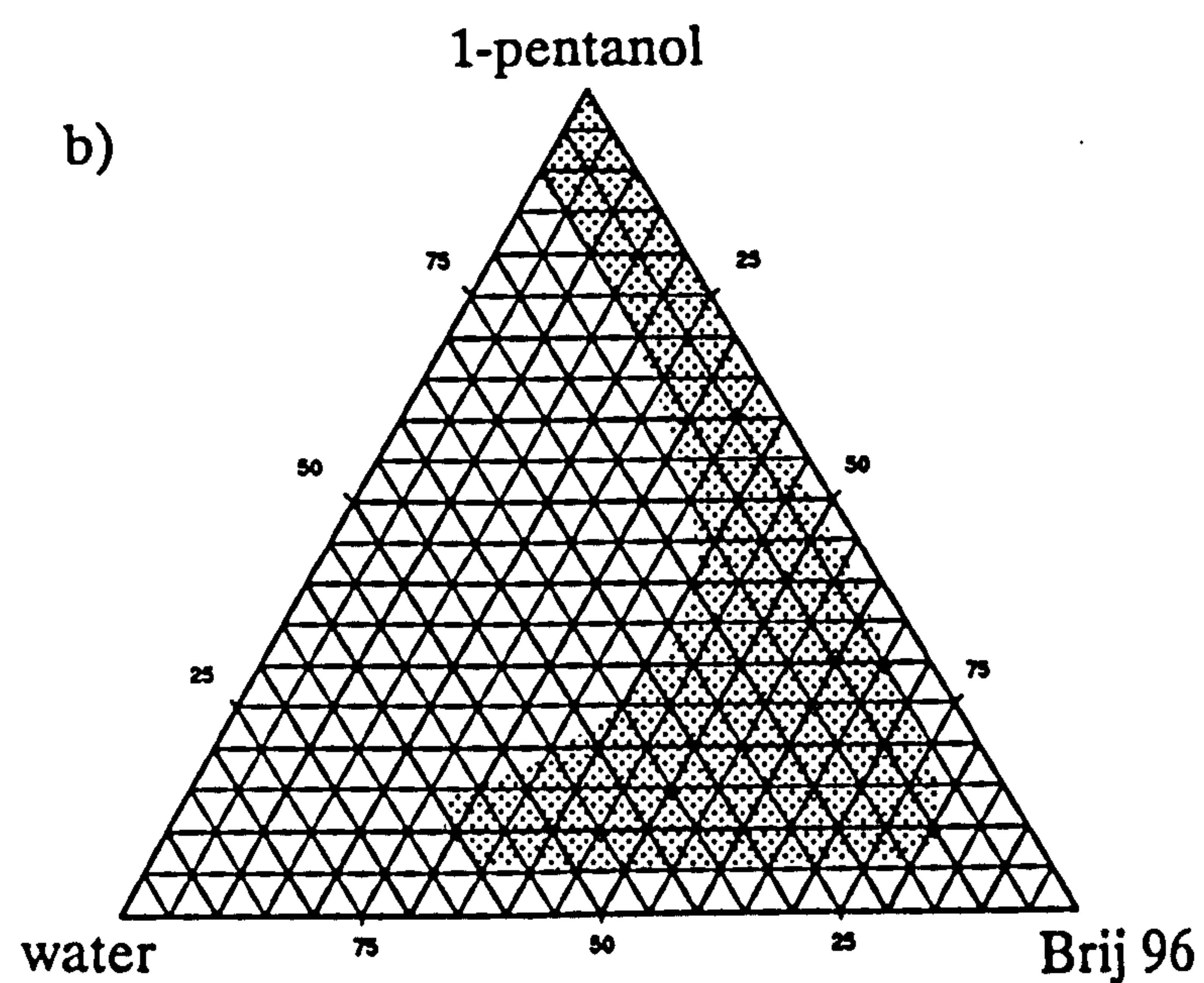
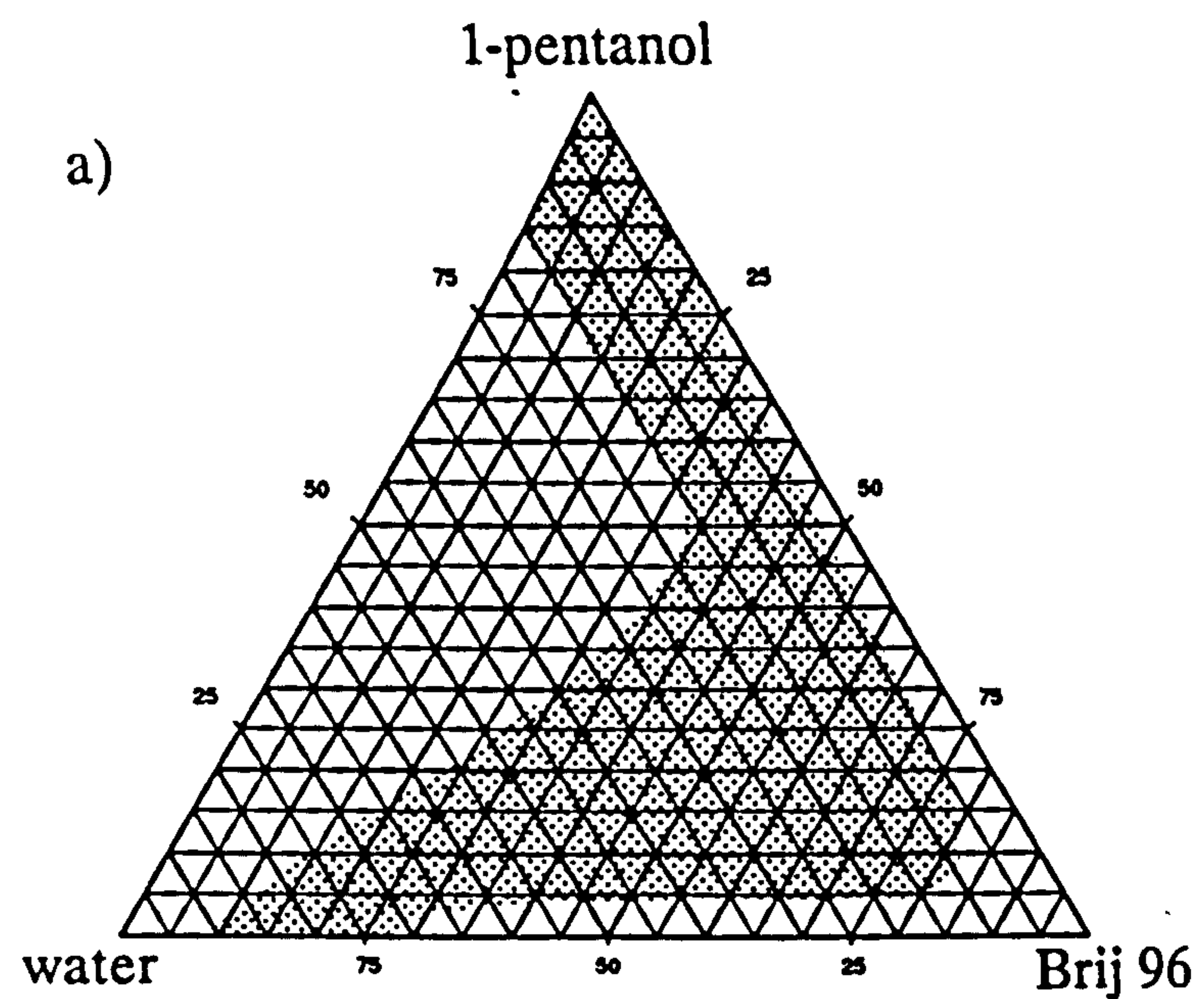


Figure 5.6: Pseudo-ternary phase diagrams showing the area of microemulsion systems containing Brij 96/1-pentanol/water and a) 2 %w/w soybean oil, b) 5 %w/w soybean oil and c) 10 %w/w soybean oil.

5.1.2 Changes in area of existence with temperature

Changes in the area of microemulsion existence with temperature of 4-component systems containing soybean oil, Brij 96, water and either methanol or butanol were investigated. A combined Brij 96:alcohol ratio of 2:1 was used. The resulting triangular plots after one months storage at 4, 25, 37 or 50°C are shown in figure 5.7.

With methanol as cosurfactant (fig.5.7a) little difference was observed between the areas of existence found at 4, 25 and 37°C. At all three temperatures two clear regions existed; an o/w region near the water apex, and an area at the combined Brij 96(2):methanol(1) apex. The area at the combined surfactant apex grew only slightly in size between 4 and 37°C. The o/w region did not appear to change at all at temperatures up to 37°C. At 50°C however there was a merging of the two regions along the water-combined surfactant axis.

The triangular plots for the same systems with butanol as cosurfactant, show that no clear microemulsion systems were possible with these 4-component systems at 4°C. At 25°C a fairly large area was found at the combined surfactant apex, with a longer arm extending towards the water apex. With increasing temperature (37 and 50°C) this arm of the microemulsion area remained fairly static, but an increase in the size of the opposite arm extending towards higher soybean oil contents was noticed.

It is anticipated that increasing temperature could result in changes in the area of microemulsion existence by two mechanisms; solubility effects, and destabilisation of the liquid crystalline phase. Firstly, the solubility characteristics of the microemulsion components will change with temperature. Mutual solubility of water and polar organic solvents may be enhanced by an increase in temperature [319]. It would also be expected that the distribution of surfactant and cosurfactant between the oil and water phases would be altered. Secondly, destabilisation of any liquid crystalline phase (a mechanism by which many cosurfactants are thought to act [306]) will increase with temperature [319].

In the Brij 96(2):methanol(1) systems viscous, one-phase compositions

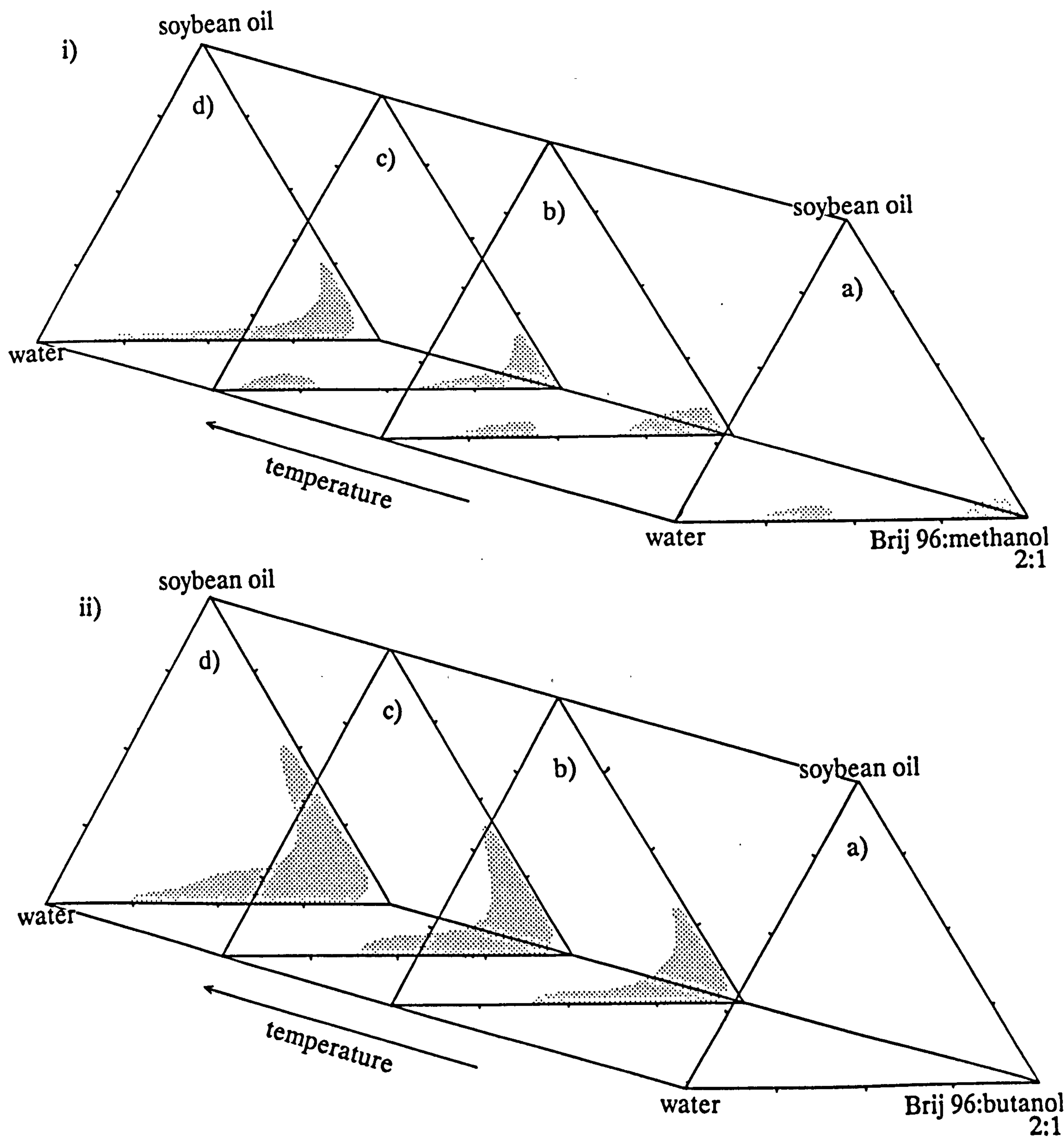


Figure 5.7: Triangular phase diagrams showing the change in microemulsion area of existence with temperature for systems containing soybean oil, water and a constant ratio of Brij 96:cosurfactant (2:1) for i) methanol and ii) 1-butanol at temperatures of a) 4°C, b) 25°C, c) 37°C and d) 50°C.

separate the two clear regions at temperatures up to, and including, 37°C. Significantly, clear regions were formed at 4°C when methanol is present in soybean oil/Brij 96/water systems which do not form when Brij 96 is used alone (3.2), or in combination with butanol. Methanol however does not appear to be a very effective agent at destroying gel phases at lower temperatures. In combination with a temperature of 50°C however, the viscous phase was replaced by clear liquid systems, resulting in the linking of the two microemulsion regions.

In contrast, although butanol was effective at destroying the gel phase at 25°C, this effect (probably in combination with unfavourable solubility and/or partitioning behaviour) was insufficient to allow microemulsions to form at 4°C. Once temperatures were reached at which microemulsion could form in this system, only one extended area of existence was observed. This area encompassed the region occupied by a gel phase in the cosurfactant-free system (3.1). Further increases in temperature extended the microemulsion region obtained with these 4-component systems towards higher incorporation of soybean oil. At lower temperatures these compositions had resulted in two phase systems, and hence it is postulated that the dominating mechanism which caused them to be included in the microemulsion region with increasing temperature is the changing solubility characteristics that occur with temperature increases.

5.1.3 Conductivity and dilution of soybean oil/Brij 96/butanol/water systems

The conductivity of microemulsion compositions, and their appearance after dilution with water was investigated in order to gain some information about the structure of 4-component systems containing butanol. Three series of microemulsion systems were selected, and results shown in figures 5.8, 5.9 and 5.10. In each case conductivity was plotted against the weight of the component(s) being considered, as a fraction of the total weight of the microemulsion composition. In two of the series, the soybean oil content was fixed at 2 %w/w, and the changes were observed with a) increasing combined surfactant of 4:1 Brij 96:butanol (fig.5.8), and b) increasing butanol when the Brij 96:water ratio was fixed at 7:3 (fig.5.9). The final series, c) (fig.5.10) followed the changes occurring in the microemulsion systems as the soybean

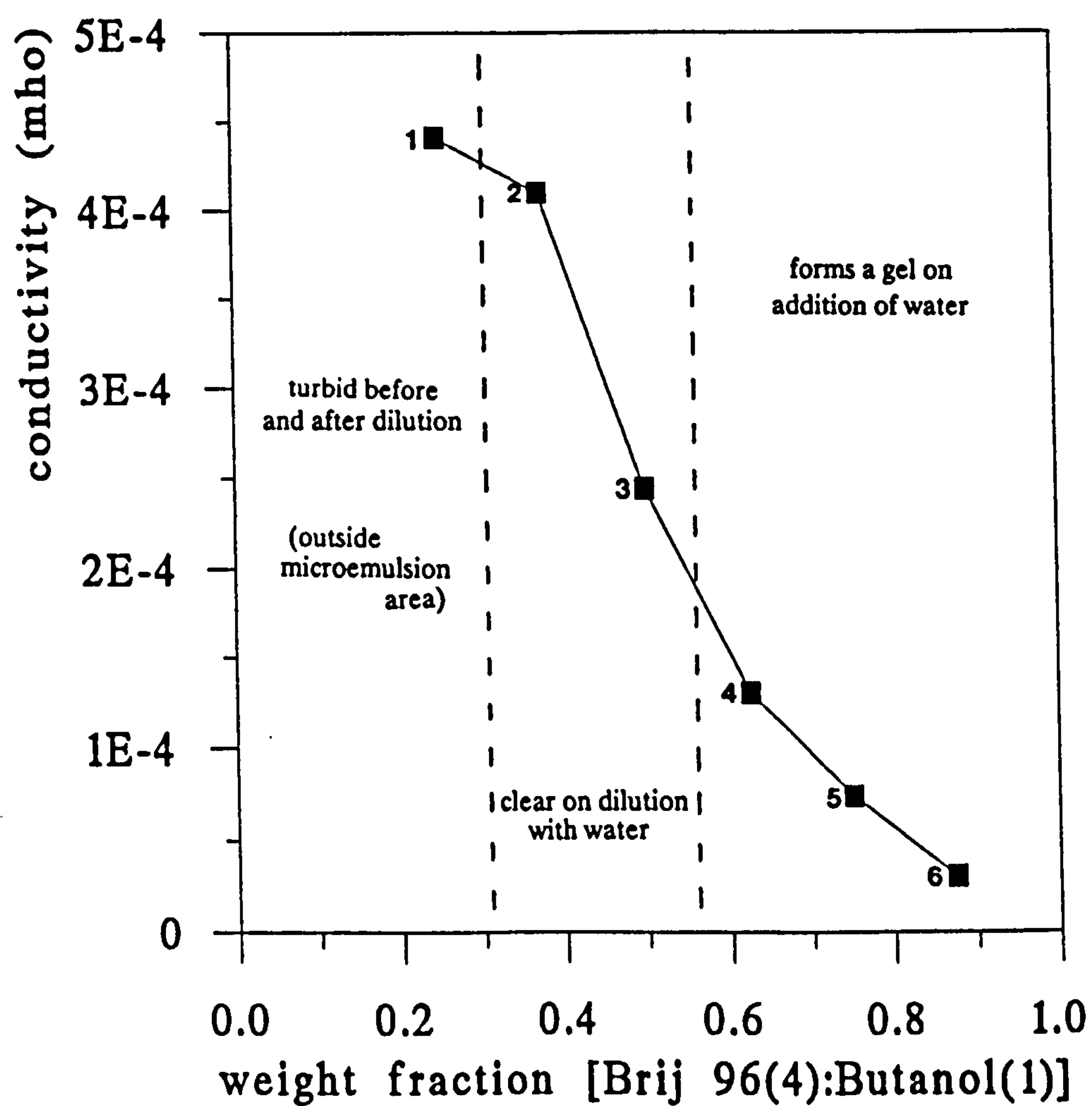
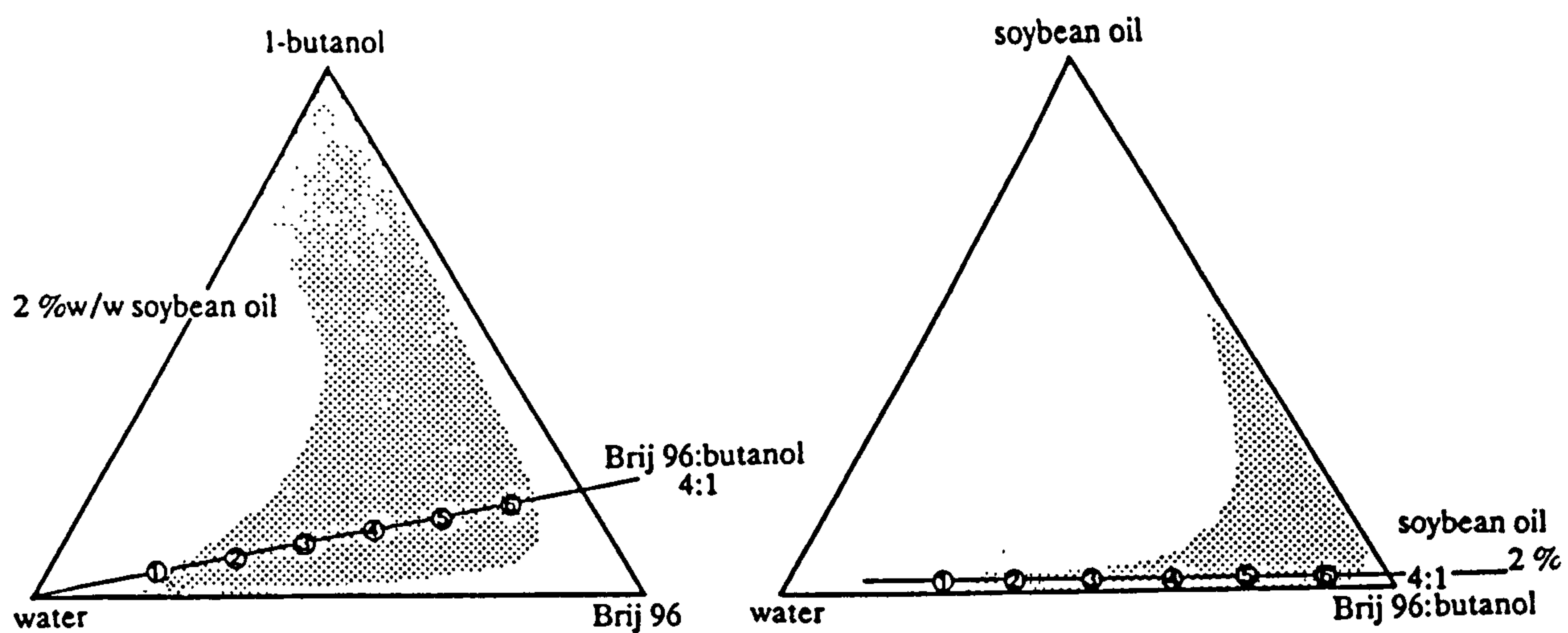


Figure 5.8: Change in conductivity and dilution characteristics in microemulsions containing 2 %w/w soybean oil and increasing weight fraction of the combined surfactant; Brij 96(4):1-butanol(1).

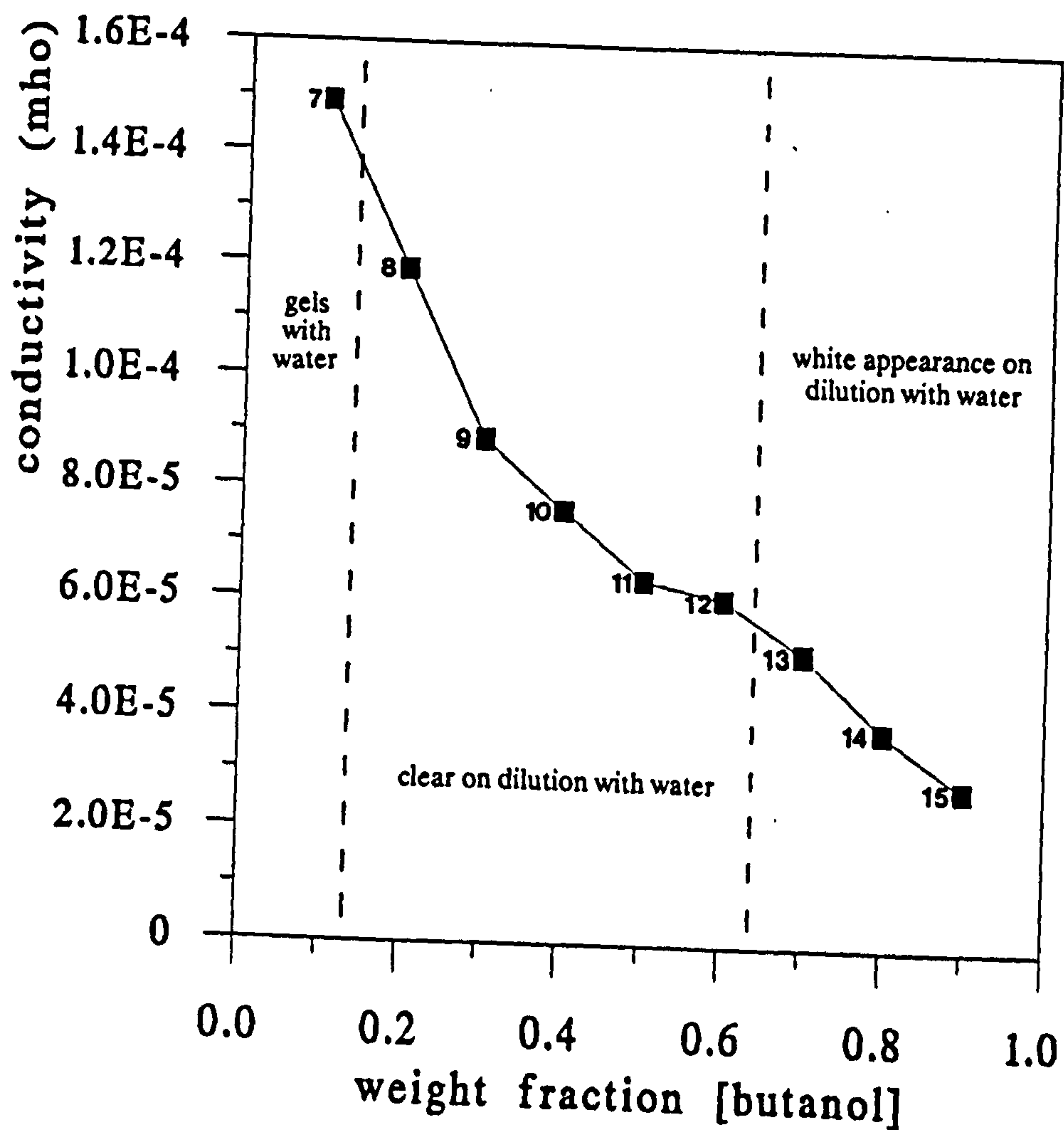
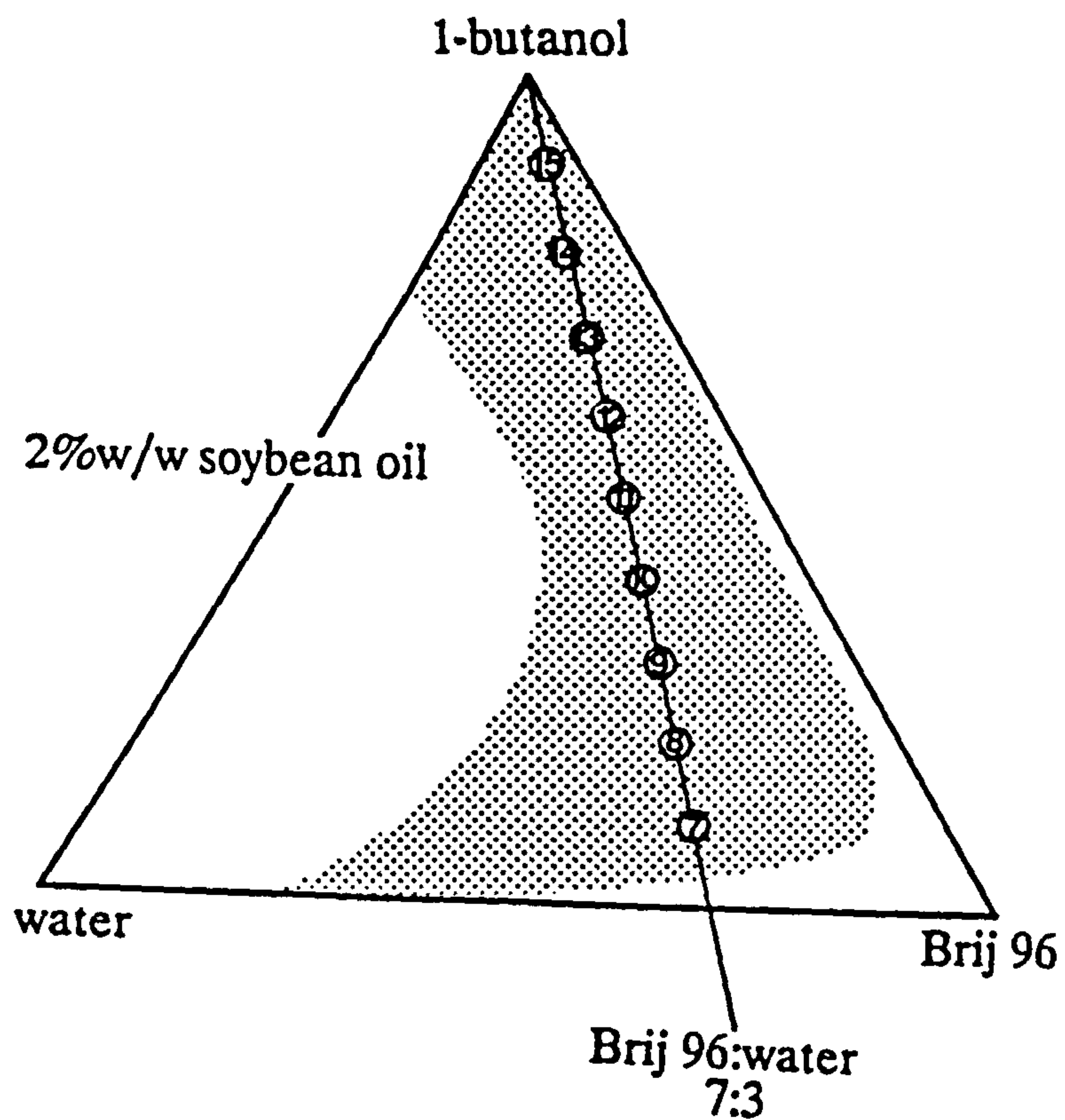


Figure 5.9: Change in conductivity and dilution characteristics in microemulsions with 2 %w/w soybean oil and increasing weight fraction of 1-butanol along the tie-line of Brij 96(7):water(3).

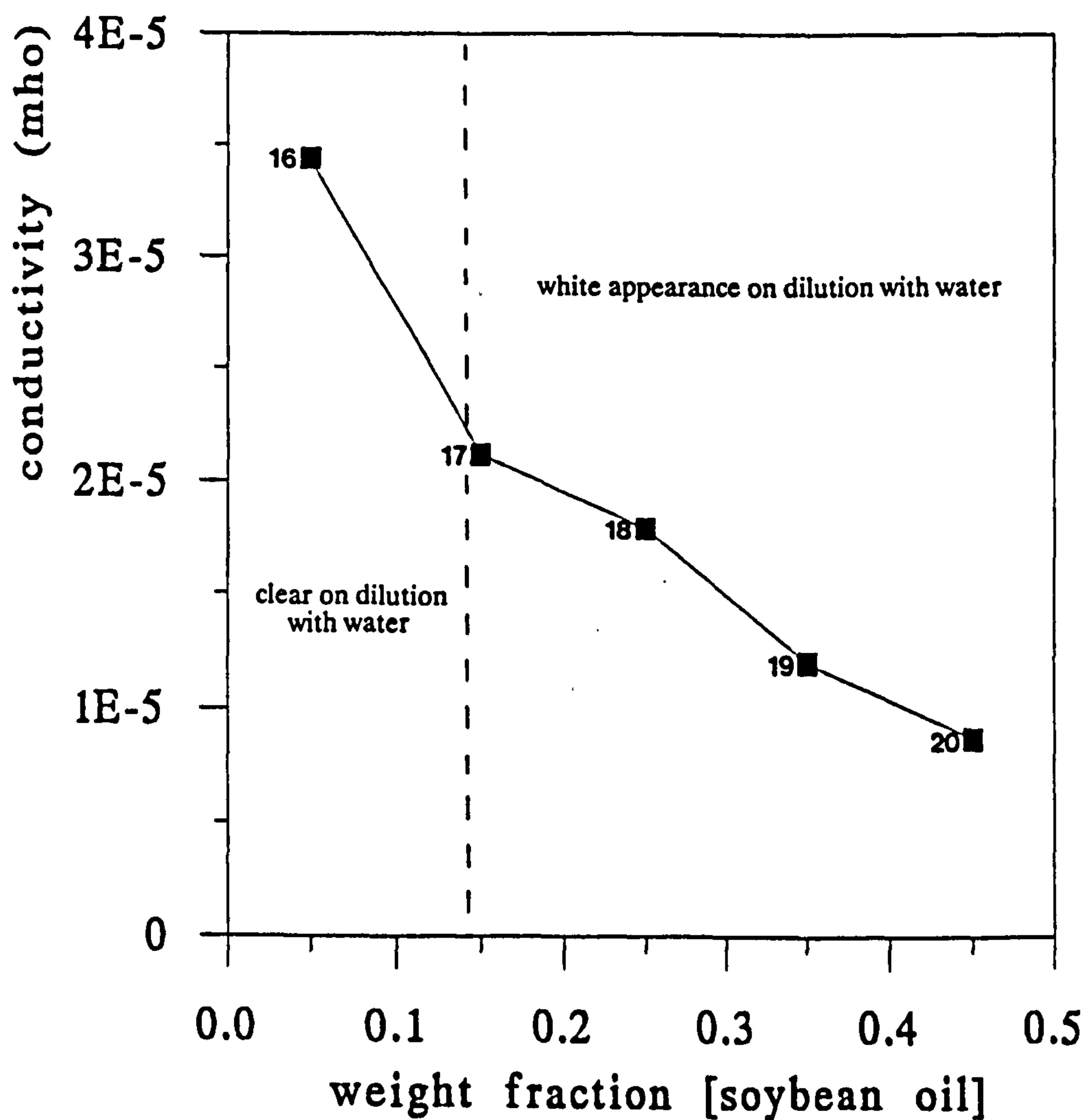
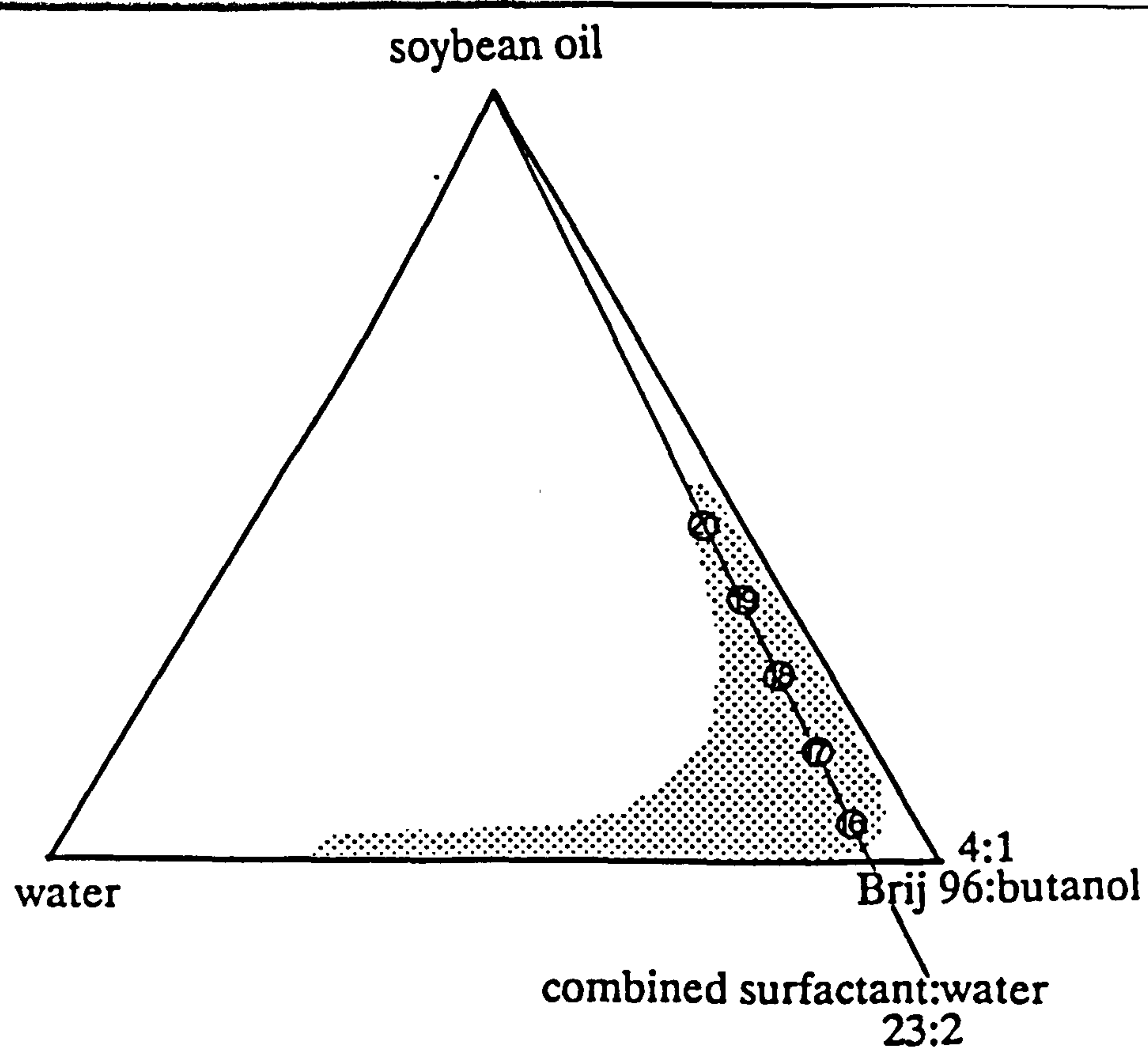


Figure 5.10: Change in conductivity and dilution characteristics in microemulsions with a constant ratio of Brij 96(4):butanol(1) with increasing soybean oil along the tie-line of combined surfactant(23):water(2).

oil content was increased along the tie-line of combined surfactant (4:1):water of 23:2.

The results show a fairly gradual decrease in conductivity for all three series; ie. as the combined surfactant, butanol or soybean oil weight fractions increase. Other workers, particularly those investigating the change in conductivity of ionic microemulsion systems, have observed very steep changes in conductivity (over several orders of magnitude) with increasing volume fractions of water or temperature. These sharp variations in conductivity have been attributed to significant and fairly dramatic changes in the structure of the systems either at the *percolation threshold*, or transition temperature [37, 38, 320].

This study did not reveal sharp changes in conductivity, which suggests that the structural changes in these systems (within the series of compositions studied) are more gradual [26]. Based on the large range of compositions and relative concentrations of components within the soybean oil/Brij 96/butanol/water microemulsion area it is however expected that changes in structure do occur.

The different responses of the microemulsion samples to dilution also imply changes within the microemulsion domain. With 2 %w/w soybean oil present, clear microemulsion compositions containing at least 50 %w/w water (samples 2 and 3 in figure 5.8) remained clear on dilution with water. Those compositions in the central region of the 2% soybean oil microemulsion area (fig.5.9) between Brij 96:butanol ratios of approximately 3:1 to 2:7 (samples 8-12) were also clear. This suggests that in these microemulsion systems the external phase is aqueous, and that the addition of further water does not sufficiently upset either the microemulsion structure, or the solubility balance of the components, to result in the formation of unstable preparations.

In contrast, in 2 %w/w soybean oil systems with higher butanol, and low water/low Brij 96, concentrations (compositions 13,14 and 15 in figure 5.9) the addition of water resulted in the production of white macroemulsions. Similarly, white macroemulsions were also produced on dilution of microemulsion systems with soybean oil contents above 15 %w/w (compositions 19, 20 and 21 in figure 5.10). At higher Brij 96 contents, as found in compositions 4,5 and 6 in figure 5.8 and sample 7 in figure 5.9,

additional water causes soft gels to form. These phenomena may suggest that the external phase in those systems which cannot be diluted is therefore not water. Although this dilution behaviour is thought to be indicative of a change in the structure of the systems, without further investigation by other techniques it is not easy to speculate on the possible structures that exist.

5.1.4 Changes in interfacial tension with the addition of butanol or pentanol

Surfactant added to an oil and water system will reduce the interfacial tension between the two phases because of its ability to accumulate at the interface. In this study, the abilities of 1-butanol and 1-pentanol to assist Brij 96 to reduce the interfacial tension between soybean oil and water were investigated.

At room temperature the interfacial tension between the soybean oil and water was found to be 21.5 mNm^{-1} . This value agrees well with the equilibrium interfacial tension between commercial soybean oil and water of 22 mNm^{-1} obtained by Gaonkar [294]. Values obtained between soybean oil and a 10 %w/w Brij 96 solution, and between soybean oil containing 10 %w/w butanol, and water were 3.6 and 6.3 mNm^{-1} respectively. The fact that butanol reduced the interfacial tension between the two phases in the absence of surfactant suggests that the alcohol can also accumulate at the interface. The interfacial tension between soybean oil with 10 %w/w butanol, and a 10 %w/w Brij 96 solution was lower still, giving in a value of 1.7 mNm^{-1} using the du Nuoy ring method.

To further investigate the low interfacial tensions that can occur in these systems a spinning drop tensiometer was used, in which a drop of soybean oil was added to an external aqueous solution containing Brij 96, as well as any cosurfactant. The interfacial tension values obtained over a range of temperatures are shown in table 5.1. All systems exhibited a decrease in interfacial tension with increasing temperature within the range of temperatures studied. No minimum in interfacial tension with temperature was observed, indicating the PIT of each system was not reached [106, 321, 322]. It was not however possible to obtain interfacial tension values for the 20 %w/w pentanol/20 %w/w Brij 96 system above 40°C , and this could have

Table 5.1: Interfacial tension (mNm^{-1}) between soybean oil and aqueous solutions of 20 %w/w Brij 96, and 0, 10 and 20 %w/w 1-butanol or 1-pentanol at varying temperatures (mean \pm SD).

Temperature (°C)	No cosurfactant	Interfacial tension \pm SD (mNm^{-1})			
		Butanol		Pentanol	
		10 %w/w	20 %w/w	10 %w/w	20 %w/w
22	—	—	—	—	0.029 ± 0.004
30	3.13 ± 0.08	0.60 ± 0.03	0.13 ± 0.05	0.25 ± 0.01	0.02 ± 0.01
40	3.02 ± 0.07	0.45 ± 0.04	0.12 ± 0.01	—	0.005 ± 0.002
45	—	—	—	0.11 ± 0.03	—
50	2.2 ± 0.1	0.38 ± 0.09	0.14 ± 0.01	—	—
55	—	—	—	0.008 ± 0.006	—
60	1.85 ± 0.08	0.27 ± 0.03	0.12 ± 0.01	—	—
67	1.6 ± 0.2	—	—	—	—

been due to the proximity of the test temperature to the PIT of the system. Introduction of the soybean oil droplet to an aqueous solution of 20% Brij 96 and 20% pentanol resulted in an immediate clouding of the system. The clarity of these systems did improve with time, but only to reveal a very diffuse droplet which could not be measured accurately.

The results show that at the same temperature, the presence of added alcohol in the aqueous phase further decreased the interfacial tension, and that 20 %w/w of either butanol or pentanol was more effective than 10 %w/w. The same trend has been found in many other surfactant/cosurfactant combinations [323, 324]. Furthermore, in soybean oil/Brij 96/water systems, the longer-chained pentanol appeared to have a greater interfacial tension-lowering effect than butanol.

5.1.5 The addition of butanol to soybean oil/Brij 76 systems

Three-component soybean oil o/w microemulsion systems were not produced when Brij 96 was replaced with Brij 76 ($C_{18}E_{10}$) containing a straight stearyl hydrocarbon in place of the oleyl hydrophobe (4.1.2). However when butanol was added to these soybean oil/Brij 76/water systems, microemulsions did form. The resulting areas of existence for 2 and 5 %w/w soybean oil are shown in figure 5.11.

A minimum butanol concentration of approximately 20 and 25 %w/w was required for 2 and 5 %w/w soybean oil microemulsions respectively to form with Brij 76. Relative to the regions found for the same concentrations of soybean oil with Brij 96 (fig.5.4) the area of microemulsion existence had shrunk away from the water apex, and further from the area that any o/w microemulsion droplets might be possible. It therefore appears that partitioning of butanol into the Brij 76 interface allowed the formation of microemulsion systems which are most likely to be of bicontinuous structure.

The observation that microemulsion formation occurred at higher minimum butanol concentrations when Brij 76, rather than Brij 96, was employed could be indicative of either the tighter packing expected in the interface, or to the lower aqueous solubility of Brij 76. The straight C_{18} hydrocarbon of Brij 76 would be expected to pack more tightly than in the Brij 96 interface, hence

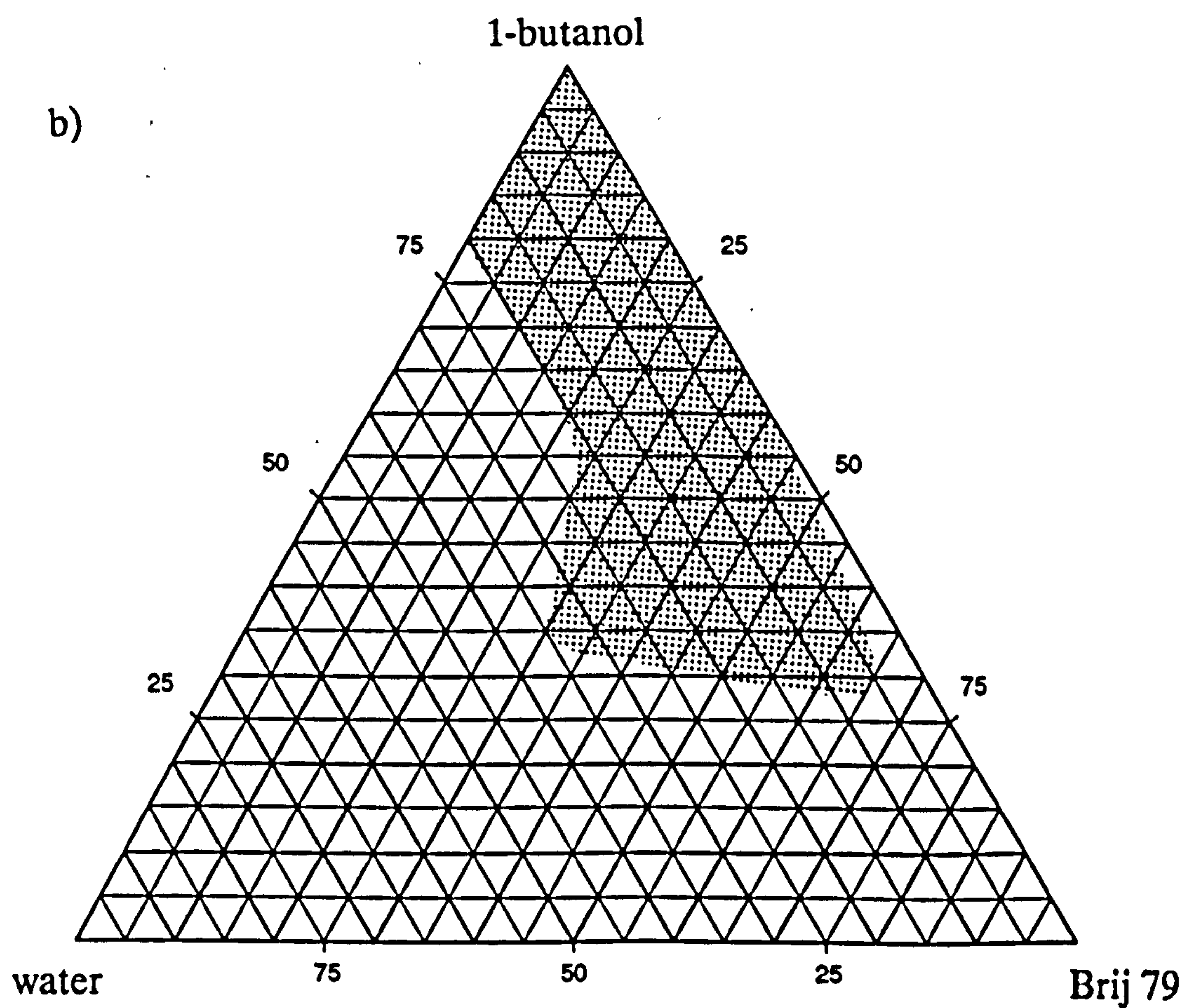
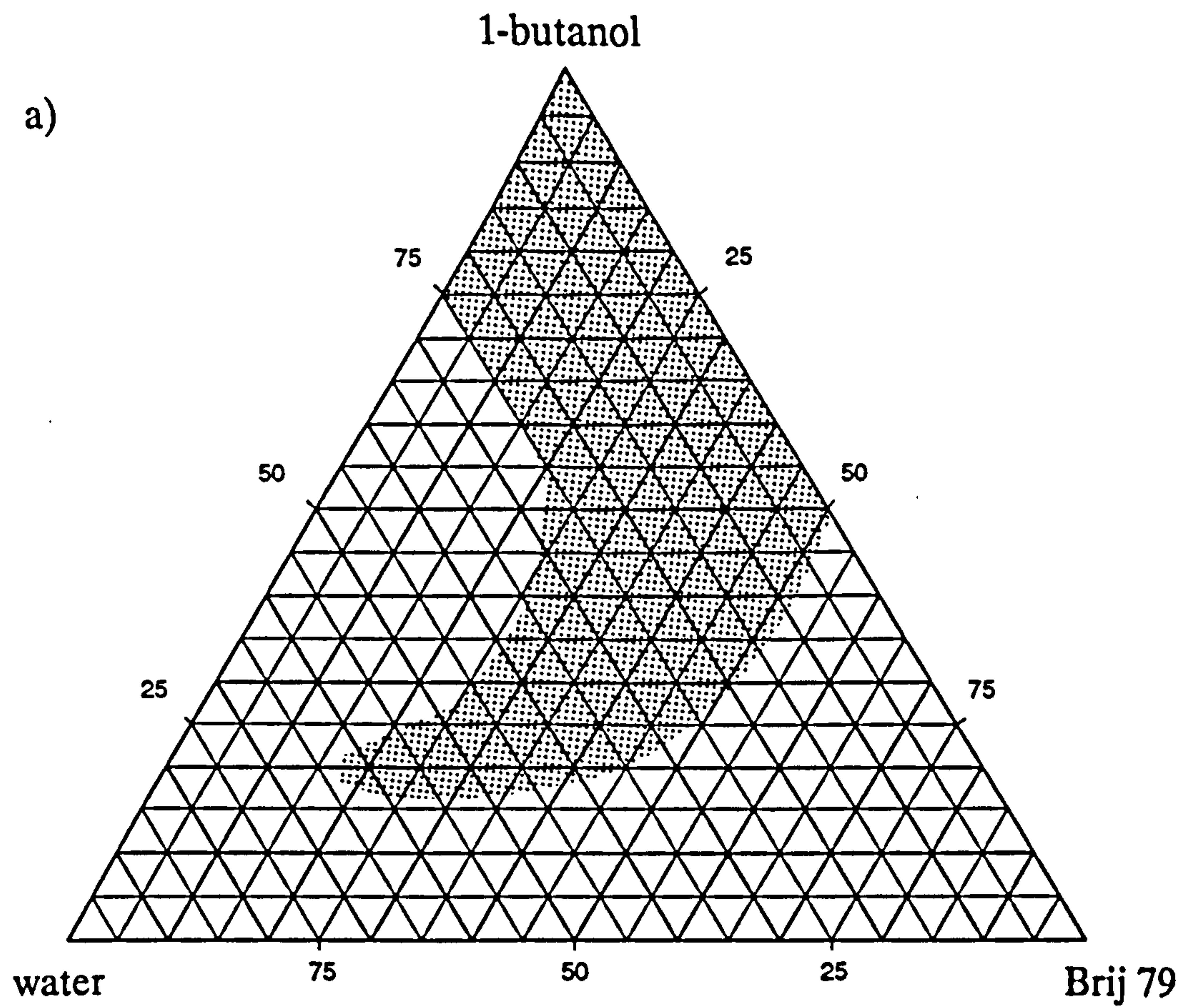


Figure 5.11: Pseudo-ternary phase diagrams showing the area of microemulsion systems with Brij 76/1-butanol/water containing a) 2 %w/w soybean oil and b) 5 %w/w soybean oil.

such systems may therefore require the partitioning of more alcohol molecules into the interface in order to achieve the required flexibility of the interface and/or disruption of any liquid crystalline phase to encourage the formation of bicontinuous, rather than droplet, microemulsion structures. Alternatively, more butanol may be required in the Brij 76 systems (compared to those containing Brij 96) in order to attain the surfactant solubility characteristics required for microemulsions to form with soybean oil and water.

5.2 The addition of polyols

5.2.1 The effect of polyols on the area of existence

The effect of adding the tri-, penta- and hexahydric alcohols; glycerol, xylitol and sorbitol, on the area of o/w microemulsion existence for soybean oil/Brij 96/water systems was investigated. Solvophobic interactions (and hence surfactant aggregation) has been shown to occur in various glycols and glycol/water mixtures [325, 326]. The high water solubility and size of all three polyols however makes it unlikely that they will penetrate far into the Brij 96 interface. Hence any possible cosurfactant effect by these three alcohols would be expected to work indirectly. The results are shown in figures 5.12-5.17.

Figure 5.12 shows that as more glycerol was added to soybean oil/Brij 96/water systems the area of existence was shifted towards the Brij 96:glycerol apex. With a Brij 96:glycerol ratio of 2:1, microemulsions existed over combined surfactant concentrations of between 12-42 %w/w, corresponding to a Brij 96 concentration of 8-28 %w/w. This range of surfactant concentration is identical to that found in the 3-component systems. Maximum soybean oil incorporation also remained unchanged. The maximum soybean oil incorporation, and range of Brij 96 concentration required for the formation of microemulsions continued to remain very much the same through ratios of Brij 96:glycerol of 1:1 and 2:3. At glycerol contents in the Brij 96:cosurfactant mix of 1:2 and above, the region of microemulsion existence began to shrink, and no more than 3 %w/w oil could be included.

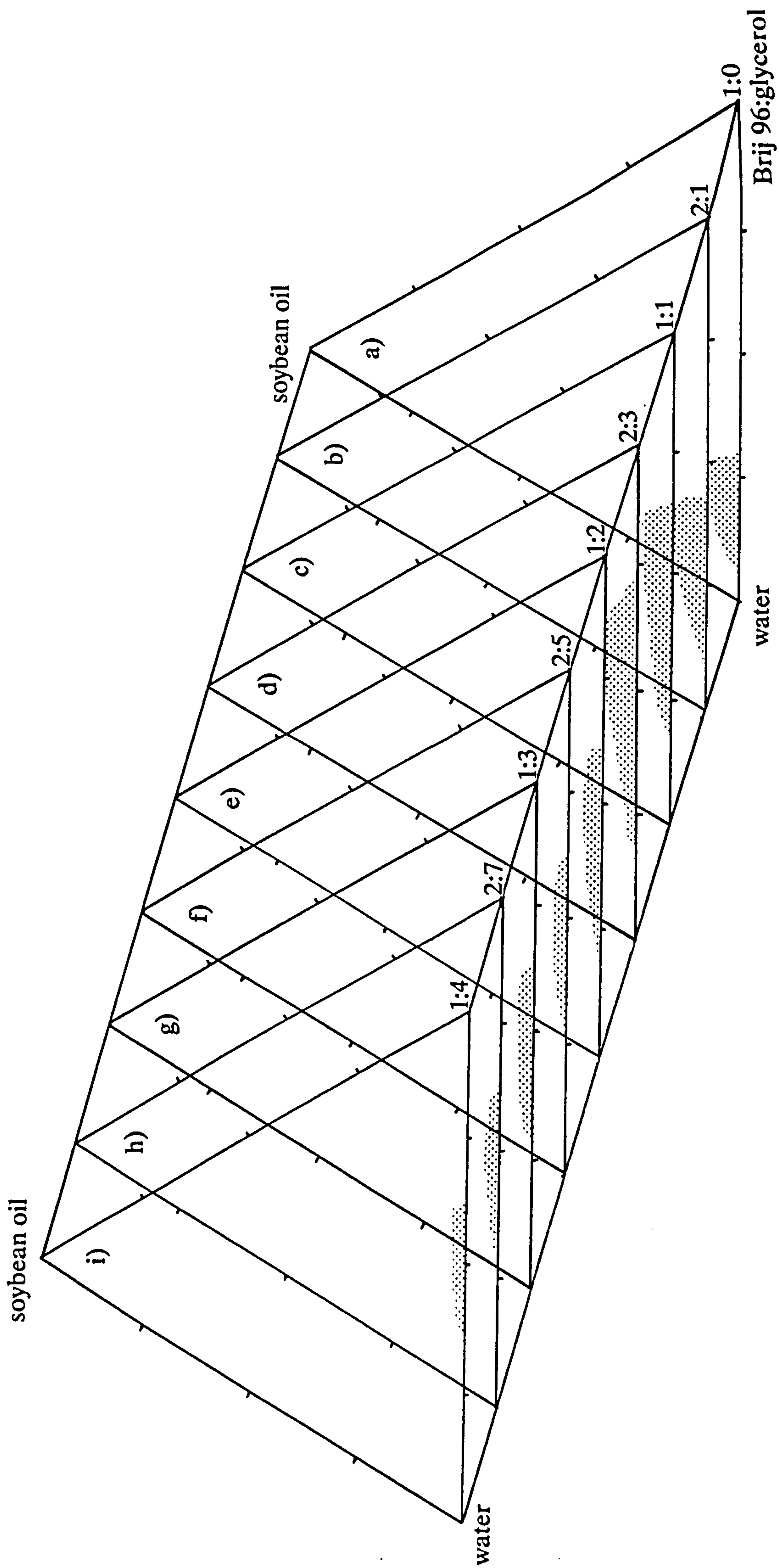


Figure 5.12: Triangular phase diagrams showing the change in microemulsion area of existence with changing weight ratio of Brij 96:glycerol; a)1:0, b)2:1, c)1:1, d)2:3, e)1:2, f)2:5, g)1:3, h)2:7 and i)1:4.

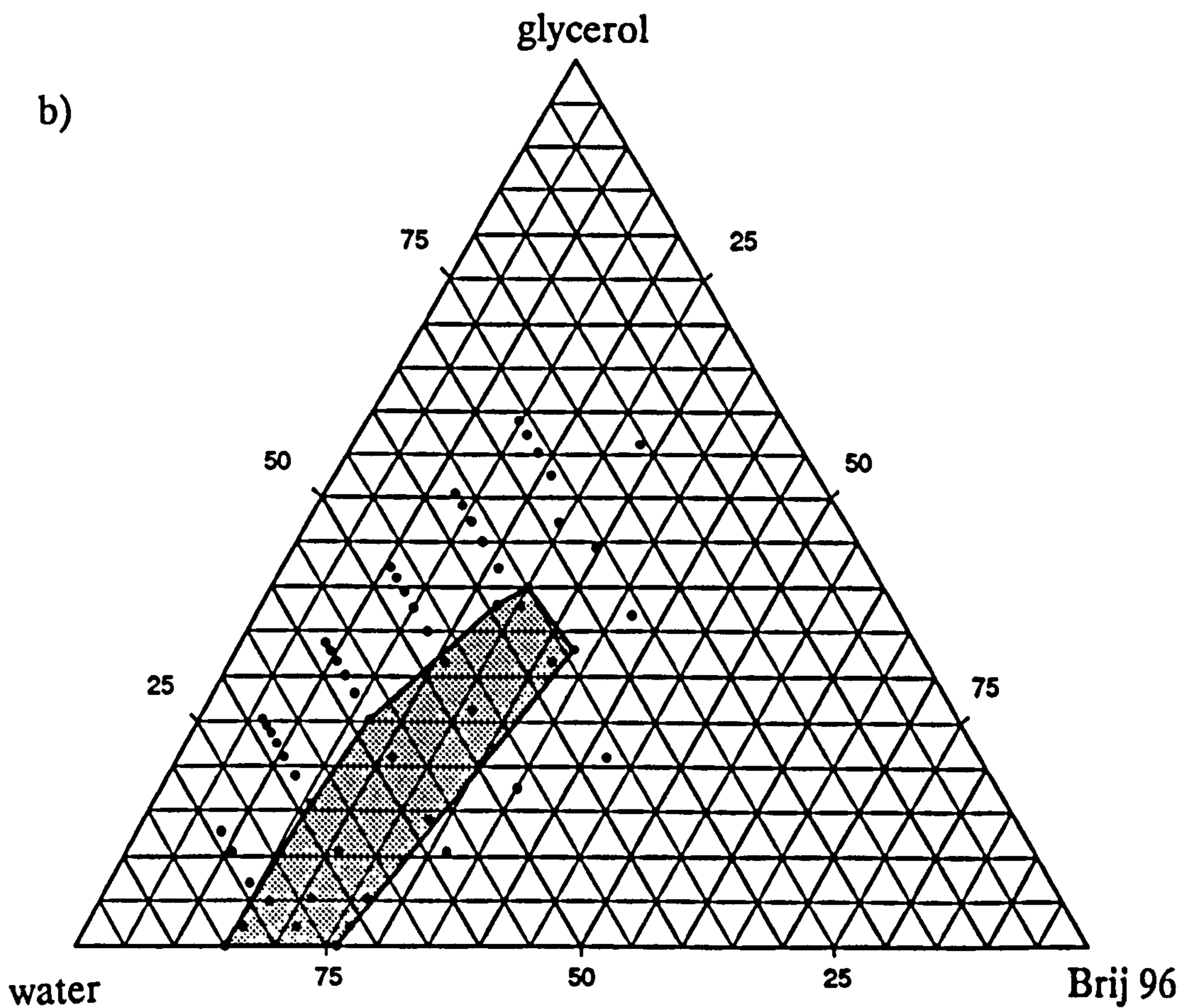
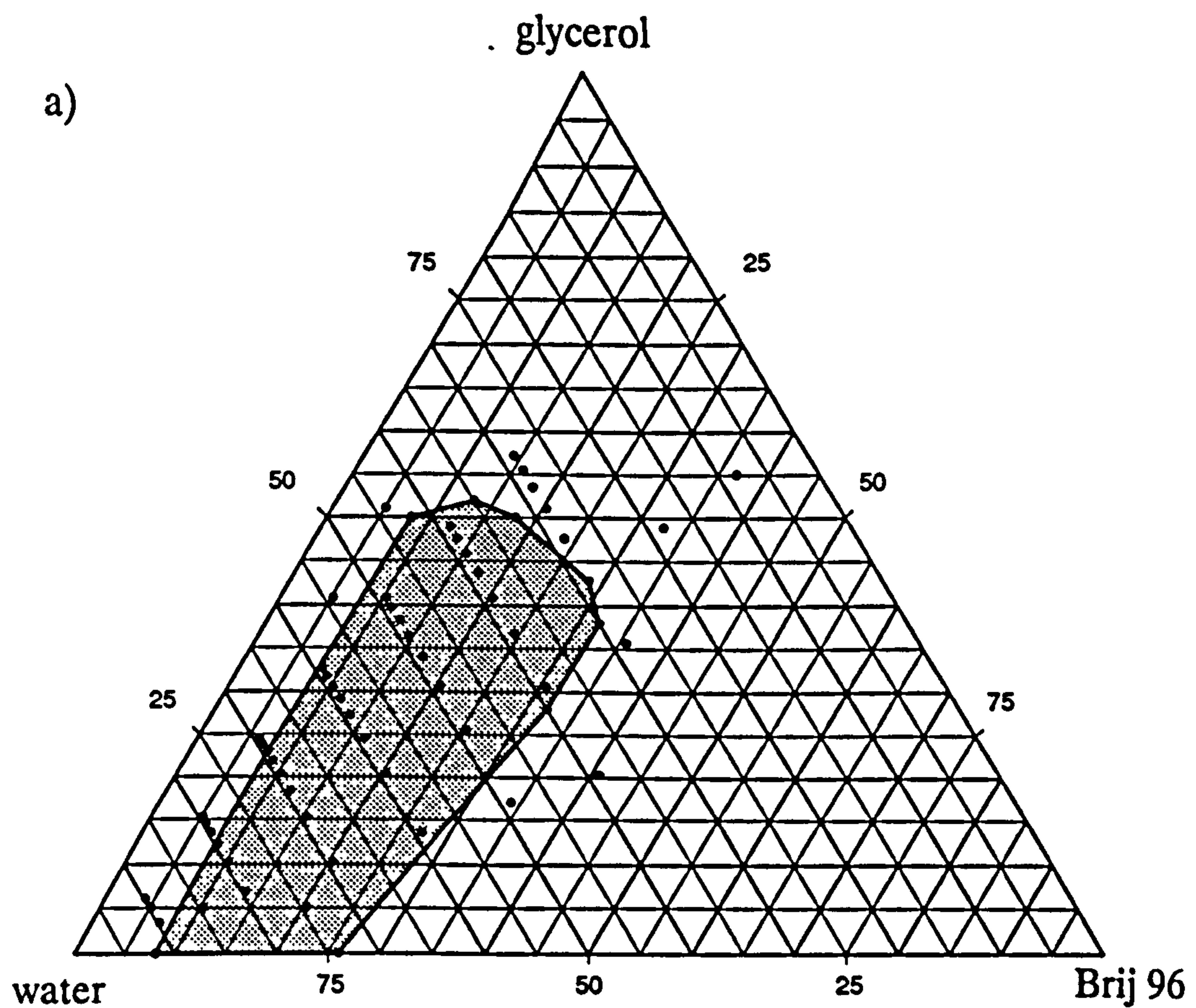


Figure 5.13: Pseudo-ternary phase diagrams showing the area of existence of microemulsion systems containing Brij 96/glycerol/water and a) 2 %w/w soybean oil, and b) 5 %w/w soybean oil.

The above situation was also reflected in the microemulsion regions containing 2 and 5 %w/w soybean oil in the presence of glycerol shown in figure 5.12. The microemulsion area formed a band, extending from the Brij 96-water axis. Microemulsion formation was generally observed within the same Brij 96 concentrations as in the systems without glycerol, but ceased after about 50 %w/w and 35 %w/w glycerol in systems containing 2 and 5 %w/w soybean oil respectively.

The implication of these results is that the glycerol does not appear to be acting as a cosurfactant at all. It did not increase the amount of soybean oil that could be incorporated, or extend the range of Brij 96 concentrations over which the microemulsions formed. On the other hand, fairly high concentrations of glycerol were tolerated without any detrimental effect on microemulsion formation.

The results described above for the addition of glycerol to soybean oil/Brij 96/water systems were essentially the same for systems in which the polyol added was either xylitol (fig.5.14 and 5.15) or sorbitol (fig.5.16 and 5.17), particularly at lower polyol and Brij 96 concentrations. For example, at a Brij 96:xylitol weight ratio of 2:1 the maximum soybean oil incorporation remained the same as in the polyol-free systems, and microemulsion formation again occurred with surfactant:glycol concentrations between 12 and 42 %w/w. With higher proportions of xylitol in the combined surfactant however (for example with a combined surfactant of 2:3 Brij 96:xylitol) the area of microemulsion existence which was found did not extend as far along the water/surfactant axis, towards the combined surfactant apex, as when glycerol was employed. Although the inhibitory nature of xylitol on microemulsion formation may therefore be slightly greater than that of glycerol (particularly at higher Brij 96 concentrations) figure 5.15 however shows that xylitol concentrations of up to 35 %w/w were tolerated by systems containing 5 % oil, and 46 %w/w xylitol in systems with 2 %w/w soybean oil.

When sorbitol was added, the areas of existence found closely resembled those of the xylitol-containing systems. It did however appear that of the three polyol systems, the larger sorbitol was tolerated least. Figure 5.17 shows that the maximum tolerated sorbitol concentration before microemulsions ceased to form was found to be 34 %w/w in 2 %w/w soybean oil systems

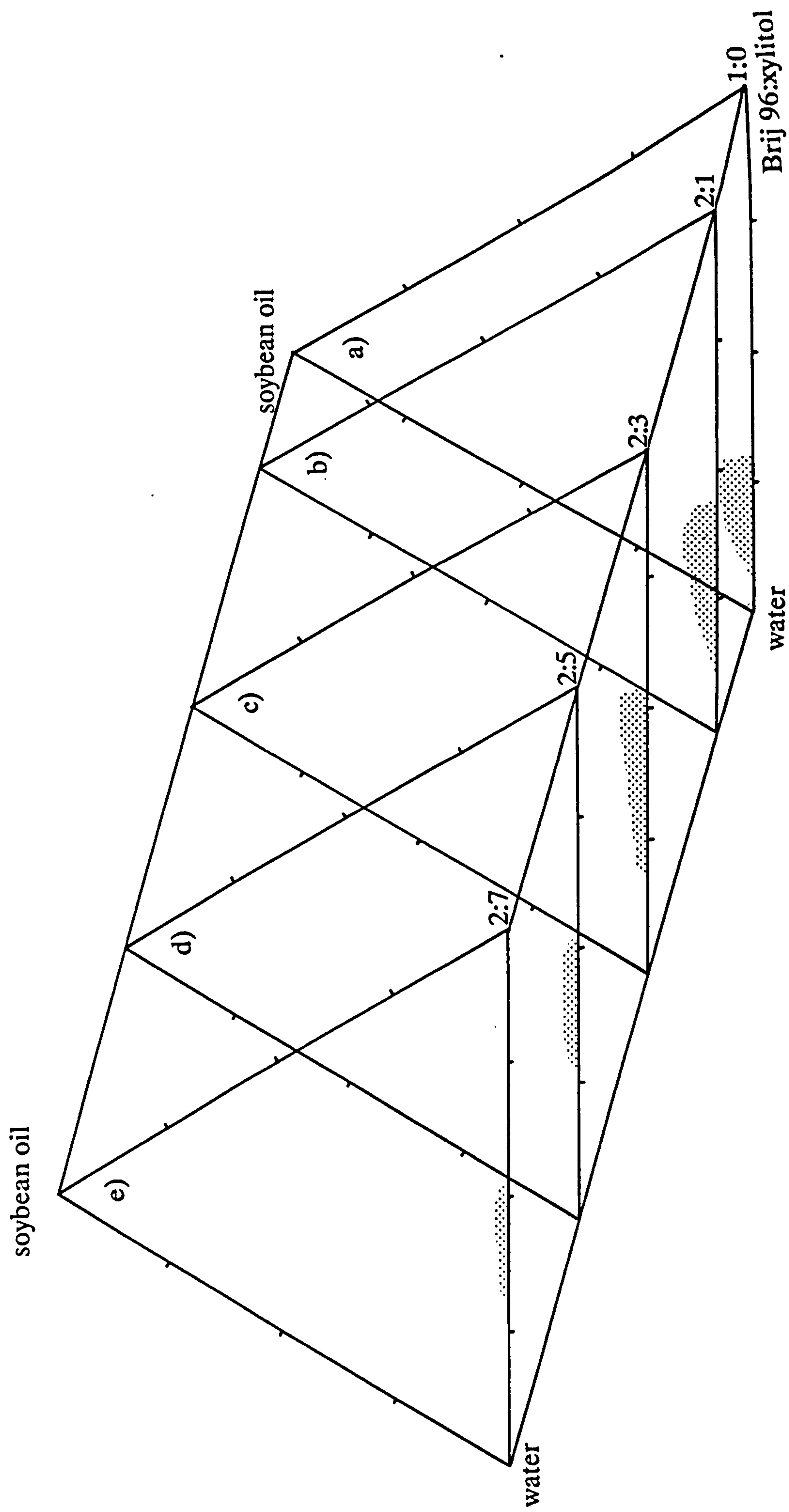


Figure 5.14: Triangular phase diagrams showing the change of microemulsion area of existence with changing weight ratio of Brij 96:xylitol; a) 1:0, b) 2:1, c) 2:3, d) 2:5 and e) 2:7.

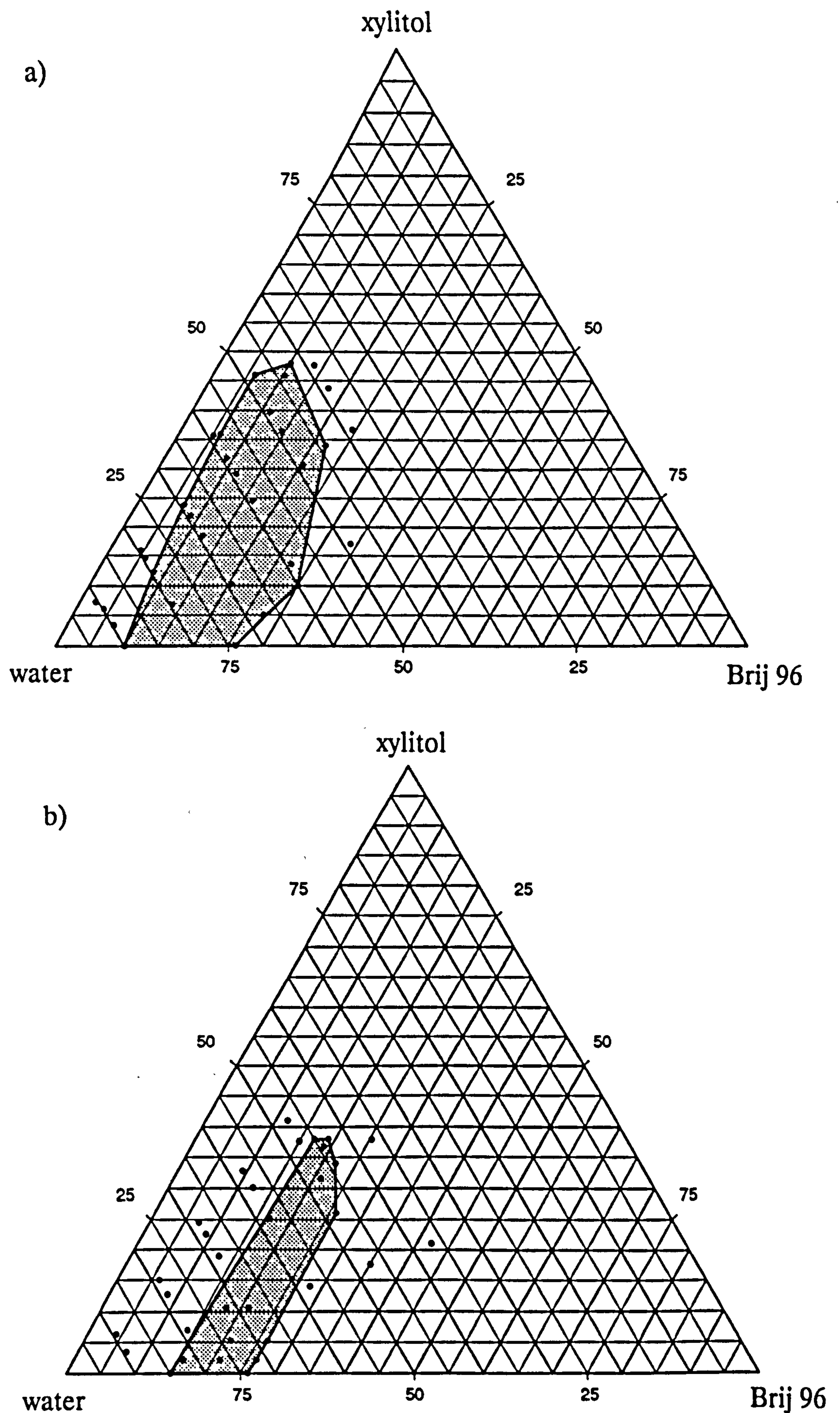


Figure 5.15: Pseudo-ternary phase diagrams showing the area of existence of microemulsion systems containing Brij 96/xylitol/water and a) 2 %w/w soybean oil, and b) 5 %w/w soybean oil.

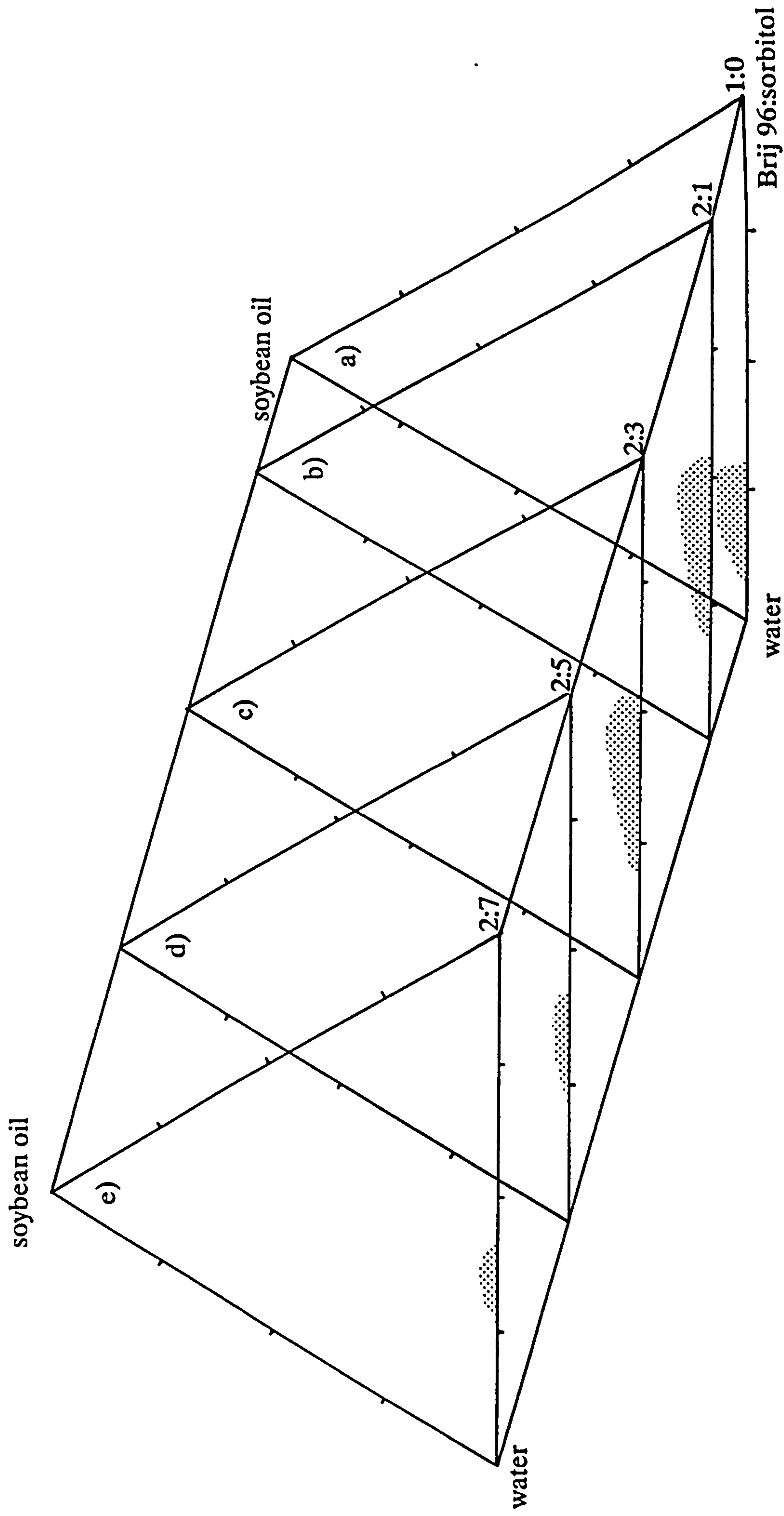


Figure 5.16: Triangular phase diagrams showing the change of microemulsion area of existence with changing weight ratio of Brij 96:sorbitol; a) 1:0, b) 2:1, c) 2:3, d) 2:5 and e) 2:7.

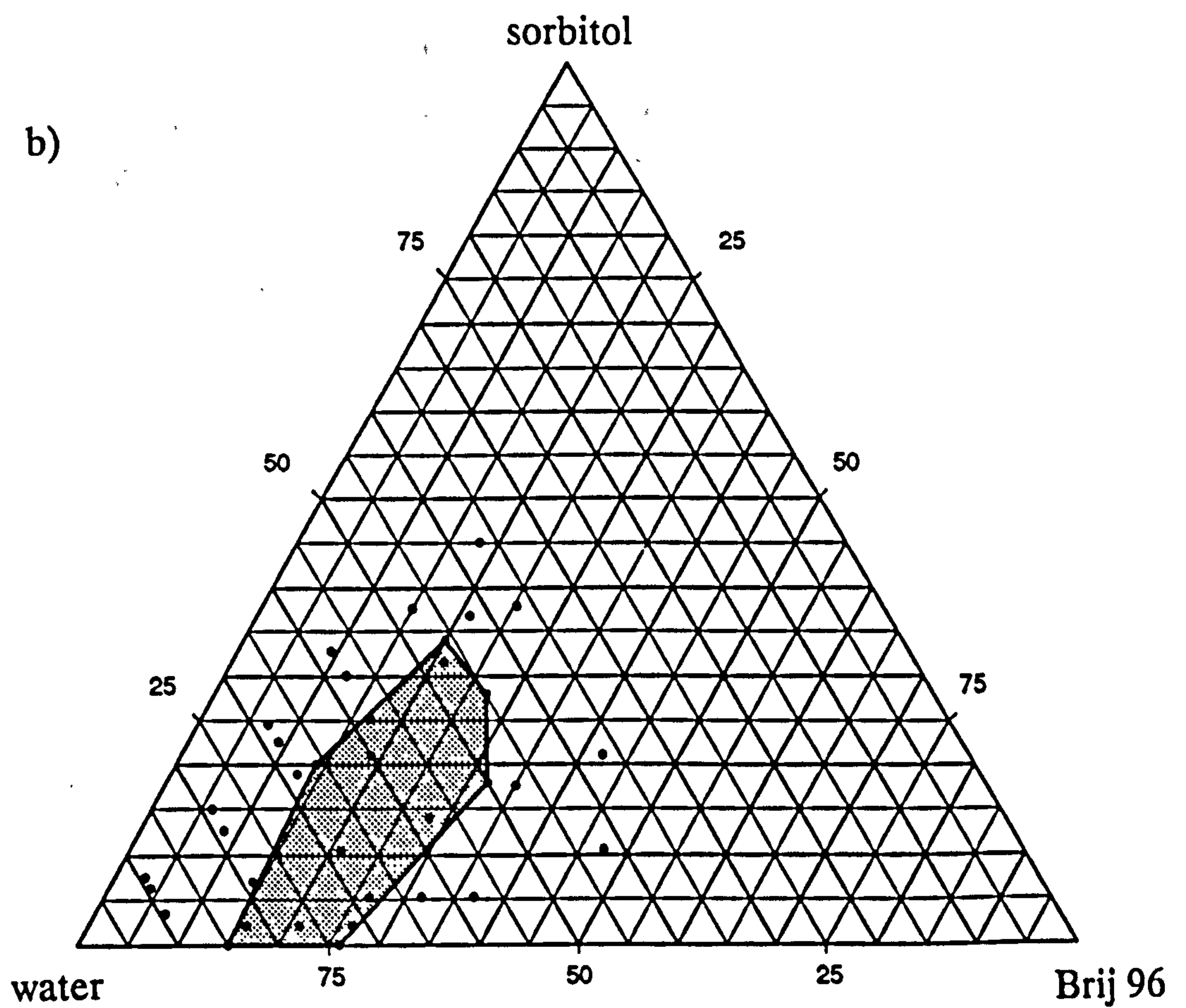
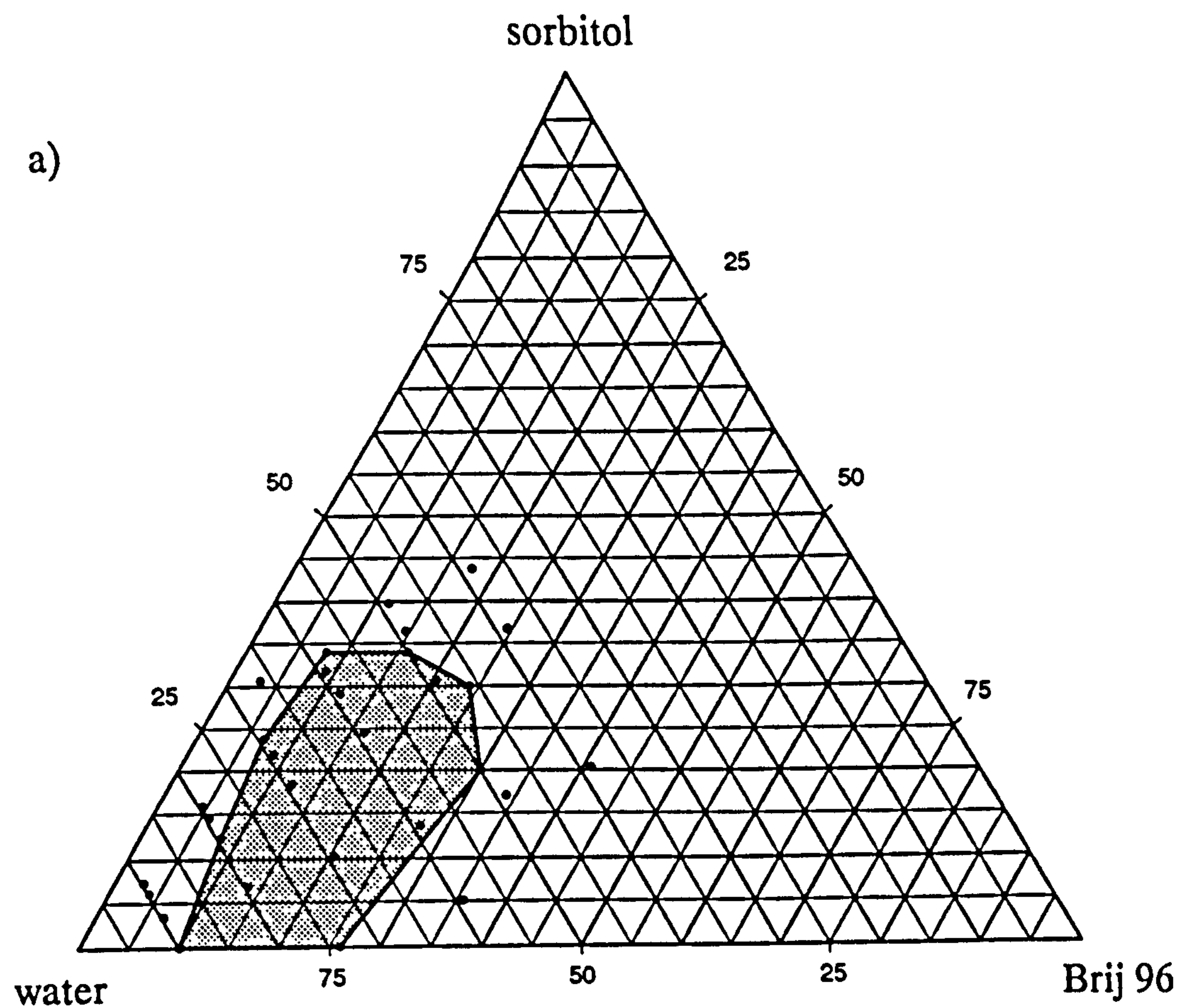


Figure 5.17: Pseudo-ternary phase diagrams showing the area of existence of microemulsion systems containing Brij 96/sorbitol/water and a) 2%w/w soybean oil, and b) 5 %w/w soybean oil.

(compared to 50 % found with glycerol and 46 % for xylitol) and 32 %w/w in 5 %w/w soybean oil microemulsions (compared to 35 %w/w for the other two polyols).

5.2.2 Changes in interfacial tension with the addition of glycerol

As with butanol and pentanol (5.1.4) the effect of added glycerol on the interfacial tension between soybean oil and Brij 96 solutions was determined. The interfacial tension between an oil phase (dodecane) and glycerol has been reported to be lower than that between dodecane and water [325]. Hence it might be expected that the presence of glycerol in the soybean oil/Brij 96/water system may contribute to further lowering of the interfacial tension.

Using the du Nuoy ring technique, at room temperature, the interfacial tension found in a system containing 10 %w/w glycerol and 10 %w/w Brij 96 (3.6 mNm^{-1}) was the same as the tension previously determined between soybean oil and 10 %w/w Brij 96 alone (5.1.4). This compares with a value of 1.7 mNm^{-1} when 10 %w/w 1-butanol was added to the soybean oil. Results obtained using the spinning drop tensiometer comparing interfacial tensions between soybean oil and 20 %w/w Brij 96 and 20 %w/w Brij 96 aqueous solutions containing either 10 or 20 %w/w glycerol, between 30 and 60°C, are shown in table 5.2. Although at higher temperatures there appears to be some small reduction in the interfacial tension values obtained when 20 %w/w glycerol was present, none of the tensions approached values in the order of 10^{-1} mNm^{-1} which had been seen when the straight-chained alcohols were added (table 5.1).

5.5.3 The effect of polyols on the phase inversion temperature

The effect of the three polyols on the cloud point of Brij 96 solutions and the PIT of microemulsions containing 2 %w/w soybean oil was studied. A decrease in the CP was seen with all three polyols. The degree of depression was concentration dependent, and for the same concentration of polyol; glycerol had the least, and sorbitol the greatest, cloud point-lowering effect. Published results also confirm that sorbitol [326, 327] and glycerol [328]

Table 5.2: Interfacial tension (mNm^{-1}) between soybean oil and aqueous solutions of 20 %w/w Brij 96 and 0, 10 and 20 %w/w glycerol at varying temperatures (mean \pm SD).

Temperature (°C)	Interfacial tension \pm SD (mNm^{-1})		
	20 %w/w Brij 96	20 %w/w Brij 96 with	
		10 %w/w glycerol	20 %w/w glycerol
30	3.13 \pm 0.08	2.7 \pm 0.2	3.2 \pm 0.1
40	3.02 \pm 0.07	2.6 \pm 0.1	2.3 \pm 0.3
50	2.2 \pm 0.1	2.3 \pm 0.3	2.0 \pm 0.1
60	1.85 \pm 0.08	1.8 \pm 0.1	1.3 \pm 0.2

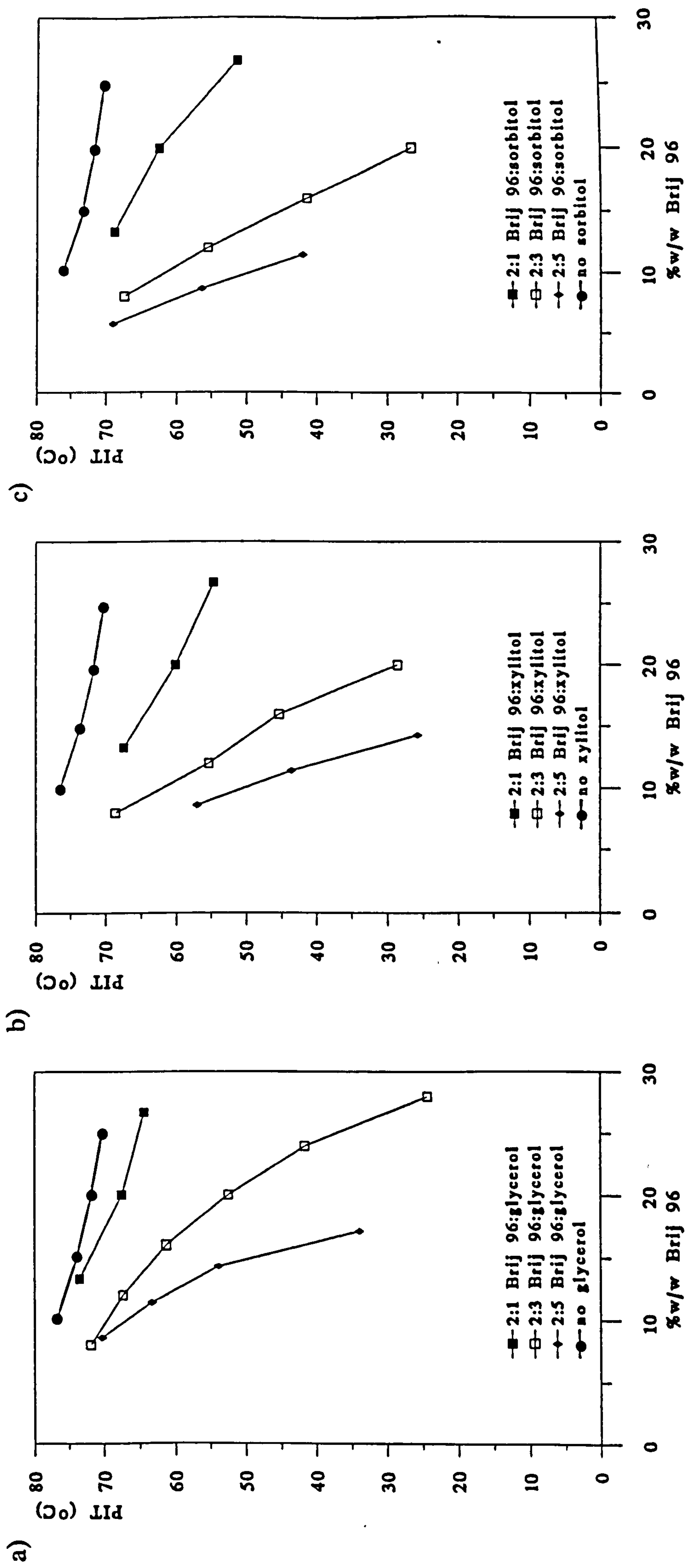


Figure 5.18: Phase inversion temperature for 2 %w/w soybean oil microemulsions with increasing Brij 96 concentration and the addition of the polyols; a) glycerol, b) xylitol and c) sorbitol.

reduce the CP of micellar systems of other ethylene oxide surfactants compared to that of water. Although glycerol has been reported to both increase and decrease the CP of an aqueous solution of nonionic surfactant, depending on the ethylene oxide chain length of the surfactant [329].

The three polyols were also found to reduce the PIT of 2 %w/w soybean oil microemulsion systems compared to that of 3-component microemulsions containing the same concentration of oil and Brij 96. Figure 5.18a-c shows the observed PITs against the Brij 96 content for systems with increasing amounts of glycol in the combined surfactant. It can be seen that greater reduction of PIT was found with increasing glycol content.

Figure 5.19 compares the effect of the three glycols, when a fixed Brij 96:glycol ratio of 2:3 was employed. It can be seen that of the three polyols considered, the depression in PIT was least for the trihydric glycol; glycerol. The PIT for systems containing xylitol and sorbitol were very similar to each other, but significantly lower than those containing glycerol. The varying degrees of PIT depression may help to explain the differences in the area of existence for the polyol systems. The differences in area were most marked at high surfactant and high polyol concentrations. The observed depression of PIT was also greatest at high surfactant and polyol concentrations and, particularly for systems containing one of the two larger polyols, the PIT may have been lower than room temperature. For example, with a Brij 96:glycol ratio of 2:3 (fig.5.19), the PITs for systems containing 50 %w/w combined surfactant (20 %w/w Brij 96) were 52.4, 28.6 and 26.6°C for glycerol, xylitol and sorbitol samples respectively. Microemulsions with higher concentrations of the combined surfactant could not be produced for the two larger polyols. Glycerol-containing microemulsions were however still produced up to a mixed surfactant concentration of 70 %w/w (28 %w/w Brij 96), at which composition a PIT of 24.3°C was recorded. No further glycerol microemulsion systems, with any higher concentration of the combined surfactant, could be encouraged to form at room temperature.

The results found for microemulsion systems containing the polyols; glycerol, xylitol and sorbitol indicate that these three polyols do not appear to function as cosurfactants when added to soybean oil/Brij 96/water microemulsion systems. They do not increase the maximum soybean oil incorporation, or the range of Brij 96 concentrations within which microemulsion formation is

possible. In addition, glycerol was found to have little effect in lowering the interfacial tension between the oil and aqueous phases. These water-soluble polyols do however have a lowering effect on the PIT of the microemulsion systems, and it appears that their presence at room temperature is tolerated until the point at which the PIT is lowered below that of ambient conditions.

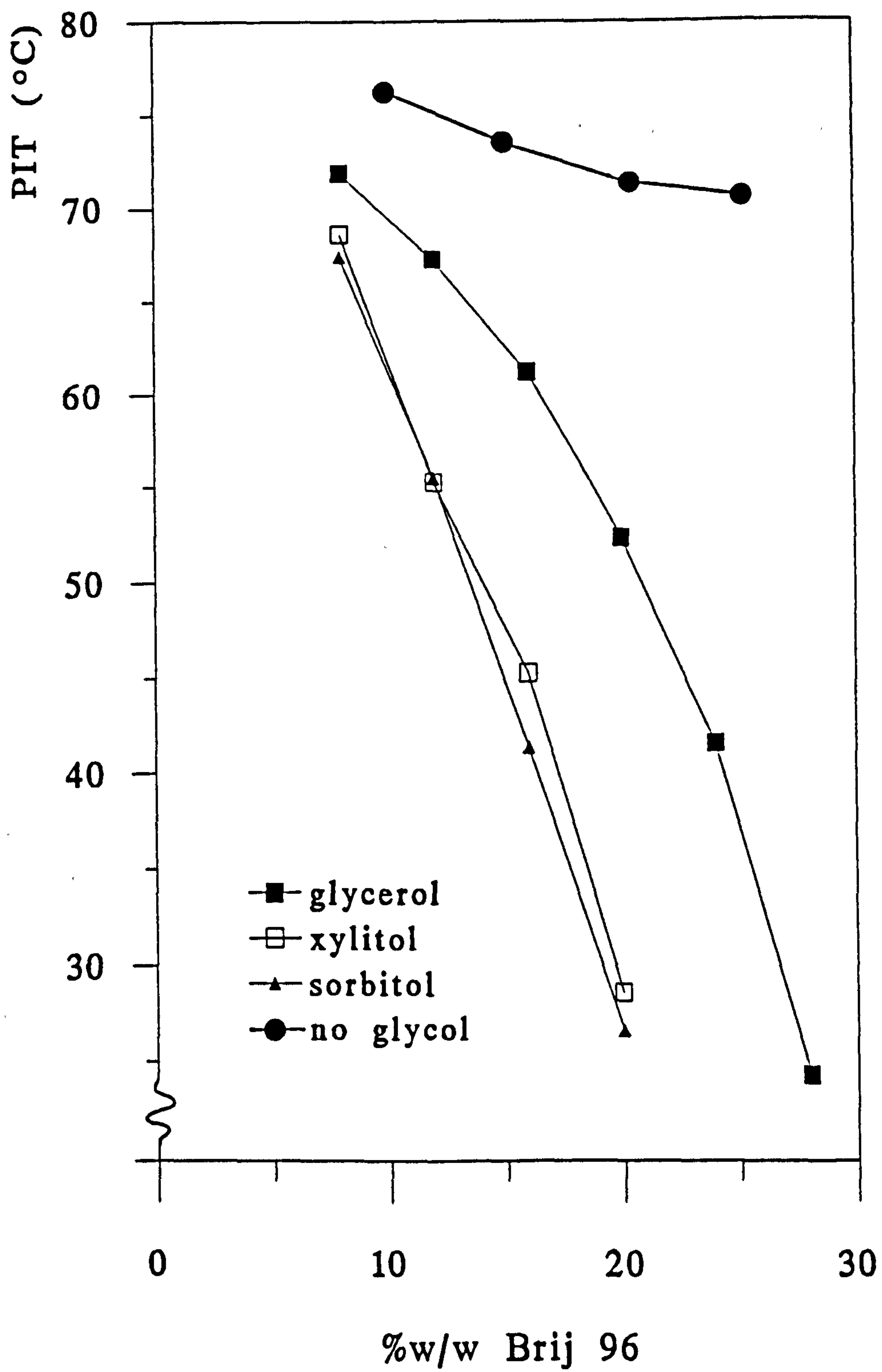


Figure 5.19: Phase inversion temperature as a function of Brij 96 concentration for 2 %w/w soybean oil microemulsions containing no added glycol, or a ratio of 2:3 Brij 96:glycol.

CHAPTER SIX: Drug incorporation into Brij 96 microemulsion systems

6.1 The incorporation of diazepam

Diazepam was selected as an example of a drug, which as a result of its poor water solubility, is difficult to formulate into an aqueous based dosage form suitable for intravenous delivery. Thrombophlebitis is a common side effect experienced with the administration of diazepam. It has been proposed that this local inflammatory response may be due to precipitation of the drug itself, if administration is too rapid [330, 331], and/or the formulation additives included to increase drug solubility such as propylene glycol, ethanol and benzyl alcohol [332].

In order to remove the need for these solubility enhancing additives, and hence reduce their painful side effects, a number of formulation alternatives have been investigated. Alternative drug delivery systems have included the use of cremophor [333], sodium salicylate solutions [334], solutions of various bile salts [335], both mixed micellar and liquid crystalline phases produced using a combination of sodium cholate and lecithin [335], vesicles of mixed short and long chained lecithins [336] and o/w soybean oil emulsions similar to Intralipid® [332, 337, 338, 339].

In this study the level of incorporation of diazepam ($\log P = 3.18$) was compared in surfactant solutions of Brij 96 and in o/w microemulsion systems consisting of 2 %w/w soybean oil or Miglyol 812 with varying concentrations of Brij 96. The possible site(s) of drug incorporation were also investigated.

6.1.1 Comparison between micellar and microemulsion incorporation

The results, given in table 6.1, showed an increase in diazepam incorporation (at 25°C) with increasing Brij 96 concentration, for micellar solutions and microemulsions produced with Brij 96 and 2 %w/w of either soybean oil or Miglyol 812. The solubility of diazepam found in triple distilled water was 0.0055 %w/w, which compares well with that of approximately 0.005 %w/v at room temperature quoted by MacDonald *et al* [340]. The experimentally determined solubility of the drug in soybean oil and Miglyol 812 was 1.3 and 2.2 %w/v respectively.

When an unpaired t-test was applied to the results; the increase in solubility between 2 %w/w soybean oil microemulsions and micellar systems of the same surfactant concentration was significant ($P=0.05$) at levels of 10, 15 and 20 %w/w Brij 96. The increase in diazepam incorporation in 2 %w/w Miglyol 812 microemulsions, compared to micellar systems, was significant at both surfactant concentrations compared (15 and 20 %w/w Brij 96). Although the mean values found for diazepam incorporation into microemulsions containing 2 %w/w Miglyol 812 were greater in systems with 15 and 20% Brij 96 than the equivalent microemulsion containing soybean oil, the differences were not significant at the three concentrations of Brij 96 (15, 20 and 25 %w/w) examined.

It therefore appears that the presence of 2% oil (either soybean oil or Miglyol 812) was sufficient to allow a small, but significant, improvement in the diazepam carrying capacity of microemulsion systems over micelles of the same surfactant concentration. The difference in solubility of the drug in the two oil phases was, however, insufficient to show a significant improvement in the drug carrying capacity of the 2 %w/w o/w microemulsion systems containing Miglyol 812 compared to those with 2 %w/w soybean oil.

6.1.2 Possible sites of incorporation

Possible sites of diazepam incorporation within the three systems were considered based on the model of an o/w microemulsion droplet proposed in figure 3.3. Due to the low water solubility of diazepam, the amount dissolved in the external aqueous phase will be small. Consequently, most diazepam

Table 6.1: Incorporation of diazepam into Brij 96 micelles and microemulsions containing 2 %w/w soybean oil or Miglyol 812 at 25°C.

%w/w Brij 96	%w/v diazepam incorporation		
	Micellar system	Microemulsion with 2 %w/w oil	
		soybean oil	Miglyol 812
0	0.0055 ± 0.0008	—	—
5	0.185 ± 0.009	—	—
10	0.37 ± 0.01	0.44 ± 0.01*	—
15	0.55 ± 0.02	0.62 ± 0.02*	0.68 ± 0.09*
20	0.68 ± 0.04	0.76 ± 0.07*	0.84 ± 0.09*
25	—	0.93 ± 0.11	0.93 ± 0.05

* indicates a significant difference (P = 0.05) between microemulsion and micellar systems.

incorporation is expected within the micellar or microemulsion droplets. However, the droplets themselves may be divided into regions of varying polarity. The nonionic micelles formed by Brij 96 would be expected to consist of a liquid hydrocarbon core surrounded by a mantle of polyoxyethylene chains. In the region closest to the core, the mantle is most likely to consist of pure polyethylene oxide. As the distance from the core increases, so does the hydration of the polyoxyethylene chains [341]. In a microemulsion droplet an oil core (soybean oil or Miglyol 812) is also present. It is anticipated that this oil core will then be surrounded by the oleyl hydrocarbon of the surfactant molecules, and finally by a mantle of ethylene oxide chains.

Table 6.2 shows the solubility of diazepam found in the two oil phases used; 1-octadecene and dimethoxytetraethylene glycol (DMTG). 1-Octadecene is a limited model chosen to represent the oleyl (9-octadecene) region which forms the central core of the micelle and the hydrocarbon region, immediately surrounding the oil, in microemulsion droplets. Diazepam exhibited only low solubility (0.2 %w/w) in this hydrocarbon.

The solubility of diazepam in DMTG and DMTG/water mixtures was undertaken in an attempt to model drug solubility in the hydrated polyoxyethylene layer of the micelle or microemulsion droplet. Pure DMTG was chosen to represent the local environment of dehydrated polyoxyethylene [342] closest to the hydrocarbon core. The lower DMTG concentrations represent increasing hydration of the polyoxyethylene as the distance from the core increases. It can be seen (fig.6.1) that diazepam showed an exponential increase in solubility with increasing DMTG. A similar trend has been previously observed for other poorly water soluble drugs [343, 344].

The combined results of these solubility investigations therefore indicate that in both micellar and microemulsion systems, most of the diazepam would be expected to dissolve in the dehydrated polyoxyethylene chains of the Brij 96. A small proportion will be present in the hydrocarbon portion of the surfactant (which constitutes the core of a micelle and the outer hydrocarbon core of a microemulsion). In addition, with microemulsion systems, some diazepam is expected to dissolve in the central oil core of the droplet.

Hence the total amount of diazepam incorporated in micelles and both the

Table 6.2: Solubilities (%w/v) of diazepam at 25°C (mean ± SD).

Solvent	Mean solubility ± SD.
water	0.0055 ± 0.0008
soybean oil	1.3 ± 0.1
Miglyol 812	2.2 ± 0.08
DMTG	12.9 ± 0.5
1-octadecene	0.2 ± 0.008

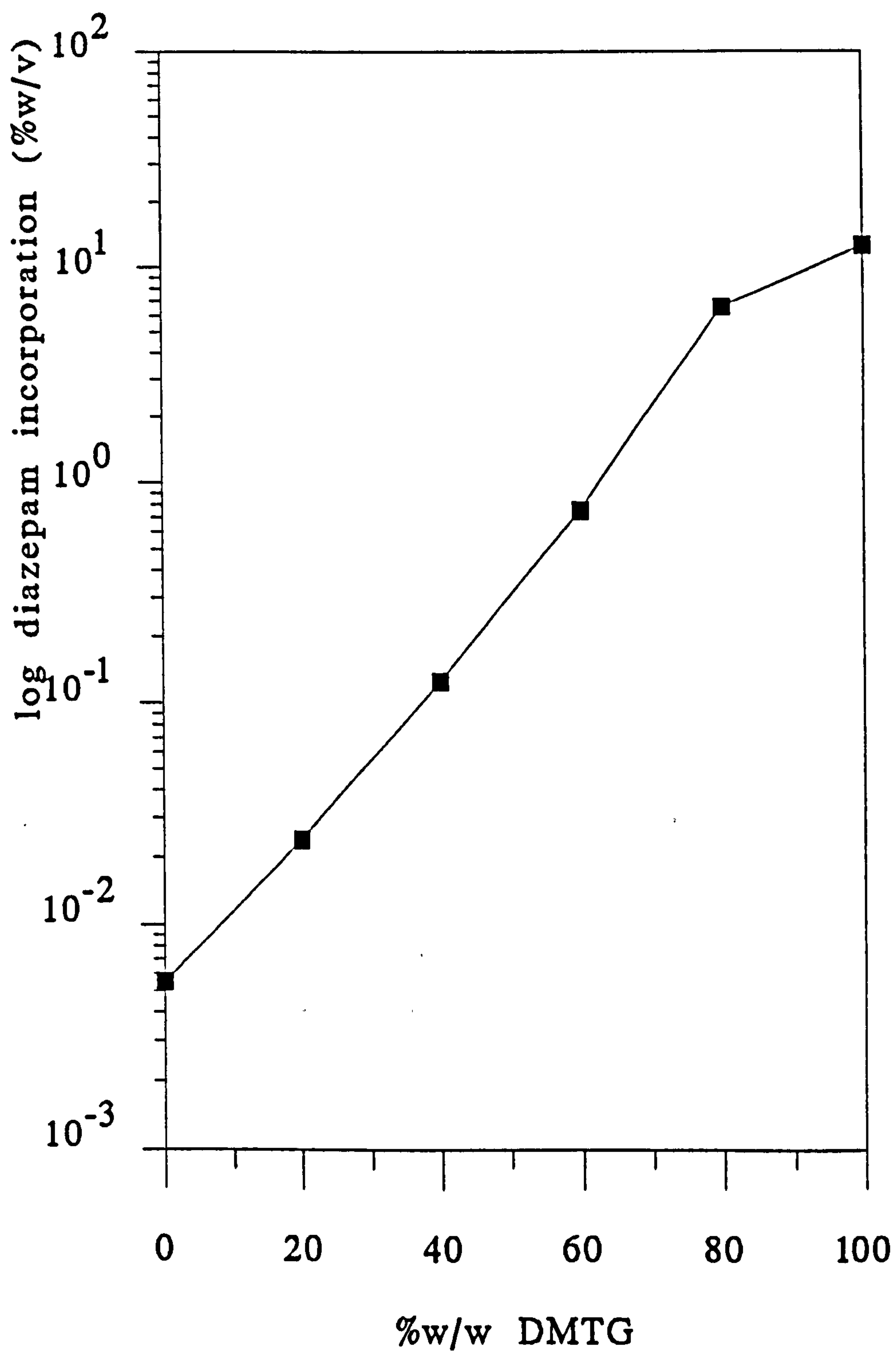


Figure 6.1: Log %w/v diazepam incorporation vs %w/w DMTG in DMTG/water mixtures.

soybean oil and Miglyol 812 microemulsion systems appears to be dominated by the Brij 96 content. Significant improvement of the diazepam carrying capabilities of an o/w microemulsion system over a micellar system of the same surfactant concentration could however be achieved, due to the presence of the 2 %w/w oil phase. Greater improvement in the capacity of a microemulsion to incorporate drug would be expected with increased solubility of the drug in the oil phase, however the difference in diazepam solubility in soybean oil and Miglyol 812 did not appear to be large enough to effect a significant change between the two microemulsion systems.

6.2 The incorporation of testosterone, testosterone propionate and testosterone enanthate

To further investigate the incorporation of drugs into microemulsion systems, a series of three poorly water soluble, structurally related steroids (testosterone, testosterone propionate and testosterone enanthate) of varying $\log P_{\text{oct}}$ (3.32, 4.78 and 6.90 respectively) was investigated. The level of incorporation into Brij 96 micellar and 3-component microemulsion systems were compared, and the effect of the drugs on the area of microemulsion existence, size and stability of the microemulsion droplets were considered.

6.2.1 Effect on the area of existence

The stability of 3-component o/w microemulsions produced from soybean oil, Brij 96 and water did not appear to be affected by the presence of the drugs. If the drug was present in excess of that which can be incorporated into the microemulsion, clear liquid systems were observed in equilibrium with excess drug.

A large number of samples of varying soybean oil and Brij 96 content (varied in increments of 2 %), which were within the o/w microemulsion region shown in figure 3.2, were produced with the addition of 0.2, 0.4 or 1 %w/w of each drug. The area of existence found containing completely clear systems, without excess drug, for all three steroids is shown in figure 6.2.

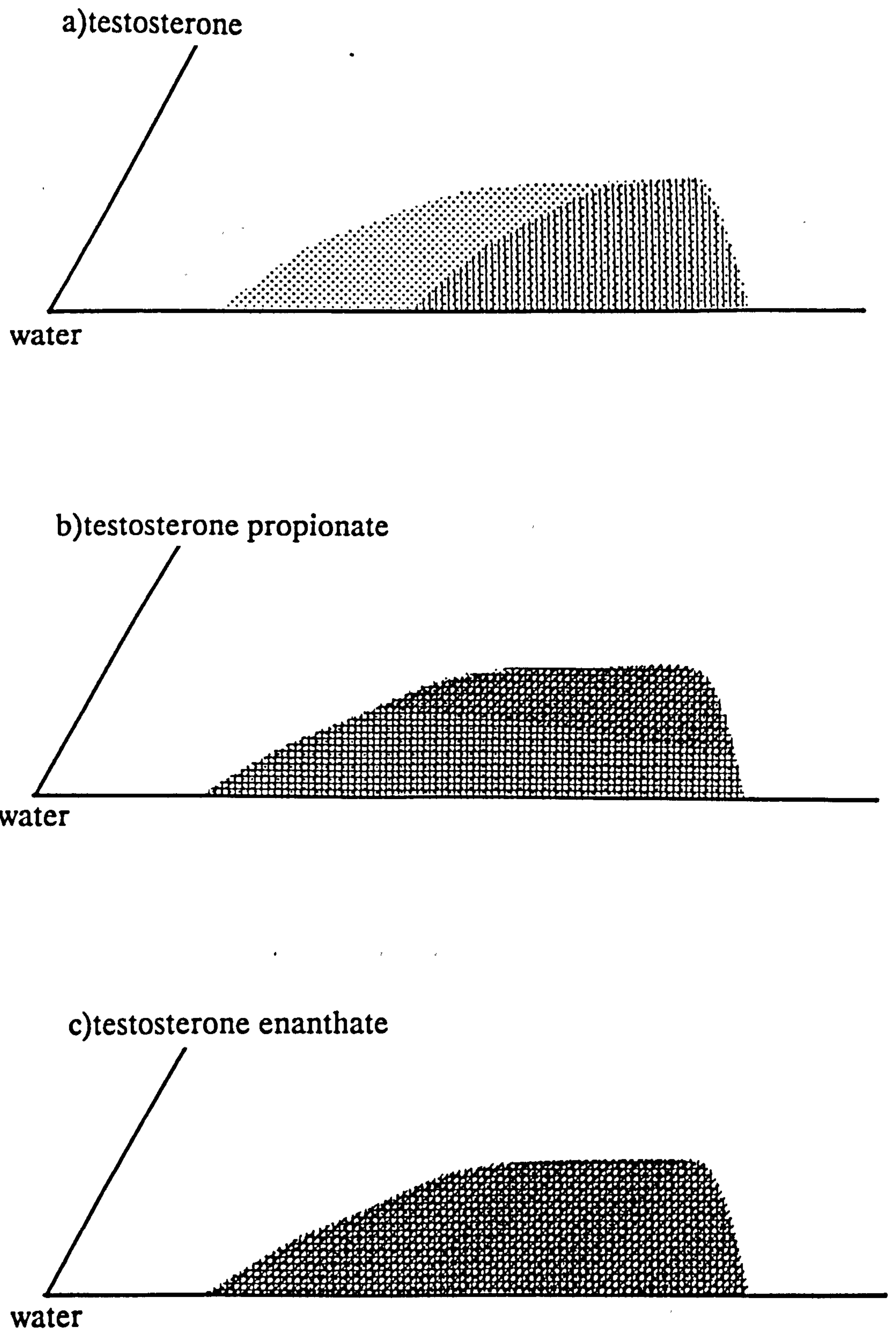


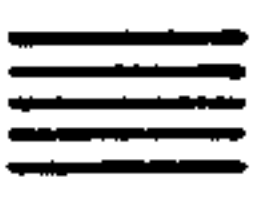



Figure 6.2: Partial triangular diagrams showing the area of existence of soybean oil/Brij 96/water microemulsions with no precipitate for systems containing a)testosterone, b)testosterone propionate, and c)testosterone enanthate.

Key:  no drug
 0.2 %w/w drug
 0.4 %w/w drug
 1 %w/w drug

It was not possible to completely incorporate 0.4 or 1 %w/w testosterone into any of the o/w microemulsion compositions. A lower concentration (0.2 %w/w) of testosterone could be included into many of the microemulsions within the area. The presence of 0.2 %w/w testosterone was however in excess of that which could be incorporated into those microemulsions with low surfactant/low oil concentrations, and consequently the area of existence for completely clear systems was reduced compared to systems without drug (fig.6.2a).

In comparison, 0.2 and 0.4 %w/w testosterone propionate could be incorporated without any visible change on the area of existence. However, as shown in figure 6.2b, 1 %w/w testosterone propionate could only be incorporated into those compositions with a higher oil component. At least 1 %w/w of the most lipophilic drug, testosterone enanthate, could be incorporated into each composition tested, resulting in clear drug-loaded microemulsions without the presence of excess drug (fig.6.2c). The PIT of ten compositions throughout the microemulsion area of existence, and containing 0.2, 0.4 or 1 %w/w testosterone enanthate were determined, and found in all cases to be lower than the equivalent drug-free composition. The reduction in PIT ranged from 0.5-13°C. The average decrease in PIT for the ten compositions were 4.7, 6.1 and 7.9°C for microemulsions containing 0.2, 0.4 and 1 %w/w testosterone enanthate respectively. The addition of 24% of the water-insoluble local anaesthetic, lidocaine, was similarly found to lower the PIT of bicontinuous microemulsions produced with IPM, water and 30% of a mixed surfactant containing 10:90 Tween 20:Tween 21, by approximately 10°C [345].

6.2.2 Comparison between micellar and 2% soybean oil microemulsion incorporation

The drug uptake in micellar solutions and 2 %w/w soybean oil microemulsions for the three steroids are given in table 6.3. In all cases drug incorporation increased with surfactant concentration. In addition the results show that there was a significant difference ($P=0.05$) in the amount of testosterone which could be incorporated in 10 %w/w Brij 96 micellar systems and a microemulsion system containing the equivalent surfactant concentration and 2 %w/w soybean oil. At higher surfactant concentrations

Table 6.3: Incorporation, at 25°C, of testosterone, testosterone propionate and testosterone enanthate into Brij 96 micelles and 2 %w/w soybean oil microemulsions (mean \pm SD).

Drug	%w/w Brij 96	%w/v Drug incorporation \pm SD	
		Micellar system	Microemulsion
testosterone	10	0.17 \pm 0.02	0.22 \pm 0.02*
	15	0.22 \pm 0.02	0.23 \pm 0.05
	20	0.31 \pm 0.02	0.30 \pm 0.02
testosterone	10	0.29 \pm 0.04	0.40 \pm 0.04*
propionate	15	0.35 \pm 0.07	0.53 \pm 0.06*
	20	0.45 \pm 0.1	0.66 \pm 0.08*
testosterone	10	3.5 \pm 0.4	5.7 \pm 0.3*
enantate	15	4.6 \pm 0.4	5.9 \pm 0.4*
	20	5.2 \pm 0.6	6.2 \pm 0.5*

* indicates a significant difference ($P = 0.05$) between microemulsion and micellar systems.

(15 and 20 %w/w) however there was no significant difference between the uptake of testosterone into microemulsions, compared to that of micellar systems of the same surfactant concentration. In comparison, there was a significant increase over the micellar solutions in the amount of testosterone propionate and testosterone enanthate found in the microemulsion systems at all three concentrations of Brij 96 tested. The increase in incorporation in the microemulsion systems, compared to the micelles, was greatest at lower surfactant concentrations.

As with diazepam, in order to try to explain these results the possible sites of drug incorporation were considered. The solubilities found at 25°C for the three test drugs in water, soybean oil, DMTG and 1-octadecene are given in table 6.4. The aqueous solubility decreases with increasing log P of the drug. This solubility is however small for all three drugs, and consequently most drug incorporation is again expected within the micelle or microemulsion droplet.

Conversely, the solubility of the three drugs in soybean oil, DMTG and 1-octadecene increases with increasing log P. In all three cases the highest solubility was found in pure DMTG. If however the ratio of the solubilities in DMTG to either soybean oil or 1-octadecene are considered the relative importance of the DMTG solubility is greatest for testosterone, and least for testosterone enanthate. For example, the ratio values obtained for the solubility in DMTG to solubility in 1-octadecene are 110, 7.9 and 1.6 for testosterone, testosterone propionate and testosterone enanthate respectively (table 6.4).

The determination of the solubilities of testosterone and its two esters in DMTG/water mixtures were also undertaken. All three drugs showed a significant increase in solubility with increasing DMTG, as illustrated in the graph of log %w/w drug incorporated vs %w/w DMTG (fig 6.3). At DMTG concentrations less than 80 %w/w, testosterone was found to have the greatest solubility and testosterone enanthate the least. In the more dehydrated samples however (< 20 %w/w water) the solubility of the drugs in the mixtures increases with increasing log P_{oct}.

Differences in the mechanism and location of solubilised steroid molecules in surfactant micelles have been reported to depend on the polarity of the drug

Table 6.4: Physicochemical properties and solubilities (%w/v) at 25°C of testosterone, testosterone propionate and testosterone enanthate (mean ± SD).

	testosterone	testosterone propionate	testosterone enantate
Mr	288.4	344.5	400.6
log Poct	3.35	4.78	6.90
Mean solubility ± SD in;			
water	0.0041 ± 0.0006	0.0009 ± 0.0002	0.00017 ± 0.0004
soybean oil	0.60 ± 0.06	3.4 ± 0.3	31.5 ± 2.1
DMTG	4.4 ± 0.006	12.0 ± 0.1	91.2 ± 4.9
1–octadecene	0.040 ± 0.009	1.51 ± 0.01	57.8 ± 3.3
Ratio of solubilities;			
DMTG / 1–octadecene	110	7.9	1.6
DMTG / soybean oil	7.3	3.5	2.9
soybean oil / 1–octadecene	15.0	2.3	0.55

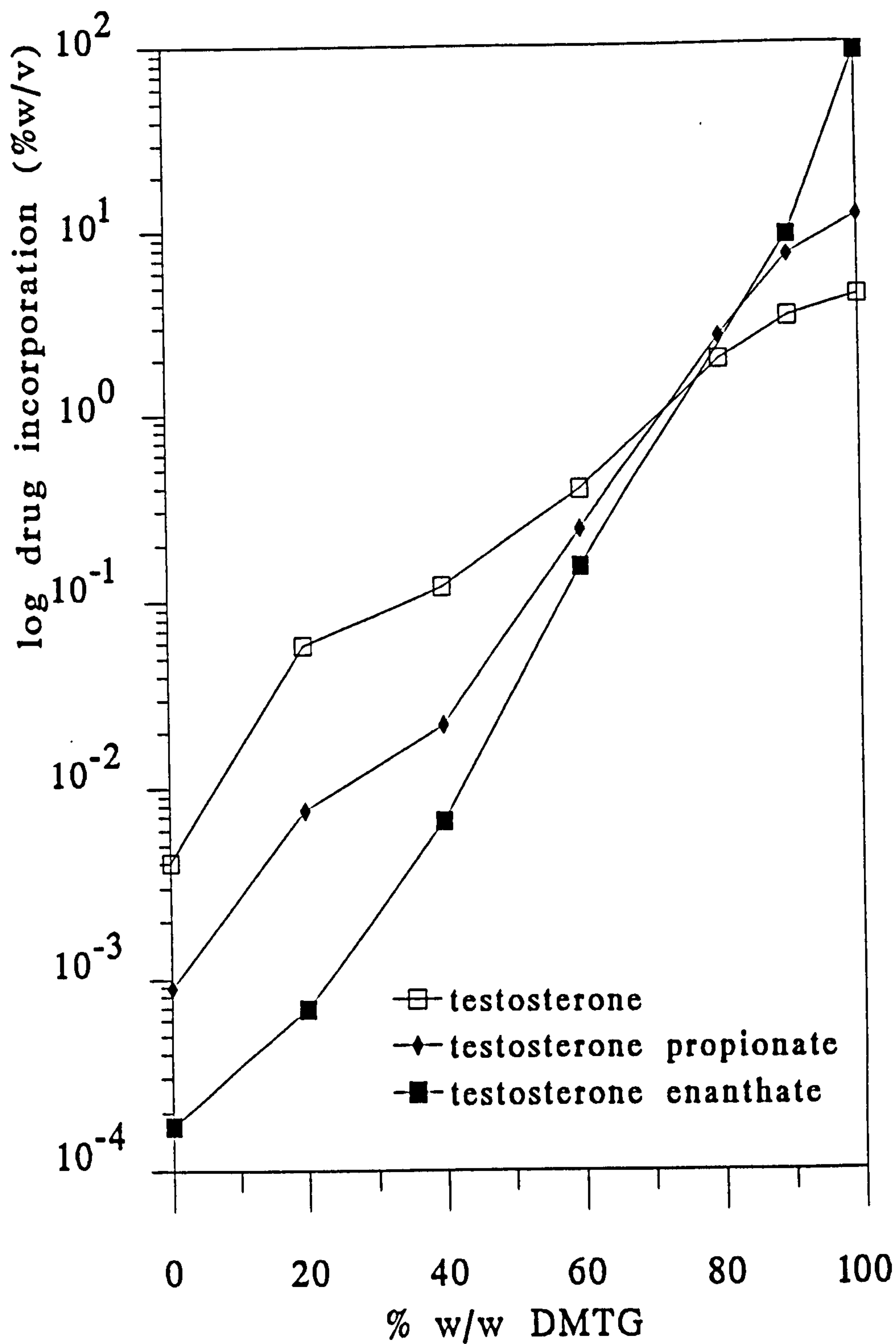


Figure 6.3: Log %w/v drug incorporated vs %w/w DMTG in DMTG/water mixtures, at 25°C, for testosterone, testosterone propionate and testosterone enanthate.

[346, 347]. It has been suggested that testosterone is more generally associated with the polyoxyethylene of an ethoxylated surfactant rather than the interior of the micelle [348, 349], and in particular in the more dehydrated region of the polyoxyethylene shell closest to the hydrocarbon core [350]. In this study, based on relative solubilities, it appeared that in Brij 96 micelles all three drugs are predominately solubilised into the dehydrated polyoxyethylene region of the hydrophilic chains. With increasing log P however an increasing proportion of the total solubilised drug would be expected within the oleyl hydrocarbon interior.

In microemulsion systems with 2 %w/w soybean oil present (forming an inner core of oil) the solubility of testosterone in the oil phase was insufficient to effect any significant increase in the drug loading capabilities of the microemulsion systems compared to that of surfactant solutions when either 15 or 20 %w/w Brij 96 was present in both systems. However when only 10 %w/w Brij 96 was present, the additional drug dissolved in the 2 %w/w soybean oil did make a significant difference to the drug loading capacities of the microemulsion compared to the micellar system. In contrast the solubility of testosterone propionate and testosterone enanthate in the soybean oil was large enough to allow a significant increase in the amount carried in the microemulsion, compared to the micellar systems, at all three concentrations of surfactant. The greatest improvement in drug incorporation was seen with testosterone enanthate, which has the largest log P_{Oct} , and the highest solubility in the soybean oil. It was however found that in those systems which exhibited an improvement in the drug carrying capacity, the increase was greater than that predicted based on the addition of the micellar solubilisation plus the amount of drug which will dissolve in the 2 %w/w soybean oil.

6.2.3 Testosterone propionate incorporation into o/w microemulsions produced with different oils

Testosterone propionate incorporation into Brij 96 o/w microemulsions containing 2 %w/w oil phase was further investigated with five other oils; heptane, 1-heptene, hexadecane, 1-hexadecene and Miglyol 812. The solubility of testosterone propionate found in each of the oil phases is given in table 6.5, and the resulting microemulsion incorporation with changing Brij 96

concentration in table 6.6. As found using soybean oil as the dispersed phase, incorporation of testosterone propionate increased in these microemulsion systems with increasing surfactant concentration up to 20 %w/w Brij 96. With all five oil phases, incorporation of the drug into microemulsions with a higher Brij 96 concentration (22.5 %w/w) was found to decrease. Possible changes in the structure of the microemulsion systems at higher surfactant concentrations may be responsible for this observation.

With microemulsion systems containing the four hydrocarbon oils, the improvement in drug incorporation over micellar systems was small. All resulted in lower levels of incorporation than those found in 2 %w/w soybean oil microemulsions of the same surfactant concentration. In contrast, microemulsions produced with 2 %w/w Miglyol 812 exhibited a much higher level of incorporation of the steroid drug compared to that found in the soybean oil microemulsions.

As observed with diazepam, the solubility of testosterone propionate was greater in the shorter triglyceride (Miglyol 812) than in soybean oil. Miglyol 812 still contains large triglyceride molecules and hence an o/w microemulsion droplet structure with a distinct oil core (fig.3.3) is predicted. The oil is therefore not expected to directly alter the drug incorporation into either the polyoxyethylene or hydrocarbon region of the surfactant, and the improvement in incorporation over soybean oil microemulsions is expected to be due solely to the increased solubility of the drug in the more polar oil.

With the hydrocarbon oil phases, the results indicate that the levels of incorporation in the o/w microemulsions formed are determined, not only by the solubility of the steroid in the oil phase, but may also be influenced by penetration of oil molecules into the surfactant interface.

The solubility of the drug in heptane was less than that found in soybean oil, and the levels of incorporation into microemulsions with 2 %w/w heptane, were lower than those found with soybean oil microemulsions of the same Brij 96 concentration. Heptane microemulsion incorporation of testosterone propionate was significantly higher than the equivalent micellar system at only one of the surfactant concentrations tested (17.5 %w/w Brij 96). In comparison, testosterone propionate showed a higher solubility in 1-heptene than in either heptane or soybean oil. However, in spite of the increased

Table 6.5: Solubilities (%w/v) of testosterone propionate in various oil phases at 25°C (mean \pm SD).

Oil	Mean solubility \pm SD.
heptane	0.92 \pm 0.01
1-heptene	4.3 \pm 0.1
hexadecane	1.0 \pm 0.1
1-hexadecene	1.7 \pm 0.1
Miglyol 812	6.2 \pm 0.4
soybean oil	3.4 \pm 0.3
DMTG	12.0 \pm 0.1
1-octadecene	1.51 \pm 0.01

Table 6.6: Incorporation of testosterone propionate, at 25°C, into Brij 96 micelles and microemulsions containing 2 %w/w of various oil phases (mean \pm SD).

%w/v testosterone propionate incorporation at 25°C							
%w/w Brij 96	Micellar systems	Microemulsion systems with 2 %w/w oil					
		heptane	1—heptene	hexadecane	1—hexadecene	soybean oil	Miglyol 812
10	0.29 ± 0.04	—	—	—	—	0.40 ± 0.04*	0.50 ± 0.05*
15	0.35 ± 0.07	0.35 ± 0.03	0.40 ± 0.02	0.43 ± 0.01*	0.39 ± 0.02	0.53 ± 0.06*	1.1 ± 0.3*
17.5	0.40 ± 0.02	0.45 ± 0.02*	0.44 ± 0.06	0.46 ± 0.02*	0.43 ± 0.01*	—	1.5 ± 0.2*
20	0.45 ± 0.1	0.48 ± 0.04	0.42 ± 0.02	0.52 ± 0.12	0.47 ± 0.04	0.66 ± 0.08*	1.3 ± 0.2*
22.5	0.49 ± 0.02	0.48 ± 0.03	0.41 ± 0.03*	0.49 ± 0.06	0.37 ± 0.02*	—	0.74 ± 0.02*

* indicates a significant difference (P = 0.05) between microemulsion and micellar systems.

solubility in the oil phase, microemulsion incorporation of the drug in the 1-heptene systems was lower than that found in the soybean oil systems. Furthermore, at 20 and 22.5 %w/w Brij 96 concentrations testosterone propionate uptake was significantly less ($P=0.05$) in 1-heptene compared to heptane-containing microemulsions.

A possible explanation for these observations is the likely penetration of the short-chained oils into the surfactant interface. Alkenes, which are more hydrophilic, are expected to penetrate to a greater extent than alkanes [293]. Although differing degrees of penetration of the oil phase into the surfactant interface did not appear to significantly alter the area of Brij 96 microemulsion existence (4.2.1.1), this penetration is expected to alter the sites available for solubilisation. In these Brij 96 microemulsion systems studied, penetration of the oil molecules into the interface would be particularly important if it is deep enough to disrupt the area of dehydrated polyoxyethylene chains which are expected to be the major site of testosterone propionate incorporation (6.2.2). Even with the greater solubility of the drug in 1-heptene, the ratio of the solubilities of testosterone propionate found in DMTG:1-heptene was still almost 3:1. Any disruption or dilution of this dehydrated polyoxyethylene region by the oil would therefore be expected to cause a reduction in the amount of drug incorporated in this area. It appears that in the case of 1-heptene, the reduction in the total incorporation of testosterone propionate due to the changes in the solubilisation site(s) available was greater than the opposing effect of the increased solubility of the drug in the oil phase.

The solubility of testosterone propionate found in the larger alkane; hexadecane, was similar to that in heptane. This similarity in solubility is unremarkable because both alkanes contain the same hydrocarbon units, the only difference being the length of the hydrocarbon chain, and hence the relative proportion of CH_3 - to $-\text{CH}_2$ - groups. Again (as with the two C_6 hydrocarbons) the presence of the terminal double bond is expected to increase the polarity of the oil, and the subsequent solubility of testosterone propionate. Hence the drug was more soluble in the 1-alkene of the same number of carbon atoms. The solubility of testosterone propionate in 1-hexadecene was however not as high as that found in 1-heptene. This observation may be explained based on the increased influence of a terminal double bond inducing polarity in a hydrocarbon of six carbon atoms compared

with a hydrocarbon with sixteen carbons. Comparison of the microemulsion incorporation shows that systems containing either of the C₁₆ hydrocarbons have lower incorporation levels than those found with microemulsions containing the triglycerides (soybean oil or Miglyol 812), and similar incorporation to those found in systems containing the smaller hydrocarbons.

At all four surfactant levels tested, 1-hexadecene microemulsion systems were found to have lower levels of testosterone propionate incorporation than systems containing hexadecane. The solubility of testosterone propionate was however found to be greater in 1-hexadecene, compared to hexadecane. These results again support the hypothesis that the alkene has a more significant and disruptive effect on the surfactant interface than the corresponding alkane, in this case resulting in reduced incorporation of the drug in 1-hexadecene compared to hexadecane microemulsion systems, even though the drug solubility is higher in 1-hexadecene.

6.2.4 Light scattering investigations of microemulsions containing testosterone enanthate

Light scattering investigations (PCS and TILS) were carried out on nine microemulsion systems in which 1 %w/w testosterone enanthate had been added (before heating) in place of 1 %w/w of the water phase. The same nine compositions (A to I) used to test the stability of the microemulsions within the o/w area of existence (section 3.5) were selected. PCS and TILS investigations of the equivalent drug-free microemulsions had already been performed (3.4.1 and 3.4.2.2). Light scattering analysis of microemulsions composed of 14 %w/w Brij 96 and either 1 or 2 %w/w soybean oil, with 0.4, 1, 2 and 3 %w/w testosterone enanthate were also carried out.

6.2.4.1 Photon correlation spectroscopy studies

Results of the PCS investigations of microemulsions containing testosterone enanthate are shown in figure 6.4. In figure 6.4a the apparent Z mean diameter of microemulsions without drug, and containing 1 %w/w drug, are plotted as a function of surfactant concentration. In all compositions compared, the apparent Z mean diameter was slightly larger in those

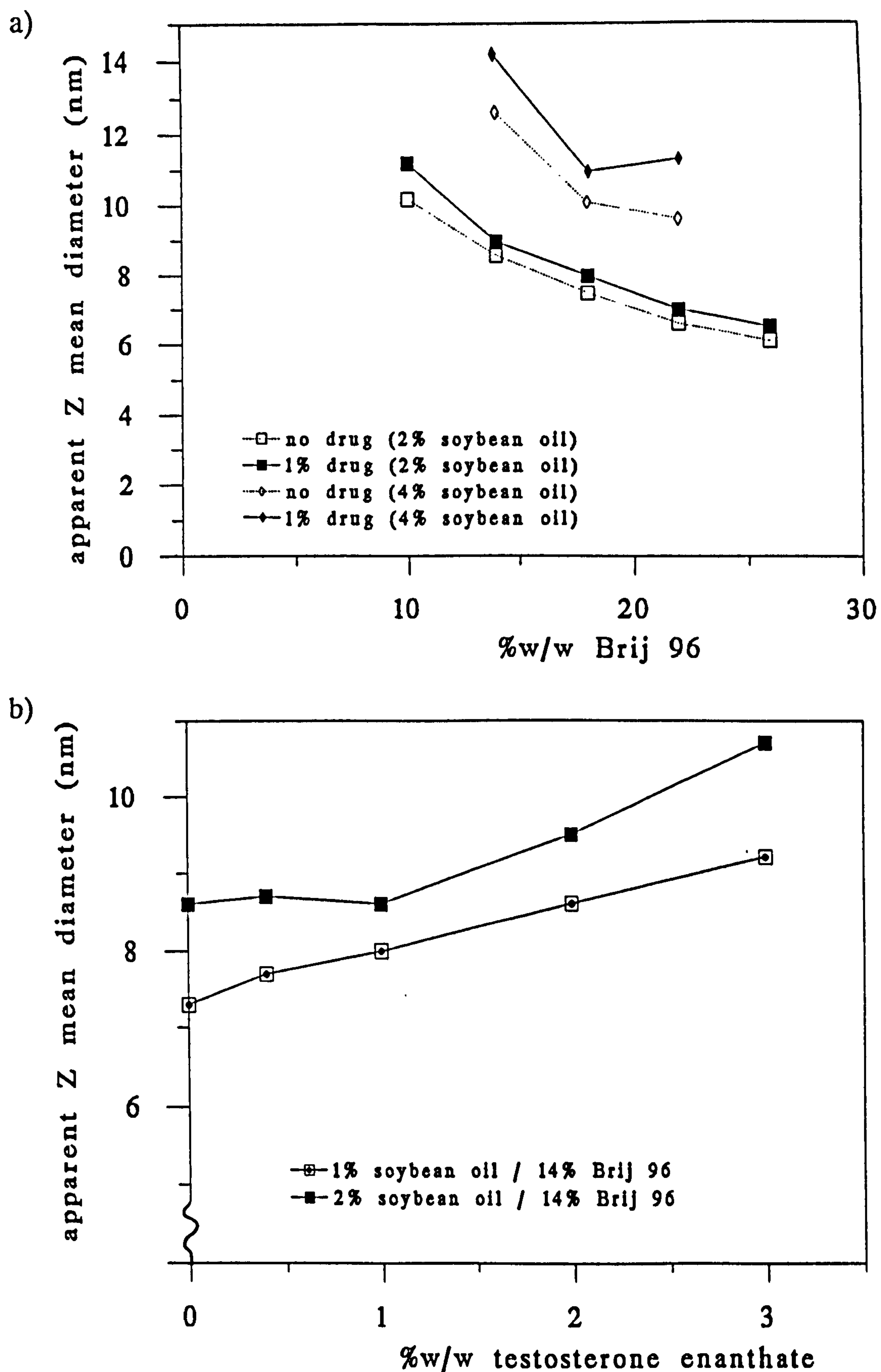


Figure 6.4: Apparent Z mean diameters (nm) determined by PCS for microemulsions with a) fixed soybean oil content (2 or 4 %w/w), in the absence and presence of 1 %w/w testosterone enanthate, as a function of surfactant concentration, and b) 14 %w/w Brij 96 with either 1 or 2 %w/w soybean oil and increasing concentration of testosterone enanthate.

microemulsions containing 1 %w/w testosterone enanthate. This increase in size is expected to be due to the presence of drug within the microemulsion droplet. However it must also be noted that (because the added drug had replaced an equivalent weight of water found in the drug-free compositions) the volume fraction of the drug-loaded microemulsion droplets was larger than the corresponding drug-free composition and so a greater possibility of interaction is anticipated. It was expected that an indication of any increased interaction in the drug-loaded microemulsions compared to the drug-free systems would be found in increased values of polydispersity. It was however found that in the microemulsion compositions containing 2 %w/w soybean oil, no increase in polydispersity was seen in microemulsions containing 1 %w/w testosterone enanthate, compared to the equivalent drug-free system. An increase in polydispersity was also not observed for the microemulsion composition containing 22 %w/w Brij 96 with 4 %w/w soybean oil, although increases of 11 and 8% were seen in the polydispersity of compositions containing 4 %w/w soybean oil with 14 or 18 %w/w Brij 96 respectively.

Figure 6.4b plots the apparent Z mean diameter for two microemulsion compositions (14 %w/w Brij 96 with either 1 or 2 %w/w soybean oil) with testosterone enanthate concentrations increasing up to 3 %w/w. It can be seen that when testosterone enanthate was added to microemulsions containing 14 %w/w surfactant and 1 %w/w soybean oil, an approximately linear increase in the apparent Z mean diameter was observed as a function of drug concentration. In comparison, the apparent Z mean diameter of microemulsions with the same surfactant concentration, but with 2 %w/w soybean oil, did not show a noticeable increase in the apparent Z mean diameter until concentrations of over 1 %w/w testosterone enanthate had been added. However the increase in size seen with the microemulsion systems with the lower (1 %w/w) soybean oil content, and up to 1 %w/w drug was less than 1nm, and so experimental variability could to some extent explain the difference in the behaviour of the two compositions. The difference between the two systems could however imply that the distribution of up to 1 %w/w testosterone enanthate within the microemulsion system composed of 14 %w/w Brij 96 and 2 %w/w soybean oil made very little impact on the size of the resultant droplets, whereas in systems with less oil, lower concentrations of the drug have a significant effect on the size of the individual droplets.

6.2.4.2 Total intensity light scattering studies

Figures 6.5a and 6.5b show the TILS results found for the same group of microemulsions studied by PCS above. The plots of R_{90} as a function of Brij 96 concentration (fig.6.5a) showed the same non-linear decrease as previously observed in the equivalent systems tested without the addition of 1 %w/w testosterone enanthate (fig.3.19b). The values of R_{90} for microemulsions with the same concentration of surfactant and oil, but containing 1 %w/w testosterone enanthate, were however slightly higher than that of the drug-free systems. Figure 6.5b plots the observed R_{90} against the weight of testosterone enanthate for microemulsions containing 14 %w/w Brij 96 and either 1 or 2 %w/w soybean oil. As with the apparent Z mean diameter found with PCS analysis of the same systems (6.2.4.1) an increase in R_{90} was seen with increasing drug content. In contrast to the apparent Z mean diameters found for these systems, there was however an increase in the value of R_{90} for microemulsions with 14 %w/w Brij 96 and both 1 and 2 %w/w soybean oil for each increasing concentration of testosterone enanthate.

In order to obtain sizes of the anhydrous radii of these drug-containing microemulsions, analysis of the TILS results was carried out using a model similar to that described in section 2.2.10.3 and previously used to analyse the TILS results of 3-component drug-free microemulsion systems (3.4.2.2). Some of the previously applied equations however needed to be adapted to allow for the presence of drug. Because the distribution of the drug within the microemulsion droplet is unknown, a further variable was also introduced. Based on studies of possible sites of incorporation (6.2.2) and the solubilities of testosterone enanthate shown in table 6.4, it was assumed that all the drug was present within the microemulsion droplet, and the aqueous concentration was taken to be zero. The relative solubilities of the drug in the droplet hydrocarbon core (soybean oil + hydrocarbon chains of the surfactant) and the ethylene oxide chains of the Brij 96 was expected to change with the relative volumes of each component, and was not known. Furthermore, analysis of the systems was carried out using an area occupied by the surfactant polar headgroup (a_0) of 48\AA^2 , and it was therefore assumed that this value did not change when drug was added.

As with the oil (eqn.30) and water component (eqn.38) the amount of drug

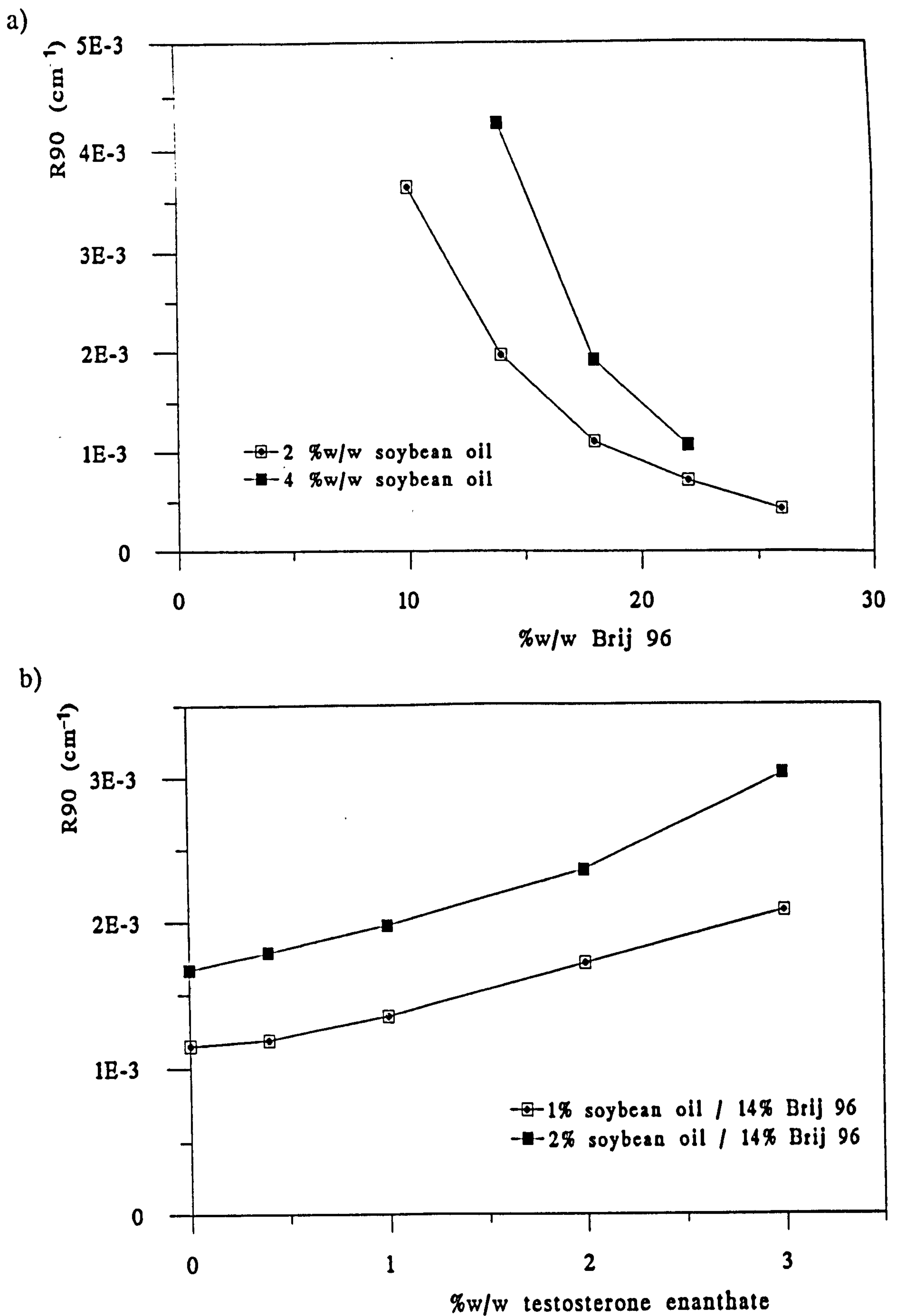


Figure 6.5: Observed R_{90} values obtained by TILS for microemulsions with a) either 2 or 4 %w/w soybean oil in the presence of 1 %w/w testosterone enanthate as a function of Brij 96 concentration, and b) 14 %w/w Brij 96 and either 1 or 2 %w/w soybean oil with increasing testosterone enanthate content.

per microemulsion droplet was thought to depend on the molar ratio of the drug to surfactant in the formulation (f_d). That is;

$$f_d = \frac{\text{weight drug}}{\text{weight surfactant}} \times \frac{M_r \text{ surfactant}}{M_r \text{ drug}} \quad \text{eqn.62}$$

and so the total number of drug molecules per droplet (n_d) may be calculated by;

$$n_d = f_d \times n_s \quad \text{eqn.63}$$

Hence if the fraction of drug found in the inner hydrocarbon core (oil + surfactant hydrophobes) of radius r_1 is g , then equation 33 may be modified to allow for the addition of drug, producing a radius, r_{1d} . So;

$$r_{1d} = \frac{3 (f v_o + v + g f_d v_d)}{a_o} \quad \text{eqn.64}$$

where v_d is the volume of the drug molecule, which because of the similarity in structure between testosterone enanthate and cholesterol, was taken to be 602\AA^3 .

Similarly, the value of r_2 (eqn.36) will also alter due to the presence of the drug in both r_{1d} and in the ethylene oxide chains of the surfactant (ie due to the total number of drug molecules in the microemulsion droplet, n_d). So that;

$$r_{2d} = \left[\frac{3 (n_o v_o + n_s [v + v_h] + n_d v_d)}{4 \pi} \right]^{1/3} \quad \text{eqn.65}$$

where v_h is the volume of the surfactant ethylene oxide chain. Using Brij 96 as surfactant, assumed to have an average hydrophilic chain of ten ethylene oxide units, a volume of 657\AA^3 was used.

A further iterative process was introduced to the program so that values of r_{1d} , r_{2d} , and a value of t_1 (corresponding to the best fit of the observed R_{90} with a hard sphere R_{90}) could be calculated for values of g between zero and one in increments of 0.05. Therefore for each drug-containing

microemulsion, 21 values of g resulted in the calculation of 21 corresponding values of r_{1d} , r_{2d} and t_1 .

Results of this analysis for microemulsions containing 1 %w/w testosterone enanthate are given in table 6.7. Inspection of the values obtained for the same microemulsion systems using an a_0 of 48\AA^2 and without any added testosterone enanthate (table 3.5) shows that as expected, in the presence of 1 %w/w drug, even the lowest value of r_{2d} is greater than the corresponding r_2 of the drug-free microemulsion. The range of values for t_1 in the presence of drug extended above and below the value of t_1 obtained in the absence of drug, except for microemulsions composed of 14 %w/w Brij 96 with 4 %w/w soybean oil, and 18 %w/w Brij 96 with 6 %w/w soybean oil for which all values of t_1 within the range were less than the t_1 found for the equivalent drug-free microemulsion. Interestingly, it is these same microemulsion compositions that were first to show signs of instability with increasing testosterone enanthate concentration when undergoing the 21-day stability test (compositions F and I in section 6.2.5). As found with analysis of the TILS data from the drug-free microemulsion systems, the values of t_1 in systems with 1 %w/w testosterone enanthate decreased with increasing soybean oil concentration, suggesting an increased possibility of interaction between droplets.

In order to compare the derived sizes, the dimensions of the drug-loaded microemulsion (of the 21 calculated with different values of g) which had the same value of t_1 expected for the equivalent volume fraction of a drug-free microemulsion was used. This was done by assuming the relationship between Φ_{r2} and t_1 was linear and determining the equation of the corresponding regression line. The resulting values of r_{2d} and $r_{2d}+t_1$ for 2 %w/w soybean oil microemulsions containing 1 %w/w testosterone enanthate, and r_2 and r_2+t_1 for the equivalent drug-free microemulsions, are plotted as a function of Brij 96 concentration in figure 6.6. Although larger than the corresponding microemulsions without drug, results for systems loaded with drug follow the same trend. A reduction in size was seen with increasing concentration of Brij 96. As found in microemulsions without added drug, the results determined for microemulsions with 1 %w/w testosterone enanthate by this method of TILS analysis were of greater size, than the hydrodynamic radius found by PCS.

Table 6.7: Analysis of TILS results (using $a_o = 48\text{\AA}$) for microemulsions containing 1 %w/w testosterone enanthate; microemulsion volume fraction, and range of r_{2d} and t_1 values for $0 \leq g \leq 1$.

microemulsion composition with 1 %w/w testosterone enanthate	Φ_{r2}	range of values $0 \leq g \leq 1$	
		r_{2d}	t_1
2% soybean oil / 10% Brij 96	0.129	59.5–65.0	1.7–6.9
2% soybean oil / 14% Brij 96	0.169	54.3–58.3	3.9–6.8
2% soybean oil / 18% Brij 96	0.208	51.4–54.5	4.9–6.8
2% soybean oil / 22% Brij 96	0.247	49.6–52.1	4.7–6.0
2% soybean oil / 26% Brij 96	0.287	48.3–50.5	4.6–5.7
4% soybean oil / 14% Brij 96	0.190	66.2–70.0	0.4–3.0
4% soybean oil / 18% Brij 96	0.229	60.7–63.7	3.8–5.4
4% soybean oil / 22% Brij 96	0.269	57.2–59.7	4.2–5.3
6% soybean oil / 18% Brij 96	0.251	69.9–72.8	-2.2– -0.7

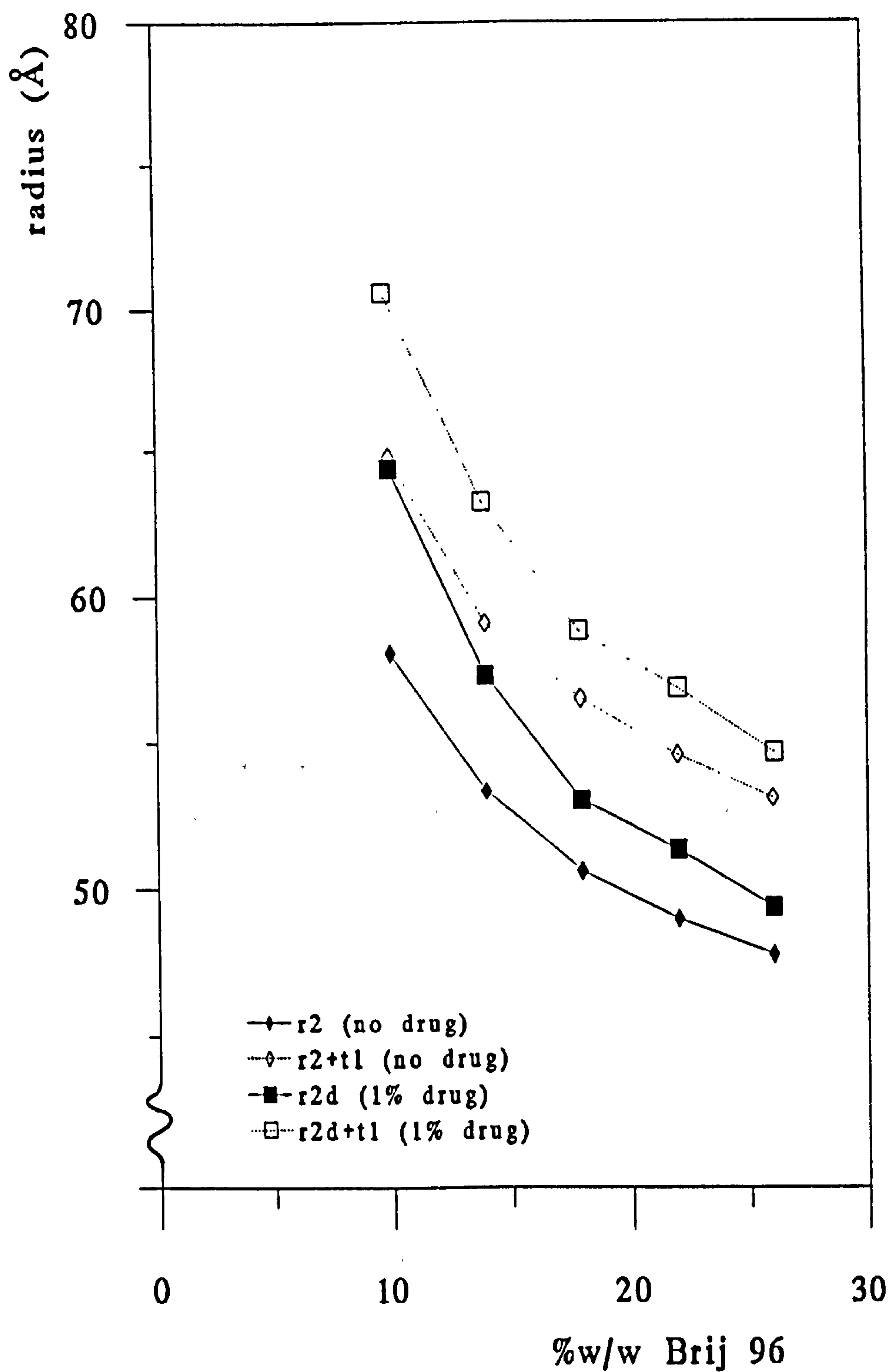


Figure 6.6: Radii of 2 %w/w soybean oil microemulsion droplets derived from TILS data for systems in the absence and presence of 1 %w/w testosterone enanthate as a function of surfactant concentration.

Similarly a range of r_{2d} and t_1 results were obtained with increasing concentration of testosterone enanthate added to the two microemulsions tested (14 %w/w Brij 96 with either 1 or 2 %w/w soybean oil). They are listed in table 6.8a and 6.8b. Results show a large range of t_1 values for these systems. Because the same microemulsion composition was present in the four concentrations of drug added, it was assumed that the drug would still distribute in the same way regardless of its concentration, and hence the value of g would remain the same. In order to compare values of r_{2d} and $t_{2d} + t_1$ the dimensions of the microemulsion corresponding to a selected value of g was used.

Figure 6.7 shows the resulting radii obtained when $g=0.5$ was selected for both microemulsion systems. A choice of g equal to 0.5 assumes that in each composition half the testosterone enanthate content distributes within the ethylene oxide chains of the microemulsion droplet and half in the hydrophobic core consisting of the soybean oil and the oleyl portions of the Brij 96. Again the values calculated were higher than the corresponding hydrodynamic radii obtained by PCS (fig.6.4b). For both microemulsion systems, as the concentration of testosterone enanthate increased, the anhydrous radius increased, but the value of t_1 decreased, suggesting that greater interaction was occurring with increasing concentration of drug in the microemulsion systems. Hence increasing instability and expulsion of the composition from the region of microemulsion existence might be expected for those microemulsions with increasing testosterone enanthate concentration. Investigations into the stability of nine microemulsions, including the composition containing 14 %w/w Brij 96 and 2 %w/w soybean oil, is reported in the following section.

6.2.5 Stability testing of microemulsions containing testosterone enanthate

The same compositions (A to I) of soybean oil/Brij 96/water microemulsions tested for stability by 21 day exposure to cycles of 4 and 30°C (16 and 8 hours respectively) in section 3.5, were similarly tested when they contained 1, 2 or 4 %w/w testosterone enanthate. Results of both the initial apparent Z mean diameter, and that found after 21 days, are given in table 6.9.

For the same composition, the initial apparent Z mean diameters observed

Table 6.8: Analysis of TILS results (using $a_0 = 48\text{\AA}$) for microemulsions containing 14 %w/w Brij 96 and either a) 1 %w/w or b) 2 %w/w soybean oil, with increasing concentration of testosterone enanthate; microemulsion volume fraction, and range of r_{2d} and t_1 values for $0 \leq g \leq 1$.

a)

%w/w testosterone enanthate	Φ_{r2}	range of values $0 \leq g \leq 1$	
		r_{2d}	t_1
0.4	0.152	47.7–49.3	5.7–7.0
1	0.158	48.2–52.3	4.3–7.4
2	0.167	49.1–57.3	1.7–7.6
3	0.176	50.0–62.2	–0.5–8.0

b)

%w/w testosterone enanthate	Φ_{r2}	range of values $0 \leq g \leq 1$	
		r_{2d}	t_1
0.4	0.163	53.7–55.3	5.0–6.2
1	0.169	54.3–58.3	3.9–6.8
2	0.178	55.2–63.2	1.7–7.2
3	0.187	56.2–68.1	–1.6–6.4

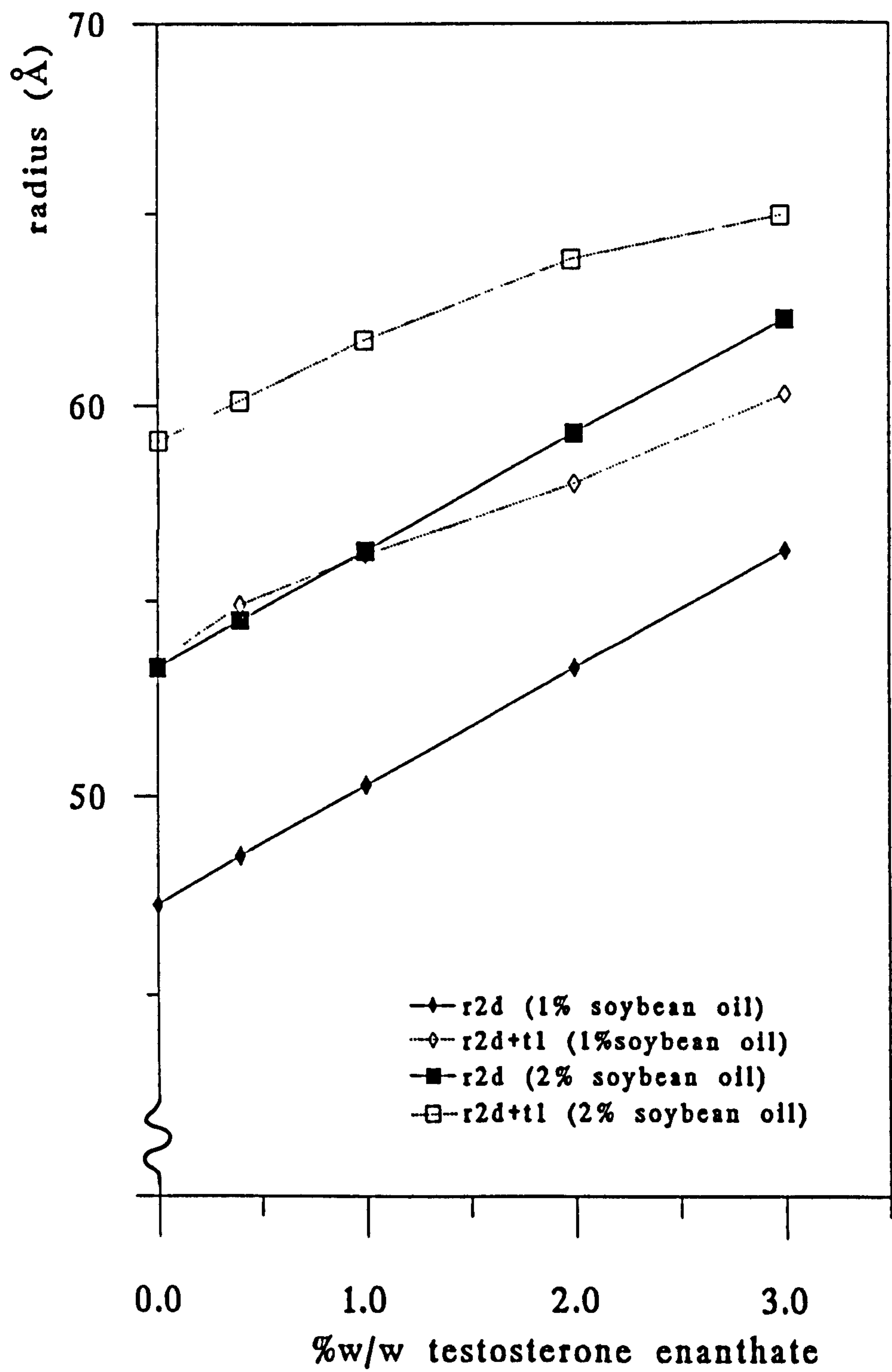


Figure 6.7: Radii of microemulsion droplets (r_{2d} and $r_{2d}+t_1$) derived from TILS data for compositions containing 14 %w/w Brij 96 and either 1 or 2 %w/w soybean oil as a function of increasing concentration of testosterone enanthate.

tended to increase with increasing drug content, as might be expected from the light scattering investigations above (6.2.4). These results also give further indication of how the area of existence was affected by the addition of drug. It has been shown that concentrations up to 1 %w/w testosterone enanthate had little effect on the area of existence (6.2.1). The apparent Z mean diameter found initially, and after 21 days, were similar for microemulsions without any drug, and for systems containing 1 %w/w testosterone enanthate. In both cases composition I (6 %w/w soybean oil/18 %w/w Brij 96) became turbid within the 21 day period of the study.

When 2 %w/w testosterone enanthate was present, the difference in size became more significant, and subsequent effects were seen on the area of existence. For example, composition I (which had been clear at the beginning of the study when 0 or 1 %w/w drug was present) was not clear when 2 %w/w testosterone enanthate was added. Also, with 2 %w/w drug incorporation, composition F (4 %w/w soybean oil/14 %w/w Brij 96) was found to be turbid at the end of 21 days of temperature cycling. Although the apparent Z mean diameter of samples A, C, D and E remained fairly small, and unaltered after 21 days, compositions A, G and H, whilst remaining clear, did show more significant increases in size (120, 160 and 157% respectively) at the end of the test.

The most significant differences were however seen in the microemulsions to which 4 %w/w testosterone enanthate had been added. Compositions A and B (2 %w/w soybean oil with either 10 or 14 %w/w Brij 96) no longer formed microemulsion systems when this level of drug was added. Instead, milky white macroemulsions were produced. Also, compositions F and I were turbid before the stability testing was initiated. At the end of 21 days, all the compositions containing 4 %w/w testosterone enanthate had become turbid, with corresponding increases in their Z mean diameter.

Results of this investigation therefore indicate that those systems containing 1 %w/w testosterone enanthate, although appearing to be slightly larger compared to microemulsions containing no drug, still seemed to be as stable as the corresponding drug-free microemulsion when exposed to temperature cycles of 4 and 30°C for 21 days.

Differences in stability behaviour did however appear to begin when a drug

Table 6.9: Apparent Z mean diameters (nm) for soybean oil/Brij 96/water microemulsions containing 0, 1, 2 and 4 %w/w testosterone enanthate, before and after 21 days of temperature cycling.

		apparent Z mean diameter (nm)							
		%w/w testosterone enanthate in microemulsion							
		0		1		2		4	
microemulsion composition		initial	21 days	initial	21 days	initial	21 days	initial	21 days
A	2% soybean oil / 10% Brij 96	10.3	10.8	11.0	12.2	12.2	14.6	–	–
B	2% soybean oil / 14% Brij 96	8.7	9.4	8.9	9.7	9.9	9.9	–	–
C	2% soybean oil / 18% Brij 96	7.6	7.7	7.8	7.8	8.2	9.0	11.0	(T)14.3
D	2% soybean oil / 22% Brij 96	6.7	7.5	7.0	7.2	7.4	7.3	9.3	(T)10.7
E	2% soybean oil / 26% Brij 96	6.1	6.3	6.5	6.8	7.4	7.1	12.1	–
F	4% soybean oil / 14% Brij 96	13.0	15.7	14.3	14.1	15.5	(T)19.1	(T)25.7	(T)26.2
G	4% soybean oil / 18% Brij 96	10.6	13.1	11.1	14.4	12.9	20.6	18.7	(T)31.4
H	4% soybean oil / 22% Brij 96	9.7	84.5	10.6	32.9	13.3	20.9	21.7	(T)154.9
I	6% soybean oil / 18% Brij 96	23.7	(T)19.2	26.4	(T)25.9	(T)32.5	(T)80.9	(T)59.4	(T)46.4

T = Turbid before filtering / size determined after filtering

load of 2 %w/w testosterone enanthate was used. Differences in the method of incorporation were also apparent with higher concentrations of testosterone enanthate. Whereas no change in the stability of the system had been noted when excess drug was added to a microemulsion which had already been formed (6.2.2), when the drug was added to the ingredients before heating and microemulsion formation had occurred, some microemulsion systems could not be produced. In the presence of 2 %w/w testosterone enanthate, although only composition I could not initially form a microemulsion, sample F also proved to be unstable within 21 days, with other compositions exhibiting small increases in size. With the addition of 4 %w/w testosterone enanthate, whilst a number of the compositions continued to form clear liquid systems initially, all were unstable at the end of 21 days of temperature cycling.

6.3 The incorporation of progesterone and medroxyprogesterone acetate

Two further drugs; progesterone and medroxyprogesterone acetate were investigated to see if the trends found with the three testosterone drugs could be used to predict the incorporation of other steroid molecules into soybean oil/Brij 96 microemulsion systems. The physicochemical properties of the two drugs in water, soybean oil, DMTG and 1-octadecene are given in table 6.10. The area of microemulsion existence when 0.4 %w/w progesterone was present showed no significant change when compared to the area found with drug-free soybean oil/Brij 96/water systems. As found with the addition of testosterone enanthate (6.2.1) there was however a reduction in the PIT of the microemulsion systems (between 0.5 and 2.8°C) in the presence of the drug.

6.3.1 Comparison between micellar and 2% soybean oil microemulsion incorporation

The calculated $\log P_{\text{Oct}}$ values [229] for progesterone and medroxyprogesterone acetate are 3.85 and 4.27 respectively. From the trends observed with $\log P$ values of the testosterone drugs (6.2.2) it might, therefore, be expected that the level of incorporation in micelles and

Table 6.10: Physicochemical properties and solubilities (%w/v) of progesterone and medroxyprogesterone acetate at 25°C (mean ± SD).

	progesterone	medroxyprogesterone acetate
Mr	314.5	386.5
log Poct	3.85	4.27
Mean solubility ± SD in;		
water	0.00004 ± 0.0002	< 0.00007
soybean oil	2.2 ± 0.2	0.43 ± 0.07
DMTG	5.1 ± 0.4	1.32 ± 0.05
1-octadecene	0.455 ± 0.009	0.042 ± 0.002

Table 6.11: Incorporation of progesterone and medroxyprogesterone acetate into Brij 96 micelles and 2 %w/w soybean oil microemulsions at 25°C (mean ± SD).

Drug	%w/w Brij 96	%w/v Drug incorporation ± SD	
		Micellar system	Microemulsion
progesterone	15	0.63 ± 0.07	0.79 ± 0.04*
	20	0.91 ± 0.2	0.91 ± 0.04
medroxyprogesterone acetate	15	0.51 ± 0.08	0.55 ± 0.05
	20	0.69 ± 0.03	0.75 ± 0.06

* indicates a significant difference (P = 0.05) between microemulsion and micellar systems.

microemulsions would be higher for medroxyprogesterone acetate. The results found however show greater solubility of progesterone (rather than medroxyprogesterone acetate) in the soybean oil, DMTG and 1-octadecene. It can also be seen in figure 6.8 that the level of incorporation of medroxyprogesterone acetate in pure DMTG and at all DMTG/water combinations was lower than that found with progesterone. Consequently the amount of progesterone incorporated into each surfactant solution and 2 %w/w soybean oil microemulsion system tested was greater than that found when medroxyprogesterone acetate was used (table 6.11).

The solubility of medroxyprogesterone acetate in soybean oil was found to be lower than that found with testosterone, and no significant difference was observed between the amount of drug incorporated into the microemulsion systems, compared to a surfactant system of the same Brij 96 concentration. The solubility found for progesterone in soybean oil was intermediate between the values for testosterone and testosterone propionate. The level of progesterone incorporation into microemulsion systems containing 15 %w/w Brij 96 was found to be significantly higher ($P=0.05$) than a surfactant system of 15 %w/w Brij 96, but at 20 %w/w Brij 96 the level of incorporation was not significantly different.

The results with these two steroid drugs confirm that considerable solubility of the drug in the dispersed soybean oil phase is required in order for a microemulsion to exhibit a significant improvement in its drug loading capabilities over a micellar solution of equivalent surfactant concentration.

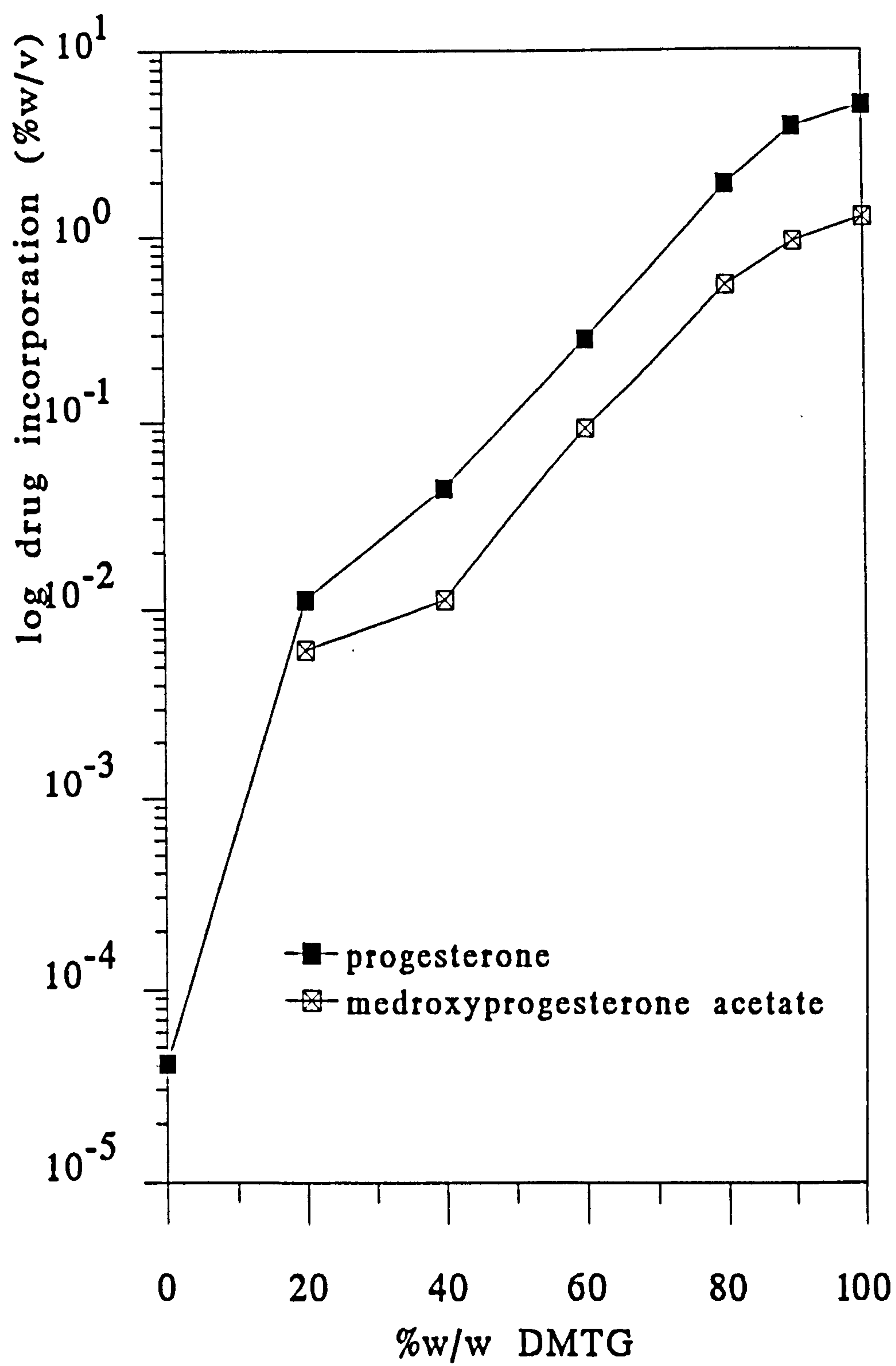


Figure 6.8: Log %w/v drug incorporated vs %w/w DMTG in DMTG/water mixtures, at 25°C, for progesterone and medroxyprogesterone acetate.

CHAPTER SEVEN: Conclusions and future work.

The potential advantages of microemulsions as a pharmaceutical drug delivery system include the ease of preparation of clear, thermodynamically stable, liquid formulations which can be sterilised by filtration and can deliver both lipophilic and hydrophilic drugs. In particular, o/w microemulsions are attractive vehicles for therapeutic agents which are not sufficiently soluble, or stable, in an aqueous environment to allow injection or other effective administration.

In this study, eight commercially available polyoxyethylene ether surfactants (C_mE_n) have been investigated for their ability to produce 3-component o/w microemulsions without the addition of a cosurfactant. The influence of surfactant headgroup size (n), hydrocarbon saturation and hydrocarbon chain length (m) and the oil phase employed, have been examined. It appears that when attached to an average of ten ethylene oxide units, a surfactant with an 18 carbon hydrophobe containing a cis double bond, is able to form microemulsions at room temperature, but surfactants with straight chained C_{18} or C_{16} hydrophobes are not. The area of existence of microemulsions produced by polyoxyethylene-10-oleyl ether (Brij 96 or $C_{18-1}E_{10}$) was found to be relatively insensitive to large changes in the properties of the oil phase. In contrast, $C_{12}E_{10}$ (which has a smaller hydrophobe) is more sensitive to the size of the oil molecules, and o/w microemulsion formation with this surfactant was favoured with oils of smaller chain lengths.

Surfactants with shorter ethylene oxide portions ($C_{18-1}E_5$ and $C_{12}E_4$) failed to produce microemulsions, even with the short hydrocarbon oil, heptane. It therefore appears that although these surfactants may have higher affinity for an oil phase than the equivalent hydrophobe attached to a longer ethylene

oxide chain, a minimum size of the hydrophilic moiety is required for o/w microemulsion formation. In comparison, microemulsions were possible, at room temperature, with the two surfactants tested with higher ethylene oxide contents ($C_{18-1}E_{20}$ and $C_{18}E_{20}$) only when hydrocarbon oils of short chain lengths were used.

This investigation has therefore shown that for a particular temperature, modification of oil and surfactant alters microemulsion formation in a complex way, which is dependent on the relative size and structure of the surfactant hydrophobe, the attached ethylene oxide chain and the oil phase to be dispersed. Further work which would be important for the development of microemulsions as drug delivery systems would be the optimisation of surfactant structure in order to produce a surfactant of low biological toxicity, which would still allow microemulsion formation with pharmaceutically acceptable oils, ideally at low amphiphilic concentrations. In this respect, investigations could be carried out to study the effect on the area of microemulsion existence of replacing the ether oxygen separating the hydrophile and hydrophobe in C_mE_n surfactants with a less toxic ester linkage, or of replacing the ethylene oxide units with alternative hydrophiles, such as sugar moieties.

Using soybean oil as the dispersed phase, the surfactant $C_{18-1}E_{10}$ (Brij 96) was found to be particularly effective at forming microemulsions of the o/w type in the concentration range of 8 to 28 %w/w at room temperature. The variation of size and structure of these 3-component Brij 96 microemulsions were investigated using photon correlation spectroscopy and total intensity light scattering techniques. The size of the microemulsion droplets were found to increase with increasing oil content, and decrease with surfactant concentration. Results suggested greater interdroplet interaction and aggregation of individual microemulsion droplets near the border of the region of microemulsion existence.

The use of light scattering techniques for investigating microemulsion systems is not however without problems. Light scattering equations strictly only apply to very dilute systems, and do not necessarily extend to concentrated, dispersed systems such as microemulsions. Hence analysis of results requires the application of mathematical models to compensate for the interdroplet interactions. In this study, total intensity light scattering data was

analysed by application of a hard sphere model, corrected for interdroplet interactions. The resulting dimensions obtained by the model were based on the assumption that a microemulsion droplet consists only of oil and surfactant, and that all the oil and surfactant in the composition is contained within the dispersed microemulsion droplets. The resulting calculated anhydrous radius of the microemulsion droplet is however dependent on knowledge of the dimensions of the oil and surfactant molecules within the droplet. In particular, the area occupied by the surfactant headgroup (a_o) at the droplet interface is very important to the calculations used in the model, but difficult to estimate. Future work investigating the value of a_o within microemulsion systems would be extremely valuable towards achieving the goal of obtaining reliable values of droplet size from TILS data.

In the photon correlation spectroscopy study of these systems, the hydrodynamic diameter was calculated using the Stokes Einstein equation for dilute, non-interacting spheres. The values obtained are useful in comparing the relative values of size, the effect of changing one of the components (such as the oil phase used), and observing the emergence of aggregate clusters as the systems become more concentrated. In order to be able to obtain absolute values of microemulsion droplet size however future work, with the aim of compensating for droplet interactions similar to that used in the TILS work, would be vital.

The effect on the area of existence of Brij 96/soybean oil/water microemulsion systems with the addition of three straight-chained alcohols (methanol, 1-butanol and 1-pentanol), or more pharmaceutically acceptable polyols (glycerol, xylitol and sorbitol), as cosurfactant were also investigated. The addition of the straight chained alcohols, in particular 1-butanol and 1-pentanol, extended the area of microemulsion existence towards compositions with higher oil and low water contents. Furthermore, the addition of 1-butanol to systems of soybean oil, water and the amphiphile with a C_{18} straight chain hydrophobe ($C_{18}E_{10}$) which could not form 3-component microemulsion systems, resulted in a substantial region of 4-component microemulsion existence.

Investigations of the interfacial tension between soybean oil and water systems in the presence of Brij 96, and either 1-butanol or 1-pentanol, confirm that one mechanism by which these alcohols may encourage the formation of

microemulsion systems is by direct action on the interface, further reducing the tension found when only surfactant was present. However in the presence of these two alcohols, lower concentrations of Brij 96 (approximately 15-28 %w/w) which had allowed the formation of 3-component o/w microemulsions, no longer resulted in the formation of clear systems. Changes in conductivity and dilution behaviour across the triangular phase diagram for systems consisting of soybean oil, Brij 96, 1-butanol and water, support the assumption that the structure of these 4-component systems changes throughout the region of existence.

In comparison, the highly water-soluble polyols; glycerol, xylitol and sorbitol did not appear to significantly extend the area of o/w microemulsion existence at room temperature. All three polyols did however reduce the phase inversion temperature of the systems. This effect was greatest for the two larger compounds, xylitol and sorbitol. Once sufficient polyol had been added to the system to reduce the PIT to temperatures below that of room temperature, o/w microemulsions were no longer observed.

Drug incorporation into microemulsions of the soybean oil/Brij 96/water type was determined for the benzodiazepine; diazepam, and five model steroid drugs; testosterone, testosterone propionate, testosterone enanthate, progesterone and medroxyprogesterone acetate, which are all poorly water soluble, with a range of log P_{oct} values. It was found that the stability of the o/w microemulsions did not appear to be affected by the presence of up to 1 %w/w of testosterone or either of its two esters. Stability studies involving higher incorporation of testosterone enanthate (2 and 4 %w/w) did however reveal that such levels of drug incorporation had a detrimental effect on the area of microemulsion existence, and on the size and interaction of the microemulsion droplets. Possible site(s) of drug incorporation in microemulsion systems were considered. Results indicated that, as with micelles, the most important site of incorporation for these six drugs appeared to be the area of dehydrated polyoxyethylene chains closest to the surfactant hydrophobe.

The level of incorporation for each drug into microemulsions containing 2 %w/w soybean oil was compared to that which could be solubilised into micellar systems produced with the equivalent concentration of surfactant. Whether or not a significant increase was observed in drug loading into

microemulsion systems compared to micellar systems appeared to depend on the solubility of the drug in the oil phase. Further investigation of testosterone propionate into microemulsions containing various oils support the importance of high drug solubility in the oil phase in order for an improvement in the drug carrying capacity of microemulsions over micellar systems to be seen.

Results of the present study suggest that o/w microemulsions could be useful drug delivery systems for drugs highly soluble in the dispersed oil phase. Future investigations would be required to determine if these drug-loaded microemulsions remain stable with the concomitant addition of other pharmaceutical ingredients such as electrolyte, flavourings and preservatives. Future *in vitro* studies of the stability and release characteristics of drugs from the microemulsions into both aqueous solutions and blood, or serum, would also be advocated. Further work involving *in vivo* investigations of drug delivery by 3-component o/w nonionic surfactant microemulsion systems will however depend on the selection and/or synthesis of surfactants with both low toxicity and the appropriate microemulsion-forming capabilities.

REFERENCES

1. Schulman, J.H., Stoeckenius, W. & Prince, L.M. (1959). Mechanism of formation and structure of micro emulsions by electron microscopy. *J.Phys.Chem.*, **63**, 1667-1680.
2. Hoar, T.P. & Schulman, J.H. (1943). Transparent water-in-oil dispersions: the oleopathic hydro-micelle. *Nature*, **152**, 102-103.
3. Rosano, H.L. (1984). Introduction. In Rosano, H.L. & Clausse, M. (eds) *Microemulsion systems*. Marcel Dekker, New York, p.xv-xix.
4. Danielsson, I. & Lindman, B. (1981). The definition of microemulsion. *Colloids Surf.*, **3**, 391-392.
5. Friberg, S.E. (1982). Comments on "the definition of microemulsion". *Colloids Surf.*, **4**, 201.
6. Friberg, S.E. (1983). Microemulsions. *Progr.Colloid Polym.Sci.*, **68**, 41-47.
7. Siano, D.B. (1983). The swollen micelle-microemulsion transition. *J.Colloid Interface Sci.*, **93**, 1-7.
8. Chevalier, Y. & Zemb, T. (1990). The structure of micelles and microemulsions. *Rep.Prog.Phys.*, **53**, 279-371.
9. Wormuth, K.R. & Kaler, E.W. (1987). Amines as microemulsion cosurfactants. *J.Phys.Chem.*, **91**, 611-617.
10. Kahlweit, M., Strey, R., Haase, D., Kunieda, H., Schmeling, T., Faulhaber, B., Borkovec, M., Eicke, H-F., Busse, G., Eggers, F., Funck, Th., Richmann, H., Magid, L., Söderman, O., Stilbs, P., Winkler, J., Dittrich, A. & Jahn, W. (1987). How to study microemulsions. *J.Colloid Interface Sci.*, **118**, 436-453.
11. Cavallo, J.L. & Rosano, H.L. (1986). Vapor pressure measurements of an

oil in water microemulsion system. *J.Phys.Chem.*, **90**, 6817-6821.

12. Aveyard, R. (1987). Ultralow tensions and microemulsions. *Chem.Ind.*, 20 July 1987, 474-478.

13. Ruckenstein, E. & Chi, J.C. (1975). Stability of microemulsions. *J.Chem.Soc., Faraday Trans.II.*, **71**, 1690-1707.

14. Ruckenstein, E. (1977). Stability, phase equilibria, and interfacial free energy in microemulsions. In Mittal, K.L. (ed.) *Micellization, solubilization and microemulsions*. Vol.2, Plenum Press, New York, p.755-778.

15. Ruckenstein, E. (1984). Phase behavior of microemulsions: The origin of the middle phase, of its chaotic structure and of the low interfacial tension. In Mittal, K.L. & Lindman, B. (eds) *Surfactants in solution*. Vol.3, Plenum Press, New York, p.1551- 1582.

16. Overbeek, J.Th.G. (1978). Microemulsions, a field at the border between lyophobic and lyophilic colloids. *Faraday Disc.Chem.Soc.*, **65**, 7-19.

17. Overbeek, J.Th.G., Verhoeckx, G.J., De Bruyn, P.L. & Lekkerkerker, H.N.W. (1987). On understanding microemulsions. II.Thermodynamics of droplet-type microemulsions. *J.Colloid Interface Sci.*, **119**, 422-441.

18. Miller, C.A. & Neogi, P. (1980). Thermodynamics of microemulsions: Combined effects of dispersion entropy of drops and bending energy of surfactant film. *AIChE Journal*, **26**, 212-219.

19. Winsor, P.A. (1948). Hydrotropy, solubilisation and related emulsification processes. *Trans.Faraday Soc.*, **44**, 376-398.

20. Robbins, M.L. (1977). Theory for the phase behavior of microemulsions. In Mittal, K.L. (ed.) *Micellization, solubilization and microemulsions*. Vol.2., Plenum Press, New York, p.713-754.

21. Langevin, D. (1986). Microemulsions and liquid crystals. *Mol.Cryst.Liq.Cryst.*, **138**, 259-305.

22. Shah, D.O. & Hamlin, Jr., R.M. (1971). Structure of water in microemulsions: Electrical, birefringence, and nuclear magnetic resonance studies. *Science*, 171, 483-485.
23. Chen, S.H., Chang, S.L., Strey, R., Samseth, J. & Mortensen, K. (1991). Structural evolution of bicontinuous microemulsions. *J.Phys.Chem.*, 95, 7427-7432.
24. Shinoda, K. & Lindman, B. (1987). Organized surfactant systems: microemulsions. *Langmuir*, 3, 135-149.
25. Rushforth, D.S., Sanchez-Rubio, M., Santos-Vidals, L.M., Wormuth, K.R., Kaler, E.W., Cuevas, R. & Puig, J.E. (1986). Structural study of one-phase microemulsions. *J.Phys.Chem.*, 90, 6668-6673.
26. Lam, A.C. & Schechter, R.S. (1987). The theory of diffusion in microemulsion. *J.Colloid Interface Sci.*, 120, 56-63.
27. Scriven, L.E. (1976). Equilibrium bicontinuous structure. *Nature*, 263, 123-125.
28. Scriven, L.E. (1977). Equilibrium bicontinuous structures. In Mittal, K.L. (ed.) *Micellization, solubilization and microemulsions*. Vol.2., Plenum Press, New York, p.877-893.
29. Davis, H.T., Bodet, J.F., Scriven, L.E. & Miller, W.G. (1989). Microstructure and transport in midrange microemulsions. *Physica A*, 157, 470-481.
30. Jahn, W. & Strey, R. (1988). Microstructure of microemulsions by freeze fracture electron microscopy. *J.Phys.Chem.*, 92, 2294- 2301.
31. Gulik-Krzywicki, T. & Larsson, K. (1984). An electron microscopy study of the L2-phase (microemulsion) in a ternary system: triglyceride / monoglyceride / water. *Chem.Phys.Lipids*, 35, 127-132.
32. Gulik-Krzywicki, T., Aggerbeck, L.P. & Larsson, K. (1984). The use of freeze-fracture and freeze-etching electron microscopy for phase analysis and

structure determination of lipid systems. In Mittal, K.L. & Lindman, B. (eds) *Surfactants in solution*. Vol.1. Plenum Press, New York, p.237-257.

33. Vinson, P.K., Sheehan, J.G., Miller, W.G., Scriven, L.E. & Davis, H.T. (1991). Viewing microemulsions with freeze-fracture transmission electron microscopy. *J.Phys.Chem.*, **95**, 2546-2550.

34. Talmon, Y., Davis, T., Scriven, L.E. & Thomas, E.L. (1979). Cold-stage microscopy system for fast-frozen liquids. *Rev.Sci.Instrum.*, **50**, 698-704.

35. Biais, J., Mercier, M., Bothorel, P. Clin, B., Lalanne, P. & Lemanceau, B. (1981). Microemulsions and electron microscopy. *J.Microsc.*, **121**, 169-178.

36. Bisal, S, Bhattacharya, P.K. & Moulik, S.P. (1990). Conductivity study of microemulsions. Dependence of structural behavior of water/oil systems on surfactant, cosurfactant, oil and temperature. *J.Phys.Chem.*, **94**, 350-355.

37. Moha-Ouchane, M., Peyrelasse, J. & Boned, C. (1987). Percolation transition in microemulsions: Effect of water-surfactant ratio, temperature, and salinity. *Phys.Rev.A*, **35**, 3027- 3032.

38. Laguës, M. & Sauterey, C. (1980). Percolation transition in water in oil microemulsions. Electrical conductivity measurements. *J.Phys.Chem.*, **84**, 3503-3508.

39. Mackay, R.A. & Agarwal, R. (1978). Conductivity measurements in nonionic microemulsions. *J.Colloid Interface Sci.*, **65**, 225-231.

40. Ktistis, G. (1990). A viscosity study on oil-in-water microemulsions. *Int.J.Pharm.*, **61**, 213-218.

41. Quemada, D. & Langevin, D. (1985). Rheological modelling of microemulsions. *J. Theoretical Appl.Mech.*, Numéro spécial, 201-237.

42. Mishra, B.K., Mukherjee, T. & Manohar, C. (1991). Probing microemulsion structure through excimer formation. *Colloid Surf.*, **56**, 229-238.

43. Zana, R., Lang, J. & Lianos, P. (1984). Fluorescence probe study of oil in water microemulsions. In Mittal, K.L. & Lindman, B. (eds) *Surfactants in solution*. Vol.3. Plenum Press, New York, p.1627-1649.
44. Mackay, R.A., Myers, S.A., Bodalbhai, L. & Brajter-Toth, A. (1990). Microemulsion structure and its effect on electrochemical reactions. *Anal.Chem.*, **62**, 1084-1090.
45. Lindman, B. & Stilbs, P. (1984). Characterization of microemulsion structure using multi-component self diffusion data. In Mittal, K.L. & Lindman, B. (eds) *Surfactants in solution*. Vol.3. Plenum Press, New York, p.1651-1662.
46. Tadros, Th.F. (1984). Microemulsions - An overview. In Mittal, K.L. & Lindman, B. (eds) *Surfactants in solution*. Vol.3. Plenum Press, New York, p.1501-1532.
47. Chen, S.H. (1986). Small angle neutron scattering studies of the structure and interaction in micellar and microemulsion systems. *Ann.Rev.Phys.Chem.*, **37**, 351-399.
48. Magid, L.J. (1986). The elucidation of micellar and microemulsion architecture using small-angle neutron scattering. *Colloids Surf.*, **19**, 129-158.
49. Carlström, G. & Halle, B. (1989). Shape fluctuations and water diffusion in microemulsion droplets. A nuclear spin relaxation study. *J.Phys.Chem.*, **93**, 3287-3299.
50. Robinson, B.H., Toprakcioglu, C. & Dore, J.C. (1984). Small-angle neutron-scattering study of microemulsions stabilised by aerosol-OT. Part 1. Solvent and concentration variation. *J.Chem.Soc.,Faraday Trans.I*, **80**, 13-27.
51. Toprakcioglu, C., Dore, J.C., Robinson, B.H. & Howe, A. (1984). Small-angle neutron-scattering studies of microemulsions stabilized by aerosol-OT. Part 2. Critical scattering and phase stability. *J.Chem.Soc.,Faraday Trans.I*, **80**, 413-422.
52. Howe, A.M., Toprakcioglu, C., Dore, J.C. & Robinson, B.H. (1986).

Small-angle neutron scattering studies of microemulsions stabilised by aerosol-OT. Part 3. The effect of additives on phase stability and droplet structure. *J.Chem.Soc.,Faraday Trans.I*, 82, 2411-2422.

53. Huang, J.S. & Kotlarchyk, M. (1986). Study of interfacial curvature in a three-component microemulsion with equal volumes of water and oil. *Phys.Rev.Lett.*, 57, 2587-2589.

54. Chen, S.H., Chang, S.L. & Strey, R. (1990). On the interpretation of scattering peaks from bicontinuous microemulsions. *Progr.Colloid Polym.Sci.*, 81, 30-35.

55. Stilbs, P. & Lindman, B. (1984). NMR measurements on microemulsions. *Progr.Colloid Polym.Sci.*, 69, 39-47.

56. Hou, M.J., Kim, M. & Shah, D.O. (1988). A light scattering study on the droplet size and interdroplet interaction in microemulsions of AOT-oil-water system. *J.Colloid Interface Sci.*, 123, 398-412.

57. Radiman, S., Fountain, L.E., Toprakcioglu, C., de Valleria, A. & Chieux, P. (1990). SANS study of polymer-containing microemulsions. *Progr.Colloid Polym.Sci.*, 81, 54-59.

58. Samseth, J., Chen, S-H., Litster, J.D. & Huang, J.S. (1988). SANS studies of the microstructure of a three-component microemulsion. *J.Appl.Cryst.*, 21, 835-839.

59. Iwunze, M.O., Sucheta, A. & Rusling, J.F. (1990). Bicontinuous microemulsions as media for electrochemical studies. *Anal.Chem.*, 62, 644-649.

60. Chen, S.J., Evans, D.F. & Ninham, B.W. (1984). Properties and structure of three-component ionic microemulsions. *J.Phys.Chem.*, 88, 1631-1634.

61. Evans, D.F., Mitchell, D.J. & Ninham, B.W. (1986). Oil, water, and surfactant: Properties and conjectured structure of simple microemulsions. *J.Phys.Chem.*, 90, 2817-2825.

62. Sjöblom, J., Skurtveit, R., Saeten, J.O. & Gestblom, B. (1991). Structural changes in the microemulsion system didodecyldimethylammonium bromide / water / dodecane as investigated by means of dielectric spectroscopy. *J.Colloid Polym.Sci.*, 141, 329-337.
63. Farago, B., Richter, D. & Huang, J.S. (1989). Shape fluctuation of microemulsion droplets. *Physica B*, 156 & 157, 452-455.
64. Farago, B., Huang, J.S., Richter, D., Safran, S.A. & Milner, S.T. (1990). Microemulsion shape fluctuation measured by neutron spin echo. *Progr.Colloid Polym.Sci.*, 81, 60-63.
65. Trotta, M., Gasco, M.R. & Pattarino, F. (1989). Effect of alcohol cosurfactants on the diffusion coefficients of microemulsions by light scattering. *J.Disp.Sci.Tech.*, 10, 15-32.
66. Lindman, B., Shinoda, K., Jonströmer, M. & Shinohara, A. (1988). Change of organized solution (microemulsion) structure with small change in surfactant composition as revealed by NMR self-diffusion studies. *J.Phys.Chem.*, 92, 4702-4706.
67. Lam, A.C. & Schechter, R.S. (1987). A study of diffusion and electrical conduction in microemulsions. *J.Colloid Interface Sci.*, 120, 42-55.
68. Khan, A., Lindström, B., Shinoda, K. & Lindman, B. (1986). Change of the microemulsion structure with the hydrophile-lipophile balance of the surfactant and the volume fractions of water and oil. *J.Phys.Chem.*, 90, 5799-5801.
69. Georges, J. & Chen, J.W. (1986). Microemulsion studies: Correlation between viscosity, electrical conductivity and electrochemical and fluorescent probe measurements. *Colloid Polym.Sci.*, 264, 896-902.
70. Clause, M., Peyrelasse, J., Heil, J., Boned, C. & Lagourette, B. (1981). Bicontinuous structure zones in microemulsions. *Nature*, 293, 636-638.
71. Roux, A.H., Roux-Desgranges, G., Grolier, J-P.E. & Viallard, A. (1981). Apparent molal volumes in microemulsions: An insight into the structures of

these systems. *J. Colloid Interface Sci.*, **84**, 250- 262.

72. Bansal, V.K., Chinnaswamy, K., Ramachandran, C. & Shah, D.O. (1979). Structural aspects of microemulsions using dielectric relaxation and spin label techniques. *J. Colloid Interface Sci.*, **72**, 524-537.

73. Ceglie, A., Das, K.P. & Lindman, B. (1987). Microemulsion structure in four-component systems for different surfactants. *Colloids Surfs.*, **28**, 29-40.

74. Stilbs, P., Rapacki, K. & Lindman, B. (1983). Effect of alcohol cosurfactant length on microemulsion structure. *J. Colloid Interface Sci.*, **95**, 583-585.

75. Lindman, B., Ahl  as, T., S  derman, O. & Walderhaug, H. (1983). Fourier transform Carbon-13 relaxation and self-diffusion studies of microemulsions. *Faraday Discuss. Chem. Soc.*, **76**, 317-329.

76. S  derman, O. & Walerhaug, H. (1986). Order and dynamics of the hydrophobic/hydrophilic interface in microemulsions of the cosurfactant type. A ^{13}C NMR relaxation study. *Langmuir*, **2**, 57-63.

77. Lindman, B., Stilbs, P. & Moseley, M.E. (1981). Fourier transform NMR self-diffusion and microemulsion structure. *J. Colloid Interface Sci.*, **83**, 569-582.

78. Lindman, B., Kamenka, N. Kathopoulis, T-M, Brun, B. & Nilsson, P-G. (1980). Translational diffusion and solution structure of microemulsions. *J. Phys. Chem.*, **84**, 2485-2490.

79. Strey, R. & Kahlweit, M. (1987). Microstructure of microemulsions. *Progr. Colloid Polymer Sci.*, **73**, 193.

80. Strey, R., Winkler, J. & Magid, L. (1991). Small-angle neutron scattering from diffuse interfaces. 1. Mono- and bilayers in the water-octane- C_{12}E_5 system. *J. Phys. Chem.*, **95**, 7502-7507.

81. Billman, J.F. & Kaler, E.W. (1991). Structure and phase behavior in four-component nonionic microemulsions. *Langmuir*, **7**, 1609-1617.

82. Shimobouji, T., Matsuoka, H., Ise, N. & Oikawa, H. (1989). Small-angle x-ray scattering studies on nonionic microemulsions. *Phys.Rev.A*, **39**, 4125-4131.
83. Olsson, U., Shinoda, K. & Lindman, B. (1986). Change of the structure of microemulsions with the hydrophilie-lipophile balance of nonionic surfactant as revealed by NMR self-diffusion studies. *J.Phys.Chem.*, **90**, 4083-4088.
84. Shinoda, K. (1967). The correlation between the dissolution state of nonionic surfactant and the type of dispersion stabilized with the surfactant. *J.Colloid Interface Sci.*, **24**, 4-9.
85. Friberg, S., Buraczewska, I. & Ravey, J.C. (1977). Solubilization by nonionic surfactants in the HLB-temperature range. In Mittal, K.L.(ed.) *Micellization, solubilization and microemulsions*. Vol.2. Plenum Press, New York. p.901-911.
86. Kunieda, H. & Shinoda, K. (1985). Evaluation of the hydrophile-lipophile balance (HLB) of nonionic surfactants. *J.Colloid Interface Sci.*, **107**, 107-121.
87. Nilsson, P-G. & Lindman, B. (1982). Solution structure of nonionic surfactant microemulsions from nuclear magnetic resonance self-diffusion studies. *J.Phys.Chem.*, **86**, 271-279.
88. Ravey, J.C. & Buzier, M. (1984). Structure of nonionic microemulsions by small angle neutron scattering. In Mittal, K.L. & Lindman, B. (eds) *Surfactants in solution*. Vol.3. Plenum Press, New York, p.1759-1779.
89. Kizling, J. & Stenius, P. (1987). Microemulsions formed by water, aliphatic hydrocarbons, and pentaethylene glycol dodecyl ether: The temperature dependence of aggregate size. *J.Colloid Interface Sci.*, **118**, 482-492.
90. Israelachvili, J.N., Mitchell, D.J. & Ninham, B.W. (1976). Theory of self-assembly of hydrocarbon amphiphiles into micelles and bilayers. *J.Chem.Soc.,Faraday Trans.2.*, **72**, 1525-1567.
91. Israelachvili, J.N., Marčelja, S. & Horn, R.G. (1980). Physical principles

of membrane organization. *Q.Rev.Biophys.*, 13, 121-200.

92. Tanford, C. (1980). Micelles. In *The hydrophobic effect: formation of micelles and biological membranes.*, Wiley & Sons, New York. p.42-59.

93. Tanford, C., Nozaki, Y. & Rohde, M.F. (1977). Size and shape of globular micelles formed in aqueous solution by n-alkyl polyoxyethylene ethers. *J.Phys.Chem.*, 81, 1555-1560.

94. Ninham, B.W. & Evans, D.F. (1986). Vesicles and molecular forces. *Faraday Discuss.Chem.Soc.*, 81, 1-17.

95. Oakenfull, D. (1980). Constraints of molecular packing on the size and stability of microemulsion droplets. *J.Chem.Soc.,Faraday I*, 76, 1875-1886.

96. Hyde, S.T., Ninham, B.W. & Zemb, T. (1989). Phase boundaries for ternary microemulsions. Predictions of a geometric model. *J.Phys.Chem.*, 93, 1464-1471.

97. Robbins, M.L & Bock, J. (1988). Model for microemulsions. I.Effect of sulfonate cation and chain size and concentration on phase behavior. *J.Colloid Interface Sci.*, 124, 462-485.

98. Robbins, M.L. & Bock, J. (1988). Model for microemulsions. II.Hydrophile-lipophile balance (HLB)-salinity-oil molar volume phase maps. *J.Colloid Interface Sci.*, 124, 486-503.

99. Robbins, M.L., Bock, J. & Huang, J.S. (1988). Model for microemulsions. III.Interfacial tension and droplet size correlation with phase behavior of mixed surfactants. *J.Colloid Interface Sci.*, 126, 114-133.

100. Langevin, D., Guest, D. & Meunier, J. (1986). Correlation between interfacial tension and microemulsion structure in Winsor equilibria. Role of the surfactant film curvature properties. *Colloids Surf.*, 19, 159-170.

101. Langevin, D. (1986). Recent advances in the physics of microemulsions. *Physica Scripta.*, T13, 252-258.

102. Helfrich, W. (1973). Elastic properties of lipid bilayers: Theory and possible experiments. *Z.Naturforsch.*, 28c, 693-703.
103. Langevin, D. (1991). Microemulsions - Interfacial aspects. *Adv.Colloid Interface Sci.*, 34, 583-595.
104. Binks, B.P., Meunier, J., Abillon, O. & Langevin, D. (1989). Measurement of film rigidity and interfacial tensions in several ionic surfactant-oil-water microemulsion systems. *Langmuir*, 5, 415- 421.
105. De Gennes, P.G. & Taupin, C. (1982). Microemulsions and the flexibility of oil/water interfaces. *J.Phys.Chem.*, 86, 2294-2304.
106. Aveyard, R., Binks, B.P. & Fletcher, P.D.I. (1989). Interfacial tensions and aggregate structure in $C_{12}E_5$ /oil/water microemulsion systems. *Langmuir*, 5, 1210-1217.
107. Meunier, J. (1985). Measurement of the rigidity coefficient of a surfactant layer and structure of the oil or water microemulsion interface. *J.Physique Lett.*, 46, L1005-L1014.
108. Aveyard, R., Binks, B.P., Clark, S. & Fletcher, P.D.I. (1989). Aggregation and adsorption behavior in nonionic surfactant/oil/water systems. *Progr.Colloid Polym.Sci.*, 79, 202- 207.
109. Farago, B., Richter, D., Huang, J.S., Safran, S.A. & Milner, S.T. (1990). Shape and size fluctuations of microemulsion droplets: The role of cosurfactant. *Phys.Rev.Lett.*, 65, 3348-3351.
110. Safran, S.A. (1991). Saddle-splay modulus and the stability of spherical microemulsions. *Phys.Rev.A*, 43, 2903-2904.
111. Lee, L.T., Langevin, D., Meunier, J., Wong, K. & Cabane, B. (1990). Film bending elasticity in microemulsions made with nonionic surfactants. *Progr.Colloid Polym.Sci.*, 81, 209-214.
112. Lee, L.T, Langevin, D., Wong, K. & Abillon, O. (1990). Microemulsions: experimental aspects. *J.Phys.:Condens.Matter*, 2, SA333-SA338.

113. Denkov, N.D., Kralchevsky, P.A., Ivanov, I.B. & Vassilieff, C.S. (1991). Effect of droplet deformation on the interactions in microemulsions. *J.Colloid Interface Sci.*, 143, 157-173.
114. Lemaire, B., Bothorel, P. & Roux, D. (1983). Micellar interaction in water-in-oil microemulsions. 1.Calculated interaction potential. *J.Phys.Chem.*, 87, 1023-1028.
115. Zemb, T.N., Barnes, I.S., Derian, P-J. & Ninham, B.W. (1990). Scattering as a critical test of microemulsion structural models. *Progr.Colloid Polym.Sci.*, 81, 20-29.
116. Talmon, Y. & Prager, S. (1977). Statistical mechanics of microemulsions. *Nature*, 267, 333-335.
117. Talmon, Y. & Prager, S. (1978). Statistical thermodynamics of phase equilibria in microemulsions. *J.Chem.Phys.*, 69, 2984-2991.
118. Talmon, Y. & Prager, S. (1982). The statistical thermodynamics of microemulsions. II.The interfacial region. *J.Chem.Phys.*, 76, 1535-1538.
119. Andelman, D., Cates, M.E., Roux, D. & Safran, S.A. (1987). Structure and phase equilibria of microemulsions. *J.Chem.Phys.*, 87, 7229-7241.
120. Widom, B. (1986). Lattice model of microemulsions. *J.Chem.Phys.*, 84, 6943-6954.
121. Widom, B., Dawson, K.A. & Lipkin, M.D. (1986). Hamiltonian and phenomenological models of microemulsions. *Physica*, 140A, 26-34.
122. Safran, S.A., Roux, D., Cates, M.E. & Andelman, D. (1986). Origin of middle-phase microemulsions. *Phys.Rev.Lett.*, 57, 491-494.
123. Cates, M.E., Andelman, D., Safran, S.A. & Roux, D. (1988). Theory of microemulsions: Comparison with experimental behavior. *Langmuir*, 4, 802-806.

124. Ninham, B.W., Barnes, I.S., Hyde, S.T., Derian, P-J. & Zemb, T.N. (1987). Random connected cylinders: A new structure in three-component microemulsions. *Europhys.Lett.*, 4, 561-568.
125. Barnes, I.S., Hyde, S.T., Ninham, B.W., Derian, P-J., Drifford, M., Warr, G.G. & Zemb, T.N. (1988). The disordered open connected model of microemulsions. *Progr.Colloid Polym.Sci.*, 76, 90-95.
126. Bansal, V.K. and Shah, O.S. (1977). Microemulsions and tertiary oil recovery. In Prince, L.M., *Microemulsions: theory and practice*. Academic Press, New York, p.149-173.
127. Neustadter, E.L. (1984). Surfactants in enhanced oil recovery. In Tadros, Th.F. (ed.), *Surfactants*. Academic Press, London, p.277-286.
128. Schomäcker, R. (1991). Chemical reactions in microemulsions: Application of microemulsions as solvents for organic synthesis., *J.Chem.Research(S)*, 92-93.
129. Pelizzetti, E., Pramauro, E. & Minero, C. (1987). Kinetics and reactivity in oil-in-water microemulsions., *Annali di Chimica*, 77, 127-143.
130. Fendler, J.H. (1980). Microemulsions, micelles and vesicles as media for membrane mimetic photochemistry., *J.Phys.Chem.*, 84, 1485-1491.
131. Mackay, R.A. & Hermansky, C. (1981). Phosphate ester-nucleophile reactions in oil-in-water microemulsions., *J.Phys.Chem.*, 85, 739-744.
132. Parra, J.L., García Domínguez, J.J., Comelles, F., Sánchez, J., Solans, C., Pelejero, C. & Balaguer, F. (1985). Use of microemulsions as vehicles for nucleophilic reagents in cosmetic formulations. *Int.J.Cosmet.Sci.*, 7, 127-141.
133. Willner, I., Ford, W.E., Otvos, J.W. & Calvin, M. (1979). Photoinduced electron transfer across a water-oil boundary as a model for redox reaction separation. *Nature*, 280, 823-824.
134. Kiwi, J. & Grätzel, M. (1980). Chlorophyll a sensitized redox processes in microemulsion systems. *J.Phys.Chem.*, 84, 1503-1507.

135. Jones, C.E. & Mackay, R.A. (1978). Reactions in microemulsions. 3. Photodegradation of chlorophyll., *J. Phys. Chem.*, **82**, 63-65.
136. Jones, C.E., Jones, C.A. & Mackay, R.A. (1979). Reactions in microemulsions. 4. Kinetics of chlorophyll sensitized photoreduction of methyl red and crystal violet by ascorbate. *J. Phys. Chem.*, **83**, 805-810.
137. Hochkoeppler, A. & Luisi, P.L. (1991). Photosynthetic activity of plant cells solubilized in water-in-oil microemulsions. *Biotech. Bioeng.*, **37**, 918-921.
138. Ovejero-Escudero, F.J., Angelino, H. & Casamatta, G. (1987). Microemulsions as adaptive solvents for hydrometallurgical purposes: A preliminary report. *J. Disp. Sci. Tech.*, **8**, 89-108.
139. Tondre, C. & Boumezioud, M. (1989). Microemulsions as model systems to study the kinetics and mechanism of reactions occurring in the extraction of metal ions by lipophilic extractants: Complexation of Nickel(II) by 8-hydroxyquinoline and Kelex 100. *J. Phys. Chem.*, **93**, 846-854.
140. Boumezioud, M., Derouiche, A. & Tondre, C. (1989). Solubilization versus microemulsification of extractant molecules in micellar systems: Comparison between 8-hydroxyquinoline and Kelex 100. *J. Colloid Interface Sci.*, **128**, 422-426.
141. Tondre, C. & Xenakis, A. (1984). Use of microemulsions as liquid membranes: Improved kinetics of solute transfer at interfaces. *Faraday Discuss. Chem. Soc.*, **77**, 115-126.
142. Kim, H.S. & Tondre, C. (1989). On a possible role of microemulsions for achieving the separation of Ni^{2+} and Co^{2+} from their mixtures on a kinetic basis. *Sep. Sci. Technol.*, **24**, 485-493.
143. Moyá, M.L., Izquierdo, C. & Casado, J. (1991). Microemulsions as a medium in chemical kinetics: The persulfate-iodide reaction. *J. Phys. Chem.*, **95**, 6001-6004.
144. Paatero, E., Sjöblom, J. & Datta, S.K. (1990). Microemulsion formation

and metal extraction in the system water/aerosol OT/extractant/isooctane. *J.Colloid Interface Sci.*, 138, 388-396.

145. Athanassakis, V., Bunton, C.A. & de Buzzaccarini, F. (1982). Nucleophilic aromatic substitution in microemulsions. *J.Phys.Chem.*, 86, 5002-5009.

146. Barnickel, P., Wokaun, A., Sager, W. & Eicke H-F. (1992). Size tailoring of silver colloids by reduction in w/o microemulsions. *J.Colloid Interface Sci.*, 148, 80-90.

147. Solans, C., Parra, J.L., Erra, P., Azemar, N., Clausse, M. & Touraud, D. (1987). Influence of microemulsion structure on cystine reactivity with keratin fibres. *Int.J.Cosmet.Sci.*, 9, 215-222.

148. Mishra, B.K., Valaulikar, B.S., Kunjappu, J.T. & Manohar, C. (1989). Influence of microemulsion structure on reaction rates. *J. Colloid Interface Sci.*, 127, 373-376.

149. Scheper, T., Makryaleas, K., Nowottny, C., Likidis, Z., Tsikas, D. & Schügerl, K. (1987). Liquid surfactant membrane emulsions: A new technique for enzyme immobilization. *Ann.N.Y.Acad.Sci.*, 501, 165-170.

150. Levashov, A.V., Khmelnitsky, Y.L., Klyachko, N.L. & Martinek, K. (1984). Reversed micellar enzymology. In Mittal, K.L. & Lindman, B. (eds) *Surfactants in solution*. Vol.2., Plenum Press, New York, p.1069-1090.

151. Hilhorst, R., Laane, C. & Veeger, C. (1982). Photosensitized production of hydrogen by hydrogenase in reversed micelles. *Proc.Natl.Acad.Sci.USA.*, 79, 3927-3930.

152. Xenakis, A., Valis, T.P. & Kolisis, N. (1991). Microemulsions as a tool for enzymatic studies: The case of lipase. *Progr.Colloid Polym.Sci.*, 84, 508-511.

153. Holmberg, K. & Österberg, E. (1990). Microemulsions as vehicles for lipase catalyzed reactions. *Progr.Colloid Polym.Sci.*, 82, 181-189.

154. Larsson, K.M., Adlercreutz, P., Mattiasson, B. & Olsson, U. (1991).

Enzyme catalysis in uni- and bi-continuous microemulsions: Dependence of kinetics on substrate partitioning. *J.Chem.Soc.Faraday Trans.*, **87**, 465-471.

155. Holmberg, K. & österberg, E. (1987). Enzymatic transesterification of a triglyceride in microemulsions. *Progr.Colloid Polym.Sci.*, **74**, 98-102.

156. Ayala, G. & Mendoza-Hernández, G. (1990). Stability and activity of 20 β -hydroxysteroid dehydrogenase in microemulsion of non-ionic detergents. *Biochem.Int.*, **22**, 717-723.

157. Oldfield, C. (1990). Evaluation of steady-state kinetic parameters for enzymes solubilized in water-in-oil microemulsion systems. *Biochem.J.*, **272**, 15-22.

158. Vulfson, E.N., Ahmed, G., Gill, I., Kozlov, I.A., Goodenough, P.W. & Law, B.A. (1991). Alterations to the catalytic properties of polyphenoloxidase in detergentless microemulsions and ternary water-organic solvent mixtures. *Biotechnol.Lett.*, **13**, 91-96.

159. Khmelnitsky, Y.L., van Hoek, A., Veeger, C. & Visser, A.J.W.G. (1989). Detergentless microemulsions as media for enzymatic reactions. Spectroscopic and ultracentrifugation studies. *J.Phys.Chem.*, **93**, 872-878.

160. Sonesson, C. & Holmberg, K. (1991). Use of a middle phase microemulsion for enzymatic lipid hydrolysis. *J.Colloid Interface Sci.*, **141**, 239-244.

161. Robinson, B.H. (1990). Microemulsions- properties and novel chemistry. *Chem.Brit.*, **26**, 342-344.

162. Luisi, P.L., Imre, V.E., Jaeckle, H. & Pande, A. (1983). Microemulsions: Proteins and nucleic acids as guest molecules. In *Top.Pharm.Sci.,Proc.Int.Congr.Pharm.Sci. F.I.P.*, 43rd., 243-255.

163. Tondre, C. & Xenakis, A. (1982). Transport of solubilized pyrene by o/w microemulsions. *Colloid Polym.Sci.*, **260**, 232-233.

164. Xenakis, A. & Tondre, C. (1987). Transport of alkali metal picrates by

w/o microemulsions used as liquid membranes: Influence of the nature of the surfactant and cosurfactant. *J.Colloid Interface Sci.*, 117, 442-447.

165. Xenakis, A. & Tondre, C. (1983). Oil-in-water microemulsion globules as carriers of lipophilic substances across liquid membranes. *J.Phys.Chem.*, 87, 4737-4743.

166. Derouiche, A. & Tondre, C. (1989). Aerosol OT reversed micelles as carrier agents. *J.Chem.Soc.,Faraday Trans.1.*, 85, 3301-3308.

167. Tondre, C. & Derouiche, A. (1990). Mechanism of solute transfer across water/oil interfaces in biphasic microemulsion systems. *J.Phys.Chem.*, 94, 1624-1626.

168. Provost, C. (1986). Transparent oil-water gels. *Int.J.Cosmet.Sci.*, 8, 233-247.

169. Rädler, J.O., Radiman, S., de Vallera, A. & Toprakcioglu, C. (1989). SANS studies of liquid crystalline microemulsion gels. *Physica B*, 156 & 157, 398-401.

170. Provost, C & Kinget, R. (1988). Transparent oil-water gels: a study of some physicochemical and biopharmaceutical characteristics. Part 1. Formation of transparent oil-water gels in the 4-component-system of Eumulgin B3, Cetiol HE, isopropyl palmitate, and water. *Int.J.Pharm.*, 44, 75-85.

171. Gradzielski, M., Hoffmann, H. & Oetter, G. (1990). Ringing gels: Their structure and macroscopic properties. *Colloid Polym.Sci.*, 268, 167-178.

172. Nürnberg, E. & Pohler, W. (1984). Zur kenntnis von transparenten 3-komponenten-tensidgelen. 4.Mitteilung: Der gelcharakter optisch isotroper tensid-H₂O-paraffinsysteme. *Progr.Colloid Polym.Sci.*, 69, 64-72.

173. Fontell, K. (1990). Cubic phases in surfactant and surfactant-like lipid systems. *Colloid Polym.Sci.*, 268, 264-285.

174. Luisi, P.L., Scartazzini, R., Haering, G. & Schurtenberger, P. (1990).

Organogels from water-in-oil microemulsions. *Colloid Polym.Sci.*, **268**, 356-374.

175. Capitani, D., Segre, A.L., Sparapani, R., Giustini, M., Scartazzini, R. & Luisi, P.L. (1991). Lecithin microemulsion gels: A NMR study of molecular mobility based on line widths. *Langmuir*, **7**, 250-253.

176. Scartazzini, R. & Luisi, P.L. (1988). Organogels from lecithins. *J.Phys.Chem.*, **92**, 829-833.

177. Schurtenberger, P., Scartazzini, R., Magid, L.J., Leser, M.E. & Luisi, P.L. (1990). Structural and dynamic properties of polymer-like reverse micelles. *J.Phys.Chem.*, **94**, 3695-3701.

178. Luisi, P.L. (1986). Process for preparing a solution of inverted micellae. Int.Pat.Appl. WO 86/02264.

179. Atkinson, P.J., Clark, D.C., Howe, A.M., Heenan, R.K. & Robinson, B.H. (1991). Characterization of microemulsion-based organo-gels. *Progr.Colloid Polym.Sci.*, **84**, 129-132.

180. Haering, G. & Luisi, P.L. (1986). Hydrocarbon gels from water-in-oil microemulsions. *J.Phys.Chem.*, **90**, 5892-5895.

181. Quellet, C. & Eicke, H-F. (1986). Mutual gelation of gelatin and water-in-oil microemulsions. *Chimia*, **40**, 233-238.

182. Petit, C., Zemb, Th. & Pileni, M.P. (1991). Structural study of microemulsion-based gels at the saturation point. *Langmuir*, **7**, 223-231.

183. Quellet, C., Eicke, H-F. & Sager, W. (1991). Formation of microemulsion-based gelatin gels. *J.Phys.Chem.*, **95**, 5642-5655.

184. Howe, A.M., Katsikides, A., Robinson, B.H., Chadwick, A.V. & Al-Mударis, A. (1988). Structure and dynamics of microemulsion-based gels. *Progr.Colloid Polym.Sci.*, **266**, 211-215.

185. Atkinson, P.J., Grimson, M.J., Heenan, R.K., Howe, A.M. & Robinson,

B.H. (1989). Structure of microemulsion-based organo-gels. *J.Chem.Soc.,Chem.Comm.*, 1807-1809.

186. Cecutti, C., Rico, I., Lattes, A., Novelli, A., Rico, A., Marion, G., Graciaa, A. & Lachaise, J. (1989). New formulation of blood substitutes: Optimization of novel fluorinated microemulsions. *Eur.J.Med.Chem.*, 24, 485-492.

187. Lowe, K.C. (1987). Perfluorocarbons as oxygen-transport fluids. *Comp.Biochem.Physiol.*, 87A, 825-838.

188. Bhargava, H.N., Narurkar, A. & Lieb, L.M. (1987). Using microemulsions for drug delivery. *Pharm.Technol.*, 11, 46-54.

189. Mathis, G. & Delpuech, J-J. (1982). Aqueous Fluorocarbide emulsions indefinitely stable at a given temperature, process for obtaining them and applications. *Int.Pat.Appl.* WO 82/01467.

190. Mukerjee, P. (1982). Fluorocarbon-hydrocarbon interactions in interfacial and micellar systems. *J.Am.Oil Chem.Soc.*, 59, 573-578.

191. Escoula, B., Rico, I., Laval, J.P. & Lattes, A. (1985). A new method of fluoroalkylation by a wittig reaction. *Synth.Comm.*, 15, 35-38.

192. Davis, B., Pearce, D.R. & Connor, P. (1975). Steroidal anaesthetic composition for intravenous injection. *US.Pat.Appl.* US 3,917,830.

193. Gauthier, R.J. (1986). Microemulsion compositions. *Eur.Pat.Appl.* EP 0 211 258.

194. Fubini, B., Gasco, M.R. & Gallarate, M. (1989). Microcalorimetric study of microemulsions as potential drug delivery systems. II. Evaluation of enthalpy in the presence of drugs. *Int.J.Pharm.*, 50, 213-217.

195. Ritschel, W.A. (1991). Microemulsions for improved peptide absorption from the gastrointestinal tract. *Meth.Find.Exp.Clin.Pharmacol.*, 13, 205-220.

196. Gallarate, M., Gasco, M.R. & Trotta, M. (1988). Influence of octanoic

acid on membrane permeability of timolol from solutions and from microemulsions. *Acta Pharm.Technol.*, 34, 102-105.

197. Comelles, F., Parra, J.L., Ferrando, C., Caelles, J. & Sánchez, J. (1990). Transparent formulations of a liposoluble sunscreen agent in an aqueous medium. *Int.J.Cosmet.Sci.*, 12, 185- 196.

198. Linn, E.E., Pohland, R.C. & Byrd, T.K. (1990). Microemulsion for intradermal delivery of cetyl alcohol and octyl dimethyl PABA. *Drug Dev.Indust.Pharm.*, 16, 899-920.

199. Gasco, M.R., Gallarate, M. & Pattarino, F. (1991). *In vitro* permeation of azelaic acid from viscosized microemulsions. *Int.J.Pharm.*, 69, 193-196.

200. Martini, M.C., Bobin, M.F., Flandin, H., Caillaud, F. & Cotte, J. (1984). Role des microemulsions dans l'absorption percutanee de l' α -tocopherol. *J.Pharm.Belg.*, 39, 348-354.

201. Muller, B.W.W., Franzky, H-J. & Kölln, C-J. (1988). Pharmaceutical multicomponent systems and method of preparing same. US.Pat.Appl. US 4,719, 239.

202. Osborne, D.W., Ward, A.J.I. & O'Neill, K.J. (1988). Microemulsions as topical drug delivery vehicles. I.Characterization of a model system. *Drug Dev.Indust.Pharm.*, 14, 1203-1219.

203. Osborne, D.W., Ward, A.J.I. & O'Neill, K.J. (1991). Microemulsions as topical drug delivery vehicles: *In-vitro* transdermal studies of a model hydrophilic drug. *J.Pharm.Pharmacol.*, 43, 451-454.

204. Kemken, J., Ziegler, A. & Müller, B.W. (1991). Investigations into the pharmacodynamic effects of dermally administered microemulsions containing β -blockers. *J.Pharm.Pharmacol.*, 43, 679- 684.

205. Kemken, J., Ziegler, A. & Müller, B.W. (1991). Pharmacodynamic effects of transdermal bupranolol and timolol *in vivo*: Comparison of microemulsions and matrix patches as vehicle. *Meth.Find.Exp.Clin.Pharmacol.*, 13, 361-365.

206. Jayakrishnan, A., Kalaiarasi, K. & Shah, D.O. (1983). Microemulsions: Evolving technology for cosmetic applications. *J.Soc.Cosmet.Chem.*, 34, 335-350.
207. Johnson, K.A. & Shah, D.O. (1986). Formulation and properties of an alcohol-free, pharmaceutical microemulsion system. In Mittal, K.L. & Bothorel, P. (eds) *Surfactants in Solution*. Vol.6. Plenum Press, New York, p.1441-1456.
208. Gasco, M.R., Pattarino, F. & Voltani, I. (1988). Behaviour of doxorubicine in o/w and w/o microemulsions. *Il Farmaco Ed.Pr.*, 43, 3-12.
209. Pattarino, F., Gasco, M.R. & Trotta, M. (1989). Accumulation of anthracyclines by a w/o microemulsion. *Il Farmaco*, 44, 339-344.
210. Gasco, M.R. & Trotta, M. (1986). Nanoparticles from microemulsions. *Int.J.Pharm.*, 29, 267-268.
211. Gasco, M.R., Morel, S. & Manzoni, R. (1988). Incorporation of doxorubicine in nanoparticles obtained by polymerization from non aqueous microemulsion. *Il Farmaco Ed.Pr.*, 43, 373-380.
212. Tarr, B.D. & Yalkowsky, S.H. (1989). Enhanced intestinal absorption of cyclosporine in rats through the reduction of emulsion droplet size. *Pharm.Res.*, 6, 40-43.
213. Ritschel, W.A., Ritschel, G.B., Sabouni, A., Wolochuk, D. & Schroeder, T. (1989). Study on the peroral absorption of the endekapeptide cyclosporin A. *Meth.Find.Exp.Clin.Pharmacol.*, 11, 281-287.
214. Ritschel, W.A., Adolph, S., Ritschel, G.B. & Schroeder, T. (1990). Improvement of peroral absorption of cyclosporin A by microemulsions. *Meth.Find.Exp.Clin.Pharmacol.*, 12, 127-134.
215. Patel, D.G., Ritschel, W.A., Chalasani, P. & Rao, S. (1991). Biological activity of insulin in microemulsion in mice. *J.Pharm.Sci.*, 80, 613-614.

216. Cho, Y.W. & Flynn, M. (1989). Oral delivery of insulin. *Lancet*, 1518-1519.
217. Owen, A.J., Morgan, E. & Sarkahian, A. (1991). Microemulsion calcitonin lowers serum calcium levels in juvenile male rats. *FASEB Journal*, 5, A1234.
218. Gasco, M.R., Pattarino, F. & Lattanzi, F. (1990). Long-acting delivery systems for peptides: Reduced plasma testosterone levels in male rats after a single injection. *Int.J.Pharm.* 62, 119-123.
219. Vigne, J-L. & Kane, J.P. (1987). Pharmaceutical microemulsions. *Int.Pat. Appl.* WO 87/01035
220. Via, D.P., Craig, I.F., Jacobs, G.W., van Winkle, W.B., Charlton, S.C., Gotto Jr., A.M. & Smith, L.C. (1982). Cholesteryl ester-rich microemulsions: Stable protein-free analogs of low density lipoproteins. *J.Lipid Res.*, 23, 570-576.
221. Ginsberg, G.S., Small, D.M. & Atkinson, D. (1982). Microemulsions of phospholipids and cholesterol esters. Protein-free models of low density lipoprotein. *J.Biol.Chem.*, 257, 8216- 8227.
222. Halbert, G.W., Stuart, J.F.B. & Florence, A.T. (1984). The incorporation of lipid-soluble antineoplastic agents into microemulsions- protein-free analogues of low density lipoprotein. *Int.J.Pharm.*, 21, 219-232.
223. Fubini, B., Gasco, M.R. & Gallarate, M. (1988). Microcalorimetric study of microemulsions as potential drug delivery systems. I.Evaluation of enthalpy in the absence of any drug. *Int.J.Pharm.*, 42, 19-26.
224. Trotta, M., Gasco, M.R. & Morel, S. (1989). Release of drugs from oil-water microemulsions. *J.Controlled Release*, 10, 237-243.
225. Gasco, M.R., Gallarate, M. & Pattarino, F. (1988). On the release of prednisone from oil in water microemulsions. *Il Farmaco Ed.Pr.*, 43, 325-330.
226. Gasco, M.R., Trotta, M. & Carlotti, M.E. (1985). Ion pairs of β blockers

with taurodeoxycholate. *Pharm.Acta Helv.*, 60, 334-338.

227. Gasco, M.R., Carlotti, M.E. & Trotta, M. (1988). *In vitro* release of propranolol from oil/water microemulsions. *Int.J.Cosmet.Sci.*, 10, 263-269.

228. Gasco, M.R., Gallarate, M., Trotta, M., Bauchiero, L., Gremmo, E. & Chiappero, O. (1989). Microemulsions as topical delivery vehicles: Ocular administration of timolol. *J.Pharm.Biomed.Anal.*, 7, 433-439.

229. Craig, P.N. (1990). Drug compendium. In Hansch, C., Sammes, P.G., Taylor, J.B. (eds). *Comprehensive medicinal chemistry. Vol.6: Cumulative subject index and drug compendium.*, Pergamon Press, New York, p.237-991.

230. Princen, H.M., Zia, I.Y.Z. & Mason, S.G. (1967). Measurement of interfacial tension from the shape of a rotating drop. *J.Colloid Interface Sci.*, 23, 99-107.

231. Coumou, D.J. (1960). Apparatus for the measurement of light scattering in liquids. Measurement of the Rayleigh factor of benzene and of some other pure liquids. *J.Colloid Sci.*, 15, 408- 417.

232. Gulari, E., Chu, B. & Liu, T.Y. (1979). Characterization of meningococcal polysaccharides by light-scattering spectroscopy. IV.Molecular weight distribution of group B meningococcal polysaccharide in buffer solution. *Biopolymers*, 18, 2943-2961.

233. Lyklema, J. (1991). *Fundamentals of interface and colloid science. Vol.1. Fundamentals.* Academic Press, London.

234. Attwood, D. & Ktistis, G. (1989). A light scattering study on oil-in-water microemulsions. *Int.J.Pharm.*, 52, 165-171.

235. Herrington, T.M., Sahi, S.S. & Leng, C.A. (1985). Apparent molar volumes for aqueous solutions of the homologous series of α -dodecyl- ω -hydroxypoly(oxyethylene) surfactants, $C_{12}EO_j$ ($j=4,5,6,8$ and 12), and of $C_{10}EO_6$. *J.Chem.Soc.,Faraday Trans.1*, 81, 2693-2702.

236. Small, D.M. (1967). Phase equilibria and structure of dry and

dehydrated egg lecithin. *J.Lip.Res.*, 8, 551-557.

237. Cebula, D.J., Ottewill, R.H., Ralston, J. & Pusey, P.N. (1981). Investigations of microemulsions by light scattering and neutron scattering. *J.Chem.Soc.,Faraday Trans.1.*, 77, 2585-2612.

238. Baker, R.C., Florence, A.T., Ottewill, R.H. & Tadros, Th.F. (1984). Investigations into the formation and characterization of microemulsions. II.Light scattering, conductivity and viscosity studies of microemulsions. *J.Colloid Interface Sci.*, 100, 332-349.

239. Kale, N.J. & Allen, L.V. (1989). Studies on microemulsions using Brij 96 as surfactant and glycerin, ethylene glycol and propylene glycol as cosurfactants. *Int.J.Pharm.*, 57, 87-93.

240. Orecchioni, A.M., Couarraze, G., Grossiord, J.L., Seiller, M. & Puisieux, F. (1984). Viscoelastic properties of paracrystalline phases appearing in water-surface agent-oil diagrams. *Int.J.Cosmet.Sci.*, 6, 131-143.

241. Lo, I., Florence, A.T., Treguier, J-P, Seiller, M. & Puisieux, F. (1977). The influence of surfactant HLB and the nature of the oil phase on the phase diagrams of nonionic surfactant-oil-water systems. *J.Colloid Interface Sci.*, 59, 319-327.

242. Olsson, U., Nagai, K. & Wennerström, H. (1988). Microemulsions with nonionic surfactants. 1.Diffusion process of oil molecules. *J.Phys.Chem.*, 92, 6675-6679.

243. Mukherjee, S., Miller, C.A. & Fort,Jr., T. (1983). Theory of drop size and phase continuity in microemulsions. 1.Bending effects with uncharged surfactants. *J.Colloid Interface Sci.*, 91, 223-243.

244. Aveyard, R., Binks, B.P. & Mead, J. (1986). Interfacial tension minima in oil-water-surfactant systems. Effects of alkane chain length and presence of n-alkanols in systems containing aerosol-OT. *J.Chem.Soc.,Faraday Trans.1*, 82, 1755-1770.

245. Sadaghiana, A.S. & Khan, A. (1991). Clouding of a nonionic surfactant:

The effect of added surfactants on the cloud point. *J. Colloid Interface Sci.*, 144, 191-200.

246. Aveyard, R., Binks, B.P., Clark, S. & Fletcher, P.D.I. (1990). Cloud points, solubilisation and interfacial tensions in systems containing nonionic surfactants. *J. Chem. Tech. Biotechnol.*, 48, 161- 171.

247. Kjellander, R. (1982). Phase separation of non-ionic surfactant solutions. A treatment of the micellar interaction and form. *J. Chem. Soc., Faraday Trans. 2*, 78, 2025-2042.

248. Aveyard, R. & Lawless, T.A. (1986). Interfacial tension minima in oil-water-surfactant systems. Systems containing pure non-ionic surfactants, alkanes and inorganic salts. *J. Chem. Soc., Faraday Trans. 1*, 82, 2951-2963.

249. Shinoda, K. & Arai, H. (1964). The correlation between phase inversion temperature in emulsion and cloud point in solution of nonionic emulsifier. *J. Phys. Chem.*, 68, 3485-3490.

250. Hoffmann, H. & Ebert, G. (1988). Surfactants, micelles and fascinating phenomena. *Angew. Chem. Int. Ed. Engl.*, 27, 902-912.

251. Jousma, H., Joosten, J.G.H., Gooris, G.S. & Junginger, H.E. (1989). Changes of mesophase structure of Brij 96/water mixtures on addition of liquid paraffin. *Colloid Polym. Sci.*, 267, 353-364.

252. Müller, B.W. & Müller, R.H. (1984). Particle size analysis of latex suspensions and microemulsions by photon correlation spectroscopy. *J. Pharm. Sci.*, 73, 915-918.

253. Chang, N.J. & Kaler, E.W. (1986). Quasi-elastic light scattering study of five-component microemulsions. *Langmuir*, 2, 184-190.

254. Cheung, H.M., Qutubuddin, S., Edwards, R.V. & Mann, Jr., J.A. (1987). Light scattering study of oil-in-water microemulsions: Corrections for interactions. *Langmuir*, 3, 744-752.

255. Ganz, A.M. & Boeger, B.E. (1986). Application of a new dilution method

to a light scattering study of interparticle repulsions in nonionic microemulsions. *J. Colloid Interface Sci.*, 109, 499-503.

256. Siano, D.B., Bock, J., Myer, P. & Russel, W.B. (1987). Thermodynamics and hydrodynamics of a nonionic microemulsion. *Colloids Surfs.*, 26, 171-190.

257. Hermansky, C. & Mackay, R.A. (1980). Light scattering measurements in nonionic microemulsions. *J. Colloid Interface Sci.*, 73, 324-331.

258. Wu, X-L., Tong, P. & Huang, J.S. (1992). Effect of elastic bending energy on the emulsification failure in a microemulsion. *J. Colloid Interface Sci.*, 148, 104-105.

259. Degiorgio, V. & Corti, M. (1984). Laser-light scattering study of nonionic micelles in aqueous solution. In Mittal, K.L. & Lindman, B. (eds) *Surfactants in solution*. Vol.1. Plenum press, New York. p.471-486.

260. Richtering, W.H., Burchard, W., Jahns, E. & Finkelmann, H. (1988). Light scattering from aqueous solutions of a nonionic surfactant (C₁₄E₈) in a wide concentration range. *J. Phys. Chem.*, 92, 6032-6040.

261. Brown, W., Rymdén, R., van Stam, J., Almgren, M. & Svensk, G. (1989). Static and dynamic properties of nonionic amphiphile micelles: Triton X-100 in aqueous solution. *J. Phys. Chem.* 93, 2512- 2519.

262. Herrington, T.M. & Sahi, S.S. (1988). Temperature dependence of the micellar aggregation number of n-dodecylpolyethyleneoxide surfactants. *J. Colloid Interface Sci.*, 121, 107-120.

263. Evans, R.M., Attwood, D., Chatham, S.M. & Farr, S.J. (1990). The effect of solubilized water on the size and shape of lecithin micelles in an apolar solvent. *J. Pharm. Pharmacol.*, 42, 601-605.

264. Mallon, C. (1991). A study on pharmaceutical microemulsions. *Ph.D Thesis*, Manchester.

265. Jousma, H., Joosten, J.G.H. & Junginger, H.E. (1988). Mesophases in mixtures of water and polyoxyethylene surfactant: Variations of repeat

spacing with temperature and composition. *Colloid Polym.Sci.*, 266, 640-651.

266. Attwood, D., Elworthy, P.H. & Lawrence, M.J. (1989). Effect of structural variations of non-ionic surfactants on micellar properties and solubilization: Surfactants with semipolar hydrophobes. *J.Pharm.Pharmacol.*, 41, 585-589.

267. Attwood, D., Currie, L.R.J. & Elworthy, P.H. (1974). Studies of solubilized micellar solutions. 1.Phase studies and particle size analysis of solutions formed with nonionic surfactants. *J.Colloid Interface Sci.*, 46, 249-256.

268. Müller, B.W. & Müller, R.H. (1984). Particle size distributions and particle size alterations in microemulsions. *J.Pharm.Sci.*, 73, 919-922.

269. Comelles, F., Solans, C., Azemar, N., Sánchez Leal, J. & Parra, J.L. (1986). Microemulsions with commercial nonionic surfactants: Study of their formation and detergency properties. *J.Disp.Sci.Technol.*, 7, 369-382.

270. Mitchell, D.J., Tiddy, G.J.T., Waring, L., Bostock, T. & McDonald, M.P. (1983). Phase behaviour of polyoxyethylene surfactants with water. Mesophase structures and partial miscibility (cloud points). *J.Chem.Soc.,Faraday Trans.1*, 79, 975-1000.

271. Aserin, A., Frenkel, M. & Garti, N. (1984). HPLC analysis of nonionic surfactants. Part IV. Polyoxyethylene fatty alcohols. *J.Am.Oil Chem.Soc.*, 61, 805-809.

272. Flanagan, P.W., Greff, R.A. & Smith, H.F. (1963). Applications of high resolution nuclear magnetic resonance spectrometry to the identification and quantitative analysis of nonionic surfactants. *Anal.Chem.*, 35, 1283-1285.

273. Crutchfield, M.M., Irani, R.R. & Yoder, J.T. (1964). Quantitative applications of high-resolution proton magnetic resonance measurements in the characterization of detergent chemicals. *J.Am.Oil Chem.Soc.*, 41, 129-132.

274. Lawrence, M.J. (1985). Physico-chemical and solubilisation studies on aqueous solutions of synthetic non-ionic surfactants. *Ph.D Thesis*,

Manchester.

275. Wormuth, K.R. & Geissler, P.R. (1991). Phase behavior of monodisperse and polydisperse ethoxylated alcohols. *J. Colloid Interface Sci.*, 146, 320-329.

276. Bostock, T.A., McDonald, M.P. & Tiddy, G.J.T. (1984). Phase studies and conductivity measurements in microemulsion-forming systems containing a nonionic surfactant. In Mittal, K.L. & Lindman, B. (eds) *Surfactants in solution* Vol.3., Plenum Press, New York, p.1805-1820.

277. Ravey, J.C. (1987). Nonionics. In Friberg, S.E. & Bothorel, P. (eds) *Microemulsions: Structure and dynamics*. CRC Press Inc., Boca Raton, Florida, p.93-117.

278. Kunieda, H., Nakamura, K., Davis, H.T. & Evans, D.F. (1991). Formation of vesicles and microemulsions in a water/tetraethylene glycol dodecyl ether/dodecane system. *Langmuir*, 7, 1915-1919.

279. Friberg, S. & Lapczynska, I. (1975). Microemulsions and solubilization by nonionic surfactants. *Progr. Colloid Polym. Sci.*, 56, 16-20.

280. Kunieda, H. & Shinoda, K. (1985). Evaluation of the hydrophile-lipophile balance (HLB) of nonionic surfactants. 1. Multisurfactant systems. *J. Colloid Interface Sci.*, 107, 107-121.

281. Kahlweit, M., Strey, R. & Firman, P. (1986). Search for tricritical points in ternary systems: Water-oil-nonionic amphiphile. *J. Phys. Chem.*, 90, 671-677.

282. Hayes, M.E., El-Emary, M., Schechter, R.S. & Wade, W.H. (1979). The relation between the $EACN_{min}$ concept and surfactant HLB. *J. Colloid Interface Sci.*, 68, 591-560.

283. Mitchell, D.J. & Ninham, B.W. (1981). Micelles, vesicles and microemulsions. *J. Chem. Soc., Faraday Trans. 2*, 77, 601-619.

284. Chen, S.J., Evans, D.F., Ninham, B.W., Mitchell, D.J., Blum, F.D. & Pickup, S. (1986). Curvature as a determinant of microstructure and microemulsions. *J. Phys. Chem.*, 90, 842-847.

285. Sowada, R., Hauthal, H.G. & Grossklaus, S. (1987). Characterization of microemulsions. *J.Prakt.Chem.*, 329, 833-840.
286. Kunieda, H. & Miyajima, A. (1989). The effect of the mixing of oils on the hydrophile-lipophile-balanced (HLB) temperature in a water/nonionic surfactant/oil system. *J.Colloid Interface Sci.*, 128, 605-607.
287. Kahlweit, M., Strey, R., Haase, D. & Firman, P. (1988). Properties of the three-phase bodies in H₂O-oil-nonionic amphiphile mixtures. *Langmuir*, 4, 785-790.
288. Saito, H. & Shinoda, K. (1967). The solubilization of hydrocarbons in aqueous solutions of nonionic surfactants. *J.Colloid Interface Sci.*, 24, 10-15.
289. Maclay, W.N. (1956). Factors affecting the solubility of nonionic emulsifiers. *J.Colloid Sci.*, 11, 272-285.
290. Gruen, D.W.R. (1981). A mean-field model of the alkane-saturated lipid bilayer above its phase transition. I. Development of the model. *Biophys.J.*, 33, 149-166.
291. Gruen, D.W.R. & Haydon, D.A. (1981). A mean-field model of the alkane-saturated lipid bilayer above its phase transition. II. Results and comparison with experiment. *Biophys.J.*, 33, 167-188.
292. Gruen, D.W.R. & Haydon, D.A. (1980). The adsorption of n-alkanes into bimolecular lipid layers: Theory and experiment. *Pure Appl.Chem.*, 52, 1229-1240.
293. Ninham, B.W., Chen, S.J. & Fennell Evans, D. (1984). Role of oils and other factors in microemulsion design. *J.Phys.Chem.*, 88, 5855-5857.
294. Gaonkar, A.G. (1992). Effects of salt, temperature, and surfactants on the interfacial tension behavior of a vegetable oil/water system. *J.Colloid Interface Sci.*, 149, 256-260.
295. Alander, J. & Warnheim, T. (1989). Model microemulsions containing

vegetable oils. Part 1: Nonionic surfactant systems. *J.Am.Oil Chem.Soc.*, 66, 1656-1660.

296. Chaiko, M.A., Nagarajan, R. & Ruckenstein, E. (1984) Solubilization of single-component and binary mixtures of hydrocarbons in aqueous micellar solutions. *J.Colloid Interface Sci.*, 99, 168-182.

297. Carroll, B.J. (1986). Solubilisation of two-component oil mixtures by micellar surfactant solutions. *J.Chem.Soc.,Faraday Trans.1.* 82, 3205-3214.

298. Thomas, D.C. & Christian, S.D. (1981). Mixed solubilization of benzene and cyclohexane in sodium deoxycholate micelles. *J.Colloid Interface Sci.*, 82, 430-438.

299. Ravey, J-C. (1983). Lower consolute curve related to micellar structure of nonionic surfactants. *J.Colloid Interface Sci.*, 94, 289-291.

300. Brown, W., Johnsen, R., Stilbs, P. & Lindman, B. (1983). Size and shape of nonionic amphiphile ($C_{12}E_6$) micelles in dilute aqueous solutions as derived from quasielastic and intensity light scattering, sedimentation, and pulsed-field-gradient nuclear magnetic resonance self-diffusion data. *J.Phys.Chem.*, 87, 4548- 4553.

301. Cebula, D.J. & Ottewill, R.H. (1982). Neutron scattering studies on micelles of dodecylhexaoxyethylene glycol monoether. *Colloid Polym.Sci.*, 260, 1118-1120.

302. Corti, M., Minero, C. & Degiorgio, V. (1984). Cloud point transition in nonionic micellar solutions. *J.Phys.Chem.*, 88, 309- 317.

303. Corti, M. & Degiorgio, V. (1981). Micellar properties and critical fluctuations in aqueous solutions of nonionic amphiphiles. *J.Phys.Chem.*, 85, 1442-1445.

304. Triolo, R., Magid, L.J., Johnson,Jr., J.S. & Child, H.R. (1982). Small-angle neutron scattering from aqueous micellar solutions of a nonionic surfactant as a function of temperature. *J.Phys.Chem.*, 86, 3689-3695.

305. Leung, R. & Shah, D.O. (1987). Solubilization and phase equilibria of water-in-oil microemulsions. II. Effects of alcohols, oils, and salinity on single-chain surfactant systems. *J. Colloid Interface Sci.*, **120**, 330-344.
306. Tabony, J. (1986). Formation of cubic structures in microemulsions containing equal volumes of oil and water. *Nature*, **319**, 400.
307. Eicke, H-F. (1979). On the cosurfactant concept. *J. Colloid Interface Sci.*, **68**, 440-450.
308. Bedő, Zs., Berecz, E., Lakatos, I. & Lakatos-Szabó, J. (1990). Effect of alcohols on micelle formation in aqueous solutions of ethoxylated nonyl-phenols. *Progr. Colloid Polym. Sci.*, **82**, 229-235.
309. Deguchi, K., Mizuno, T. & Meguro, K. (1974). Solvent effects on the micellar destruction of nonionic surfactant. *J. Colloid Interface Sci.*, **48**, 474-480.
310. Schwab, A.W. & Pryde, E.H. (1985). Triglyceride-methanol microemulsions. *J. Disp. Sci. Tech.*, **6**, 563-574.
311. Schwab, A.W., Nielson, H.C., Brooks, D.D. & Pryde, E.H. (1983). Triglyceride / aqueous ethanol / 1-butanol microemulsions. *J. Disp. Sci. Tech.*, **4**, 1-17.
312. Roux-Desgranges, G., Grolier, J-P.E., Villamañan, M.A. & Casanova, C. (1986). Role of alcohol in microemulsions. III. Volumes and heat capacities in the continuous phase water-n-butanol-toluene of reverse micelles. *Fluid Phase Equilibria*, **25**, 209-230.
313. Ceglie, A., Das, K.P. & Lindman, B. (1987). Effect of oil on the microscopic structure in four-component cosurfactant microemulsions. *J. Colloid Interface Sci.*, **115**, 115-120.
314. Stilbs, P., Rapacki, K. & Lindman, B. (1983). Effect of alcohol cosurfactant length on microemulsion structure. *J. Colloid Interface Sci.*, **95**, 583-585.

315. Ceglie, A., Das, K.P. & Lindman, B. (1987). Microemulsion structure in four-component systems for different surfactants. *Colloids Surf.*, 28, 29-40.
316. Starkovskii, A.V. & Trapeznikov, A.A. (1988). Effect of the nature of an alcohol on its distribution between the phases in a microemulsion system. *Colloid J.USSR.*, 50, 346-348.
317. Guo, J.S., Sudol, E.D., Vanderhoff, J.W., Yue, H.J. & El-Aasser, M.S. (1992). Partitioning behaviour and thermodynamic model for styrene o/w microemulsions. *J.Colloid Interface Sci.*, 149, 184- 196.
318. Guo, J.S., El-Aasser, M.S., Sudol, E.D., Yue, H.J. & Vanderhoff, J.W. (1990). Phase compositions of styrene oil-in-water microemulsions. *J.Colloid Interface Sci.*, 140, 175-184.
319. Friberg, S.E. & Fang, J-H. (1984). Temperature dependence of the solubility areas for w/o microemulsions with nonionic/anionic surfactants. *J.Am.Oil Chem.Soc.*, 61, 801-804.
320. Ito, M., Takisawa, N. & Shirahama, K. (1990). Conductivity fluctuation of a microemulsion system at transition temperature. *J.Phys.Chem.*, 94, 3726-3728.
321. Aveyard, R., Binks, B.P., Lawless, T.A. & Mead, J. (1985). Interfacial tension minima in oil+water+surfactant systems. Effects of salt and temperature in systems containing nonionic surfactants. *J.Chem.Soc.,Faraday Trans.1*, 81, 2155-2168.
322. Aveyard, R., Binks, B.P. & Mead, J. (1986). Interfacial tension minima in oil-water-surfactant systems. Effects of alkane chain length and presence of n-alkanols in systems containing aerosol OT. *J.Chem.Soc.,Faraday Trans.1*, 82, 1755-1770.
323. Verhoeckx, G.J., De Bruyn, P.L. & Overbeek, J.Th.G. (1987). On understanding microemulsions. 1.Interfacial tensions and adsorptions of SDS and pentanol at the cyclohexane/water interface. *J.Colloid Interface Sci.*, 119, 409-421.

324. Zhou, J.S. & Dupeyrat, M. (1990). Alcohol effect on interfacial tension in oil-water-sodium dodecyl sulphate systems. *J.Colloid Interface Sci.* 134, 320-335.
325. Wärnheim, T., Jönsson, A. & Sjöberg, M. (1990). Phase diagrams for cationic surfactants in polar solvent systems. *Prog.Colloid Polym.Sci.*, 82, 271-279.
326. Attwood, D., Ktistis, G., McCormick, Y. & Story, M.J. (1989). Solubilization of indomethacin by polysorbate 80 in mixed water-sorbitol solvents. *J.Pharm.Pharmacol.*, 41, 83-86.
327. Zatz, J.L. & Lue, R-Y. (1987). Flocculation of suspensions containing nonionic surfactants by sorbitol. *J.Pharm.Sci.* 76, 157- 160.
328. Cantù, L., Corti, M., Degiorgio, V., Hoffmann, H. & Ulbricht, W. (1987). Nonionic micelles in mixed water-glycerol solvent. *J.Colloid Interface Sci.*, 116, 384-389.
329. Marszall, L. (1977). The effect of alcohols on the hydrophile-lipophile balance of nonionic surfactants. *J.Colloid Interface Sci.*, 60, 570-573.
330. Jusko, W.J., Gretch, M. & Gassett, R. (1973). Precipitation of diazepam from intravenous preparations. *JAMA*, 225, 176.
331. White, M. & Yalkowsky, S.H. (1991). Studies in plebitis. III. Evaluation of diazepam and phenytoin. *Pharm.Res.*, 8, 1341-1342.
332. Jeppsson, R. & Ljungberg, S. (1975). Anticonvulsant activity in mice of diazepam in an emulsion formulation for intravenous administration. *Acta Pharmacol.Toxicol.*, 36, 312-320.
333. Mattila, M.A.K., Ruoppi, M., Korhonen, M., Larni, H.M., Valtonen, L. & Heikkinen, H. (1979). Prevention of diazepam-induced thrombophlebitis with cremophor as a solvent. *Br.J.Anaesth.*, 51, 891-893.
334. Badwan, A.A., El-Khordagui, L.K., Saleh, A.M. & Khalil, S.A. (1980). The solubility of benzodiazepines in sodium salicylate solution and a

proposed mechanism for hydrotropic solubilization. *J.Pharm.Pharmacol.*, 32, 74P.

335. Rosoff, M. & Serajuddin, A.T.M. (1980). Solubilization of diazepam in bile salts and in sodium cholate-lecithin-water phases. *Int.J.Pharm.*, 6, 137-146.

336. Schmidt, D. (1981). Pharmaceutical compositions for parenteral or local administration. US Pat.Appl.4,271,196

337. Von Dardel, O., Mebius, C. & Mossberg, T. (1976). Diazepam in emulsion form for intravenous usage. *Acta Anaesth.Scand.*, 20, 221- 224.

338. Thorn-Alquist, A-M. (1977). Parenteral use of diazepam in an emulsion formulation. A clinical study. *Acta Anaesth.Scand.*, 21, 400-404.

339. Von Dardel, O., Mebius, C., Mossberg, T. & Svensson, B. (1983). Fat emulsion as a vehicle for diazepam. A study of 9492 patients. *Br.J.Anaesth.*, 55, 41-47.

340. MacDonald, A., Michaelis, A.F. & Senkowski, B.Z. (1972). Diazepam. In Florey, K.(ed.), *Analytical profiles of drug substances*. Vol.1. Academic Press, New York, p.79-99.

341. Elworthy, P.H. & Patel, M.S. (1982). Demonstration of maximum solubilization in a polyoxyethylene alkyl ether series of nonionic surfactants. *J.Pharm.Pharmacol.*, 34, 543-546.

342. Patel, M.S., Elworthy, P.H. & Dewsnap, A.K. (1981). Solubilisation of drugs in nonionic surfactants. *J.Pharm.Pharmacol.* 33(suppl.), 64P.

343. Elworthy, P.H. & Lipscomb, F.J. (1968). Solubilization of griseofulvin by nonionic surfactants. *J.Pharm.Pharmacol.*, 20, 817- 824.

344. Groves, M.J., Bassett, B. & Sheth, V. (1984). The solubility of 17 β -oestradiol in aqueous polyethylene glycol 400. *J.Pharm.Pharmacol.*, 36, 799-802.

345. Carlfors, J., Blute, I. & Schmidt, V. (1991). Lidocaine in microemulsion - A dermal delivery system. *J.Disp.Sci.Tech.*, 12, 467-482.
346. Lundberg, B., Lövgren, T. & Heikius, B. (1979). Simultaneous solubilization of steroid hormones II: Androgens and estrogens. *J.Pharm.Sci.*, 68, 542-545.
347. Tomida, H., Yotsuyanagi, T. & Ikeda, K. (1978). Solubilization of steroid hormones by polyoxyethylene lauryl ether. *Chem.Pharm.Bull.*, 26, 2832-2837.
348. Thakkar, A.L. & Kuehn, P.B. (1969). Solubilization of some steroids in aqueous solutions of a steroidal nonionic surfactant. *J.Pharm.Sci.*, 58, 850-851.
349. Thakkar, A.L. & Hall, N.A. (1967). Micellar solubilization of testosterone. I. In aqueous solutions of polysorbates. *J.Pharm.Sci.*, 56, 1121-1125.
350. Barry, B.W. & El Eini, D.I.D. (1976). Solubilization of hydrocortisone, dexamethasone, testosterone and progesterone by long-chain polyoxyethylene surfactants. *J.Pharm.Pharmacol.*, 28, 210-218.